AUTOMATIC CONTROL OF MULTISTAND COLD ROLLING MILL

by

R.F. Darlington, B.Sc.(Eng.)

A Thesis submitted for the Degree of Doctor of Philosophy in the Faculty of Engineering of the University of London

June 1965

Mechanical Engineering Department,
Imperial College of Science and Technology,
London.

ABSTRACT

The Bland and Ford equations describing the mechanics of cold rolling, including the entry and recovery elastic zones, are programmed for a digital computer. This programme includes the calculation of the coefficients required in the control equations used to describe the dynamic behaviour of a multistand cold rolling mill. Forward slip is expressed as a function of the stand input and output gauges and tensions enabling a convenient equation for forward slip to be obtained; for which the coefficients are determined by digital computation. The control equation coefficients are tabulated for a range of roll gap coefficients of friction for the mill schedule used.

Utilising these results, a four stand cold rolling mill is simulated on an analogue computer so as to allow the acceleration and deceleration phases of mill operation to be represented. Variable time delays and modified servomultipliers are used in conjunction with a general purpose analogue computer to achieve this end.

With a model of the mill simulated, experiments are performed to study the nature of the process with a view to automatic gauge control. The response of

the process alone, to a number of strip output velocity profiles, incoming strip variations and schedule deviations is recorded and discussed. The experiments are conducted with and without forward slip included as a variable to indicate its effects on the mill variable transients.

A variety of automatic gauge control systems are simulated and imposed on the mill model. Their ability to control strip tensions and gauges when the mill is subjected to a number of strip output velocity profiles and incoming strip variations are recorded and discussed.

ACKNOWLEDGEMENTS

The author wishes to thank Professor R.D. Hoyle, Ph.D., M.I.Mech.E. for his supervision of the initial research, and Professor J.M. Alexander, D.Sc., Ph.D., M.I.Mech.E., M.I.Prod.E., F.I.M. for his supervision in the latter part of the work.

While conducting the research the author held an Athlone Fellowship and is grateful to the British Board of Trade and the Athlone Fellowship Managing Committee.

The author is also particularly grateful to Jarry Hydraulics Ltd., Montreal, for their financial assistance; and Mr. J.P. Fullam, Vice-president thereof, for his encouragement during this period.

CONTENTS

LIST OF SYMBOLS

A	=	Constant in yield stress equation A.19.
A	=	Cross sectional area of strip
a_{1r}, a_{2r} a_{3r}, a_{4r}	=	Coefficients relating change in r^{th} stand output gauge to change in tensions, roll gap and incoming gauge changes in B.I.S.R.A. eqns.
b_{1r}, b_{2r} b_{3r}, b_{4r}	=	Coefficients relating change in r^{th} stand roll speed to changes in tensions, roll gap and incoming gauge changes in B.I.S.R.A. eqns.
B	=	Constant in yield stress equation A.19.
C	=	Electrical capacitance.
c	=	Constant in Hitchcock's Equation A.15.
c_1, c_2, c_3	=	Integral controller gains.
D_r	=	r^{th} stand motor droop.
E	=	Young's modulus.
e	=	Unit strain.
e	=	voltage.
F_r	=	Forward slip of strip leaving r^{th} stand.
f_{1r}, f_{2r} f_{3r}, f_{4r}	=	Coefficients relating change in slip to changes in incoming and outgoing gauges and tensions of r^{th} stand.
G_{or}	=	Motor torque of r^{th} stand.
G_p	=	Rolling torque due to plastic zone.

G_{eo} = Rolling torque due to exit elastic zone.

G_{ei} = Rolling torque due to entry elastic zone.

G_r = Total rolling torque of r^{th} stand.

g_{1r}, g_{2r}, g_{3r}, g_{4r} = Coefficients relating change in rolling torque to changes in incoming and outgoing gauges and tensions of r^{th} stand.

H_r = Gauge of strip leaving r^{th} stand.

H'_{r-1} = Gauge of strip entering r^{th} stand.

H_r^* = Strip thickness signal to X-ray gauge.

J = Dimensionless quantity defined by equation A.9.

J_n = Value of J at neutral point.

J_i = Value of J at entry to plastic zone.

k = Proportional controller gain.

k = Analogue computer scale factors.

k = Yield stress of strip.

$k_{0.6}$ = Mean yield of strip in roll gap.

L_r = Distance from r^{th} stand to next stand.

l = Length of arc of contact.

M_r = Stiffness constant of r^{th} stand.

P_p = Roll force due to plastic zone.

P_{eo} = Roll force due to exit elastic zone.

P_{ei} = Roll force due to entry elastic zone.

P_r = Total roll force of r^{th} stand.

p = Operator d /dt; Laplacian operator.

p_{1r}, p_{2r}	=	Coefficients relating change in roll
p_{3r}, p_{4r}		force to changes in incoming and out-
		going gauges and tensions of r^{th} stand.
q	=	Compressive stress perpendicular to
		surface of strip in roll gap.
R	=	Radius of undeformed roll.
R'	=	Radius of circular arc of contact of
		loaded roll.
r	=	Strip reduction as a fraction of original
		thickness.
S_r	=	Roll gap setting of r^{th} stand.
S_{or}	=	No-load roll gap of r^{th} stand.
ΔS_{or}	=	Roll neck bearing oil film thickness
		change.
s	=	Vertical compressive stress in roll gap.
T	=	Interstand tension force - tons.
t	=	Time
u	=	Coefficient of friction.
V_r	=	Velocity of strip
V'_{r-1}	=	Velocity of strip entering r^{th} stand.
w_r	=	Angular speed of rolls of r^{th} stand.
W_{Dr}	=	Speed setting of r^{th} stand.
Z	=	Electrical impedance.

α = Amplifier gain.

γ = Poissons ratio.

δ = Draft = $H_i - H_o$.

= Damping ratio.

θ = Constant in yield stress formula A.19.

λ = Denotes independent variable (Ref. Fig. 5.5).

σ = Interstand tension stress - tons/inch^2.

τ = Time constant - seconds.

ϕ = Angular coordinate in roll gap.

w = Natural frequency.

Subscripts

i = Denotes entry side to roll gap.

o = Denotes exit side of roll gap.

r = Denotes stand number.

n = Neutral point.

D = Denotes demanded value of variable.

R = Denotes variables associated with wind reel.

Prefixes

δ = Small change in variable due to perturbation.

Δ = Denotes a deviation from scheduled value of a variable.

1. INTRODUCTION

Although the concept of obtaining metal strip of a desired gauge and width dates back to a feasible design of a 4-high rolling mill sketched by Leonardo da Vinci in 1495, it is only in this century that true tandem mills, operating with the strip under tension between the stands, have been developed; and it was the past decade that saw the first successful applications of automatic gauge control to tandem cold rolling mills (1).

To investigate the automatic control of any process or machine it is useful to study the process itself and to obtain a mathematical model which will allow insight into the preferable methods of control.

In this thesis a method of investigating multistand cold rolling mills with computers is described and applied to this end. The resulting model is also used to illustrate and evaluate the effects of a variety of automatic gauge control systems.

1.1. THE MULTISTAND COLD ROLLING MILL

A multistand cold rolling mill is used to reduce the thickness of metal strip by passing it, unheated, through a series of up to six stands of work rolls. Each stand consists of two work rolls (about 20 inches in diameter) and a back up roll (about 50 inches in diameter) for each

work roll to provide stiffness. Thus each stand consists of 4 rolls in a vertical plane, supported by bearings mounted in the stand housing.

The work rolls of each stand are driven by D.C. motors; there usually being separate drives for each stand. The gap between the work rolls is adjustable to allow for various strip thicknesses desired and for adjustments to be made during a production run. The rolls are positioned by motor driven screws attached to yokes supporting the roll bearing.

While the strip is passed through the roll gap a vertical force is applied to the strip via the work rolls; a torque is applied to the work rolls by the drive motors to force the strip through the rolls; and the strip is put under tension by the relative roll speeds of the stands. The condition of plasticity states that the algebraic sum of the vertical compressive stress and the horizontal tensile stress must equal the yield stress of the strip at every point in the roll gap in order to produce a plastic zone in the strip to insure permanent reduction to the strip gauge as it passes between the rolls. Various theories exist on the mechanics of cold rolling (2).

The theory for the mechanics of the rolling process used (Chapter 2) is that of Bland and Ford (3, 6) and Bland, Ford and Ellis (4, 5). The equations describing this

theory (Appendix A) were programmed for the digital computer by the author and so enables convenient analysis of the process. The programme including the effects of the elastic zones in the roll gap is described in Chapter 5, and the programme itself is in Appendix C.

Fig. 2.1 shows the layout of the 4-stand tandem mill at the Abbey Works of the Steel Company of Wales. This mill has been used for investigation into rolling mill gauge by others at Imperial College (7, 8) and by the British Iron and Steel Research Association (9, 10, 11) and is also used as a reference in this thesis.

1.1.1. Mill Operation

The strip to be rolled; consisting of several separate strips from the hot rolling mill butt welded together to form a total length in the order of 5000 feet, is coiled and mounted on the unwind reel. The strip is fed through the mill stands and connected to the wind reel. Both the wind and unwind reels are powered to control the input and output tensions of the mill. The rolls having been positioned to the desired gap, the rolling speed of the mill is then increased to full operating speed. The operating speed in this case is in the order of 2000 feet per minute. Although the operating speed of a mill may be of this order, some

modern mills can be run at speeds exceeding 6000 feet per minute (1). Reference (1) also states that strip for many applications may be produced at a rate of up to 1000 tons per shift.

While the strip is being rolled, manual or automatic control is exerted through the motors to keep the gauge within the required thickness tolerance and to prevent strip breakage or 'cobbles'. Cobbles are the tangles of metal that may result if the strip becomes too slack and buckles over on itself.

Satisfactory operation of the mill implies that the maximum amount of on-gauge strip with good surface finish and good physical properties has been obtained economically. To achieve this, work is being devoted to increasing mill speeds, increasing the amount of gauge within tolerance, lowering the tolerances and optimising the energy consumption of the process. In the course of this thesis schemes for the automatic control of gauge are evaluated using the electronic analogue computer.

1.2. AUTOMATIC CONTROL OF GAUGE

During operation of the mill continuous adjustment of the mill settings is required due to disturbances caused by changes in the values of the parameters of the strip and mill. Incoming thickness variations can originate in the hot mill due to skid marks, loss of

tension at strip ends and eccentricity of the rolls. In the cold mill, disturbances may be caused by a change in hardness of the strip; a change in screw setting, speed, tension or roll gap frictional conditions; or in bearing roll neck frictional conditions. Over the long term, temperature rises in the mill during operation can cause effective changes in the roll gap settings. The butt weld at the strip joints is a particularly severe disturbance which requires the mill speed be reduced to allow its passage.

In the 4-stand mill being considered, the distance between the first and last stands is approximately 40 feet. With the strip travelling at an average speed in the mill at about 1200 feet per minute, the strip enters and leaves the mill in about 2 seconds. With higher speeds being introduced it is obvious that the most a manual controller can do is to note the trend of any deviations and make attempts to correct them. Since a proper balance of loads, speeds and tensions is required there exists the danger of a severe upset to the mill, such as strip breakage or cobbles, from an improper corrective action.

A reliable control system would remove this risk, allow more strip to be rolled to gauge and in general

tend to achieve the goals noted in section 1.1.1. There can be a considerable economic gain as all strip not rolled to within the gauge tolerances must be cut out of the produced strip as scrap.

The requirement is for a method by which a change in output gauge thickness, from the desired value, will produce a signal which may be used to actuate a control system to supply corrective action, rapidly and without instability. This problem has received considerable attention (Ref. 7 to 30).

1.2.1. Application of Computers to Gauge Control Analysis

As mentioned, to evaluate control systems for a given process, a mathematical model is required and it must be such that it accounts for the dynamics of the process. In this instance the process is taken to mean the rolling mill and its associated electric drives. To use the rolling equations as developed from the theory of rolling mechanics has been found impracticable at present and it has been necessary for the equations to be linearised (12, 16, 17, 18) to obtain 'control equations' which enable the dynamics to be conveniently described for a specific point, or mill speed.

This has limited previous work utilising computers to trials at a particular mill speed. This

thesis describes and utilises a method developed by the author which allows a multistand rolling mill to be simulated on an analogue computer so that mill speed or the strip velocities are variable. This allows the acceleration and deceleration phases of mill operation to be simulated and studied. Also slip - a factor relating stand roll speed to strip velocity - is included as a variable as is the varying roll neck bearing oil film thickness effect on the roll gap setting.

These control equations (Chapter 4) require partial differential coefficients to be evaluated. This was done by repeated solutions of the original rolling equations. These calculations are included in the digital programme in Appendix C which is described in Chapter 5. It calculates the coefficients for a range of mill speeds and a given mill schedule.

The most efficient manner of investigating many processes and their control systems is by analogue computer simulation. Analogue computers (Chapter 6) enable the process and its control system to be simulated by electronic analogy.

Two analogue computers were used in this work. Initial tests were run on the International Research and Development Company analogue computer. The final

and majority of tests were conducted on the Imperial College Mechanical Engineering Department's analogue computer. It is a general purpose analogue computer (Chapter 6) but its component specification was such that it lends itself particularly to the problem at hand.

The analogue simulations of the mill developed (Chapter 7) and the control systems used (Chapter 5) were used to investigate the mill behaviour. The results of these tests are described in Chapters 8 and 9.

2. THE COLD ROLLING PROCESS

2.1. MECHANICS OF THE ROLLING PROCESS

The mill and its operation were described in section 1.1 where it was mentioned that the rolling theory of Bland Ford and Ellis was employed in the study. Fig. A.1 in Appendix A shows the geometry of the roll gap and the forces acting on the plastic zone of the strip in the roll gap. The assumption of plane strain makes the Von-Mises yield stress criterion valid which gives the yield stress as 1.15 times the yield stress in uniaxial tension. Because friction exists between the strip and the rolls, the distribution of vertical pressure on the strip is modified. The distribution is found using the equations of force equilibrium. The equations for the plastic zone are listed in Appendix A.1 and their derivation employed the following assumptions.

2.1.1. Assumptions for the Plastic Zone Calculations

1) The coefficient of friction is of constant value in the roll gap and changes sign at the neutral point.
2) The arc of contact is circular.
3) Elastic compression is negligible.
4) Plane-strain exists in the roll gap.
5) Von-Mises criterion of plasticity holds.

6) Plane vertical sections remain plane.

7) Small angle relations hold as $\emptyset$ is usually less than 6°.

2.1.2. Yield Stress as Function of Strip Reduction

To solve equation A.16 for the roll force Bland and Ford suggest the use of a mean yield stress in the roll gap. However, with the digital computer it was possible to include the yield stress (Fig. A.2) as a function of strip reduction, which in turn may be expressed in terms of $\emptyset$, the roll gap angle. The equation relating yield stress to reduction was developed by B. Kafranoglu at Imperial College (31). It is based on a least squares fit to a logarithmic function. The constants in the equation (A.19) were determined with the digital computer from a set of points taken from Fig. A.2. Up to 200 points may be accommodated; in this instance 50 points were used and the following values were obtained for the equation's coefficients.

$$A = 55.2982 \text{ tons/in}^2$$

$$B = 0.00202317$$

$$\theta = 0.271503$$

2.1.3. Elastic Zone Equations

At the boundaries of the elastic and plastic zones, the elastic plane-strain must be compatable with the

plastic plane-strain. Commencing with these boundary conditions, and Hookes law for a three dimensional state of stress, the forces in the elastic zones may be found. The equations for the elastic zones, according to the theory of Bland, Ford and Ellis, are given in Appendix A.2. Fig. A.2 shows the elastic zones and the notation peculiar to Appendix A.2.

The effects of both the entry and exit elastic zones are included, although the entry elastic zone does not make a significant contribution. Once the effects of the elastic zones on the roll force and torque have been found, a modified radius of the circular arc of contact can be found considering the strip deflections. The equations are listed in Appendix A.3.

The equations discussed above have been included in Appendix A as it is these equations which are later programmed for the digital computer in Chapter 5.

2.2. MILL CONSTANTS AND SCHEDULE DATA

The calculations in this thesis are based on a particular schedule run on the Abbey Works mill. The data concerning this schedule is listed in Table 2.1. The same schedule has been used by the British Iron and Steel Research Association (9, 10, 11) and by others at Imperial College (7, 8) in their investigations of cold rolling mill control.

Table 2.1 Mill Schedule Data

Symbol	Quantity	Std.1	Std.2	Std.3	Std.4
H'_{r-1}	Input gauge-inches	.093	.078	.055	.041
H_r	Output gauge-inches	.078	.055	.041	.036
δ_r	Draft - inches	.015	.023	.014	.005
r_r	strip reduction	.161	.409	.559	.613
T_{r-1}	Tension force - tons	0	18	18.2	10.9
T_r	Tension force - tons	18	18.2	10.9	0
σ_{r-1}	Back tension $\frac{\text{tons}}{\text{in}^2}$	0	4.99	7.15	5.77
σ_r	Front tension $\frac{\text{tons}}{\text{in}^2}$	4.99	7.15	5.77	0
b	Strip width-inches	46.25	46.25	46.25	46.25
A'_{r-1}	Strip area in^2	4.30	3.608	2.544	1.896
A_r	Strip area in^2	3.608	2.544	1.896	1.665
R	Roll radius-inches	10.0	10.0	10.0	10.0
M_r	Mill stiffness $\frac{\text{ton}}{\text{in}}$	10000	10000	10000	10000
L	Distance to next stand-ins.	156	156	156	

Fig. 2.1 denotes the variable notation that will be used in this analysis and also shows the layout of the mill. Fig. 2.2 illustrates the general notation used - by substitution of the stand number for 'r' the notation of Fig. 2.1 is obtained.

2.3. THE MILL DRIVES

The mill rolls are driven by Ward-Leonard sets in which the drive motor is a D.C.-shunt motor. The steady-state characteristics of such motors can be expressed by the equation:

$$G_r = A_r + 1/D_r \, W_r \qquad 2.1$$

The torque output to the rolls can be controlled by varying A, which corresponds to varying the motor armature voltage. D_r is the motor droop. When the motors are operating at a set speed, any disturbance causing a change in torque will result in a change in rolling speed due to the motor 'droop'. The droop can vary when the motor speed is changed by varying the shunt field excitation.

For a given setting of A, the steady state change in speed is given by:

$$\delta W_r = 1/B_r \delta G_r = D_r \delta G_r \qquad 2.2$$

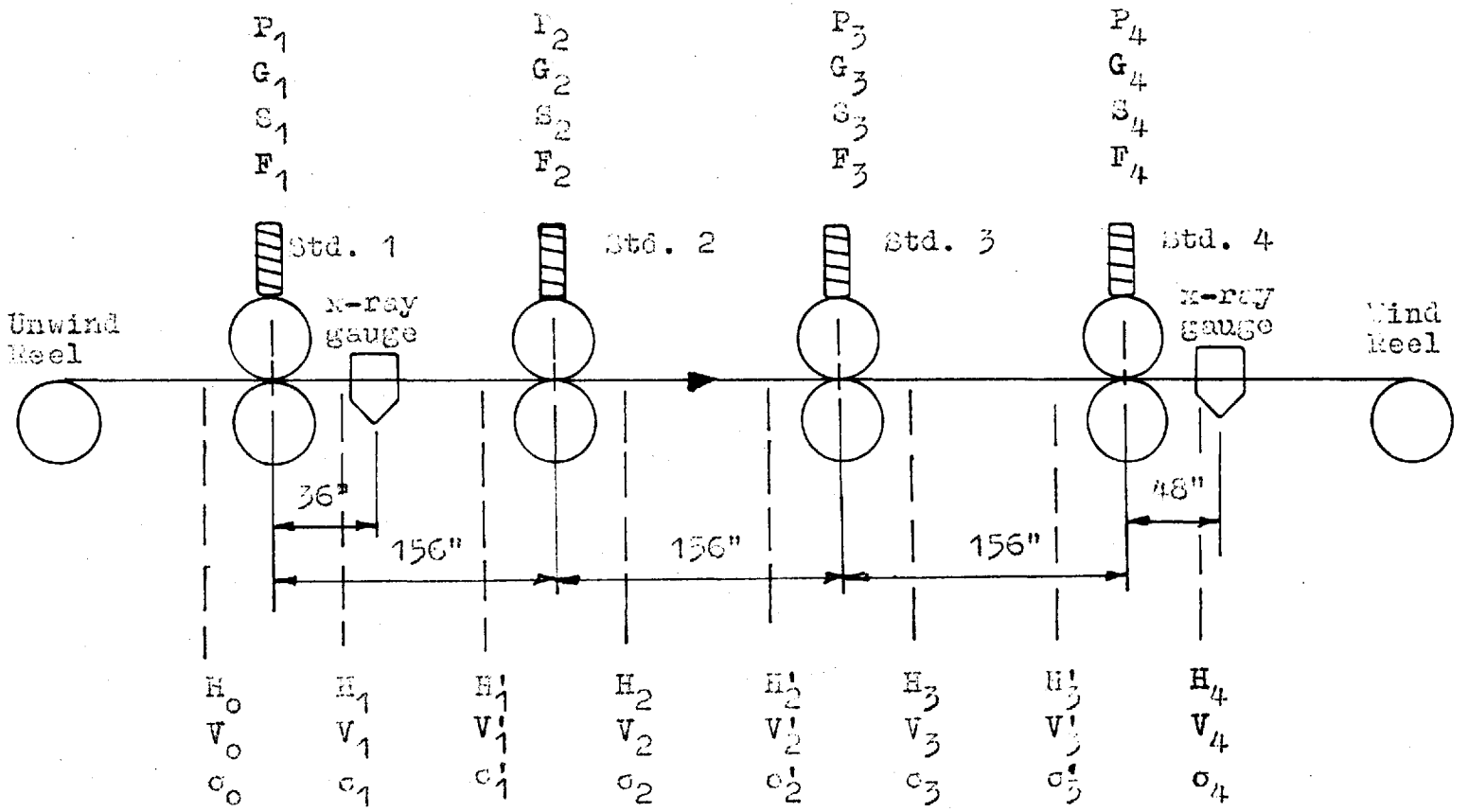

Note: $\sigma_1 = \sigma_1'$, $\sigma_2 = \sigma_2'$, $\sigma_3 = \sigma_3'$

Fig. 2.1. Layout of Mill and Notation of Variables Throughout Mill

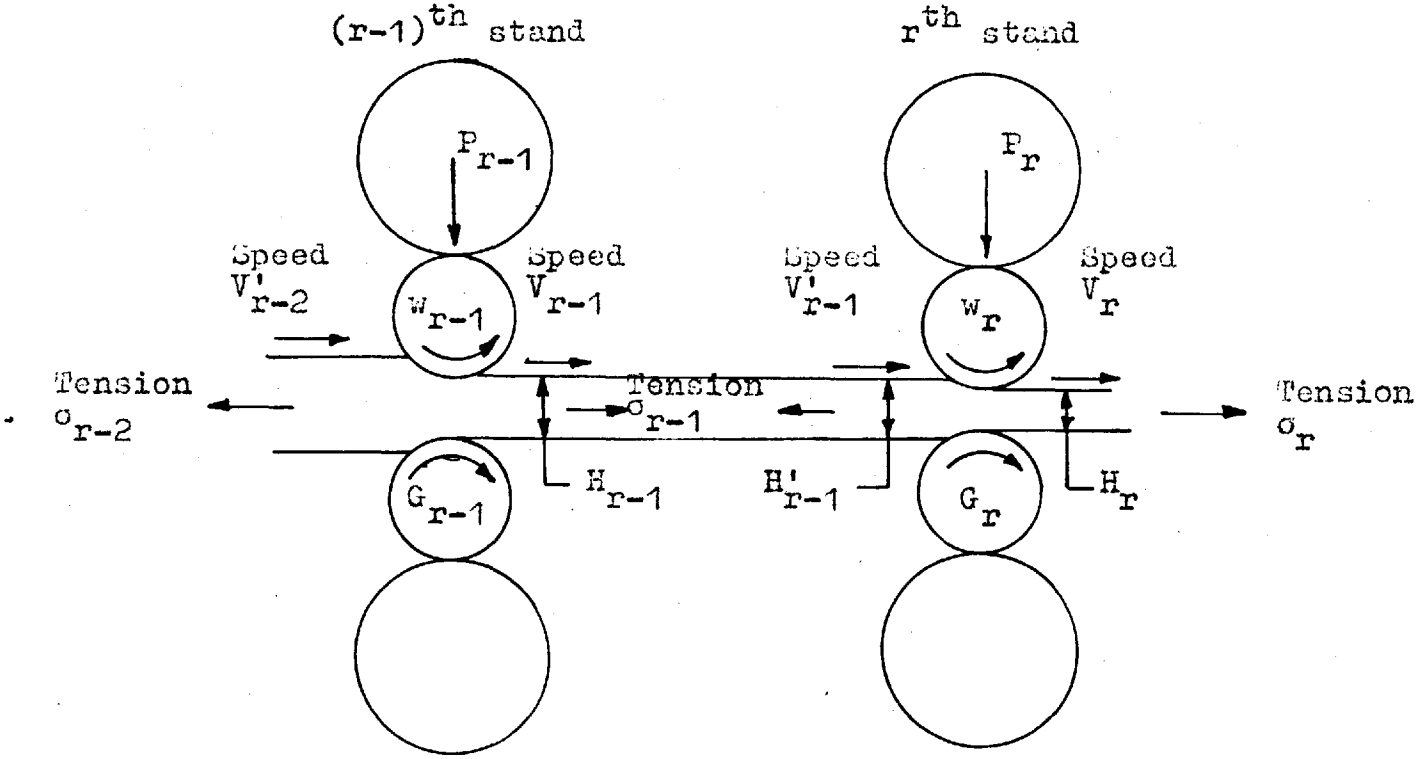

Fig. 2.2. General Notation For Mill

The results of Table 2.2 are based on equation A.39.

2.4. ROLL GAP FRICTION

As the strip is being rolled it slides against the roll surfaces due to the change in speed of the strip relative to the rolls as it passes through the roll gap. Only at the neutral point (Fig. A.1) does the strip speed equal the roll speed. The greater the coefficient of friction, the greater the tangential forces generated; hence, the greater the roll forces and roll torques. A reduction in the coefficient of friction allows a greater reduction of the strip gauge, for the same roll force and hence a more efficient mill design.

Sliding friction, as described in reference (34), is mainly due to the formation and destruction of minute bridges between the asperites of sliding surfaces. A film of lubricant, itself easily sheared, separates the surfaces and reduces the number of asperite bridges.

2.4.1. Types of Lubrication

The type of lubrication is defined by the film thickness. The extreme cases are boundary and hydrodynamic; with 'thin-film' being an intermediate condition.

With boundary lubrication the film is only one or two molecules thick (34). It occurs under heavy loads and

Table 2.2 Mill Motor Schedules

	Total Horse Power	Flatout RPM	1950 FPM Output		975 FPM
			Droop %	Droop r/s/Ton-in	Droop r/s/Ton-in (estimated)
1	3500	270	6	-.00472	-.00944
2	5000	408	5.33	-.00682	-.01364
3	5000	545	4.67	-.001065	-.02130
4	5000	635	4.00	-.0126	-.0252
Wind reel	1250	730	EST. 1.0	-.0173	-.0173

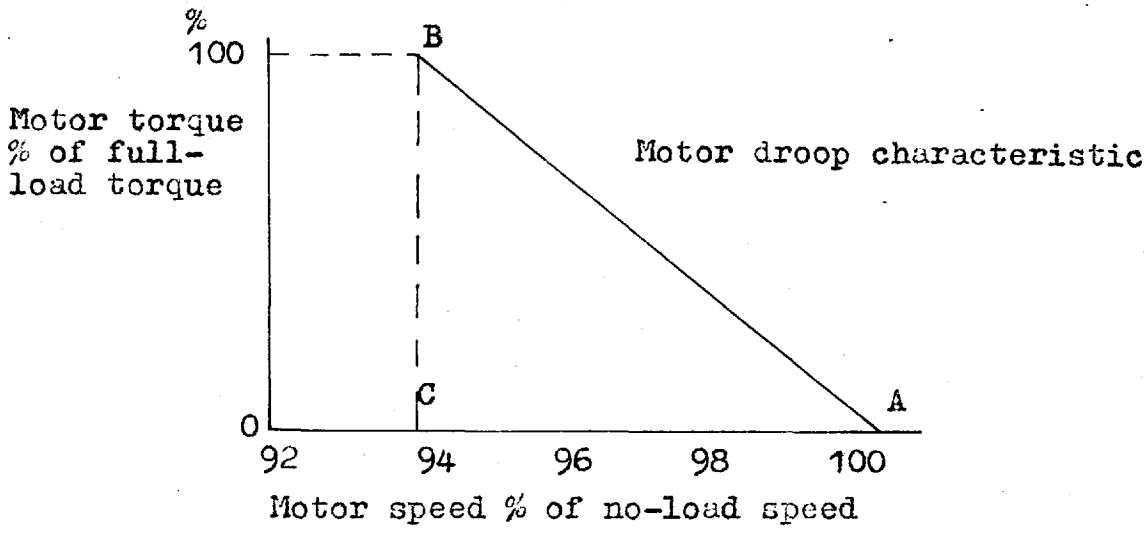

Fig. 2.3 Motor Droop Characteristic

low speeds. The nature of the surface and the chemistry of the lubricant play an important role in this type of lubrication.

In hydrodynamic lubrication the surfaces are separated by a film of considerable thickness and the resistance to motion is due to viscosity and other bulk properties of the fluid. There is, ideally, no wear and an oil wedge is created if the pressures are sufficiently high. This type of lubrication might exist in cold rolling at high speeds (34, 35).

2.4.2. Cold Rolling Aspects

The type of lubrication which exists in the roll gap is still not certain. The production of metal dust during rolling and of measured values of u in the order of 0.07 indicate boundary type lubrication. But as u decreases with increasing strip speed, some hydrodynamic effect is indicated.

J.M. Thorpe (34) carried out a series of experiments with a variety of lubricants on a single stand experimental mill. His results for pure paraffin lubricants show a marked transition zone where u falls to a lower value with increasing strip velocity. The explanation put forward was that during the transition period liquid is trapped in the surface irregularities to produce some

hydrodynamic effect. With palm oil - a base for many rolling lubricants - the coefficient of friction exhibited a gradual decrease with speed. Strip precoated with stearic acid in 100% concentrations, which fills the surface irregularities, did not show any change in u for speeds up to several hundred feet/minute. However, stearic acid by itself is not a practical lubricant, although it is used in small percentages in many rolling lubricants.

2.5. CONTROL OF STRIP GAUGE

2.5.1. Roll Force Equilibrium

Hessenberg and Sims (12) considered the stand housing as reacting as a stiff spring to the load imposed on the strip by the rolls; the overall stiffness being the combination of the roll stiffness and stand housing stiffness. The rolling load will thus cause the roll gap to increase over its value with no load. Assuming the strip output thickness to be equal to the roll gap under rolling load, they expressed the roll force as:

$$P_r = M_r(H_r - S_{or}) \qquad 2.4$$

Equation 2.4 is called the elastic equation of the stand. Fig. 2.4 shows the state point describing the equilibrium of the deformation of the strip due to load

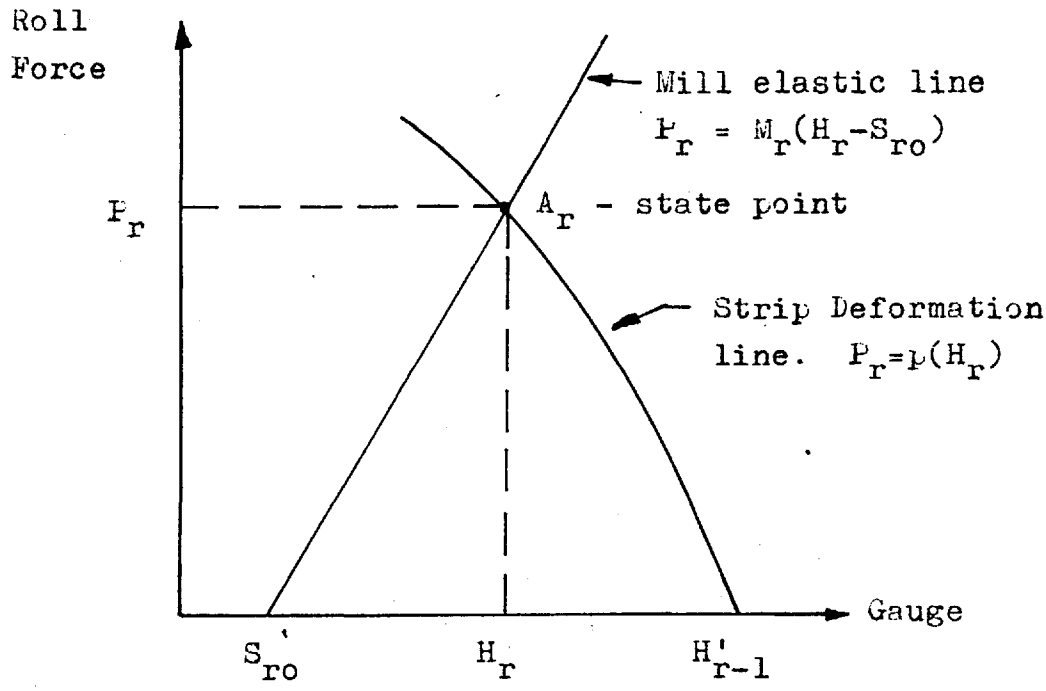

Fig. 2.4 Roll Force Equilibrium

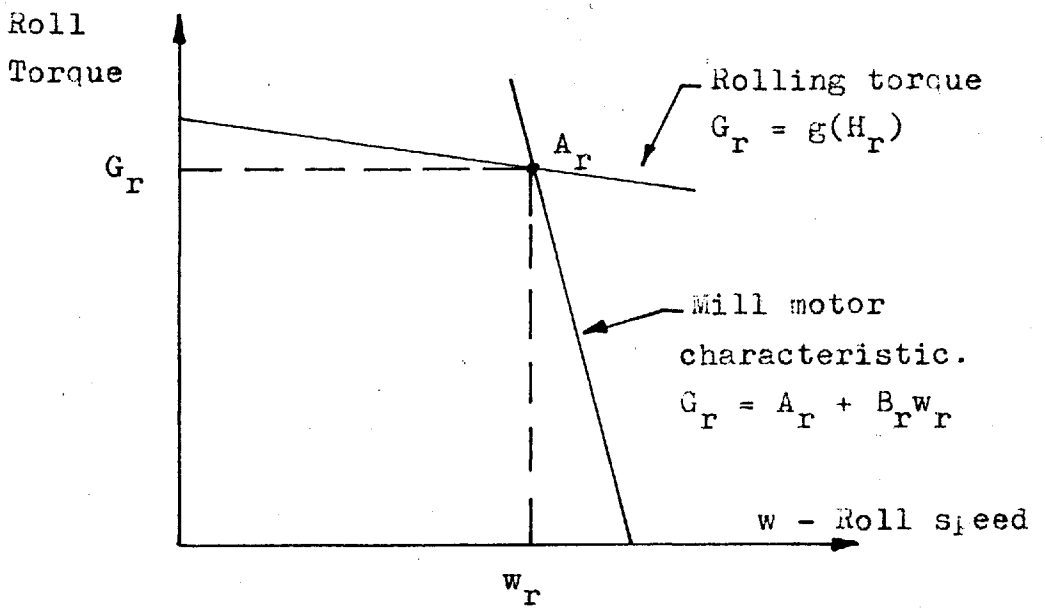

Fig. 2.5 RollTorque Equilibrium

and the elastic deflection of the stand (12, 16). The strip deformation characteristic is calculated from the roll force equations in Appendix A for varying output thickness; other variables being held constant. That is:

$$P_r = P(H_r) \qquad 2.5$$

Therefore, for a given roll setting S_o, there is a particular state point A.

2.5.2. Roll Torque Equilibrium

During a rolling operation the torque supplied by the drive motors is balanced by the rolling torque defined by the torque equations in Appendix A. For a particular stand and given strip parameters the rolling torque can be expressed as a function of output thickness (17). Thus:

$$G_r = g(H_r) \qquad 2.6$$

The state point A denotes the equilibrium condition which defines a particular value of operating speed of the rolls. The value of H_r in equation 2.6 is that defined by Fig. 2.4. Fig. 2.5 shows the rolling torque as decreasing with speed - an effect which is discussed

in section 2.5.5. It is due to the reduction of the coefficient of friction with increasing speed.

2.5.3. The Speed Effect

Experiments and observations on operating mills (11, 22, 27, 34, 35, 36), as discussed, indicate that as the rolling speed of the mill is increased, the coefficient of friction in the roll gap decreases. The consequent reduction in roll force and roll torque, predicted by the rolling theory in Appendix A, give rise to new state points. This is shown in Fig. 2.7 by the movement of the force state point from A1 to A2 for decreasing u.

There is, however, the added effect of the movement of the necks of the rolls in their bearings. The hydrodynamic film - for non antifriction type bearings - tends to increase in thickness with increasing roll speed. This causes the rolls to move closer together, decreasing the gap, and shifting the state point to A3; at which point there has been a reduction in output gauge, but an overall increase in roll force (22). This effect is taken into account in the simulation of Chapter 7 by modifying equation 2.4 to:

$$P_r = M_r(H_r - S_{or} - \Delta S_{or}) \qquad 2.7$$

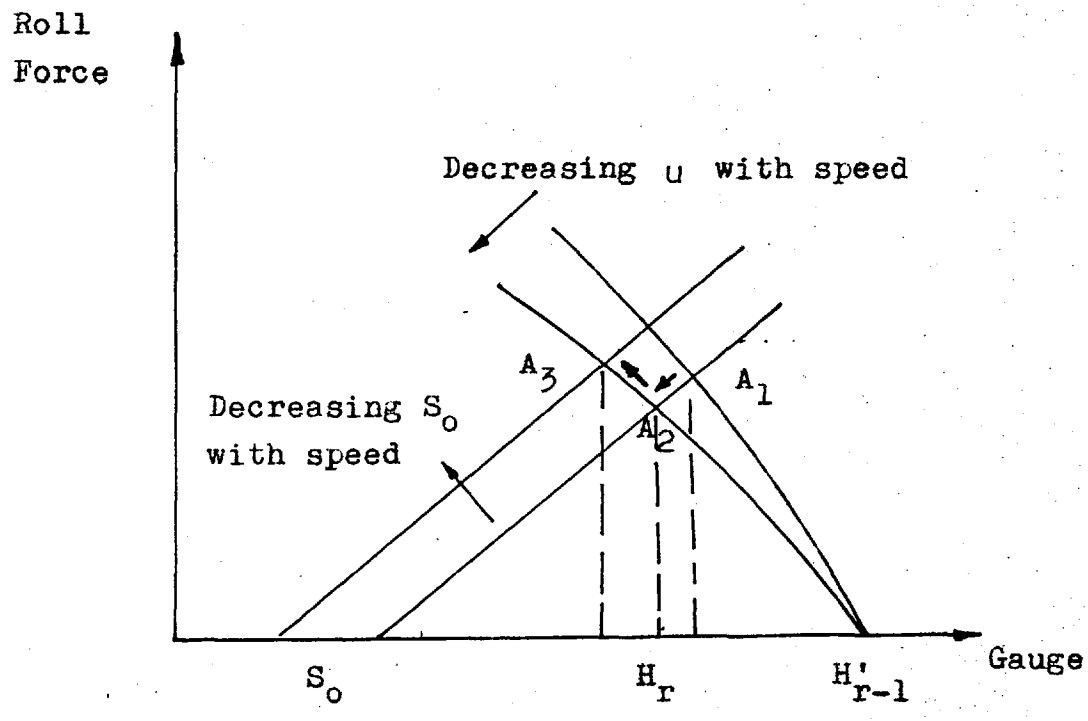

Fig. 2.6 Illustration of Speed Effects.

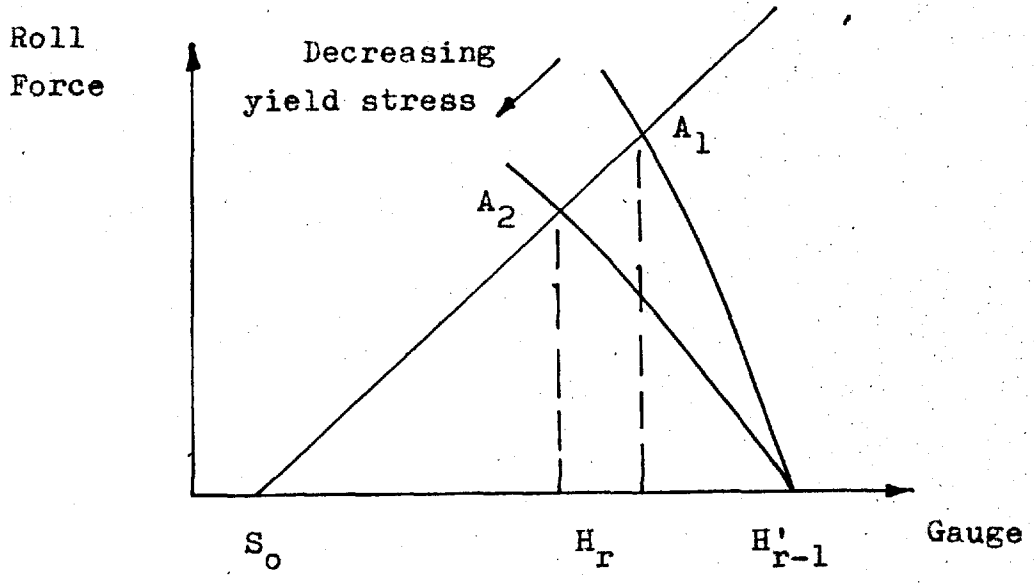

Fig. 2.7 Effect of Changing Yield Stress on Gauge.

Where ΔS_{or} is the roll neck bearing oil film thickness change. Roll movements are considered positive when tending to increase the roll gap.

2.5.4. Control Modes

The effect of some common disturbances on gauge is illustrated in Figs. 2.6 to 2.9. In each case a shift in the state point has changed the output gauge.

A method of correcting the effects of a perturbation by adjusting the roll gap is illustrated in Fig. 2.8. An increase in incoming gauge has caused the state point to shift from A1 to A2. To bring the output back to the desired value, the roll gap opening is decreased to point 2, causing the state point to shift to A3, thus correcting the output gauge (12).

In Fig. 2.9 the correction for an increase in incoming gauge is obtained by increasing the tension applied to the strip. The increased tension, acting in accordance with the roll force equation A.16, reduces the roll force required to produce a given output gauge. The state point, having been shifted to A2, can thus be brought back to A1 which gives the correct output gauge (16).

Figs. 2.8 and 2.9 thus indicate two modes of automatic gauge control. They are the basis of most

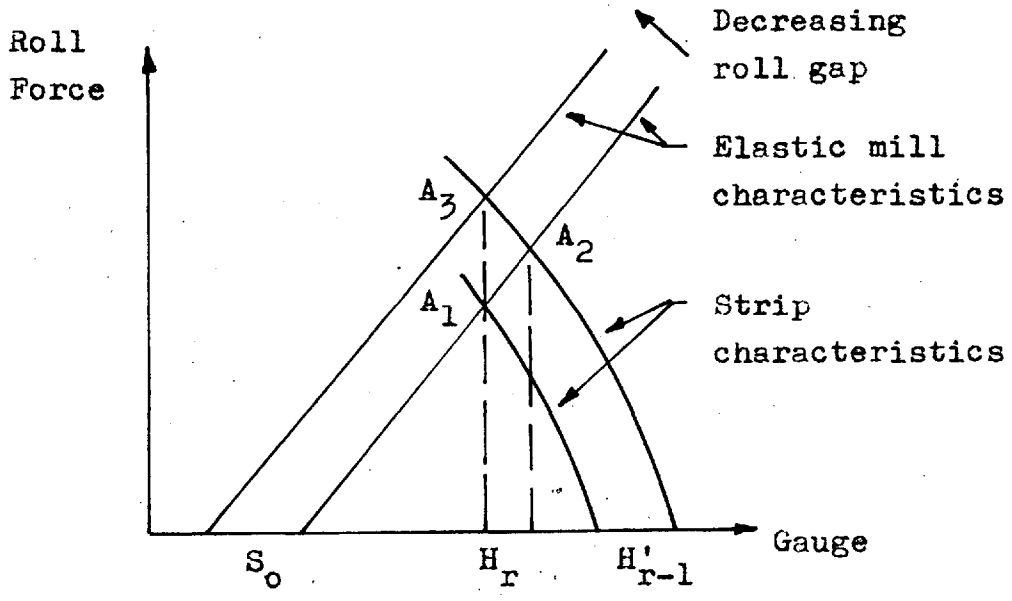

Fig. 2.8 Controlling Gauge by Roll Gap Setting.

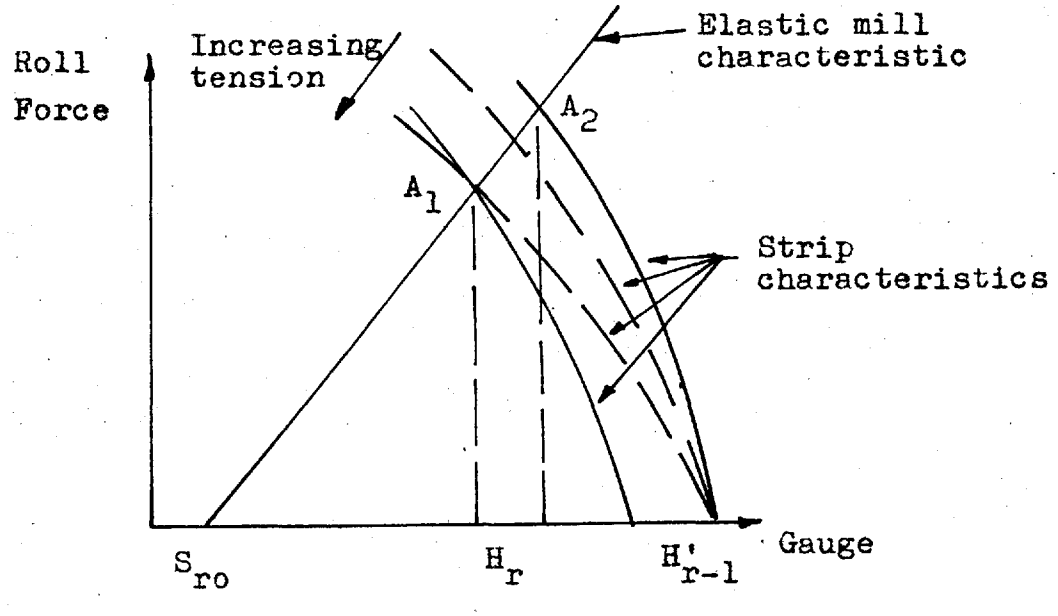

Fig. 2.9. Controlling Gauge by Tension Adjustments.

cold rolling mill control systems. Usually the tensions are adjusted for rapid control of gauge and the roll gap setting for coarse, or long term control. This is due to the drive motors being able to vary the tensions more rapidly than the screw down motor can vary the roll gap setting. Controlling gauge by varying the roll gap setting is usually undertaken in the earlier stands before the strip has been work hardened. Although with the introduction of digital computers for mill control there is usually facilities available for the control of the roll gap of each stand (11).

3 AUTOMATIC CONTROL THEORY

3.1. OPEN LOOP CONTROL

An open-loop control system is illustrated in Fig. 3.1. In this system the thickness of the outgoing gauge is proportional to the setting of the roll gap S_o. By adjusting the roll gap the desired output gauge may be obtained. If the strip deviates from the desired gauge a manually introduced signal would have to be supplied to the screwdown motors to reposition the rolls.

3.2. CLOSED-LOOP FEEDBACK CONTROL

Fig. 3.2. shows the system with closed-loop control. There is now a closed sequence of cause and effect; an unwanted variation in any quantity initiates actions which tend to reduce the initial variation. Thus, if the gauge were too heavy, a signal, proportional to the gauge, would be obtained from the x-ray gauge and it would differ from the signal corresponding to the desired gauge. A voltage or current signal proportional to, or some function of, this error would then actuate the motor to position the rolls so as to reduce the deviation until the error signal; Desired gauge - Actual gauge, is equal to zero.

The above discussion holds for slowly varying disturbances. For rapid variations the dynamic responses of the system elements become important, and tend to

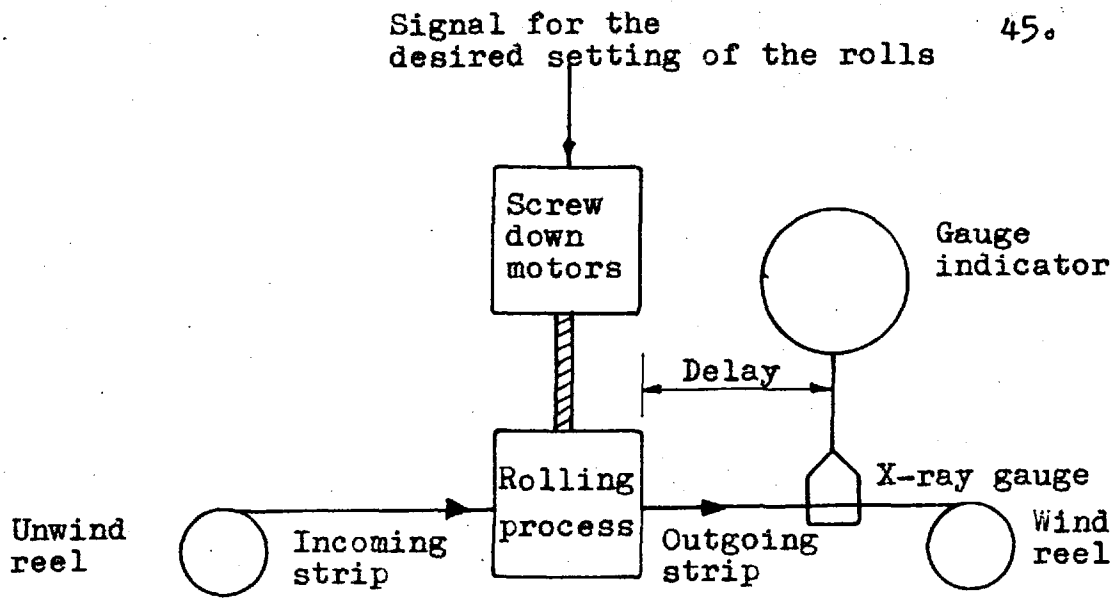

Fig. 3.1 Open-loop type of Gauge Control.

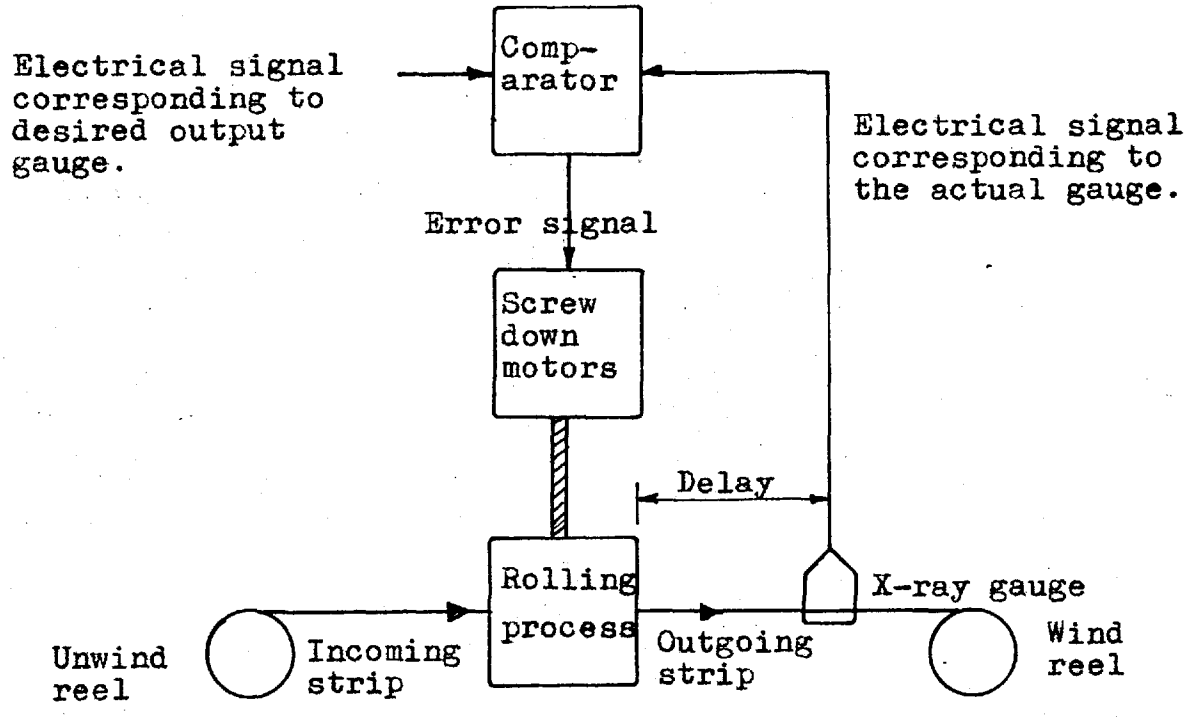

Fig. 3.2 Closed-loop Type of Gauge Control.

limit the behaviour of the system.

3.2.1. Dynamic Responses

In the mill a signal into the screwdown motors takes time to have effect as the motor must accelerate, position the rolls, and return to rest. Also, due to the inability to measure thickness in the roll gap, a delay occurrs until the corrected strip reaches the x-ray gauge and is measured.

The response of the system to a sudden desired change in thickness is important as it determines the transient response. The response of the system, and hence the change in thickness, must be such that the correction is obtained rapidly and without excessive oscillation. Such information is available from the transient response.

Also important is the response of the system to sinusoidal signals. It reveals how a poor system can oscillate continuously - be unstable - and so be useless as a control system. The reaction of control systems to sinusoidal inputs is termed their frequency response.

The strip entering a cold mill may have, among other deviations, a sinusoidal variation due to the eccentricity of the rolls in the hot rolling mill. The outgoing strip would then also have such variations, as would the error signal. The error signal would act to

reduce the error, but due to delays it would be lagging in phase.

3.2.2. Instability

Instability may be explained by considering what happens when a sinusoidal signal is applied to a component which cannot respond instantaneously; the response of the component is a sinusoidal waveform delayed in time relative to the input. There is a phase lag between the input and output. For several such components in cascade, the overall phase lag is the sum of the lags of the individual components. Should, at some particular frequency, the overall phase lag from output strip thickness; to measured gauge; to error signal; to roll gap adjustment S_o, be equal to 180 degrees, then the response of the feedback system would be such as to increase the original gauge error rather than decrease it.

Consider a gauge control system as in Fig. 3.2 acting at stand 1. Assume that the output gauge of stand 1 is varying sinusoidally with time - which can occur if the input gauge has a sinusoidal variation -

at a frequency which gives an overall phase lag of 180 degrees. If the corrective action under these conditions is too large, the system will continue to oscillate. This is illustrated in Fig. 3.3. At time t_0, the strip has the maximum positive deviation. Due to the delay until the deviation is recorded by the x-ray gauge the error does not reach the motor until time t_1; and the screws are not set until time t_2. However at time t_2, the output fluctuation is of the same phase as that initially assumed; the screws are thus merely following the contour of the strip, and may actually increase the deviation should the loop gain be greater than one.

The preceding discussion indicated how an unstable control system would oscillate continuously; if the gain of the system were higher the oscillations would tend to grow. The presence of inertia and time lags are the basic causes of instability. Considering the action of a control system in a more general manner; a signal demanding an action on the part of the control system causes the load to be driven, the kinetic energy of the moving parts causes an overshoot the magnitude of which depends on the damping in the system. There must be some damping in a satisfactory control system.

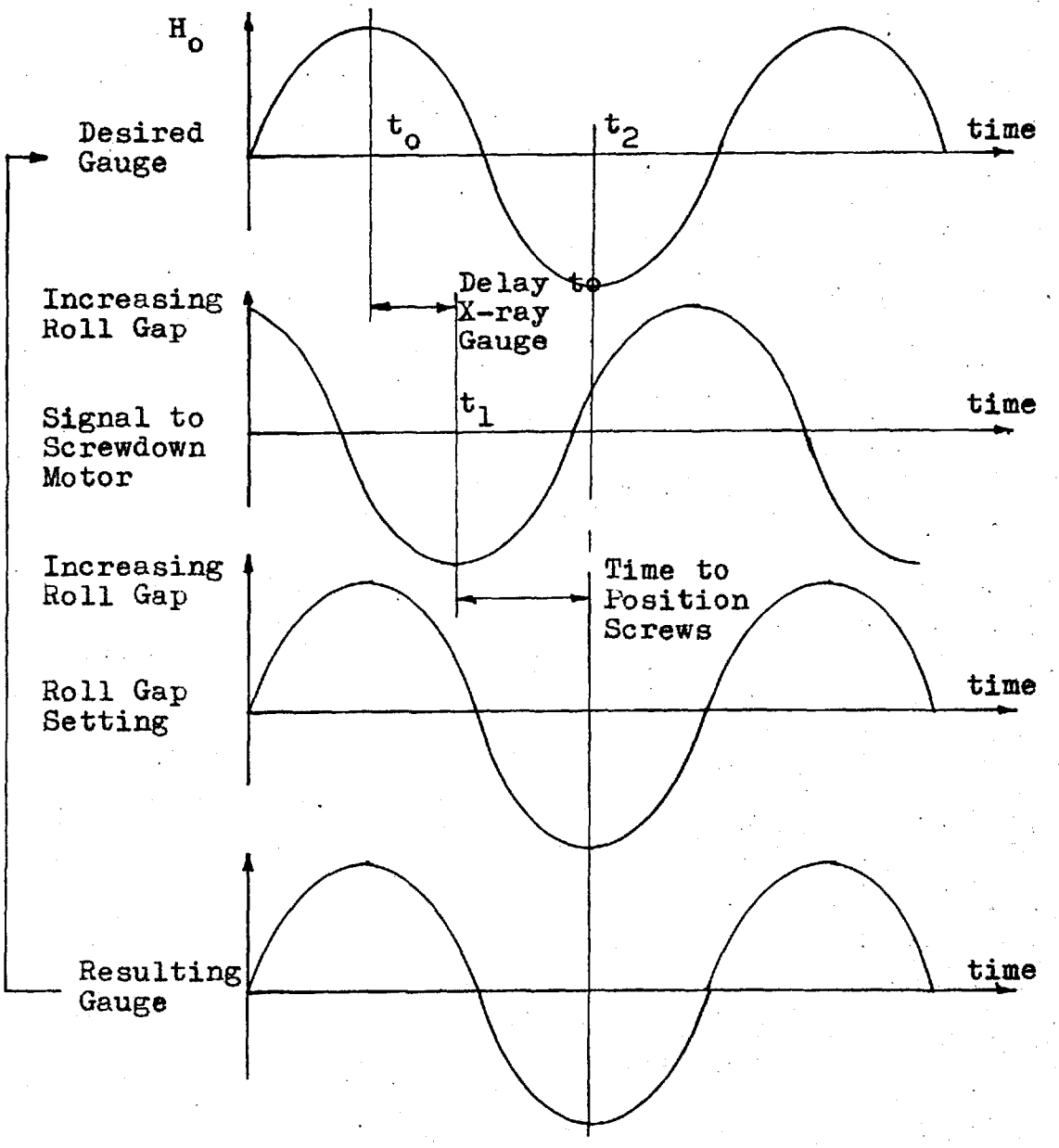

Fig. 3.3 Illustration of Oscillation Caused by Delays in the Control System of Fig. 3.2.

Instability may also be explained in terms of loop gain. As control systems are described by at least a second order differential equation, the classical solution of which indicates that the equation coefficients can be such that an oscillatory response will be obtained for a step input. As the equation coefficients correspond to the gains in the control loop an oscillation indicates that the gains are incorrect or too great.

In the majority of texts on control systems (39, 40, 41, 42) stability is analysed by specially adapted techniques such as the root-locus method which demonstrates the degree of stability by considering the roots of the complementary solution of the system differential equations. In general it may be said that if any derivative term is missing from the differential equation or if all the coefficients are not of the same sign the system will be unstable.

The above methods are more difficult to apply to complex systems such as the rolling mill in this instance. In such cases investigation by analogue computer simulation is both convenient and informative.

3.2.3. Requirements of Control Systems

In any automatic control system there are three basic requirements which must be met.

1) The variable which is to be controlled must be measured. This is usually done by a device called a transducer which converts the measurement into an easily handled voltage, current, hydraulic or pnuematic signal. The transducer accuracy is important as it limits the maximum accuracy that can be achieved with the control system.

2) The error that exists between the desired value and the existing value of the output must be determined. If the signals are in voltage form, the voltage from the transducer, which corresponds to the measured value of the output, must be compared and subtracted from the voltage corresponding to the desired value of the quantity being controlled.

3) The error must be used to control the output. The error signal, being of small power, is used to modulate or control a power source or primemover which supplies the power to adjust the output quantity. The term 'amplifier' is used to describe equipment which performs this function.

3.2.4. Basic Performance Considerations

Three important considerations in the design of control systems are noted below.

1) Steady-state error: when the system is disturbed or a new value of output demanded the system

will experience a transient period. After the transient has died out and the variables have reached new constant values, the error must be within tolerance. Increasing the system amplification - the gain - will reduce the steady-state error; too large an increase will cause instability.

2) Response time: to a sudden change in demanded output the system should respond as fast as possible. The new desired steady-state value must be reached as rapidly as possible without excessive overshoot or oscillation. If the input is sinusoidal or periodic the system must respond and reproduce the appropriate output without excessive error.

3) Stability: the system must be stable; that is, it must not oscillate.

3.3. EQUATIONS OF PHYSICAL SYSTEMS

Although the differential equation expressed in the classical form contains a systems dynamic characteristics, they are labourious to solve, particularly if of a higher order. Their solution can also obscure the fundamental relationships between the responses for various inputs. The Laplace transformation method (39, 40, 41, 42) tends to overcome these difficulties.

The Laplace transform of a differential equation is an algebraic equivalent from which the dynamic

characteristics may be computed. The transform can incorporate initial conditions, but for most control system analysis the mathematical treatment assumes the system is initially at rest. An outline of the Laplace transforms used in this study is given in Appendix B.1.

3.3.1. Transfer Function Analysis

If the transformed equation is manipulated so that the ratio of the output signal to the input signal is obtained, (magnitude and phase) the ratio is called the components transfer function. The transfer function form assumes the initial conditions to be zero. For a system which is initially at a steady-state operating condition, the response may be obtained by adding the initial value to the response for the case in which all the initial conditions are zero. The transfer function allows ready assessment of the effect of each component in the system, and it is independent of the input function it must operate on.

Techniques such as the frequency response and root locus methods (39, 40, 41, 42) allow the transfer function to be handled numerically or graphically. By determining the inverse Laplace transform; that is reverting back to the time domain which gives the solution of the differential equation, the transient response for various inputs may be found.

The analysis of a system respresented wholely or partly by transfer functions or differential equations may be performed on an electronic analogue computer as described below.

3.3.2. Analogue Computer Analysis

There are two methods in general use for analysing equations; of the type encountered in control system studies, on an analogue computer

One method, the differential analyser approach, analogues the entire system term by term. Using this method the correspondance between each computer element and the component it represents is lost.

Another approach, called the simulation method, is to obtain the equation of one or several components at a time and to analogue them. When all the components or equations have been analogued they are interconnected in the proper sequence. The simulation method is often used in control system analysis as it allows the study of each component, as well as the entire system. This is the method employed in this thesis to analyse gauge control systems. Using an analogue computer allows changes or adjustments of any of the system parameters to be easily made.

In many complex processes and control systems, an analogue computer study is the only feasible method of

analysis. For many systems, particularly in studying dynamic responses, it is faster and more flexible than a digital computer.

3.3.3. Block Diagrams

Block diagrams are useful in illustrating the order of events in control systems. The output quantity of each block is formed by the multiplication of the input to the block by the operating equation or transfer function in the block. Complex operations can be factored into simple operations, each one being represented by a separate block, and the complete operation can then be represented by a series of cascaded blocks. Since the effect of each block on its input can be easily assessed, insight into the operation of the system is facilitated.

In the case of the screwdown motor the error signal voltage is the input to the block representing the motor and the ouput is the screw rotation which sets the roll gap.

3.4. TYPES OF CONTROLLERS

There are a variety of manipulations that may be exerted on the signals in a control system in order to obtain the desired output response. This action may be exerted by a controller as indicated in Fig. 3.5 and is described in references (38, 39, 40, 44).

The rolling mill gauge control systems in chapter 8 were tested with proportional, integral and proportional plus integral controllers as required in the various control loops.

Using proportional control, the controller (~~Fig. 3.4~~) consists simply of an amplifier to increase the magnitude of the error signal before it reaches the motors. The transfer function is thus a pure gain, k, which is usually adjustable. Since the control action is proportional to error; for a small error there is a small control action. The control system thus tends to allow a steady-state error to exist. This error may be reduced by increasing the gain, but with increasing risk of instability. To eliminate it entirely additional control signals are required.

With integral control the controller transfer function is of the form c/p, where c is a constant and 1/p represents the integration. The error is thus integrated before it is applied to the motors. This eliminates the steady-state errors as the output of the controller will increase indefinitely with time for a constant error; thus to produce any finite motor signal, zero steady-state error is required. The amount of integral control must be consistent with system stability.

By applying proportional plus integral control, the advantage of the integral action are combined with the desired transient response of the proportional control which applies the error signal immediately to the motors without having to wait for the error to be integrated. The transfer function for this type of controller is $(k + c/p)$.

4. CONTROL EQUATIONS OF THE ROLLING PROCESS

4.1. LINEARISING THE ROLLING EQUATIONS

Due to the non-linear nature of the equations describing the rolling process - Appendix A - it is difficult to develop equations that will account for the dynamic behaviour of the mill. This can be overcome by linearising the rolling equations about a selected operating point. The resulting equations then hold for small deviations about that operating point. This is satisfactory for a study of the process with a view to automatic gauge control as only small deviations are expected to be encountered.

The experience of mill operators and previous work (7, 10, 12, 17, 18) indicate that the roll force and roll torque for a mill stand may be expressed for a given operating point as:

$$P_r = \text{function } (H'_{r-1}, H_r, \sigma_{r-1}, \sigma_r) \qquad 4.1$$

$$G_r = \text{function } (H'_{r-1}, H_r, \sigma_{r-1}, \sigma_r) \qquad 4.2$$

As equations A.16 and A.17 indicate, P and G are also functions of the coefficient of friction; and in section 2.5.5 the coefficient of friction is described as being

a function of strip velocity. Thus, equations 4.1 and 4.2 hold at a selected mill velocity, which determines a particular value of u.

4.1.1. Roll Force and Roll Torque Control Equations

By applying partial differentiation to the equations 4.1 and 4.2, they have been expressed for small changes in the variables as shown below (7, 10, 12, 17, 18, 20). The general notation illustrated in Fig. 2.2 is used.

$$\delta P_r = \frac{\partial P_r}{\partial H'_{r-1}} \delta H'_{r-1} + \frac{\partial P_r}{\partial H_r} \delta H_r + \frac{\partial P_r}{\partial \sigma_{r-1}} \delta \sigma_{r-1} + \frac{\partial P_r}{\partial \sigma_r} \delta \sigma_r \qquad 4.3$$

$$\text{or } \delta P_r = p_{1r}\delta H'_{r-1} + p_{2r}\delta H_r + p_{3r}\delta \sigma_{r-1} + p_{4r}\delta \sigma_r \qquad 4.3$$

$$\delta G_r = \frac{\partial G_r}{\partial H'_{r-1}} \delta H'_{r-1} + \frac{\partial G_r}{\partial H_r} \delta H_r + \frac{\partial G_r}{\partial \sigma_{r-1}} \delta \sigma_{r-1} + \frac{\partial G_r}{\partial \sigma_r} \delta \sigma_r \qquad 4.4$$

$$\text{or } \delta G_r = g_{1r}\delta H'_{r-1} + g_{2r}\delta H_r + g_{3r}\delta \sigma_{r-1} + g_{4r}\delta \sigma_r \qquad 4.4$$

The method of calculation of the coefficients (8) is described below using stand 2 roll force as an example. The control equation is:

$$\delta P_2 = \frac{\partial P_2}{\partial H'_1} \delta H'_1 + \frac{\partial P_2}{\partial H_2} \delta H_2 + \frac{\partial P_2}{\partial \sigma_1} \delta \sigma_1 + \frac{\partial P_2}{\partial \sigma_2} \delta \sigma_2$$

H_1', H_2, σ_1, and σ_2 are known scheduled quantities from Table 2.1. To evaluate the coefficient $\frac{\partial P_2}{\partial H_1'}$; the roll force was calculated for a small increment added to H_1', that is; $H_1' + \delta H_1'$; and again for a small increment subtracted from H_1', that is; $H_1' - \delta H_1'$. The remaining independent variables, H_2, σ_1, and σ_2 were held constant during the calculations.

Letting $H_1' + \delta H_1'$ equal $H_1'^+$ and the corresponding roll force equal P_2^+ and again letting $H_1' - \delta H_1'$ equal $H_1'^-$ and its corresponding roll force equal P_2^- we have:

$$P_{12} = \frac{\partial P_2}{\partial H_1'} \simeq \frac{P_2^+ - P_2^-}{H_1'^+ - H_1'^-} \qquad 4.5$$

This process is repeated for each independent variable and for each equation in the set described by equations 4.3, 4.4 and equation 4.15 which is discussed in section 4.2.1. The control equation coefficients were evaluated using a digital programme developed by the author and described in Chapter 5.

4.1.2. Constraint Equations

As there is no storage or depletion of strip as it passes through the mill the mass flow through the mill must be constant at all points. Since the width of

the strip throughout the mill is constant the continuity equation may be expressed as (7, 18):

$$V'_{r-1}H'_{r-1} = V_rH_r = V'_rH'_r = \ldots . \qquad 4.6$$

In incremental form it becomes:

$$V'_{r-1}\delta H'_{r-1} + H_{r-1}\delta V'_{r-1} = V_r\delta H_r + H_r\delta V_r = \ldots 4.7$$

The stands are effectively connected by the tension existing in the interstand strip. Disturbances at a stand may cause a change in interstand tensions and so transmit a disturbance to the neighbouring stands. The following equation (7, 10 , 19, 29) has been used to describe the interstand tensions. In incremental form:

$$\delta T_r = \frac{A_rE}{L_r}\int(\delta V'_r - \delta V_r)dt$$

In terms of tension stress it becomes:

$$\delta\sigma_r = \frac{E}{L_r}\int(\delta V'_r - \delta V_r)dt \qquad 4.8$$

The mass flow concept implies that when the speeds of the mill stands are fixed, the strip gauges are constrained to certain ratios, and the interstand tensions must go to the values necessary to maintain these ratios. However in practice it is necessary to keep the tension fluctuations within limits as too low a tension will cause cobbles and too high a tension may break the strip.

For convenience and to conserve equipment in the analogue computer simulation, equations 4.7 and 4.8 are combined to give equation 4.9. Using the relationship:

$$\frac{H_{r+1}}{H'_r} = \frac{V'_r}{V_{r+1}} \quad ; \quad \text{we get:}$$

$$\delta\sigma_r = \frac{E}{L}\int\left(\frac{V'_r}{V_{r+1}}\delta V_{r+1} + \frac{V'_r}{H_{r+1}}\delta H_{r+1} - \frac{V'_r}{H'_r}\delta H'_r - \delta V_r\right) dt \qquad 4.9$$

Since a change in thickness of the strip at one stand takes a finite time to reach the following stand there exists a 'transport delay', τ_r. The delay is equal to the time required for the strip to travel from one stand to the next. Thus:

$$\delta H'_r(t) = \delta H_r(t - \tau_r) \qquad 4.10$$

As in previous work (7, 10, 12, 17) the roll force control equation 4.3 is combined with the mill spring equation 2.5. In this case however the oil film thickness parameter is included to yield:

$$\delta H_r = \frac{1}{(M-p_{2r})}\left(p_{1r}\delta H'_{r-1} + M_r\delta S_{or} + M_r\Delta S_{or} + p_{3r}\delta\sigma_{r-1} + p_{4r}\delta\sigma_r\right) \qquad 4.11$$

This step eliminates the roll force from the simulation. Because of this the simulations of Chapter 7 were attempted without combining equations 4.3 and 2.5, but there was a tendency for the simulation in this form to be unstable. Hence equation 4.11 has been used.

4.2. INCLUDING SLIP AS A VARIABLE

As mentioned, previous analogue simulations of rolling mill control equations have generally assumed the slip (equation A.20) to be constant. That is, it does not change value should the mill experience any perturbations from its operating point.

The strip velocity leaving a mill stand is related to the peripheral velocity of the rolls by equation A.20, which for any stand is:

$$F_r = \frac{V_r - W_r R}{W_r R} \qquad 4.12$$

This is the definition of F; the slip.

The strip output velocity may be expressed from 4.12 as

$$V_r = W_r R(1 + F_r) \qquad 4.13$$

The incremental form; obtained by partial differentiation is (9, 10):

$$\delta V_r = R(F_r + 1)\delta W_r + W_r R \delta F_r \qquad 4.14$$

Assuming the slip constant would cause the second term on the right hand side to become zero.

By including slip as a variable the above assumption may be eliminated. The slip may be calculated from the expression; $\frac{R'\phi n^2}{H_r}$, equation A.20 in Appendix A. However as the formula for ϕn (equation A.15) is difficult to solve in the dynamic sense, it is necessary to linearise again. To do this the slip was expressed as:

$$F_r = f(H'_{r-1}, H_r, o'_{r-1}, \sigma_r) \qquad 4.15$$

This is the same form as the equations developed by others for roll force and roll torque. In differential form the slip control equation is:

$$\delta F_r = \frac{\partial F_r}{\partial H'_{r-1}} \delta H'_{r-1} + \frac{\partial F_r}{\partial H_r} \delta H_r + \frac{\partial F_r}{\partial \sigma'_{r-1}} \delta \sigma'_{r-1} + \frac{\partial F_r}{\partial \sigma_r} \delta \sigma_r \qquad 4.16$$

$$\text{or} \quad \delta F_r = f_{1r} \delta H'_{r-1} + f_{2r} \delta H_r + f_{3r} \delta \sigma'_{r-1} + f_{4r} \delta \sigma_r \qquad 4.16$$

The coefficients for equation 4.16 were evaluated in the same manner as those for roll force and torque, using equation A.20 for the repeated calculations of the slip, F. Their values, calculated with the digital computer are listed in Tables C.1 to C.6.

4.3. MOTOR TRANSFER FUNCTIONS

4.3.1. The Roll Drive Motors

A Ward-Leonard set drive may be characterised in incremental form by the equation:

$$\delta w_r = f_w(p) \delta W_{Dr} - f_G(p) D_r \delta G_r \qquad 4.17$$

The functions $f_w(p)$ and $f_G(p)$ represent the dynamics, in Laplace transfer form, associated with the response to demanded speed changes (δw_{Dr}), or load torque changes (δG_r) respectively.

At a particular speed setting the steady-state response to a load torque disturbance is:

$$\delta w_r = - D_r \delta G_r; \quad \text{which is equation 2.2.}$$

4.3.2. The Screwdown Motors

The transfer function for the screw down motors is the relationship between the signal for the demanded position and the actual position of the rolls; however, since a constant signal to the motors drives the screws at a constant velocity, the transfer function contains an integral term in order to yield the roll gap setting. In incremental form the transfer function becomes:

$$\delta S_r = \frac{f_s(p)}{p} \delta S_{Dr} \qquad 4.18$$

where $f_s(p)$ represents the remaining dynamics of the transfer function representing the screw down motors.

4.3.3. Wind Reel Motor

In order to maintain the strip tension between the last stand and the wind reel constant the speed and torque of the wind reel must be under a form of control. Torque changes result from changes in the strip tension and the speed must be adjusted to allow for the increasing diameter of the coil of strip as it is wound. The transfer function becomes in incremental form (Ref. Appendix A.5):

$$\delta V_R = f_\sigma(p) D_R \delta\sigma_4 + f_V(p) \delta V_{DR} \qquad 4.19$$

where D_R is a factor relating the effect of tension

changes on the strip velocity at the wind reel.

4.4. THE CONTROL EQUATIONS AS FUNCTIONS OF MILL SPEED

The equations 4.3 to 4.9 contain terms or coefficients which are functions of mill speed. The nature of the coefficients is determined in Chapter 5. To programme the equations on an analogue computer in a manner that will allow acceleration and deceleration phases of mill operation to be simulated will thus require varying the coefficients during a trial on the analogue computer. Sections 6.9 and 6.10 describe a method which achieves this, and Chapter 7 describes its application.

5. DIGITAL COMPUTER DETERMINATION OF CONTROL EQUATION COEFFICIENTS

5.1. INTRODUCTION

The determination of the coefficients in the control equations of Chapter 4 involves considerable computation. They have been calculated by hand (8) for the roll force and roll torque equations; using the plastic zone equations, the schedule of Table 2.1 and a value of $u = 0.07$ for all stands. Bryant and Butterfield (10) have reported a set of coefficients, for the roll force and roll torque equations, applicable to slightly differing control equations (Appendix C). They were obtained by applying statistical techniques to experimental data. However slip was not included as a variable in this work.

Since the speed differs for each stand, the coefficient of friction is different for each stand. To determine the correct value to use for the schedule selected it is necessary to do repeated calculations until a value of roll force is obtained to match an experimental value; or to solve the equations of Appendix A for u,using an experimental value of roll force. The former procedure was adopted as it suited the intention of calculating a series of stand roll forces, torques steps and coefficients for a range of u values

corresponding to a range of mill speeds.

5.2. PROGRAMME DESCRIPTION

Two final programmes were developed; one which used the plastic zone equations only, and another which included the effects of the entry and exit elastic zones. A third programme was developed in the latter stages which performed the trial and error process, necessary to find roll force, to a particular error of convergence. It ran satisfactorily with a trial set of data; the results of which indicated that the other two programmes, which repeated the trial and error process a fixed number of times, were converging to at least 0.05%. Although the equations being solved are accurate to several% (5), a precise answer is required as it is necessary to subtract quantities of comparable size (equation 4.5) to obtain the control equation coefficients.

Each of the two final programmes included the print-out of roll force, torque, slips, coefficients and equivalent BISRA coefficients (Appendix C.2).

Fig. 5.2 is the flow diagram for a complete programme. The data required for the 4 mill stands is termed one set. Each set is similar except for a different value of u. The thirteen sets of data are for the following values of u

Data Index			Variable Index			
A1	H_f	inches	B0	H_i/H_f	G^o	$(s\phi)^o$
A2	H_i	inches	B1	H_o/H_f	to	to
A3	H_o	inches	B2	$H_{0.6}/H_f$	G^{18}	$(s\phi)^{18}$
A4		tons/inch^2	B3	k_i	H2	
A5		tons/inch^2	B4	k_o	H5	P_{eo}
A6	R	inches	B5	$k_{0.6}$	H7	
A7	u	-	B6	δ	H9	P_{ei}
A8	k_i	tons/inch^2	B7	$\sqrt{R\delta}$	H10	G_{ei}
A9	k_o	tons/inch^2	B8	Approx.P	H11	δ_2
A10	c	inch^2/ton	B10	R'	H12	δ_t
A11	P	tons/inch	B11	ϕ_1	H16	R'
A12	b	inches	B20	ϕ_n	H17	G
A13	w	RPM	B30	P_p	H18	F
A14	γ	-	B33	G_p	U12	$b\partial P/\partial H_i$
A15	E	tons/inch^2	C0	ϕ^o	U13	$b\partial G/\partial H_i$
A16	-		to	to	U14	$\partial F/\partial H_i$
A17	-		C18	ϕ^{18}	U23	$b\partial P/\partial H_o$
A18	A	tons/inch^2	D0	$\exp(uJ)^o$	U24	$b\partial G/\partial H_o$
A19	B	-	to	to	U25	$\partial F/\partial H_o$
A20	θ	-	D18	$\exp(uJ)^{18}$	U34	$b\partial P/\partial \sigma_i$
A21	A_i	inch^2	E0	S^o	U35	$b\partial G/\partial \sigma_i$
A22	A_o	inch^2	to	to	U36	$\partial F/\partial \sigma_i$
A23	M	tons/inch	E18	S^{18}	U45	$b\partial P/\partial \sigma_o$
A24	D	rad/sec/ton-inch	F0	k^o	U46	$b\partial G/\partial \sigma_o$
			to	to	U47	$\partial F/\partial \sigma_o$
			F18	k^{18}		

Fig. 5.1. Digital Programme Data and Variables.

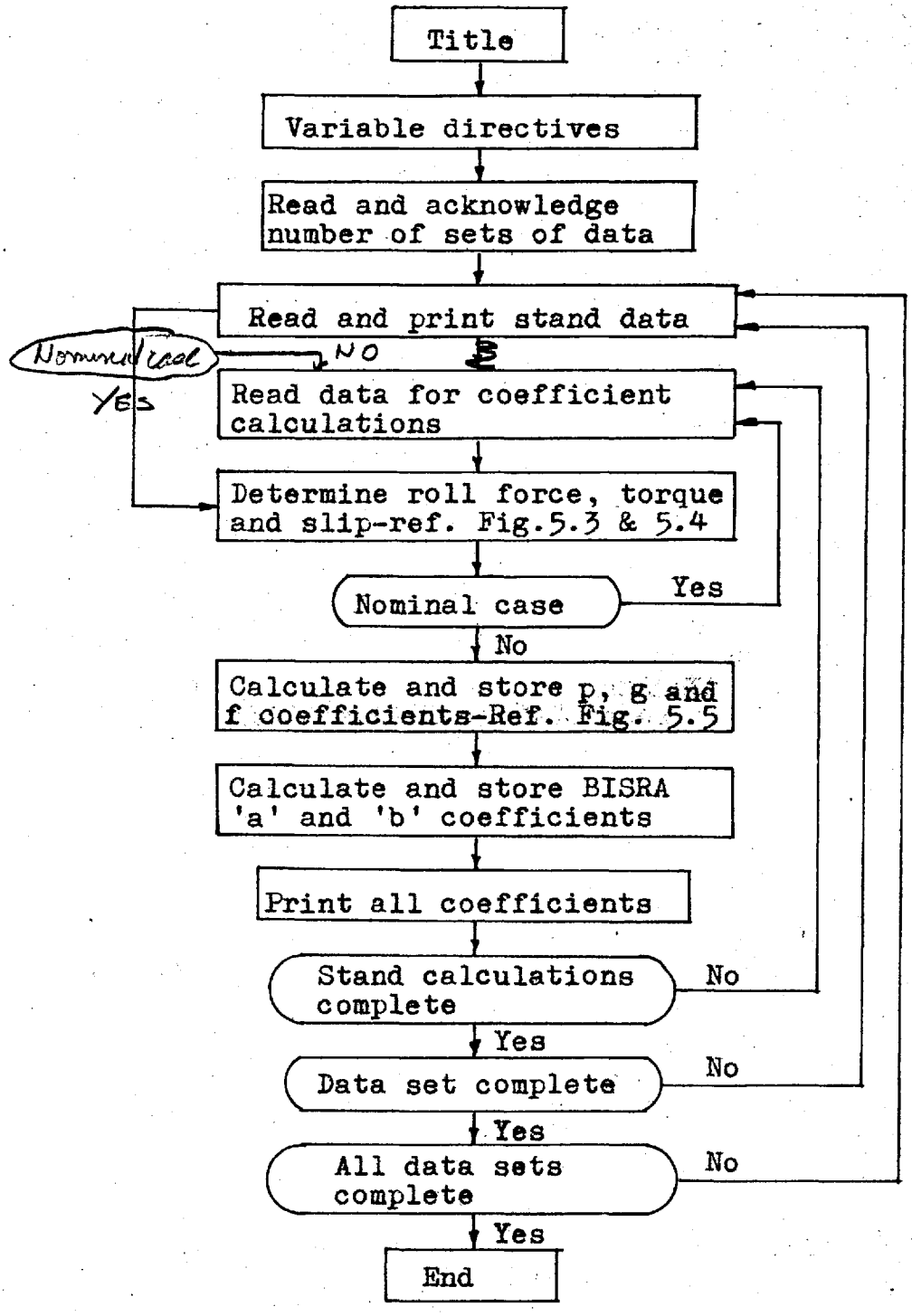

Fig. 5.2 Flow Diagram for the Calculation of the Control Equation Coefficients. Reference Appendix C for the Digital Computer Programme.

.01, .02, .03, .04, .05, .06, .07, .08, .09, .10, .11, .12, .15

The first 24 data are termed the nominal data (Fig.5.1); the remaining 8 data describe the incremental changes in H_i; H_o; σ_i; σ_o; respectively. After the computer has read the nominal data for one stand it prints the data then proceeds with the calculations as indicated in Fig. 5.2.

5.2.1. Calculation of Roll Force, Roll Torque and Slip in the Plastic Zone

Fig. 5.3 shows the flow diagram for the calculation of P_p. Using equation A.15 and A.18, a first approximation for R' is obtained. From equations A.1, A.10, A.13 and A.14 we obtain: ϕ_i, J_i, J_n and ϕ_n. To evaluate the integral for roll force (equation A.16) Simpsons Rule is used. The angle ϕ_n is divided into six increments and $(\phi_i - \phi_n)$ is divided into twelve increments. The value of vertical stress, s; and sϕ, is evaluated for every point using the relations A.9, A.1 and A.19. By summing according to Simpsons Rule the roll force is obtained. This cycle is repeated four times, to give the final value of P_p. At this stage the roll torque and slip are evaluated using equations A.17 and A.20 respectively.

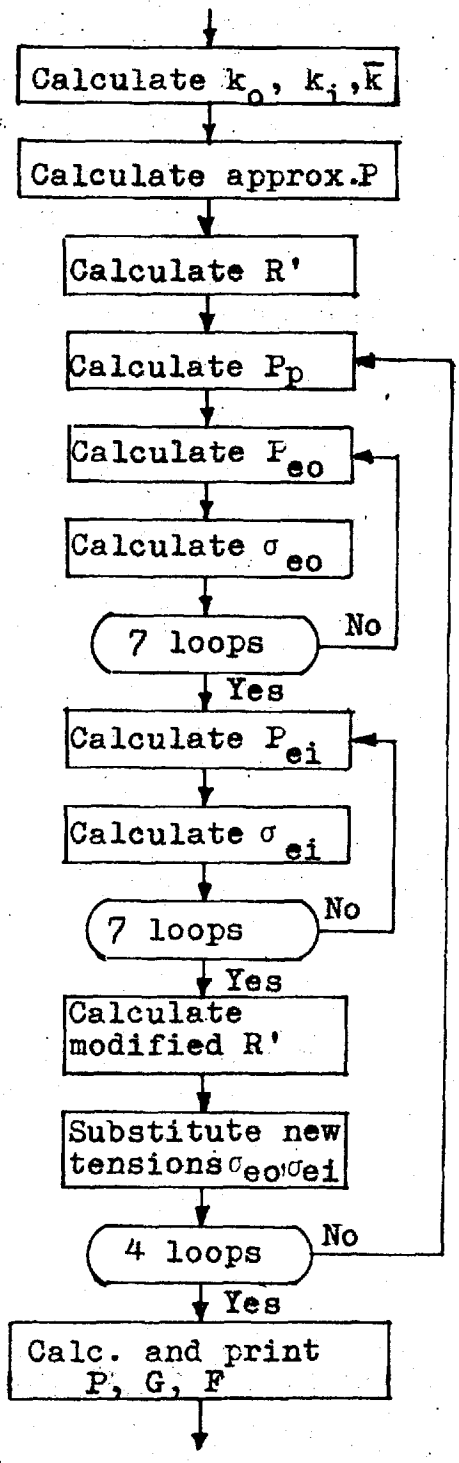

Fig. 5.4 Calculation of Roll Force, Torque and Slip Including the Elastic Zones

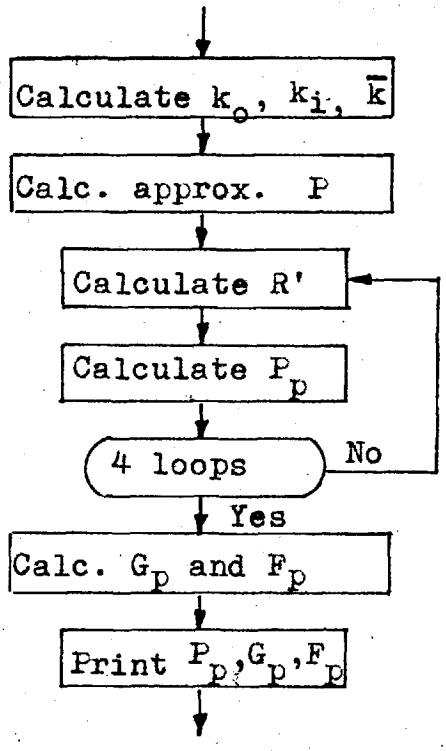

Fig. 5.3 Calculation of Roll Force, Torque and Slip for the Plastic Zone.

5.2.2. Calculation of Roll Force, Torque and Slip Including the Elastic Zones

The flow diagram of Fig. 5.4 shows the basis of the procedure used. Here P_p is calculated as above. Then using equations A.30 and A.28, the roll force for the exit elastic zone, P_{eo}, and the new tension stress, σ_{eo}, applied to the exit side of the plastic zone is found. This latter calculation is repeated seven times due to slow convergence.

The roll force on the input elastic zone, P_{ei}, and the new tension stress σ_{ei}, applied to the entry side of the plastic zone are then found in the same way; using equations A.32 and A.34.

Having found the roll forces for the three zones in the roll gap the modified radius of the circular arc of contact, R', is calculated from equations A.38 and A.35. With the new R' the calculation for P_p is repeated using the newly formed tension stresses σ_{eo} and σ_{ei} existing on the boundaries of the plastic zone.

As indicated in Fig. 5.4, the complete process is then repeated 4 times to converge to a value of P found to be converged to 0.05% (section 5.2). With the total roll force available the roll torque and slip can be calculated using equations A.36 and A.20.

5.2.3. Calculation of the Coefficients for the Control Equations

The coefficients in the equations of Chapter 4 were obtained using the plastic zone equations only, and again using the equations for the three zones. In each case the portion of the programme required to calculate the coefficients is identical. Both cases were done to afford a comparison.

After having obtained the roll force, roll torque and slip the computer proceeds to the part of the programme shown in the flow diagram of Fig. 5.5.

The Q counter controls the flow of events. The computer reads the value of H'^{-}_{r-1} from the data tape then calculates P^{-}, G^{-} and F^{-} which are defined in Chapter 4. It then reads H'^{+}_{r-1} and calculates P^{+}, G^{+} and F^{+}. By this method the values of the relevant coefficients p_{1r}, g_{1r} and f_{1r} are obtained.

Fig. 5.5 shows how this process is repeated for H_r, σ'_r and σ_r to obtain the complete complement of coefficients for the stand in question. Using the above coefficients, the programme then directs the computer to calculate the equivalent BISRA coefficients (Appendix C).

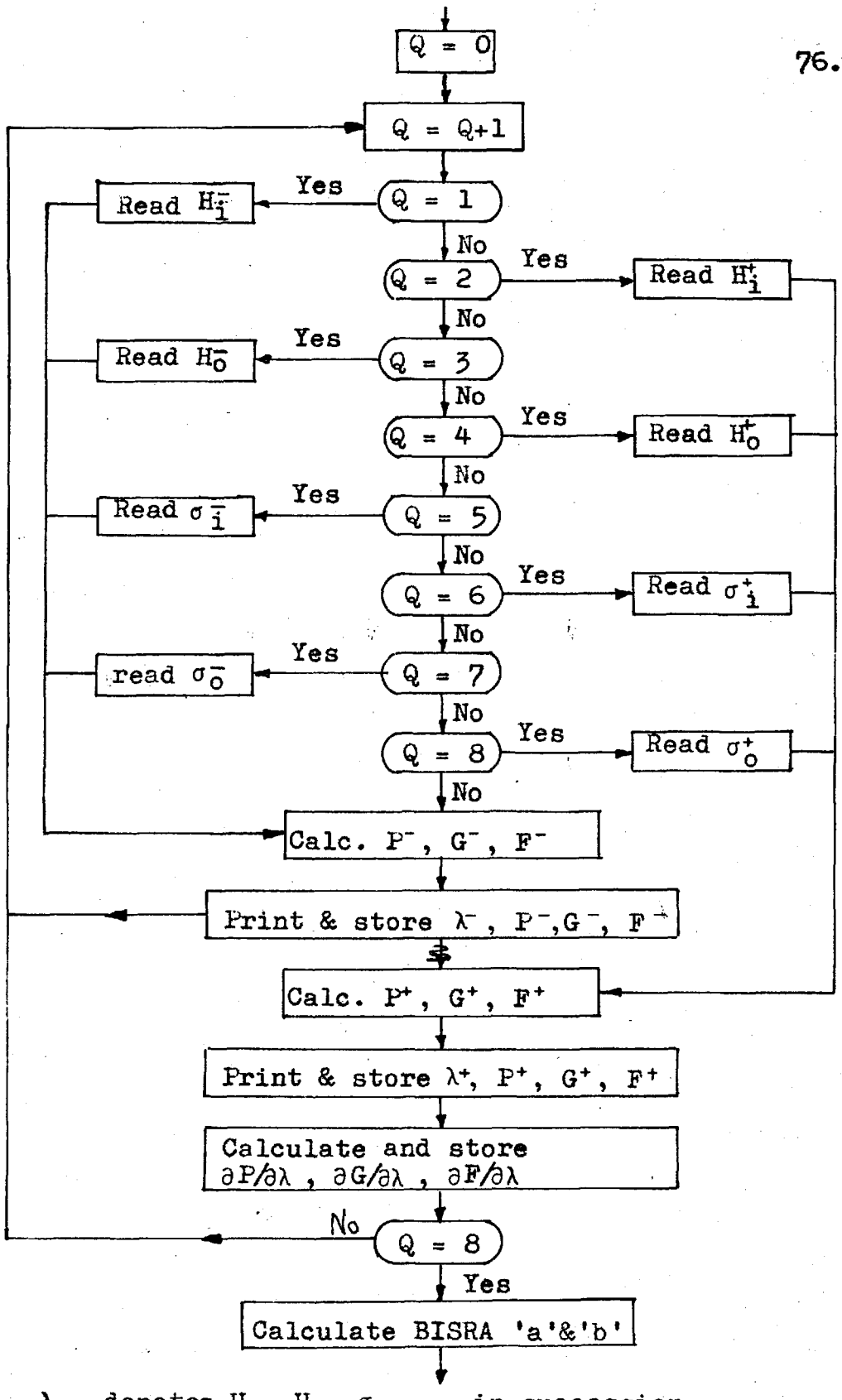

λ - denotes H_i, H_o, σ_i, σ_o in succession.

Fig. 5.5 Flow Diagram for the Calculation of the Coefficients.

5.3. RESULTS OF DIGITAL COMPUTER COMPUTATIONS

The main results obtained from the digital computer computations are tabulated in the Tables of Appendix C. From these, the coefficient values used in the analogue simulations (Chapter 7) were selected. Figs. 5.6 to 5.10; graphs of the results for stand 3 of the mill, illustrate the trend of the variations with the roll gap coefficient of friction.

5.3.1. Roll Force, Torque and Slip

Fig. 5.6 shows the increase in roll force, torque and slip with increasing u for the plastic zone and plastic plus elastic zone cases. The force and torque rise more steeply the higher u in accordance with the exponential term in equation A.8.

The exception to this as indicated in Table C.2 is the rolling torque for stands 1 and 4 when the elastic zones are included. At stand 1 the effects of taking the stand back tension as zero - which it is generally assumed to be in practice - results in the drive aiding front tension (equation A.17) and the aiding torque due to the exit elastic zone yielding a negative torque requirement. This becomes more negative as the roll gap friction is increased due to the increase in negative torque from the exit elastic zone. It is

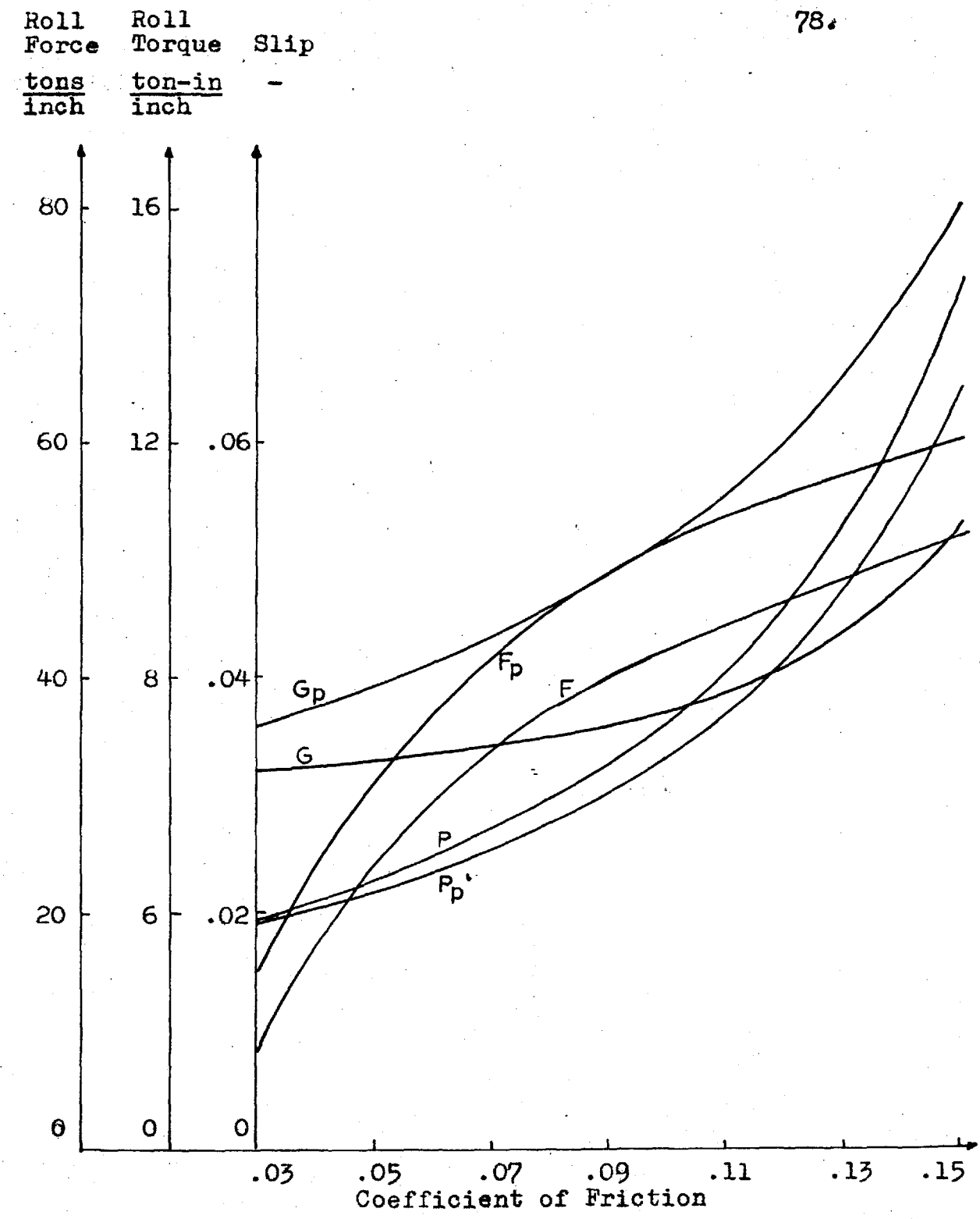

Fig. 5.6 Roll Force, Torque and Slip for Stand 3, with and without the Effects of the Elastic Zones Included, as a Function of the Coefficient of Friction.

probable that the theory used (6) is giving an excessive value for the torque due to the exit elastic zone.

The torque required at stand 4 is shown in Table C.2 to decrease rapidly with increasing roll gap friction. An analysis of the elastic zone loads indicated that this was due to the increase in exit elastic zone roll force giving an increase in negative torque.

In all cases calculated the exit elastic zone roll force was from twenty five to upwards of two hundred times larger than the entry elastic zone roll force.

Tables C.1 and C.2 indicate that for a given u the roll force is greater and the rolling torque and slip smaller for the case including the elastic zones. The roll force increases due to the added effect of the elastic zones. The roll torque decreases due to the negative torque of the exit elastic zone as discussed above. The slip (equation A.20) is reduced due to a reduction in R' - the circular arc of contact - and a relatively larger reduction in ϕ_n - the neutral angle - which being squared in the equation has the overriding effect in reducing the slip.

5.3.2. Control Equation Coefficients

The effect of varying u on the control equation coefficients is shown in Figs. 5.7 to 5.10 for stand 3.

The complete set of coefficients for the case including the elastic zones is in Appendix C. That the coefficients do vary with u is apparent; as is the fact that the variations are non-linear in nature.

The signs of the coefficients would appear to be correct as: 1) The p_{1r} and g_{1r} coefficients indicate that the roll force and roll torque increase with increasing incoming gauge. 2) The p_{2r} and g_{2r} values indicate that the roll force and roll torque decrease for increasing outgoing stand gauge. 3) The p_{3r} and g_{3r} indicate that the roll force decreases and roll torque increases for increasing strip back tension. 4) The p_{4r} and g_{4r} values indicate that the roll force and roll torque decrease for increasing strip front tension. The sign of the slip coefficients is not so apparent but can be traced through the changes in ϕ_n. 5) An increase in incoming gauge would increase the roll gap angle ϕ_i, and hence ϕ_n, and an increase in outgoing gauge would decrease the roll gap angle and ϕ_n. This would lead to a positive value of f_{1r} and a negative value of f_{2r} as shown. 6) If the strip back tension is increased the neutral point is shifted towards the exit side of the roll gap, thus giving a decrease of ϕ_n, and hence, a negative value of f_{3r} as shown. The reverse process

causes an increase in front tension to give a positive value of f_{4r} as indicated in the Tables of Appendix C. The tables show some deviations from the above for the slip coefficients and these are discussed below.

The computations were carried out for a range of u values from 0.01 to 0.15. However the results for u equal 0.01 and 0.02 were discarded; as in several coefficient calculations ϕ_n was negative, which is an impossible physical condition. The neutral angle can become zero when the strip is not passing through moving rolls; that is the rolls are moving faster than the strip throughout the roll gap, but a negative value would be meaningless. The intermediate results from the digital computer indicated that the scheduled tensions did not result, for these cases, in a neutral angle of sufficient magnitude to handle the incremental changes in the variables required to calculate the coefficients. In a physical situation this would probably mean that the tension schedule would be unsatisfactory for high speeds where such coefficients of friction would be encountered. Equation A.13 indicated that as u decreases there is an increasing tendency for J_n to go negative which would result in ϕ_n becoming negative - equation A.14. From equation A.13 it is apparent that J_n will tend to remain positive

if the front tension, σ_o is increased or if the back tension σ_i is decreased. Thus it appears that for the high speeds associated with the low values of u to be achieved the interstand tension settings must be properly selected. An interstand tension schedule could be checked by equation A.13.

Experimentally derived coefficients (9, 10) for the equations of Appendix C agree generally with the coefficients obtained in this study for these equations (Tables C.7 and C.8). However the assumption made in reference (9, 10) that p_{4r} is approximately equal to p_{3r} in determining the 'a' coefficients from experimental data would lead to some discrepancy as this assumption is not supported by the results obtained in this study with the digital computer. Further for a comparison to be made for the 'b' coefficients, the coefficients must be adjusted according to the motor droops existing or assumed for each analysis.

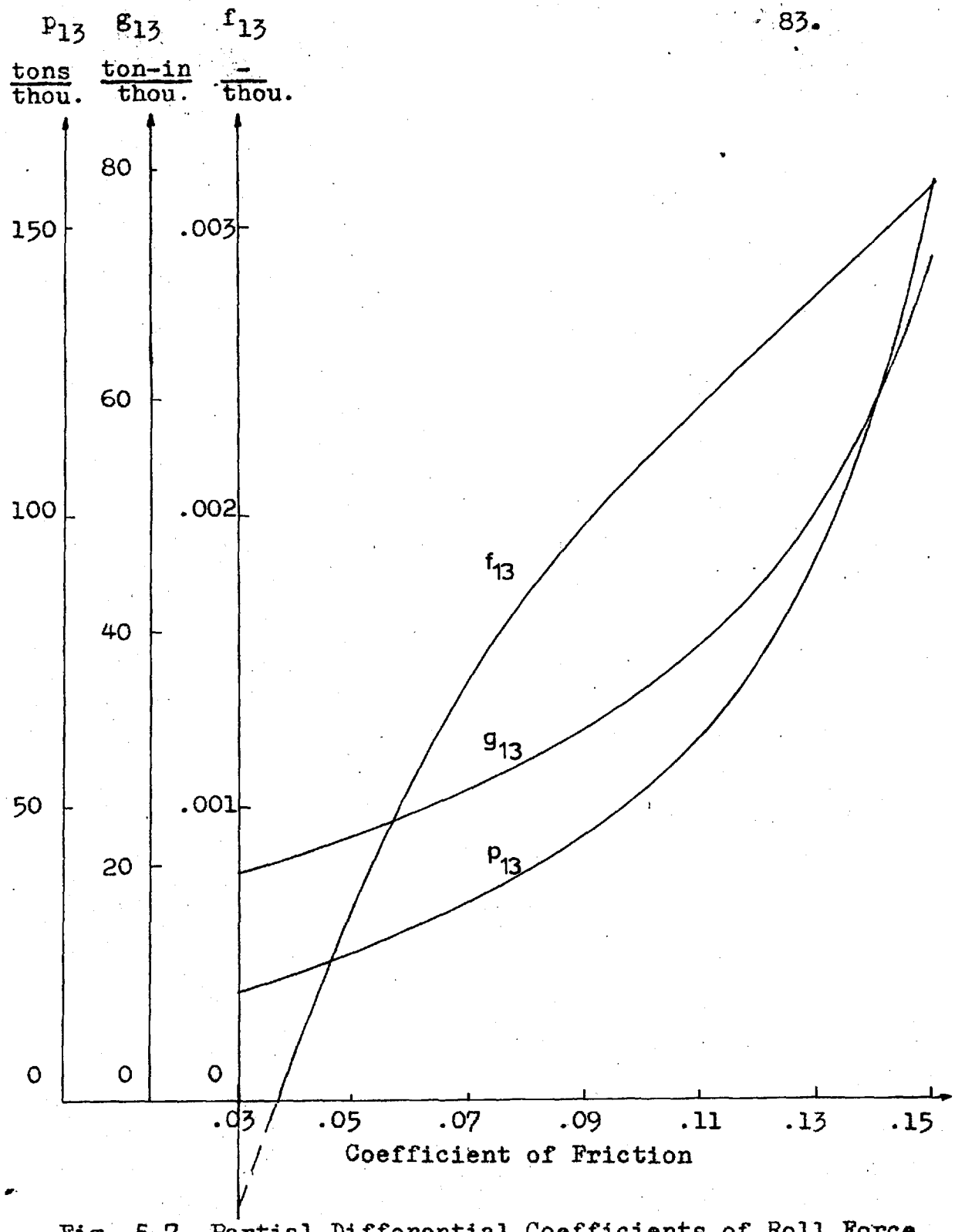

Fig. 5.7 Partial Differential Coefficients of Roll Force, Torque and Slip with respect to Incoming Strip Thickness for Stand 3; Including the Effects of The Elastic Zones, as a Function of the Coefficient of Friction.

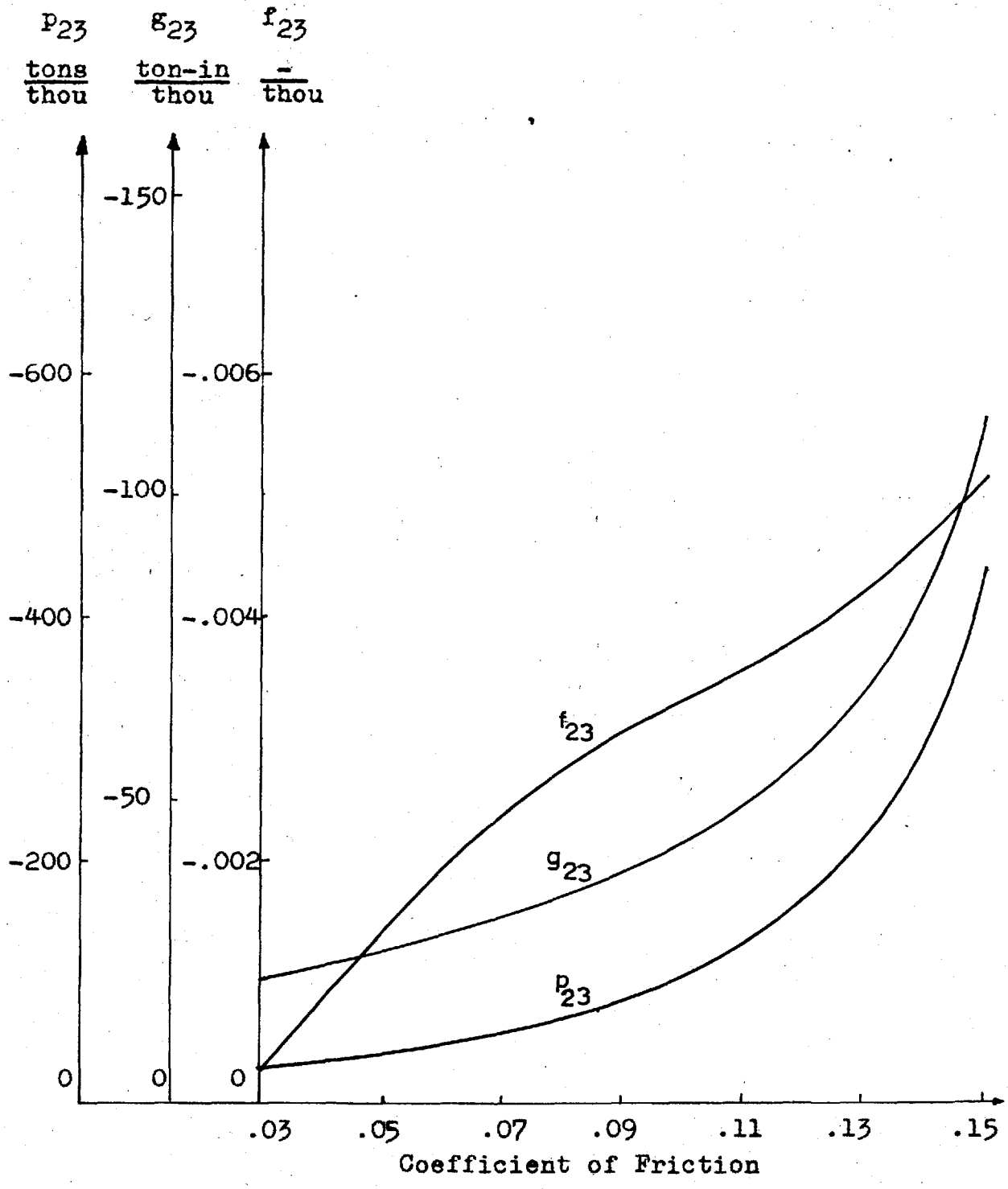

Fig. 5.8 Partial Differential Coefficients of Roll Force, Torque and Slip with respect to Outgoing Strip Thickness for Stand 3, Including the Effects of The Elastic Zones, as a Function of the Coefficient of Friction.

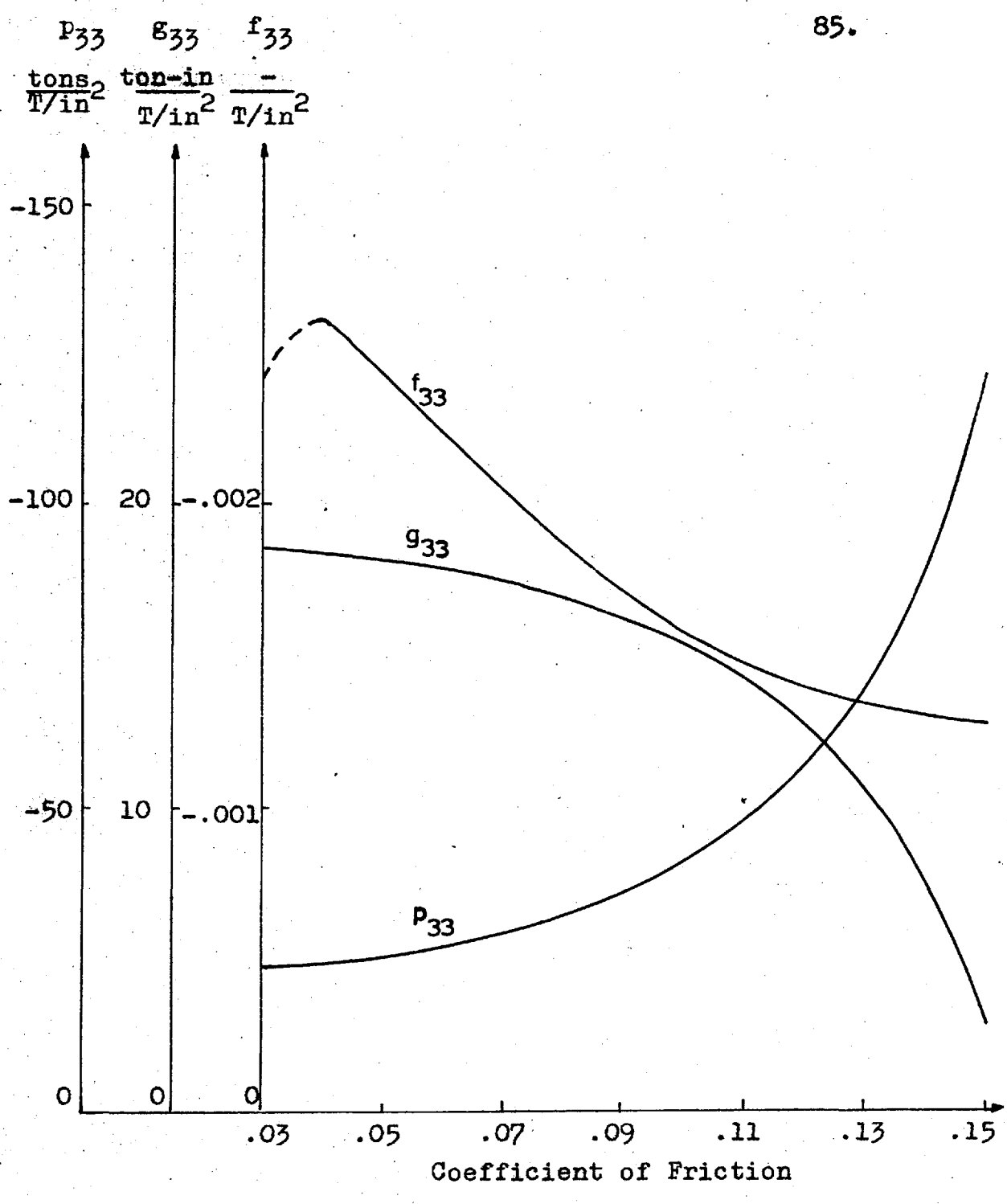

Fig. 5.9 Partial Differential Coefficients of Roll Force, Torque and Slip with respect to Back Tension Stress for Stand 3, Including the Effects of the Elastic Zones, as a Function of the Coefficient of Friction.

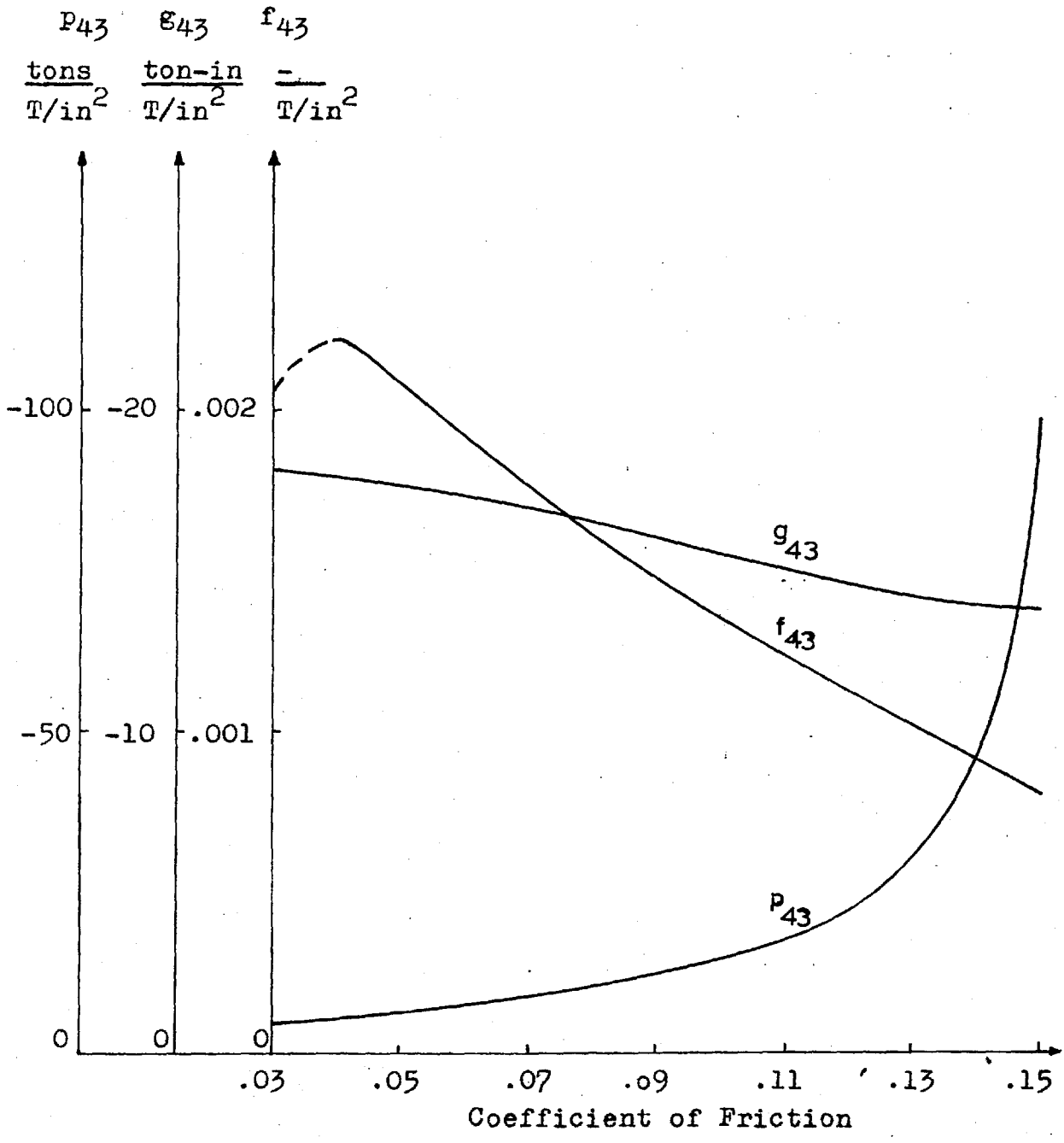

Fig. 5.10 Partial Differential Coefficients of Roll Force, Torque and Slip with respect to Front Tension Stress for Stand 3, Including the Effects of the Elastic Zones, as a Function of the Coefficient of Friction.

6. ELECTRONIC ANALOGUE COMPUTERS

6.1. INTRODUCTION

The electronic analogue computer, often referred to as an analogue computer, is a means of representing the variables of a problem by voltages or shaft rotations. The voltages or shaft rotations are called machine variables. References (46, 47, 48) describe analogue computers.

Using analogue computing elements, the machine variables are forced to obey mathematical relations analogous to those of the original problem. Records of these voltages and shaft rotations constitute solutions of the original problem.

6.1.1. Standard Components

The basic component is the very high gain feedback amplifier. When used in conjunction with resistors, capacitors and inductors the operations of addition, subtraction, multiplication, integration, and differentiation may be performed. Normally due to electrical noise problems differentiation is not used. Multiplication by a constant less than one is carried out with a potentiometer. By using diodes, resistors and amplifiers a function of a variable may be generated.

6.1.2. The General Purpose Analogue Computer

To facilitate efficient use of analogue computing equipment, the general purpose analogue computer has come into being. The various computing elements are mounted in readily accessible racks and all the connections are brought to a central terminal board at which the interconnections of components are made with plugs or plug-in wires. These boards are removable to allow 'patching' to be done while the computer is being used with another patched board.

On medium and large size analogue computers there is usually a digital voltmeter on which the output voltage of any component may be displayed in numerals through the use of a push-button address system.

The accuracy of an installation of any significant size is about 0.1% or less, with 0.01% capable of being attained with expensive equipment. This refers to the accuracy of an individual computing component. The overall accuracy of a problem solution will be correspondingly less depending on the size of the programme, although the decrease is minimised by the effects of the feedback loops inherent in any programme.

Given satisfactory amplifiers the accuracy is determined mainly by the matching of the computing resistors and capacitors, in this case better than 0.1%.

6.2. D.C. FEEDBACK AMPLIFIER

Fig. 6.1. shows the symbol for a high gain d.c. amplifier in which the gain is represented by α. When drawing the block diagram the earths are usually omitted as shown. The amplifier always reverses the sign of the input signal in order to provide negative feedback.

The amplifier is usually used in conjunction with an input impedance, Z_1; and a feedback impedance, Z_f. According to the type of impedance inserted, various operations may be performed. In this form the whole is referred to as an 'operational' amplifier.

The important characteristics of the d.c. amplifier are listed below; values of these parameters for the Imperial College, Mechanical Engineering Department's analogue computer are given.

1) Very high gain; 3×10^7.
2) Low grid current: Less than 5×10^{-11} amps.
3) Low drift: As an integrator with unity time constant 25 microvolts/sec. or 0.1% error in over an hour. As a summer with unity gain 0.001%.
4) Low noise level: 2 millivolts r.m.s.
5) Large bandwith: 20 kc
6) Low output impedance: 0.1 ohms.
   High input impedance assured by 2).

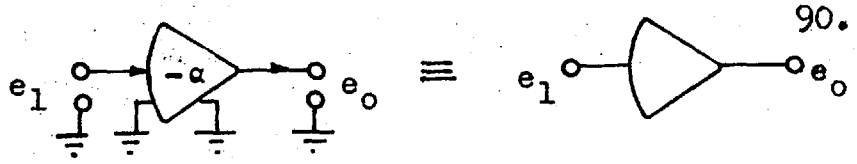

Fig. 6.1 High Gain Amplifier and its Equivalent Symbol.

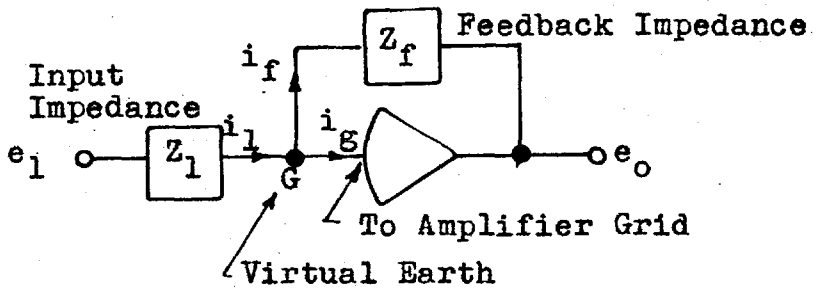

Fig. 6.2 General Operational Amplifier Configuration.

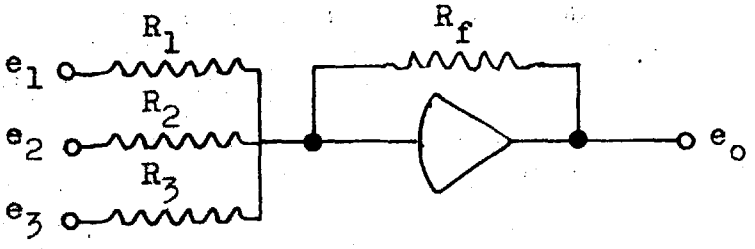

Fig. 6.3 A Summer with 3 Inputs.

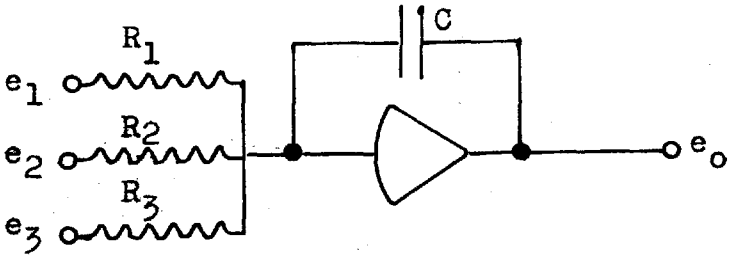

Fig. 6.4 An Integrator with 3 Inputs.

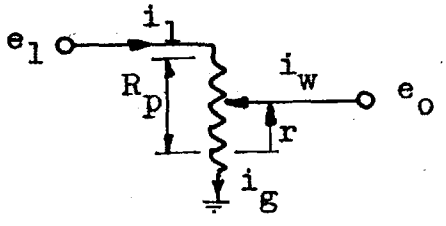

Fig. 6.5 A Potentiometer.

6.2.1. General Transfer Function

Fig. 6.2 shows the general operational amplifier configuration.

Applying Kichoff's current law to point G:

$$i_1 = i_f + i_g$$

Applying Ohm's law:

$$\frac{e_1 - e_g}{Z_1} = i_1$$

$$\frac{e_g - e_o}{Z_f} = i_f$$

The amplification is:

$$e_g = -\frac{1}{\alpha} e_o$$

From characteristic 2, the grid current is small therefore:

$$i_1 = i_f$$

and

$$\frac{e_1 - e_g}{Z_1} = \frac{e_g - e_o}{Z_f}$$

Using the amplification relationship gives:

$$\frac{e_i}{Z_1} + \frac{e_o}{\alpha Z_1} = -\frac{e_o}{\alpha Z_f} - \frac{e_o}{Z_f}$$

From characteristic 1; α is very large and we get:

$$\frac{e_o}{e_1} = -\frac{Z_f}{Z_1} \qquad 6.1$$

Equation 6.1 is the transfer function of the circuit of Fig. 6.2. For multiple inputs the equation would become:

$$e_o = -\left[\frac{Z_f}{Z_1} e_1 + \frac{Z_f}{Z_2} e_2 + \cdots\right] \qquad 6.2$$

The need for characteristics 1 and 2 is indicated in the preceding derivation. Characteristic 3 refers to the error in the amplifier output voltage that tends to accumulate with time. Low drift means that the amplifier will not require nulling for intervals of several days, and that during this time the drift will not be large enough to effect computation accuracy. Number 4 implies that there will be little electrical noise on the machine voltage signals. Number 5 determines the upper limits of the signal frequencies that can be handled by the amplifiers without amplitude attenuation or phase shift. Number 6 is a characteristic necessary to ensure that

circuits in cascade do not effect or 'load' each other. When the conditions of 6 are satisfied the amplifier effectively isolates the computer components by acting as buffers and ensures that each computer component enforces the proper relationship.

6.3. THE SUMMING AMPLIFIER

Recalling that the voltage drop across a resistor is; $e = Ri$, the impedance is then the resistance R. By changing the impedances in equations 6.1 and 6.2 to resistances a summing amplifier is obtained.

$$e_o = \frac{R_f}{R_1} e_1 \qquad 6.3.$$

For multiple inputs:

$$e_o = -\left[\frac{R_f}{R_1} e_1 + \frac{R_f}{R_2} e_2 + \ldots .\right] \qquad 6.4.$$

The inputs can be merely summed, or summed and multiplied by a constant depending on the values of the resistances used. Fig. 6.3 shows a summing amplifier with three inputs.

6.4. THE INTEGRATING AMPLIFIER

By replacing the feedback impedance by a capacitor and the input impedance by a resistor, an integrator is obtained. The voltage drop across a capacitor is:

$$e = \frac{q}{C} = \frac{1}{C}\int i\,dt$$

$$= \frac{1}{Cp} x\ i; \quad \text{in operational form.}$$

Thus the impedance is; $\frac{1}{Cp}$.

The transfer function of an integrator is then:

$$\frac{e_o}{e_1} = -\frac{1}{R_1 Cp} \qquad 6.5.$$

For multiple inputs:

$$e_o = -\left[\frac{1}{R_1 Cp} e_1 + \frac{1}{R_2 Cp} e_2 + \ldots\right] \qquad 6.6.$$

An integrating amplifier with three inputs is shown in Fig. 6.4.

From equation 6.6 it can be seen that each of the input machine variables is integrated as well as multiplied by the constant factor 1/RC. Measuring the resistance R, in megohms (M) and the capacitance in microfarads (UF) results in 'real' time units as:

$$1/RC = 1/M \times UF = \text{seconds}^{-1}$$

The values of R and C are selected to give the desired multiplying factor or 'gain' consistent with the time scale desired - section 6.7.1. - which in this study was

real time, that is the computer solutions occurred in the same time as they would have taken on the actual rolling mill.

If initial conditions are present they can be introduced into the output of the integrator before computation starts. In a general purpose analogue computer there is switching equipment - integrator resetter - that allows the capacitor in the feedback to be charged to a value equivalent to the initial condition and then switches the capacitor back to its normal computing connections when computation is to begin.

6.5. POTENTIOMETERS

Potentiometers multiply a voltage by a constant k; where, $0 \leq k \leq 1.0$.

Referring to Fig. 6.5 we have:

$$i_1 = i_g; \quad \text{as } i_w \text{ is negligible}$$

$$\frac{e_1 - e_o}{R_p - r} = \frac{e_o}{r}$$

Which gives:

$$\frac{e_o}{e_1} = \frac{r}{R_p} = k; \quad \text{the potentiometer setting} \qquad 6.7$$

The potentiometer transfer function, equation 6.7, holds when it is not 'loaded' by the following circuit. This is partly ensured by having a high resistance

following the potentiometer, which prevents a significant current from flowing in the wiper. The following resistance is usually the input resistance of an operational amplifier. Since this resistance cannot have an infinite impedance there is always some loading effect.

To overcome the loading effect, potentiometers are not set by their dials, but by applying a reference 100 volts to their inputs with the succeeding equipment connected to give the loading effect. The potentiometer is then adjusted while monitoring the wiper voltage on the voltmeter until it indicates the correct value; that is the desired k times 100 volts.

The potentiometers associated with the computers used have a resistance of 50 kΩ; a linearity of .25% (deviation from straight line relationship); and a resolution of ± 0.3% (steps due to the movement of the wiper over the wire element).

Operations	Computing Elements	Block Diagram Symbols	Machine Equations
Summation, multiplications by Constant coefficients (with sign change)	Summing Amplifier	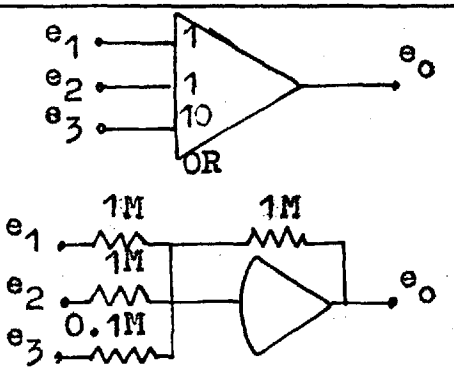	$e_o = -(e_1+e_2+10e_3)$
Summation, multiplication by constant coefficients (with sign change) and integration with respect to machine time from initial value $e_o]_o$	Summing Integrator	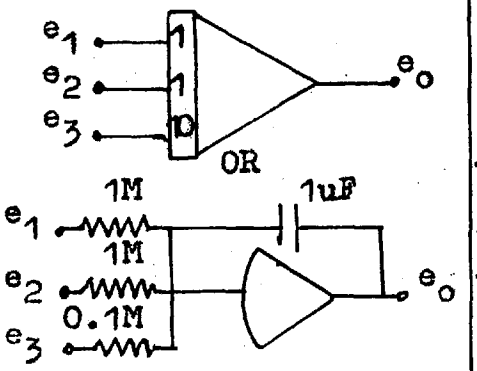	$e_o = -\int(e_1+e_2+10e_3)dt = -\frac{1}{p}(e_1+e_2+10e_3)$
Multiplication by constant coefficients	Potentiometer	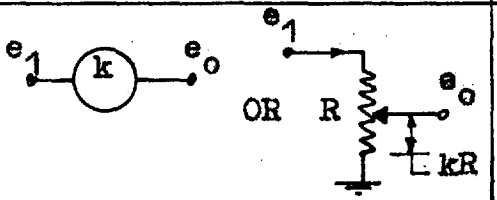	$e_o = ke_1$ $0 \le k \le 1$

Fig. 6.6 Computing Elements and Symbols

6.6 SERVOMULTIPLIERS

A servomultiplier capable of multiplying one variable by three others to form three products is shown in Fig. 6.7. The servo drive and feedback potentiometer form a position control system which is governed by the relations described in Chapter 3. A signal at e_1 causes the motor to position the shaft and feedback potentiometer wiper so that $e_1 = -e_f$.

Consider a fixed value of e_1 which positions the feedback potentiomer wiper, and hence the other potentiometer wipers which are fixed to the same shaft, to a value of k. At this point the shaft will stop rotating; as $e_1 + e_f$, which equals the voltage to the servo, will be zero. This gives:

$$e_f = -100k$$

$$-e_1 = -100k$$

$$\text{and} \quad k = e_{1/100} \qquad 6.8$$

$$\text{Also:} \quad e_5 = ke_2 = e_1e_{2/100}$$

$$e_6 = ke_3 = e_1e_{3/100} \qquad 6.9$$

$$e_7 = ke_4 = e_1e_{4/100}$$

For a continuously varying signal the shaft follows

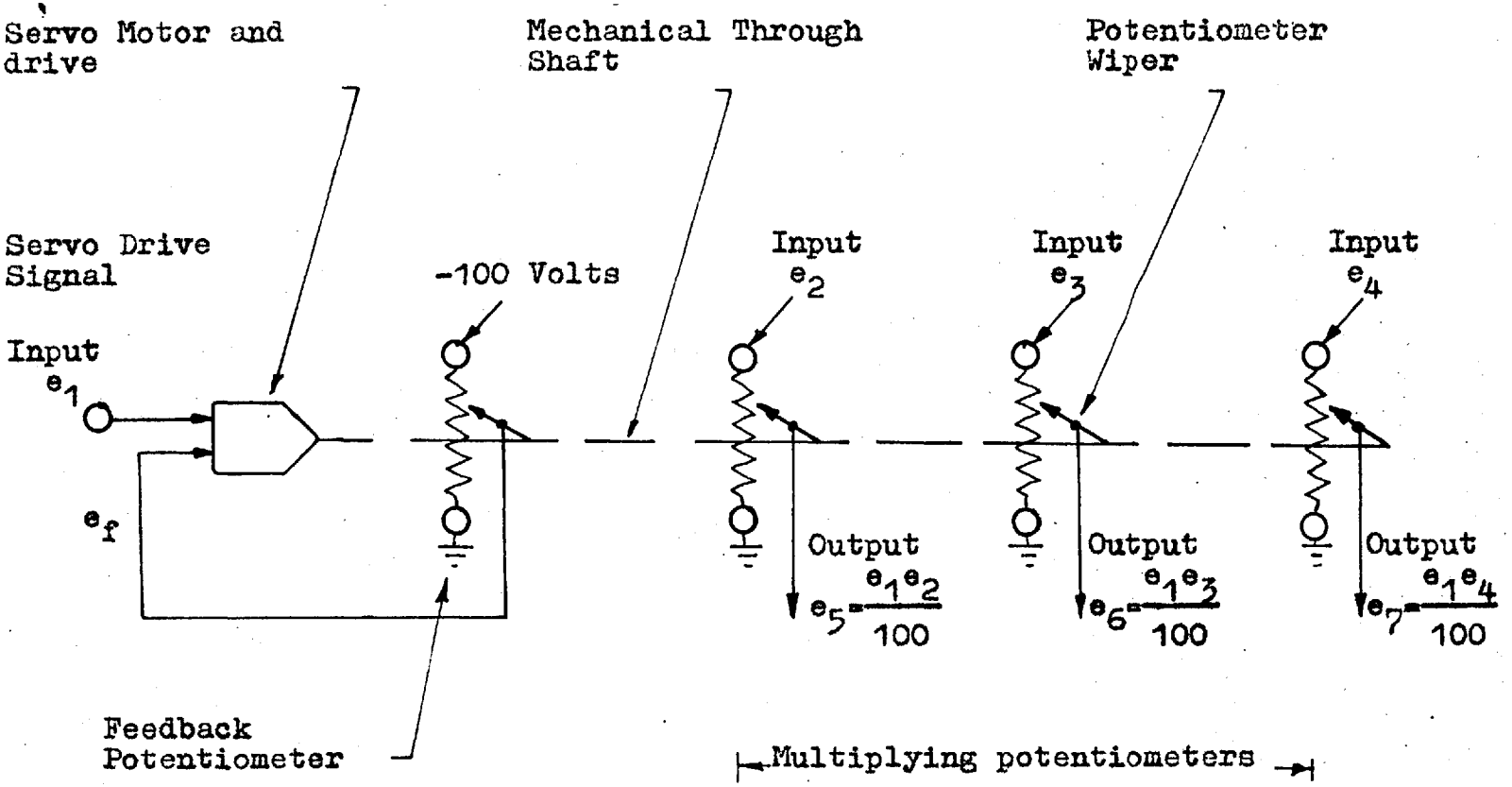

Fig. 6.7 Computing Servo Multiplier with 3 Ganged Multiplying Potentiometers

the input e_1, and yields continuously the desired products of equation 6.9.

6.7 PROGRAMMING PROCEDURE

An outline of the steps taken in obtaining a solution of a problem on an analogue computer is given in the following section. This procedure is applied, in Chapter 7, to the equations of Chapter 4.

6.7.1. Scaling

Having obtained the mathematical model (equations of original system) of the problem, the next step in an analogue computer solution is to transform the model into equations in which the variables are represented by the machine voltages.

The analogue representation may thus be considered a type of scale model, but with the scale factor varying for different parts of the analogue. This need for differing scale factors is due to the inherent limitation of the analogue computer voltages which, as mentioned, are usually limited to the range of $\pm$ 100 volts.

The problem must be amplitdue scaled and may also be time scaled. That is, the time scale of the computer may be speeded up or slowed down relative to the 'real time' of the original problem. The ability to change the time scale is very useful in studying rapidly varying phenomena.

The first step in amplitude scaling is to estimate, by approximate calculations, the maximum value of the problem variables.

Consider the equation:

$$\delta\sigma_1 = \frac{1}{p}(60.7\delta V_2 + 247\delta H_2 - 174\delta H_1 - 86\delta V_1) \qquad 6.10$$

This is the physical equation for the tension between stands one and two of the rolling mill. The coefficients are from Table 7.1.

By approximate calculations and previous work the maximum values for the equation 6.10 were estimated. They are shown in Table 6.2. The scale factor is then obtained by dividing this maximum expected value of the variable into 100 volts. This ensures that 100 volts will not be exceeded during computation. The amplitude scale factor can then be defined as:

$$k = \frac{\text{analogue computer voltage}}{\text{original system value}} = \frac{e}{x} \qquad 6.11$$

Where:

k is the scale factor.

x is the value of the physical system variable.

e is the corresponding analogue voltage.

For ease of handling the scale factors are usually rounded off to one significant digit.

The scale factors are now used to obtain the machine equation by substitution into the physical equation, the relations:

$$\delta\sigma_1 = e_o/k_o$$

$$\delta V_2 = e_1/k_1$$

$$\delta H_2 = e_2/k_2$$

$$\delta H_1' = e_3/k_3$$

$$\delta V_1' = e_4/k_4$$

This gives the equation:

$$\frac{e_o}{20} = \frac{1}{P}\left(\frac{60.7}{25}e_1 + \frac{247}{50}e_2 - \frac{174.5}{10}e_3 - \frac{86}{10}e_4\right) \qquad 6.12$$

$$e_o = \frac{1}{p}(48.56\, e_1 + 98.8\, e_2 - 349\, e_3 - 172\, e_4)$$

Equation 6.12 is the machine equation (Appendix D.1).

6.7.2. Analogue Computer Block Diagram

Using the symbols of Fig. 6.6, equation 6.12 may be represented as in Fig. 6.8, which also shows the values of the components required. The more convenient form of

Physical Variable	Maximum Value	Scale Factor	Machine Variable
δ_1	5 tons/in^2	k_o =20 volts/ton/in^2	$e_o = k_o\delta_o$
δV_2	4 in/sec	k_1 = 25 volts/in/sec	$e_1 = k_1\delta V_1$
δH_2	2 thou	k_2 = 50 volts/thou	$e_2 = k_2\delta H_2$
$\delta H_1'$	10 thou	k_3 = 10 volts/thou	$e_3 = k_3\delta H_1'$
δV_1	10 in/sec	k_4 = 10 volts/in/sec	$e_4 = k_4\delta V_1$

Table 6.1 Scale Factors for Equation 6.8.

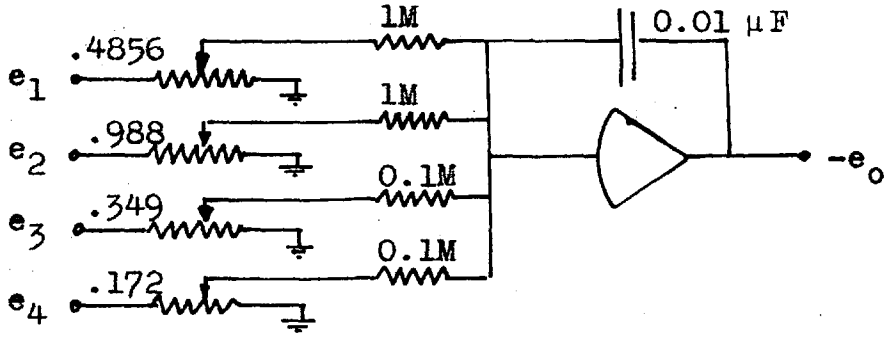

Fig. 6.8 Analogue Block Diagram of Equation 6.10.

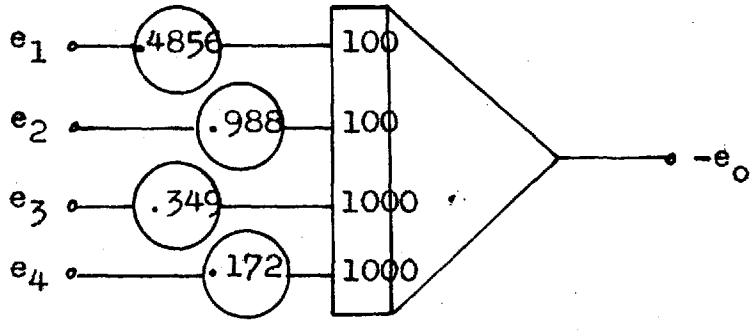

Fig. 6.9 Convenient Representation of Equation 6.10.

representation is shown in Fig. 6.9. Here the numbers in the circles represent the potentiometer settings and those in the integrator symbol represent the gains required (section 6.4.X.) that is; the 1/RC terms.

The outlined procedure is carried out for each equation in the original system. To aid this operation each equation should be manipulated into a form similar to that of equation 6.10. That is, with one variable on the left hand side of the equation - the output - which is equal to the expression of the right hand side, which in turn must be formed by performing the indicated operations on the variables - the inputs - contained in the expression. When this is completed each input variable required will be available as the output of another block. This holds except for the forcing functions or inputs to the system as a whole; such as the incoming thickness to stand 1 of the rolling mill. Aside from these system inputs the analogue block diagram will be composed completely of closed loops as in Fig. 7.2 Chapter 7.

In the above discussion the symbol e has been used to denote a machine variable as it aids the discussion. However, in an actual programme the same symbols may be used for the machine variables as for the physical variables. This system is used in Chapter 7 as the

machine equations and block diagrams become more meaningful.

6.7.3. Programming the Analogue Computer

The majority of the programming is done by making the connections on the patch board as indicated on the block diagram of the problem. The patch board is then placed on the computer forming the desired connections within the computer. The potentiometers are then set and any special functions set up.

The programming being completed, a useful check is to compare the steady-state analogue computer solution for a step input against a solution obtained manually or by trying the solution in the equations. This gives a steady-state check only but indicates whether the patching, scaling, potentiometer settings and computer operation are satisfactory.

6.8. CONTROL STATES

The general purpose analogue computer has a number of control states, selected by push buttons from a central control panel, to allow for the necessary operations during set-up and computation. These control states are listed and described below.

1) Balance State

In the balance state all inputs to the summers

and integrators are disconnected, allowing the amplifier outputs to be easily corrected for any drift. Connections or adjustments between components are usually made in this state as there is less danger of overloading the amplifiers.

2) Reset State

When the computer is switched to the reset state all integrator amplifier grids are disconnected from the input networks. Voltages corresponding to the initial values desired are simultaneously applied across the feedback capacitors of all integrators; then when the computer is put in the operate state the initial condition will exist at the output and normal integration can proceed.

The desired value of initial condition is obtained by passing an accurate 100 volt reference voltage through a potentiometer and setting the potentiometer while monitoring the voltage output on the voltmeter.

3) Hold State

If the computer is switched to the hold state during computation, the voltages existing in the computer will be 'frozen' at the values existing at that instant. All variables may thus be inspected at any time during a problem solution.

The hold state is accomplished by disconnecting the inputs to the integrators so that their output cannot vary. The computer may be kept in this mode .. until capacitor leakage results in inaccuracies.

4) Operate State

During operate all the connections shown on the completed block diagram are enforced. Thus the machine variables are forced to obey the mathematical relations of the original problem.

The operate state is the only one in which the inputs to the integrators are connected.

6.9. MODIFIED SERVOMULTIPLIER TO OBTAIN VARIABLE COEFFICIENTS

In the description of the servomultiplier given in section 6.6 it was shown that each of e_2, e_3, and e_4 are multiplied by the same factor k. However, to carry out the study of the rolling mill acceleration and deceleration phases it is necessary to multiply the mill variables by varying coefficients all having differing values. To do this it is necessary to multiply the variable applied to each servomultiplier potentiometer by a continuously varying factor which differs for each potentiometer.

To achieve this a scheme was developed whereby

resistors were placed in series ('padding') with each multiplying potentiometer to give the continuously varying value of k, the multiplying factor, desired for all positions of each potentiometer. Fig. 6.10 illustrates the scheme. The feedback potentiometer is not padded as it is desirable to utilise the full range of analogue computer voltage to achieve maximum accuracy. To pad the multiplying potentiometers to the values of k desired, a fixed resistor and a computing potentiometer is used on each side of a multiplying potentiometer.

The limits of the feedback potentiometer multiplying factor, when set up as shown, are $0 \leq k \leq 1.0$. However, with the padding resistors inserted, the multiplying factors for the other potentiometers have the new limits:

$$k_{2L} \leq k_2 \leq k_{2H}$$

$$k_{3L} \leq k_3 \leq k_{3H}$$

$$k_{4L} \leq k_4 \leq k_{4H}$$

Also when $k_1 = k_{1H} = 1.0$ we have:

$$k_{1H} \neq k_{2H} \neq k_{3H} \neq k_{4H}$$

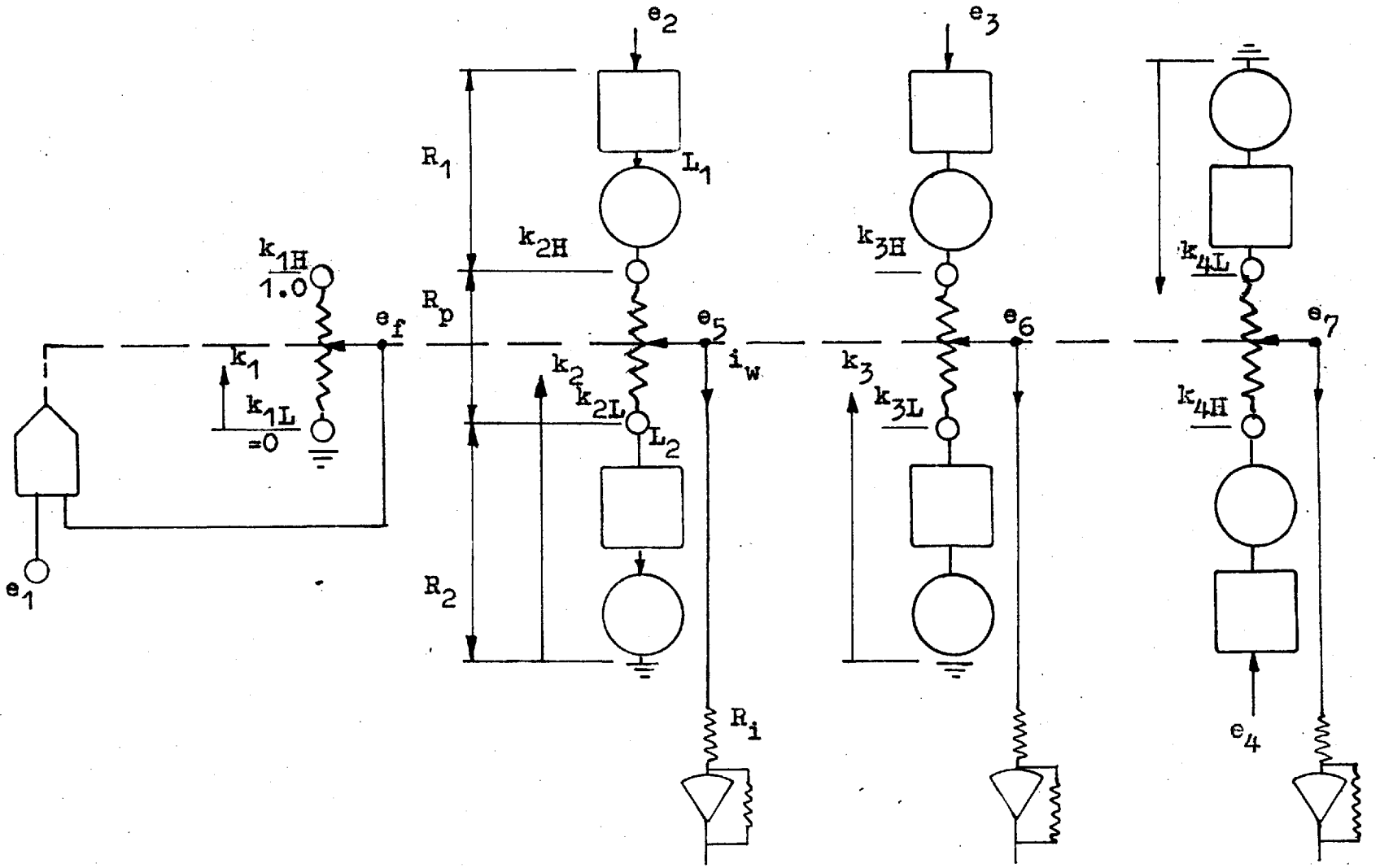

Fig. 6.10 Servo multiplier Modified to Give a Variable Coefficient at Each Potentiometer

and when $k_1 = k_{1L} = 0$ we have:

$$k_{1L} \neq k_{2L} \neq k_{3L} \neq k_{4L}$$

which is the situation desired.

It now remains to determine the values of the padding resistors to give the desired k values. If linear interpolation is used - the scheme is not limited to this case however - then it is required to find the values of the multiplying coefficients when $k_1 = 0$ and $k_1 = 1.0$.

From the chain in Fig. 6.10 with input e_2 and the wiper current i_w assumed to be negligible, we have:

$$i_1 = i_2$$

or $$\frac{e_2 - e_5}{R_1(1 - k_1)R_p} = \frac{e_5}{R_2 + k_1 R_p}$$

Solving for the ratio e_5/e_2; which is k_2, the multiplying factor of the padded potentiometer in question yields:

$$k_2 = \frac{e_5}{e_2} = \frac{R_2 + k_1 R_p}{R_1 + R_2 + R_p} \qquad 6.13$$

Knowing the values of k_2 desired when $k_1 = 0$ and $k_1 = 1.0$ the resulting equations may be solved for

R_1 and R_2. However the effects of the loading resistance (the input resistance of the following amplifier) cannot be ignored. It may be accounted for analytically or experimentally. The latter method was convenient to use when programming the circuits of Chapter 7 as the tolerances of the padding resistors could be taken into account directly.

Having calculated the approximate values of the resistances required, the circuit was patched onto the computer and the padding potentiometers adjusted until the correct coefficient values are obtained at the servomultiplier outputs with reference input signals of zero volts and 100 volts applied to each servo-multiplier input. In Fig. 6.10, input e_4 is shown multiplied by a factor which decreases as the others increase.

With the procedure described above completed, multiplying coefficients of the correct value proportional to a signal at e_1 (Fig. 6.10) are achieved. By making the signal e_1 correspond to mill speed, coefficients proportional to mill speed are obtained.

6.10. A PURE TIME DELAY UTILISING ANALOGUE COMPUTER EQUIPMENT

Fig. 6.11 illustrates the sample and hold technique used to obtain a delay of the analogue voltages corresponding to the strip thicknesses emerging from the individual stands of the mill. The resetters and integrators shown are standard computing elements. The oscillator and drive units are designed specifically for this purpose and are housed in the computer framework.

The integrator resetters are normally used to switch in initial conditions to the integrator outputs, applied at the terminals marked I.C., at the start of a problem solution, and to switch the initial condition out when the integrator capacitors have stored the initial condition and computation begins. The initial condition voltages are imposed when the resetter relay is closed by a voltage pulse.

This aspect of resetter operation is made use of to build the time delay shown in Fig. 6.11. Here the resetters are driven by synchronised voltage pulses from the drive units. When a resetter is closed for the duration of a pulse (3 milliseconds) the voltage currently at the relevant I.C. terminal is stored on

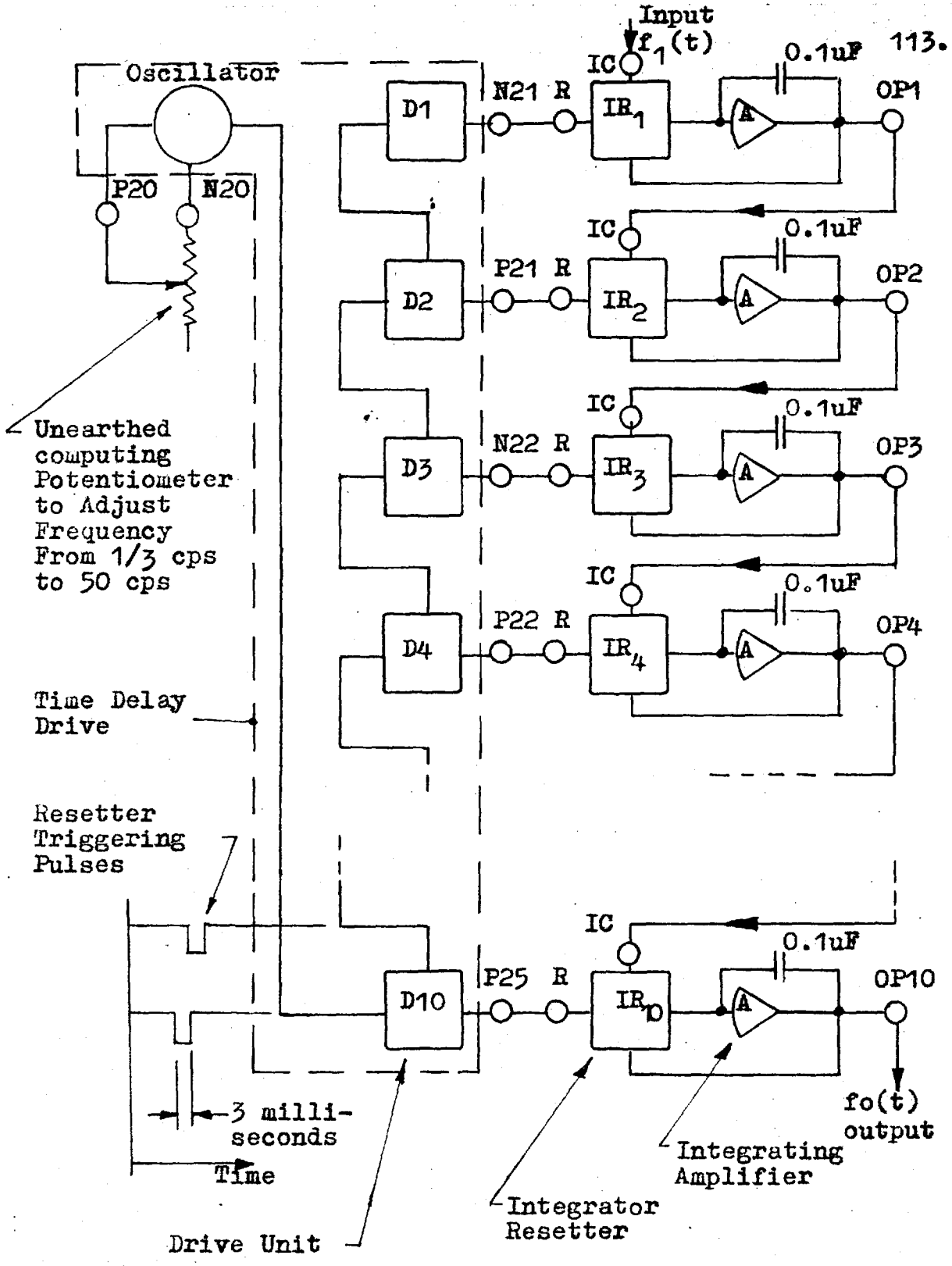

Terminals indicated are those on computer patch board
IC - initial condition terminals

Fig. 6.11 Time Delay Circuit Utilising Analog Computer Components

the integrator capacitor in the normal manner. When the pulse passes and the resetter relay is open the voltage is held on the capacitor until the next pulse closes the resetter relays causing the new existing voltage at I.C. to be stored on the capacitor.

The use of the device to delay a ramp signal is shown in Fig. 6.12 using three delay sections. Here pulse 1.1 to IR1 (integrator resetter 1) yields voltage $-V_1$; the voltage existing at I.C1 at the moment, but of reversed sign. At an interval of time Δ later the next pulse 1.2 gives $-V_2$ at OP1 and at another interval Δ, pulse 1.3 gives $-V_3$ at OP1. This process is continuous with the train of pulses. The result is the step approximation of the ramp signal delayed in time as shown. This describes the output of one section of the delay. However at given times the other resetter units are being pulsed as indicated.

Thus pulse 2.1 applies voltage V_1 to OP2 and pulse 3.1 applies V_1 to OP3. Similarly with V_2 and so forth. The pulse trains are synchronised so that the lagging edge of the pulse to IR_{n+1} triggers the leading edge of the pulse to IR_n. That is when pulse 3.1 has passed the relay of IR_3 having caused $-V_1$ to appear at OP3 it triggers pulse 2.2 which

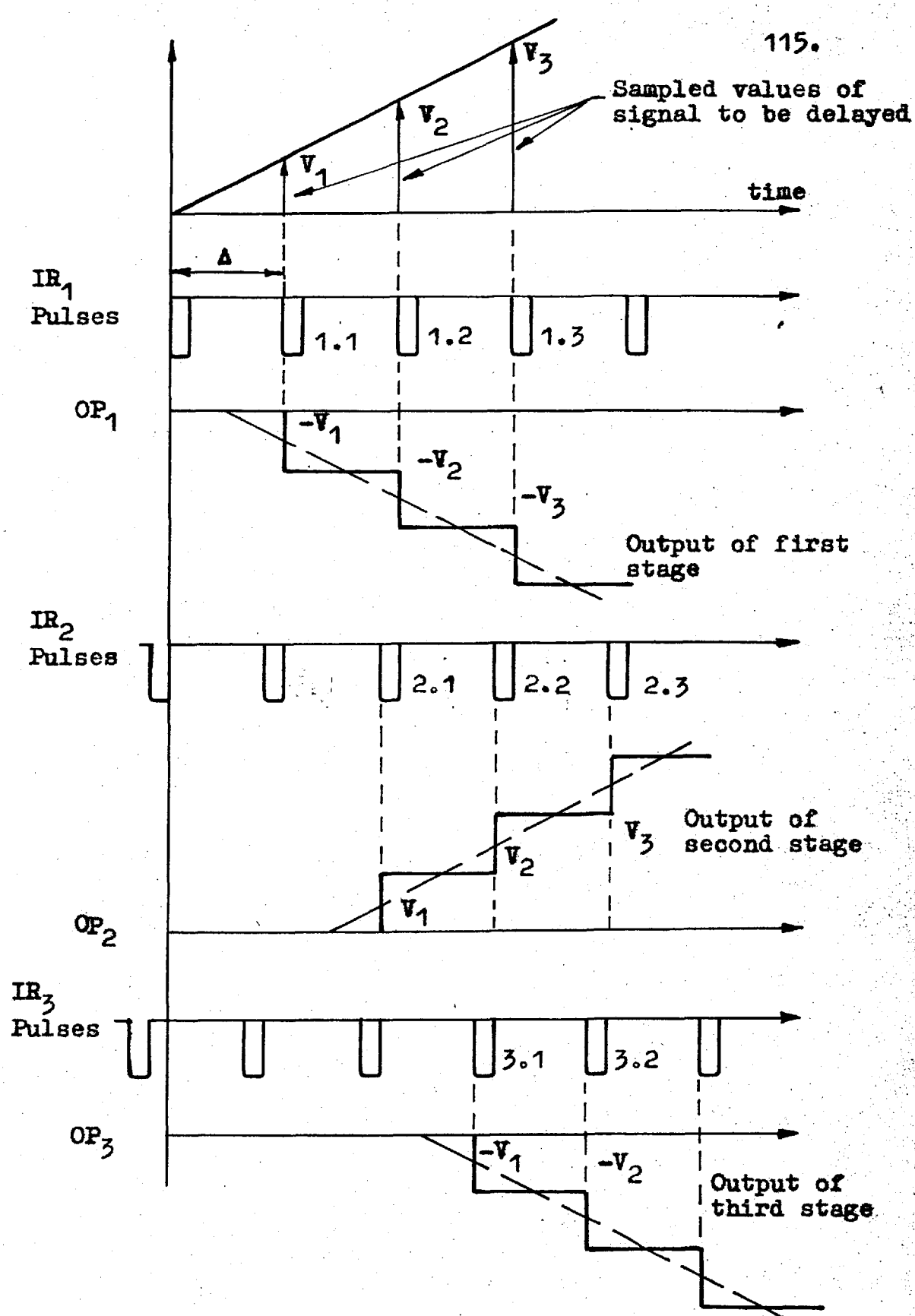

Fig. 6.12 Illustration of Delay of a Ramp with the Circuit of Fig. 6.11. Exaggerated Step Size

immediately causes V_2 to appear at OP2. This in turn triggers 1.3 which gives $-V_3$ at .OP1. The process appears to be viewed in reverse but due to the continuous pulsing the sampled voltages are passed through the circuit and give a step approximation to a ramp delayed in time. For n delay sections the relationship of the signal to be delayed $f_1(t)$ and the delayed signal $f_o(t)$ is:

$$f_o(t) = (-1)^n f_1\left(t - \frac{(2n-1)}{2}\Delta\right) \qquad 6.14$$

From equation 6.14 it can be seen that the time a signal is delayed is proportional to the number of sections n and the pulse frequency $1/\Delta$. For a given delay time the best response is obtained by using the maximum number of sections so that the maximum pulse frequency can be used.

6.10.1. A Continuously Variable Time Delay Unit

The pulse frequency, and hence the time a signal is delayed, can be varied by a potentiometer as indicated in Fig. 6.11. This potentiometer is ungrounded as it is a current control device, which controls the oscillator frequency that determines the rate at which

pulses emanate from the drive units.

For a simulation of the rolling mill acceleration phase, the delay time representing the time the strip takes to travel from stand to stand must be varied in accordance with the mill speed. That is, the resistance represented by the potentiometer must be varied during the simulation.

The method used is illustrated in Fig. 6.13. The principle is as discussed in section 6.9; a servo-multiplier potentiometer, whose resistance can be varied by a signal corresponding to mill speed is inserted in series with the potentiometer controlling the oscillator frequency.

The delay time is not a linear function of the resistance between the terminals P20 and N20 if one padding resistor is added in parallel as required for current control. To overcome this the resistance is subdivided in increments across the taps of the servo-multiplier potentiometer as shown.

Fig. 6.14 shows the values measured from the time delays used in the simulation of Chapter 7 for a mill output speed varying from 975 FPM to 1950 FPM using this scheme. Other methods of achieving a pure time delay are discussed in references (48, 50, 51).

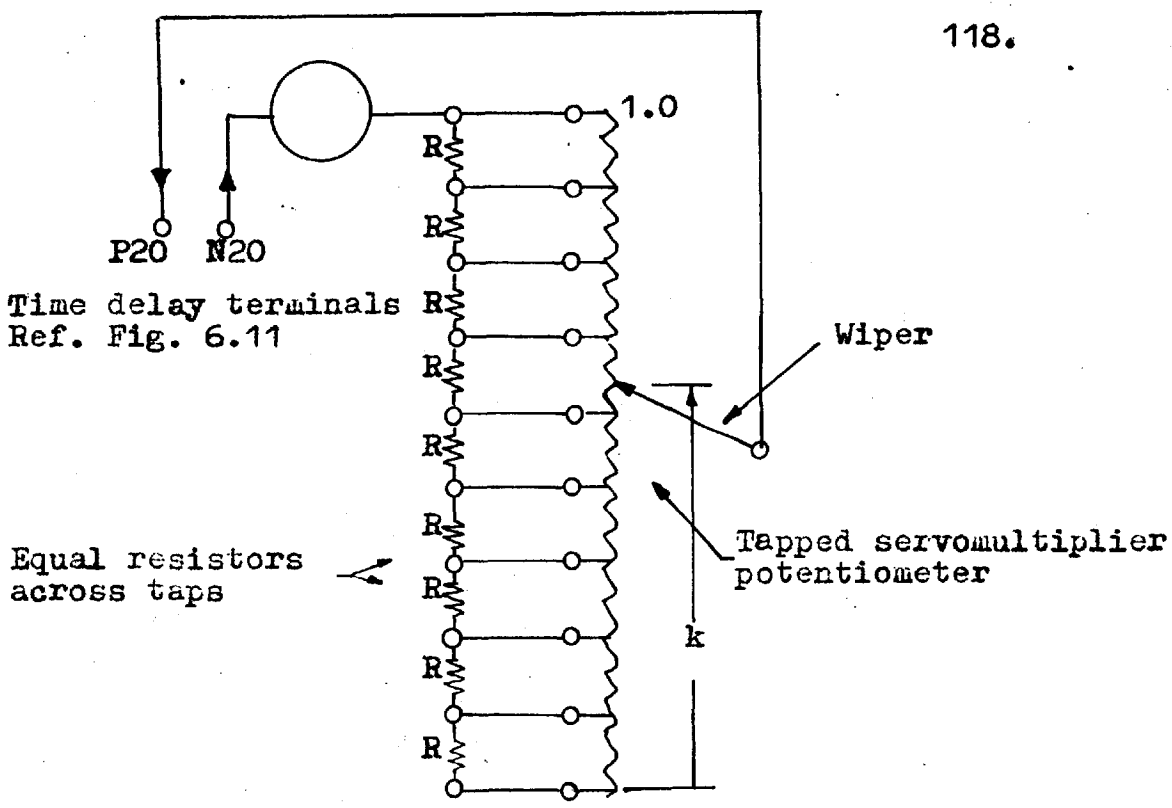

Fig. 6.13 Method used to obtain a Linear Variation of Delay Time with Varying Mill Speed.

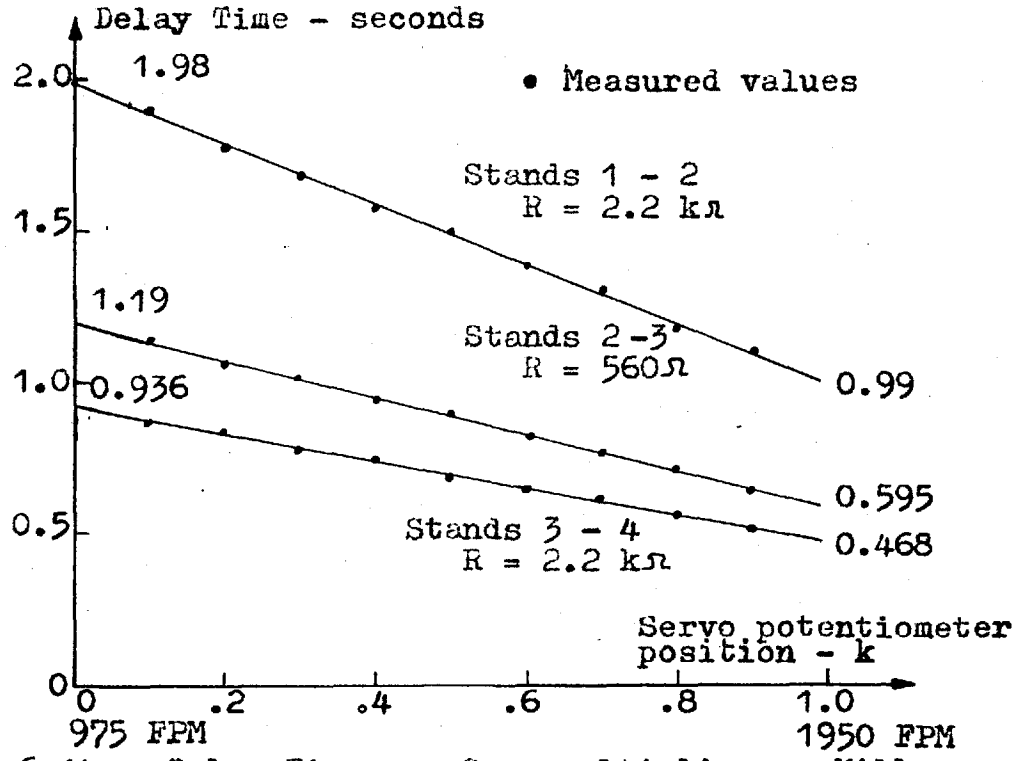

Fig. 6.14 Delay Time vs. Servomultiplier or Mill Speed Setting

6.10.2. Response of the Time Delays

A figure of merit for the time delay units is their frequency response; which in this case is the ratio of the amplitude of the sine wave received at the output, to the original sine wave imposed at the input of a delay unit. The phase angle is not important as it is equivalent to delay time which is desired here. By varying the frequency of the sine wave the point at which attenuation begins, and its effect, can be determined. Figures 6.15 and 6.16 show the response for the delays used. For the high speed case, attenuation commences at about 25 radians/second and for the low speed case, with the longer delay times, the attenuation starts at close to 10 radians/second, with 90% of the amplitude or better being achieved at 30 radians/second. Due to the sampling method of achieving the delays the signal deteriorates at frequencies over 70 radians/second for the high speed case and at over 40 radians/second for the low speed case - with the exception of delay number 3 for which the figure is 60 radians/second. This range of frequencies is sufficient to allow the majority of signals encountered in a cold rolling mill control study to be passed.

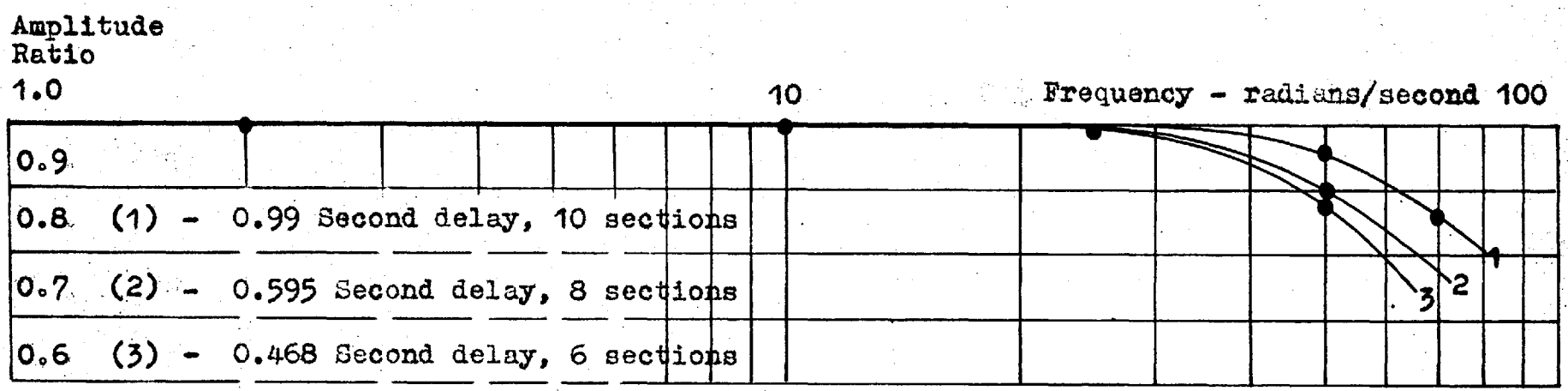

Fig. 6.15 Measured Values of Frequency Response of Time Delays at Delays Corresponding to 1950 FPM Mill Output Speed.

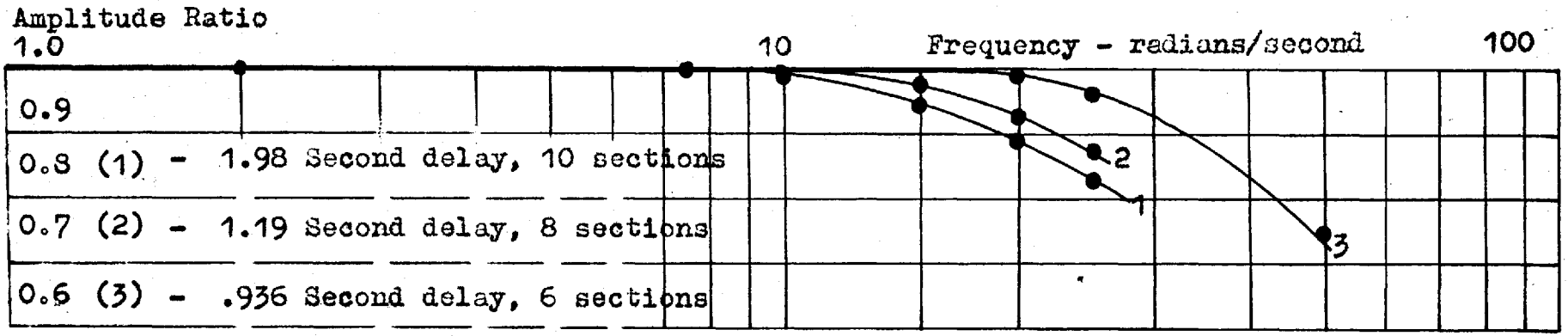

Fig. 6.16 Measured Values of Frequency Response of Time Delays at Delays Corresponding to 975 FPM Mill Output Speed.

6.11. IMPERIAL COLLEGE MECH. ENG. DEPT. ANALOGUE COMPUTER

This chapter described the major components of the Imperial College Mechanical Engineering Department's analogue computer, the specification and equipment complement of which was determined by the author to enable a multistand cold rolling mill to be simulated. However, it also serves as a general purpose analogue computer allowing a broad range of problems to be handled. The component complement is thus such as would normally be found in a general purpose analogue computer but with the special purpose time delay and servomultiplier equipment required for the rolling mill simulation.

6.11.1. Recording Equipment

An x-y plotter with a static accuracy of 0.075% and a dynamic accuracy of 0.2% was used to record the results of Chapters 8 and 9.

7 ANALOGUE SIMULATIONS OF THE 4-STAND TANDEM ROLLING MILL

7.1. CONTROL EQUATIONS FOR A SELECTED OPERATING SPEED

A mill output strip velocity of 1950 FPM was chosen as this is in accordance with Table 2.1. From the Tables C.3 to C.6 the coefficients for equations 4.4, 4.11 and 4.16 can be selected. The values selected, which are listed in Table 7.1, are a comprise between satisfying the experimental roll force values, the accuracy of which is not certain, and meeting the envelope of expected u values versus speed (Fig. 7.1).

This figure shows a plot of u versus strip velocity for a palm oil and water mixture; however since the rolling lubricant used in the schedule of Table 2.1 contained many additives this curve is only representative of the nature of the relationship.

Using the data of Fig. 2.1, Table 2.1 and Table 7.1 the constants in a set of control equations representing the rolling mill at the speed mentioned were obtained. These equations were transformed into machine equations in accordance with section 6.7. The scale factors of Table 7.2 were used. The resulting set of machine equations are listed in Appednix D.1.

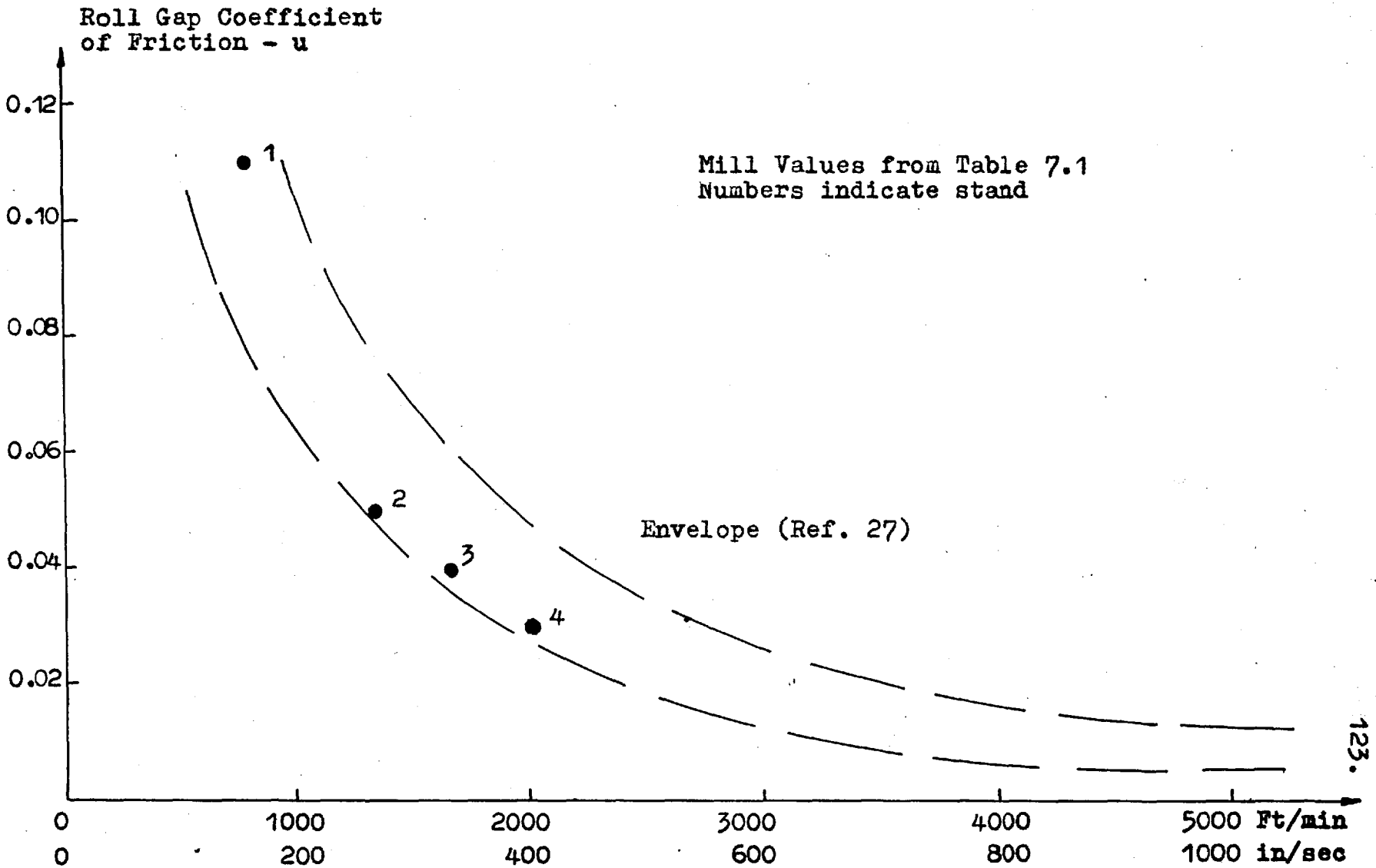

Fig. 7.1 Roll Gap Coefficient of Friction vs. Stand Output Velocity

Quantity	Units	Stand			
		1	2	3	4
V_r	inches/sec	158	262	334	390
V_r	feet/min	790	1310	1670	1950
V'_{r-1}	inches/sec	132.5	158	262	334
w_r	radians/sec	15.25	25.5.	32.9	38.9
τ_r	seconds	.989	.595	.468	-
τ_g	seconds	.228	-	-	.123
D_r	rad/sec/ton-in	-.00472	-.00682	-.01065	-.0126
u_r	-	.11	.05	.04	.03
P_{Er}	tons	-	935	750	712
P_r	tons	823	1050	980	754
G_r	ton-inches	-39.4	340.5	300	170.5
F_r	-	.03609	.02678	.01735	.00393
p_{1r}	tons/thou	44.61	10.67	21.31	47.21
p_{2r}	tons/thou	-51.33	-27.46	-32.75	-55.21
p_{3r}	tons/ton/in^2	-	-29.12	-23.65	-18.12
p_{4r}	tons/ton/in^2	-18.72	-11.30	-9.018	-
g_{1r}	ton-in/thou	18.46	15.18	20.92	24.73
g_{2r}	ton-in/thou	-22.33	-21.95	-22.99	-23.06
g_{3r}	ton-in/ton/in^2	-	23.38	18.32	16.63
g_{4r}	ton-in/ton/in^2	-32.66	-24.23	-17.72	-
f_{1r}	-/thou	.00143	-.00021	.00013	.00059
f_{2r}	-/thou	-.00171	-.00045	-.00076	-.00093
f_{3r}	-/ton/in^2	-	-.00393	-.00259	-.00119
f_{4r}	-/ton/in^2	.00252	.00309	.00220	-
$R(1+Fr)$	inches	10.361	10.268	10.174	10.039
$w_r R$	rad-inch/sec	152.5	255	329	389
V'_{r-1}/V_r	-	.606	.746	.878	-
V'_{r-1}/H_r	inch/sec/thou	2.873	6.390	9.278	-
V'_{r-1}/H'_{r-1}	inch/sec/thou	-2.026	-4.764	-8.146	-

Table 7.1 Physical Data For Simulation of Fig. 7.2.

Variable	Maximum Value	Scale Factor
$\delta H_0'$	20 thousandths	5 volts/thou.
δH_1, $\delta H_1'$	10 "	10 volts/thou.
δH_2, $\delta H_2'$	2 "	50 volts/thou.
δH_3, $\delta H_3'$, δH_4	2 "	50 volts/thou.
$\delta\sigma_1$, $\delta\sigma_2$	5 tons/in^2	20 volts/ton/in^2
$\delta\sigma_3$	10 tons/in^2	10 volts/ton/in^2
δG_1	200 ton-inches	0.5 volts/ton-in.
δG_2, δG_3	100 "	1 volt/ton-in.
δG_4	50 "	2 volt/ton-in.
δV_1, $\delta V_1'$	10 inches/second	10 volts/inch/sec.
δV_2, $\delta V_2'$	4 "	25 "
δV_3, $\delta V_3'$	4 "	25 "
δV_4	4 "	25 "
δS_1	10 thousandths	10 volts/thou.
δS_2, δS_3, δS_4	2 "	50 "
δP_1	200 tons	0.5 volts/ton
δP_2, δP_3, δP_4	400 "	.25 "
δF_1	0.02	5000 volts/unit
δF_2, δF_3, δF_4	0.01	10000 "
δw_1	1 radian/second	100 volts/rad/sec.
δw_2, δw_3, δw_4	0.5 "	200 "

Table 7.2 Scale Factors for Simulation of Fig. 7.2.

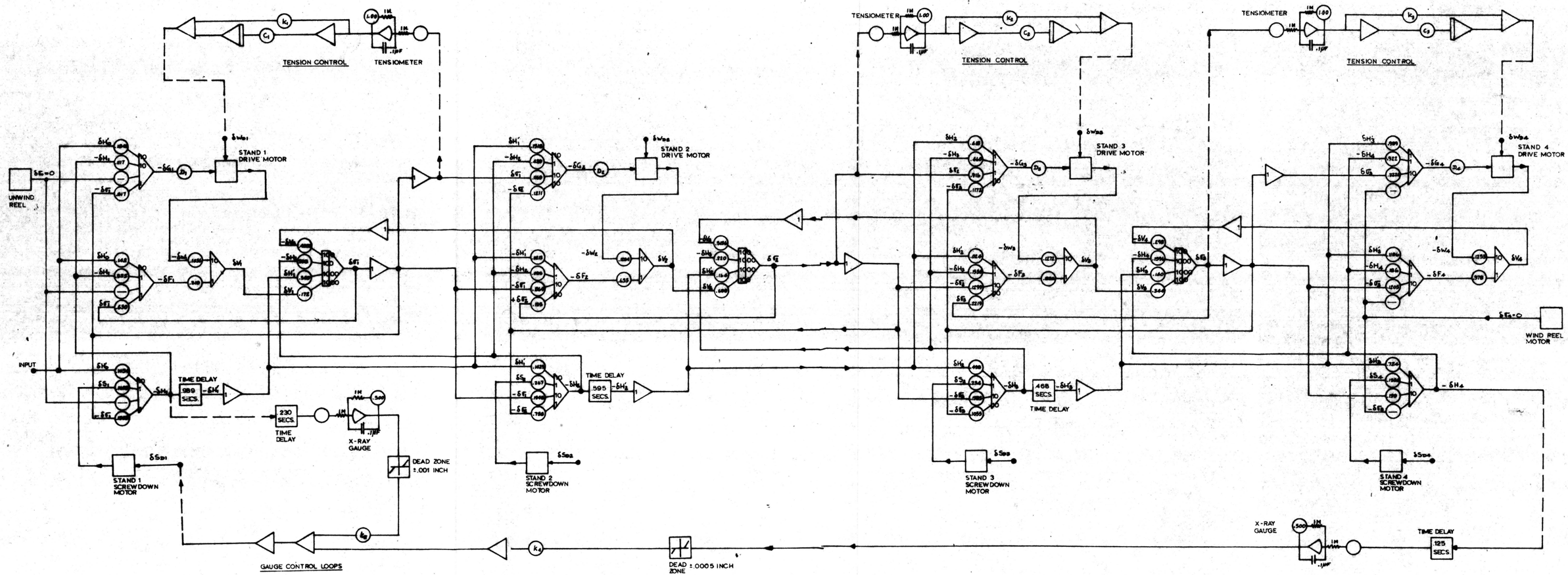

FIG. 7.2

4-STAND COLD ROLLING MILL SIMULATION
WITH CONTROL SYSTEM NUMBER 5
R.F. DARLINGTON JUNE 1964

In Appendix D.1 the equations for the drive motors (equation 4.17) are represented by first order lags (Appendix B.2) with the time constants noted. This representation is a generalisation rather than an assumption, as the motor responses are often such - as in recordings made by BISRA - although they may at times be more complex.

The screw down motors (equation 4.18) are represented by a lag and integral term. The time constant is larger than for the drive motors as the screw down motors have a slower response.

7.1.1. The X-Ray Gauge

An x-ray gauge (Fig. 7.3) utilises a radioisotope to ionise the gases in the chamber. The steel strip, acting as an absorber of energy, causes the energy entering the chamber to vary with strip thickness. The current flow is proportional to the energy entering the chamber. A voltage, inversely proportional to the strip thickness can thus be obtained by passing the current through a resistor. This voltage is then amplified and used to actuate the recorder from which an error signal proportional to the strip gauge error may be obtained. The transfer function of the x-ray gauge is given (9) in analogue form as:

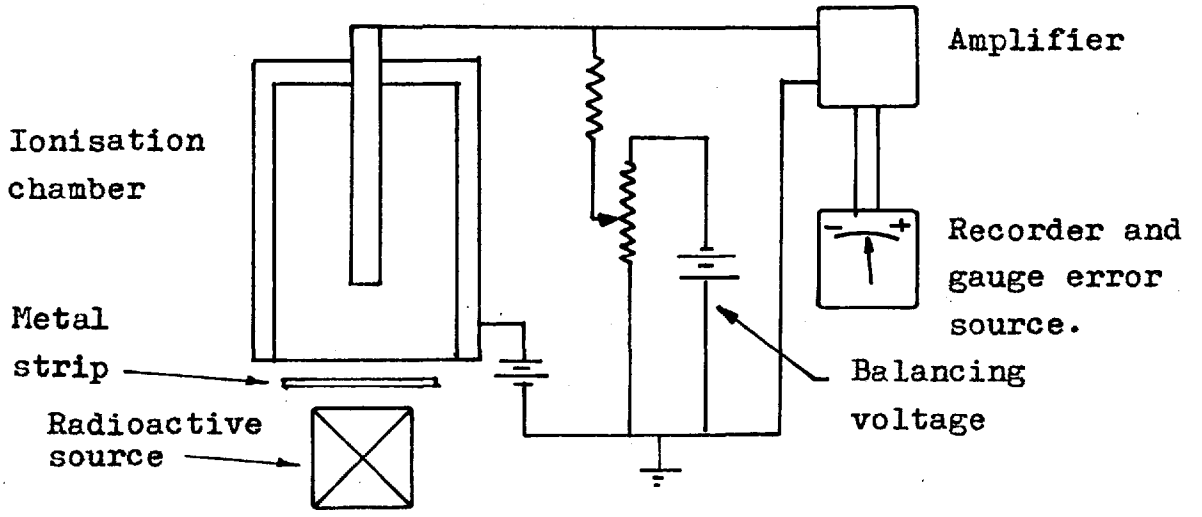

Fig. 7.3 X-ray Gauge.

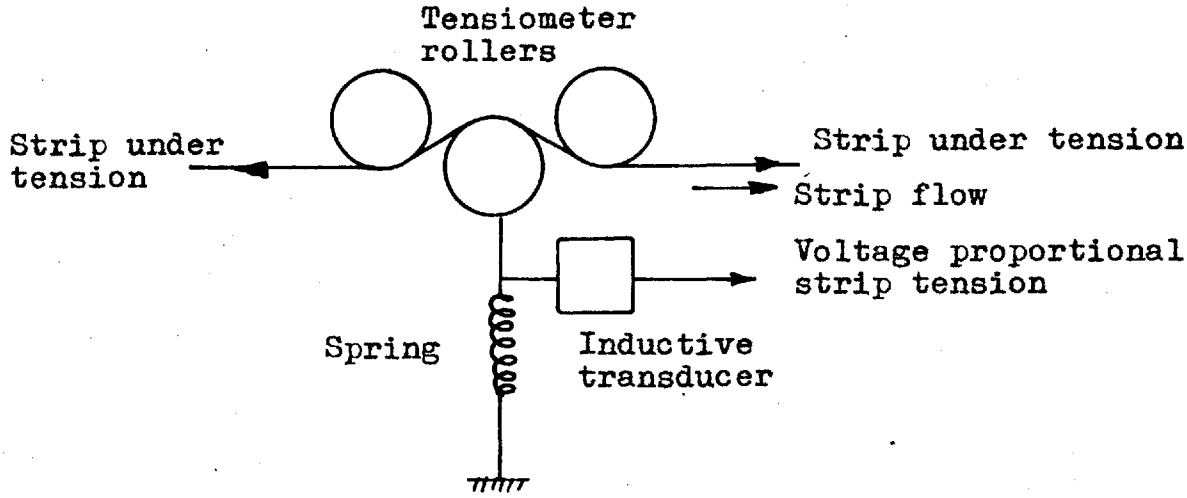

Fig. 7.4 Tensiometer.

$$\frac{\text{output voltage}}{\text{input voltage}} = \frac{1}{1 + 0.2p} \qquad 7.1$$

7.1.2. The Tensiometer

To measure interstand tension a system of rollers is fitted between the mill stands through which the strip passes. Fig. 7.4 shows the system; the variations in tension of the strip acting in accordance with the required equilibrium of forces cause the spring mounted roll to move in a vertical plane. A calibrated induction transducer produces an electrical signal proportional to the change in tension. The transfer function of this tension measuring system has been estimated (9) in analogue form as:

$$\frac{\text{output voltage}}{\text{input voltage}} = \frac{1}{1 + 0.1p} \qquad 7.2$$

7.1.3. Analogue Simulation

From the set of equations in Appendix D.1 the analogue simulation circuit of Fig. 7.2 was drawn. The symbols defined in Table 6.6 are used. The lag circuit of Fig. B.1 was used to represent the motors, x-ray gauges and tensiometers.

In Fig. 7.2 the layout follows the mill layout, that is, stand 1 is to the left and stand 4 to the right as may be noted from the variable subscripts. The

connections made with the dashed lines represent control system number 5 which is later described in Chapter 9. Five time delays are used, three for the interstand spacing and two for the time the strip takes to reach the x-ray gauges.

The wind and unwind reels are shown although they have no effect on the actual simulation as their respective strip tensions have been assumed zero, which they are usually assumed to be in practice. The circuit illustrates the method of including their effects if it is desired.

The interaction of the mill variables is apparent from Fig. 7.2. This δV_2 is fed back to the integrator yielding $\delta\sigma_1$, and δV_3 is fed back to effect $\delta\sigma_2$. The terms $\delta\sigma_1$, $\delta\sigma_2$ and $\delta\sigma_3$ are fed forward to effect the force, torque and slip at the succeeding stands. Since equation 4.9 is used to determine the interstand tensions, the integrators yielding $\delta\sigma_1$, $\delta\sigma_2$ and $\delta\sigma_3$ have four inputs. The circuit illustrates the point that perturbations in any variable eventually effect all other variables to some degree.

The ancillary circuits of Appendix B.3 were used to facilitate the use of the analogue computer.

7.2. ANALOGUE SIMULATION FOR A SELECTED SCHEDULE AND SPEED RANGE

Section 7.1 described the simulation of the rolling mill at a selected operating speed. Below is described a method of simulation which holds over a selected speed range permitting acceleration tests on the analogue computer (in the following discussion reference will be made to acceleration tests only, however, deceleration is also implied).

To amplify the discussion in preceding chapters leading to the conclusion that this is possible the original schedule (Table 2.1) will first be considered. The results from the digital computer computations (Tables C.1 and C.2) of the roll forces and torques indicate that it is necessary to adjust the mill roll forces, torques and speeds (mill settings) during acceleration to account for the changes due to the varying roll gap friction. The interstand tensions may also be varied (27) although for this schedule they are held constant. The means of controlling a rolling mill are through the drive motor speeds, which enables interstand tensions to be controlled; the drive motor torque, and the screw down motors which control the roll gap setting or roll force. A schedule is maintained through control of these motors. At

the present time work is progressing in applying digital computers to mill scheduling (11) in place of a manual operator.

As adjustements are made in the mill settings to maintain the gauge schedule, the coefficients in the control equations change (Tables C.3 to C.6), the calculation of which is based on a known schedule. There is no restriction as to the type of schedule (except for practical restrictions) but it should be predetermined and able to maintain the gauges desired at the output of the stands over the expected operating speed range.

There are two aspects to the problem of maintaining the gauge schedule when acceleration is taking place. One is the maintenance of the gauge in the face of changing roll gap friction and roll neck bearing oil film thickness change and the other is the control of the effects of variations in the character of the incoming strip. The former requires adjustments in mill settings which must be made even with the entering strip maintaining a constant character.

Changes in the incoming strip gauge, hardness etc require adjustments of mill settings to correct the perturbations they cause. These can occur during

acceleration; and mill setting changes to correct for them must be superimposed on those being made for the adherence to the original schedule. They may be considered as small changes about the nominal schedule values existing when they occur. This is the same assumption as has been made to obtain the control equations at a selected operating point and holds at any mill velocity. Using the method described in section 6.9 the correct control equation coefficients can be obtained in the analogue simulation of the mill acceleration phases. That is, using servomultipliers with padded potentiometers which respond to signals representing mill speed and position the potentiometers to give the correct coefficients. If the servomultiplier were to position the potentiometers to represent any mill speed, the correct coefficients would exist and a series of simulations of the type described in Fig. 7.2 representing any desired operating point speed would be available. Since the servomultiplier can respond to a continuously varying signal, representing mill speed, acceleration may be simulated. Such simulations would hold for the cases in which the schedule is being maintained. However deviations from the schedule can be introduced. These deviations from the scheduled

or desired nominal values of the mill variables can be treated exactly as those that would exist when a variation in incoming strip causes perturbations. In an analogue simulation the deviations from the desired schedule are able to be programmed into the simulation by introducing signals representing any quantity of roll force, torque or tension change, again by means of the servomultiplier potentiomers. If the schedule is maintained these signals would be of zero value. Figure 7.5 shows in skeleton form the simulation of stand 1 as depicted in Fig. 7.2 with the added circuitry required to introduce signals for simulating schedule changes and deviations. Taking the low speed case as the base, at which the servo drive signal is zero, the voltage signals coming from the servomultiplier vary as the servomultiplier drive signal is varied.

Several possible situations are:

1) That the schedule is maintained with acceleration by adjusting the roll forces, torques and speeds.

2) That the schedule is maintained by the adjustments of (1) and of the interstand tensions.

3) That it is attempted to adjust the schedule as in (2) but it is not perfectly maintained. In each of these cases the effects of the roll neck bearing oil

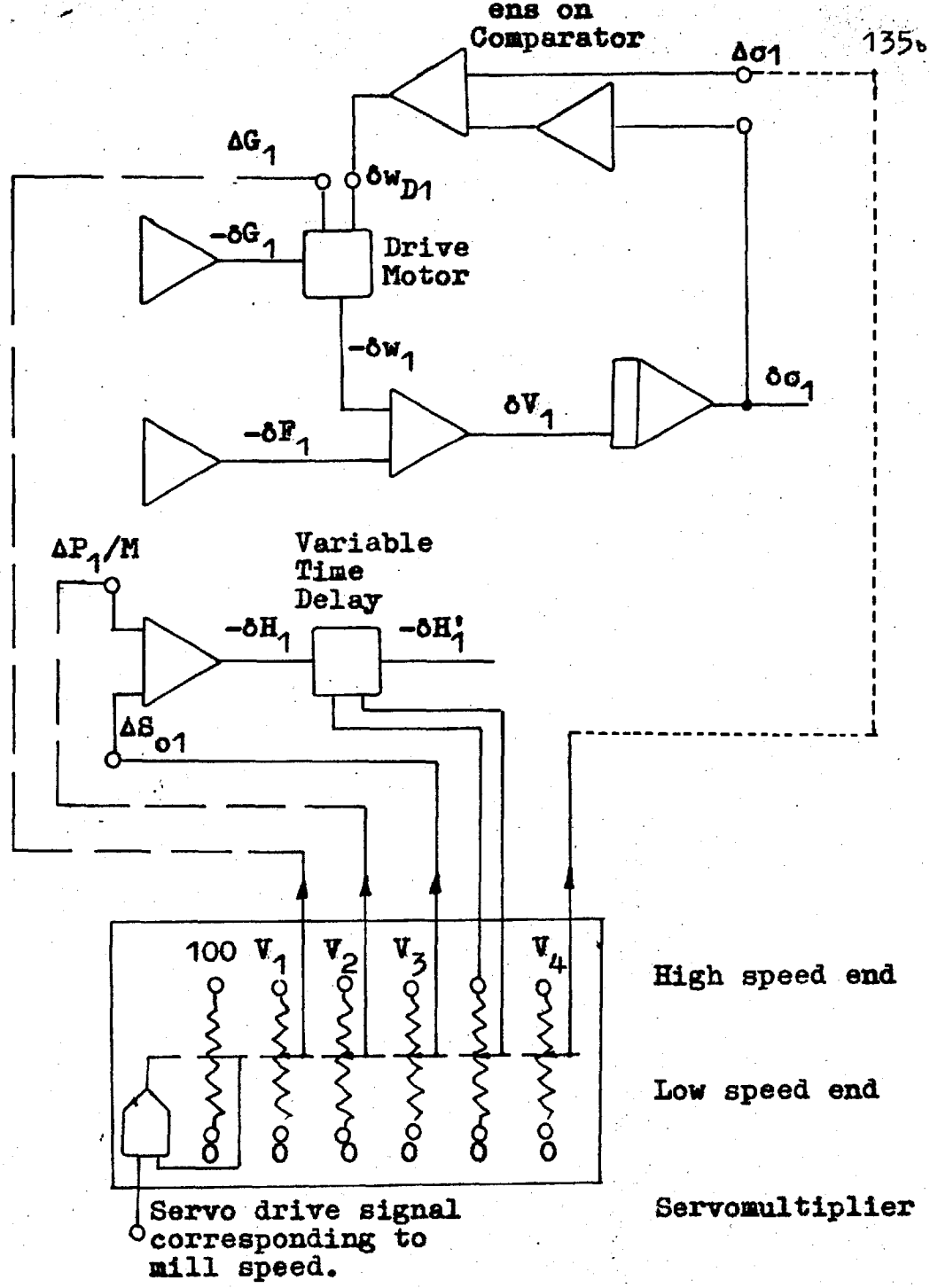

V_1, V_2, V_3, V_4, V_5 represent voltage signals corresponding to changes in nominal values of variables indicated at high speed end.

Fig. 7.5 Method of Introducing Schedule Changes into the Simulation

film thickness changes, ΔS_{or}, can exist and for this discussion are considered separate from the schedule deviations. In later sections, reference to a maintained schedule implies the mill has been adjusted to counter the oil film effects.

In case (1), Fig. 7. would show a connection only to ΔS_{o1} input (other than the time delay control shown) as indicated. The dotted and dashed lines could be omitted since, as the schedule is maintained, ΔG_1, $\Delta P_{1/M}$ and $\Delta \sigma_1$ are zero. In case (2) the dotted connection to $\Delta \sigma_1$ would have to be added to bring the interstand tension to the desired value as is discussed later. For the third case the dashed connections to ΔG_1 and $\Delta P_{1/M}$ would have to be added and would transmit signals from the servomultiplier potentiometers corresponding to the deviations from the scheduled values. By changing the voltages applied to the multiplying potentiometers, or by inserting other signals of any desired form at any time it is possible to represent any schedule deviation.

To maintain the schedule of Table 2.1 during acceleration adjustments must be made in roll force and torque. If these are made correctly and at all stands in unison then there will be no steady-state change in the gauge or tension schedule; each stand will just be required to follow the changing equilibrium point. However this cannot be said if adjustments are made in

the tension schedule as roll force and torque have been expressed as functions of tensions (and gauges) as in equations 4.3 and 4.4, hence their adjustment for scheduled changes affects roll force and torque. For this reason changes in the tension schedule must be expressed in the simulation and cannot be assumed as eliminated simply because the schedule has been perfectly maintained during acceleration.

To obtain the scheduled tension, which in Fig. 7.5 is shown accomplished by controlling stand 1 motor speed, the desired change in interstand tension from base level (low speed case) is compared with the tension existing and a signal representing the difference is fed to the stand drive motor speed control which tends to bring the existing interstand tension to the desired value. It should be noted that this is not an actual tension control loop with controllers such as is discussed later in Chapter 9 but is a loop inserted in the simulation to cause it to adhere to the schedule for the mill tensions during acceleration. Tension control loops used to correct for gauge errors would be inserted in addition to loop to maintain scheduled tension.

The above discussion can be further summarised by

the following extension of equation 4.8.

$$\delta\sigma_r = \frac{E}{L_r}\int(\delta V'_r - \delta V_r)dt + \Delta\sigma_r(\Delta V_r, \Delta V'_r) \qquad 7.1$$

Here the scheduled change in tension is represented by $\Delta\sigma_r$ which is shown as a function of the variables that can be varied by the motor settings to yield it.

It is possible to express deviations from the roll force and torque schedule by including the terms ΔP_r and ΔG_r, representing the deviations, in the equations 4.11 and 4.8 respectively.

$$\delta H_r = \frac{1}{M-p_{2r}}(p_{1r}\delta H'_{r-1} + M_r\delta S_{or} + M_r\Delta S_{or} + p_{3r}\delta\sigma_{r-1} + p_{4r}\delta\sigma_r - \Delta P_r) \qquad 7.2$$

$$\delta G_r = g_{1r}\delta H'_{r-1} + g_{2r}\delta H_r + g_{3r}\delta\sigma_{r-1} + g_{4r}\delta\sigma_r - \Delta G_r \qquad 7.3$$

For a schedule maintained with speed the terms ΔP_r and ΔG_r are zero. However as previously discussed the $\Delta\sigma_r$ term in equation 7.1 must be included to represent changes in interstand tensions if such changes are scheduled.

7.3. ANALOGUE SIMULATION FOR A MILL OUTPUT SPEED RANGE OF 975 FPM TO 1950 FPM

This simulation enables acceleration and deceleration phases of the mill operation between the output velocity range of 975 FPM and 1950 FPM to be represented on the analogue computer. This range is selected due to limitations of the delay times obtainable at the low speed end and by some evidence that the schedule of tensions given in Table 2.1 would have to be revised for speeds much in excess of 1950 FPM (section 5.3) which in any case is the expected maximum operating speed for this schedule. Inspection of the coefficients in Tables C.2 to C.6 and Figures 5.6 to 5.10 show that over the speed range considered for each stand the coefficients are close to linear. Hence coefficient values were selected for each end of the speed range and intermediate values obtained by interpolation using the servomultiplier technique described. Tables 7.3 and 7.4 gave the values for the extreme speed cases. From the resulting sets of equations, the machine equations given in Appendix D.2.1 and D.2.2 were obtained using the scale factors of Table 7.5 and the scaling technique of section 6.7.

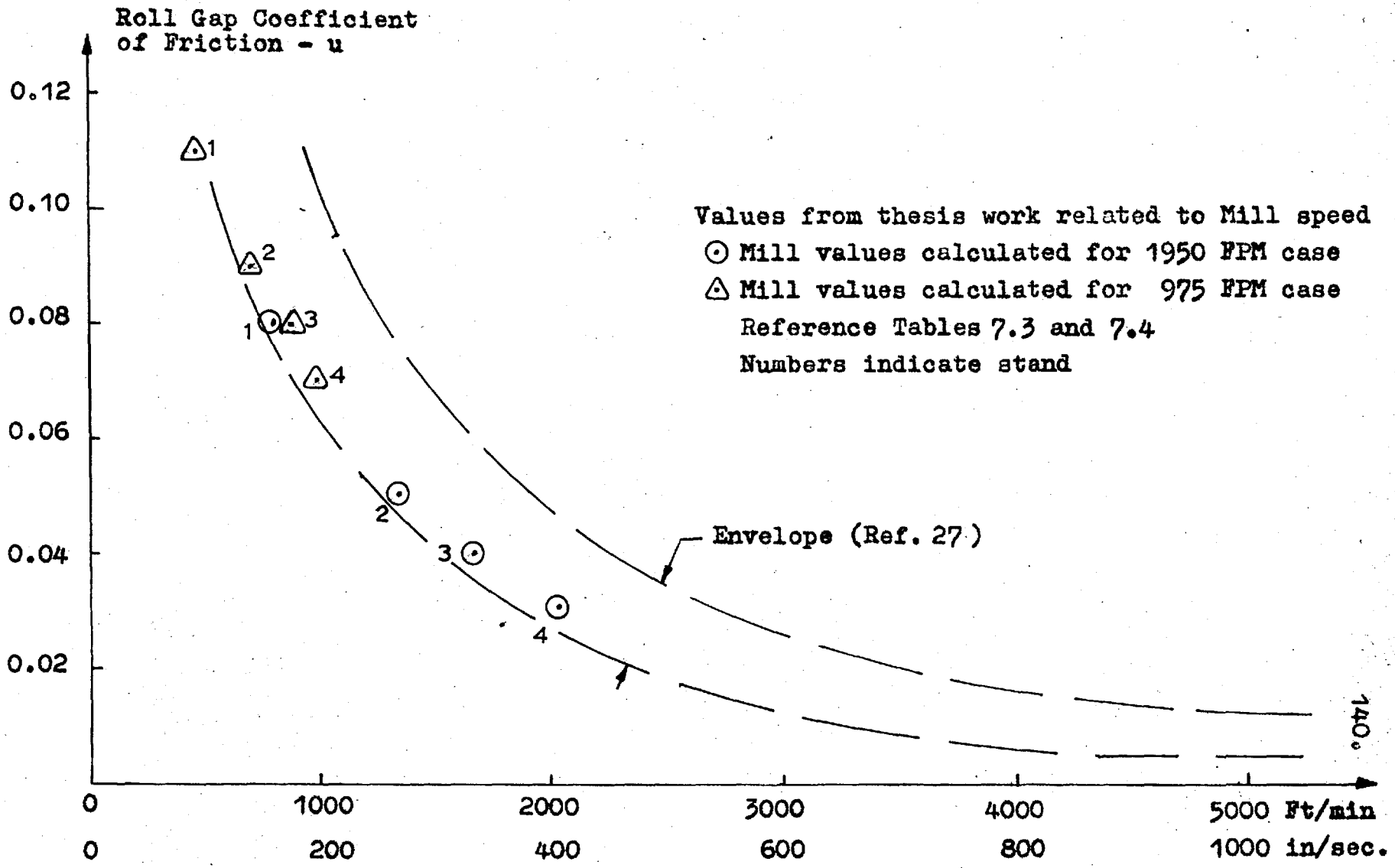

Fig. 7.6. Roll Gap Coefficients of Friction vs. Stand Output Velocity

Quantity	Units	Stand			
		1	2	3	4
V_r	inches/sec	158	262	334	390
V_r	feet/min	790	1310	1670	1950
V'_{r-1}	inches/sec	132.5	158	262	334
w_r	radians/sec.	15.24	25.51	32.83	38.85
τ_r	seconds	.989	.595	.468	-
τ_g	seconds	.228	-	-	.123
D_r	rad/sec/ton-in.	-.00472	-.00682	-.01065	-.01260
u_r	-	.08	.05	.04	.03
P_{Er}	tons	-	935	750	712
P_r	tons	734	1050	980	754
G_r	ton-inch	-31.5	340.5	300	170.5
F_r	-	.03579	.02678	.01735	.00393
p_{1r}	ton/thou	37.31	10.67	21.31	47.21
p_{2r}	ton/thou	-41.96	-27.46	-32.75	-55.21
p_{3r}	ton/ton/in^2	-	-29.12	-23.65	-18.12
p_{4r}	ton/ton/in^2	-15.96	-11.3	-9.02	-9.0
g_{1r}	ton-in/thou	16.64	15.18	20,92	24.73
g_{2r}	ton-in/thou	-20.10	-21.95	-22.99	-23.06
g_{3r}	ton-in/ton/in^2	-	23.38	18.32	16.63
g_{4r}	ton-in/ton/in^2	-34.14	-24.22	-17.72	-15.0
f_{1r}	-/thou	.00107	0	.00013	.00059
f_{2r}	-/thou	.00128	-.00045	-.00076	-.00093
f_{3r}	-ton/in^2	-	-.00393	-.00259	-.00119
f_{4r}	-ton/in^2	.00344	.00309	.00220	.002
$R(1+Fr)$	inches	10.37	10.27	10.17	10.04
w_rR	rad-inch/sec	152.4	255.1	328.3	388.5
V'_r/V_{r+1}	-	.6031	.7844	.8564	-
V'_r/H_{r+1}	inch/sec/thou	2.873	6.390	9.278	-
V'_r/H'_r	inch/sec/thou	-2.026	-4.764	-8.146	-

Table 7.3 Physical Data for Simulation of Fig. 7.7 (1950 feet per minute case)

Quantity	Units	Stand			
		1	2	3	4
V_r	inches/sec	79	131	167	195
V_r	feet/min	395	655	835	975
V'_{r-1}	inches/sec	66.3	79	131	167
w_r	radians/sec	7.625	12.52	16.10	19.23
τ_r	seconds	1.98	1.19	.936	-
τ_g	seconds	.456	-	-	.246
D_r	rad/sec/ton-in	-.00944	-.01264	-.02130	-.02520
r	-	.11	.09	.08	.07
P_{Er}	tons	-	-	-	-
P_r	tons	823	1370	1365	1045
G_r	ton-inches	-39.4	388	321	113
F_r	-	.03609	.04595	.03719	.01431
p_{1r}	ton/thou	44.61	18.99	38.21	77.83
p_{2r}	ton/thou	-51.33	-49.15	-68.36	-101.20
p_{3r}	ton/ton/in^2	-	-36.25	-31.79	-23.20
p_{4r}	ton/ton/in^2	-18.72	-19.90	-19.22	-19.0
g_{1r}	ton-in/thou	18.46	20.28	28.67	35.31
g_{2r}	ton-in/thou	-22.33	-30.09	-33.75	-34.17
g_{3r}	ton-in/ton/in^2	-	21.07	16,76	16.69
g_{4r}	ton-in/ton/in^2	-32.66	-23.34	-16.33	-14.0
f_{1r}	-/thou	.00143	.00087	.00172	.00284
f_{2r}	-/thou	-.00171	-.00178	-.00275	-.00346
f_{3r}	-/ton/in^2	-	-.00284	-.00185	-.00092
f_{4r}	-/ton/in^2	.00252	.00226	.00159	.0015
$R(1+Fr)$	inches	10.361	10.46	10.37	10.14
$w_r R$	rad-inch/sec	76.25	125.2	161.0	192.3
V'_r/V_{r+1}	-	.6031	.7844	.8564	-
V'_r/H_{r+1}	inch/sec/thou	1.436	3.195	4.639	-
V'_r/H'_r	inch/sec/thou	-1.013	-2.382	-4.073	-

Table 7.4 Physical Data for Simulation of Fig. 7.7 (975 feet per minute case

Variable	Maximum Value	Scale Factors
$\delta H_0'$	20 thousandths	5 volts/thou
$\delta H_1, \delta H_1', \delta H_2, \delta H_2'$	10 "	10 "
$\delta H_3, \delta H_3', \delta H_4$	5 "	20 "
δG_1	200 tons	0.5 volts/ton-in
δG_2	100 "	1 "
δG_3, δG_4	50 "	2 "
δV_1, $\delta V_1'$	10 inch/sec	10 volts/inch/sec
$\delta V_2, \delta V_2', \delta V_3, \delta V_3'$	5 "	20 "
δV_4, δV_R	5 "	20 "
δS_1, δS_2	10 thou	10 volts/thou
δS_3, δS_4	5 thou	20 "
ΔS_{01}, ΔS_{02}	10 thou	10 volts/thou
ΔS_{03}, ΔS_{04}	5 thou	20 "
δF_1	.02	5000 volts/unit
δF_2, δF_3, δF_4	.01	10000 "
δw_1	1 rad/sec	100 volts/rad/sec
δw_2, δw_3, δw_4	.5 "	200 "
$\delta\sigma_1, \delta\sigma_2, \delta\sigma_3, \delta\sigma_4$	5 tons/in^2	20 volts/ton/in^2

Table 7.5 Scale Factors for Simulation of Fig. 7.7.

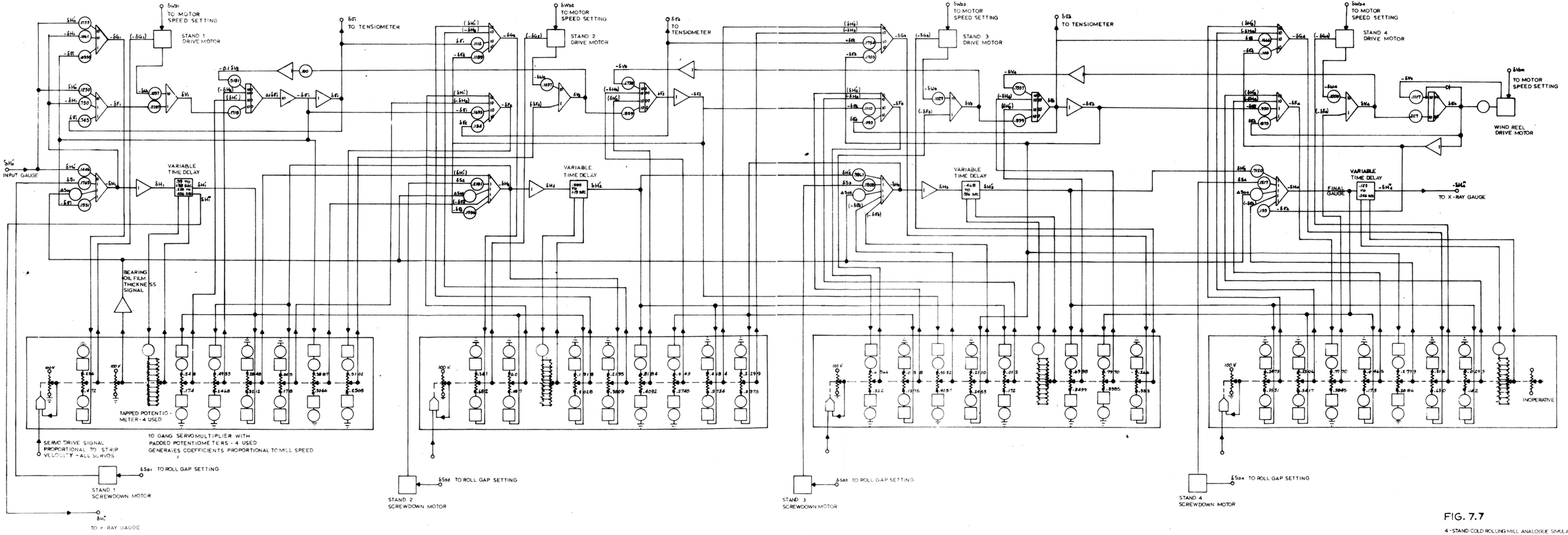

FIG. 7.7

4-STAND COLD ROLLING MILL ANALOGUE SIMULATION FOR MILL OUTPUT VELOCITIES FROM 1000 TO 2000 FEET PER MINUTE.

R. F. DARLINGTON. DECEMBER 1964

Figure 7.7 is the resulting analogue circuit. It is basically similar to Figure 7.2 but for the addition of four servomultipliers each with ten potentiometers to generate the varying coefficients and signals corresponding to schedule deviations. The top of the potentiometers gives the 1950 feet per minute values, the bottom gives the 975 feet per minute values and any other point corresponds to an intermediate mill speed.

To simulate the acceleration of the mill, a voltage signal representing mill speed is imposed on each servomultiplier drive (voltage e_1 in Fig. 6.10). At zero volts the servomultiplier positions the potentiometers at values corresponding to 975 feet per minute and 100 volts represents the 1950 feet per minute values. For example a ramp signal starting at zero volts and rising to 100 volts in 5 seconds would represent a constant acceleration of approximately 200 feet per minute per second.

The results in Tables C.1 to C.6 were for a constant tension schedule hence scheduled tension changes do not appear in Fig. 7.7. The roll neck bearing oil film thickness changes ΔS_{or}, are included as shown. In Chapter 8 results are also given for

deviations from the scheduled values of roll speed and roll force. The roll force deviations can be included with the ΔS_{or} changes as they are similar in effect.

From Fig. 7.7 it is apparent that not all the varying coefficients could not be included due to the limited quantity of servomultiplier equipment available.

7.3.1. Motor Dynamics

The motor dynamics were first represented, as in the simulation of Fig. 7.2, by first order lags. The equations of Appendix D.2.1 and D.2.2 give the relation for the wind reel motor. Following this the drive motor torque-speed relation was represented by a second order transfer function. In this case equation 4.17 becomes:

$$\delta w_r = \frac{\delta w_{Dr}}{(1 + 0.25p)} - \frac{D_r \delta G_r}{\frac{1}{w_n^2} p^2 + \frac{2\zeta}{w_n} p + 1} \qquad 7.3$$

where the denominator of the δG_r term is the transfer function of a second order relationship between δG_r and δw_r. The term w_n is the natural frequency and ζ is the damping ratio. Figs. 7.7 and 7.8 show the response obtained for a step input of torque and the analogue circuit used to achieve the relationship.

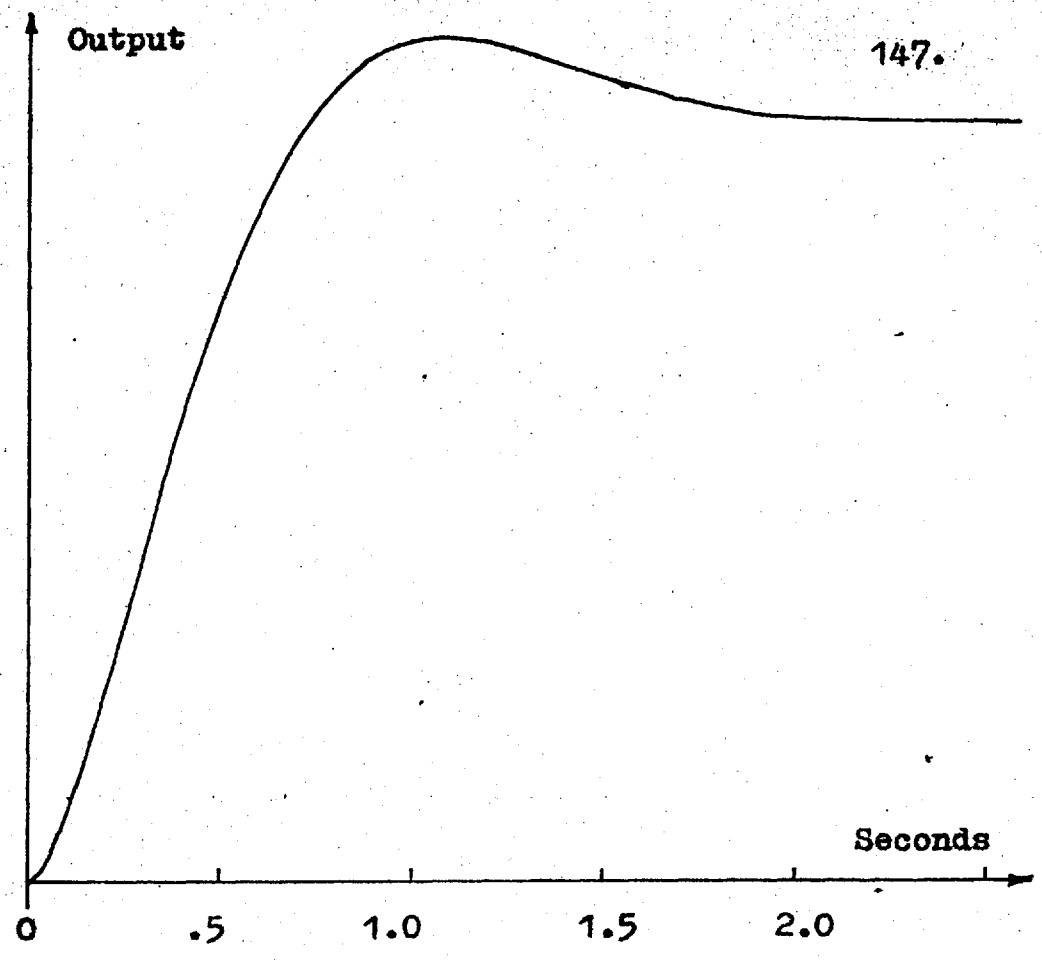

Fig. 7.8 Response of 2nd order simulation of Drive motors to a step input

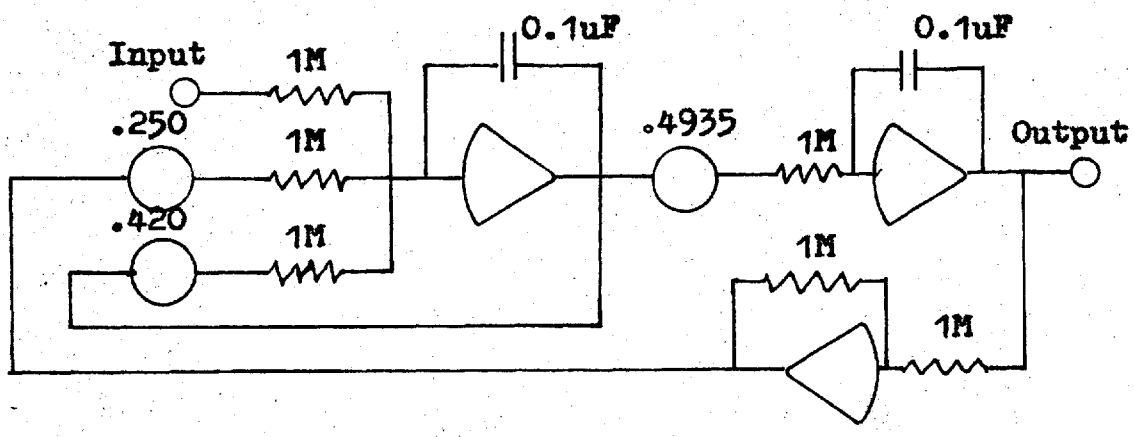

Fig. 7.9 Analogue Circuit of 2nd Order Drive Motor Simulation

8. RESULTS FROM THE ANALOGUE SIMULATIONS OF THE ROLLING MILL PROCESS

The following discussion is of information obtained from a series of experiments on the analogue simulations of the 4 stand tandem mill discussed in Chapter 7. It is inferred that the rolling mill itself would behave in a similar manner given the limitations of the simulations as discussed in previous chapters. Where possible comparison is made with published data logged directly from rolling mills.

The experiments in this chapter are open loop tests on the simulated mill without any form of gauge control being exerted. The purpose is to study the nature of the mill behaviour and to evaluate the circuit permitting simulation of the acceleration and deceleration phases of operation.

8.1. ACCURACY OF THE ANALOGUE SIMULATIONS

Table D.1. gives an indication of the accuracy with which the equations of Appendix D.2 were simulated. The columns 1 and 4 are lists of the steady-state values of the variables read from the analogue computer for a value of δH_o equal to a 40 volt step (0.008 inches). The columns 2 and 5 are the calculated values of these variables arrived at by solution of the equations of

Appendix D.2 through substitution of the values of the independent variables in each equation. Each equations must be checked and found satisfactory. Columns 3 and 6 show the deviations to be small. For a small value of a variable the percentage error can be significant, as in the case of δG_4 at 1950 feet per minute.

However, when the variable achieves a significant value the percentage error is greatly reduced, as for δG_4 in the 975 feet per minute case, as the voltage error remains in the same order. Thus any variable trace cannot be said to have a given percentage error (considering the analogue computation errors alone) but rather a voltage error which becomes less significant the larger the voltage. This is shown by the errors (columns 3 and 6) for δG_4.

The integrators were checked by summing their imputs; which should equal zero in the steady-state. This is shown in Table 8.1 for the interstand tensions which are the outputs of integrators. The sums of their inputs is small.

The columns 1 to 6 thus indicate that a reasonably accuract solution of the equations of Appendix D.2 has been obtained for this case. This means that the

simulation has been correctly programmed with the proper connections, amplifier gain settings and potentiometer settings.

Columns 7 and 8 show a comparison between the steady-state solution for the simulations of Fig. 7.2 and 7.7 for δH_o equal 20 volts (0.004 inches). The values should not be equal as different coefficients are used in each simulation. The results do show, however, that there is still close correspondence between the gauges and tensions for these differing schedules. The results in columns 7 were obtained using the analogue computer of the International Research and Development Company and those for column 8 using the analogue computer of the Mechanical Engineering Department at Imperial College.

8.2. EXPERIMENTS AT THE LIMITS OF THE SPEED RANGE

These experiments were conducted mainly on the simulation of Fig. 7.7. The servomultiplier potentiometers were set to give the 1950 feet per minute mill output speed coefficients and then the 975 feet per minute values.

Schedule deviations or oil film effects are not included as the experiments are at a specific operating

point speed. In effect the simulation of Fig. 7.7 is being used to give two cases of a simulation of the type of Fig. 7.2.

The test signal used was a step in incoming gauge error δH_o. The response of the variables to a step signal gives their transient behaviour. The response to a sine wave input is also shown for one case.

8.2.1. With Strip output speed 1950 feet per minute

Experiment (1) - With Slip Included

With the coefficients at the required value and the wind reel circuit included as shown in Fig. 7.7 the simulation was subjected to a 0.004 inch step (20 volts) in δH_o; the deviation in incoming gauge. (In the following discussion the word deviation or change etc. to account for the δ prefix in the variables, denoting changes about the nominal value of a variable, is used only where it may be misleading not to do so) In a number of these tests the diode across the integrator (Fig. 7.7) which yields $\delta\sigma_4$ is used to prevent this tension from going negative.

Figure 8.1(a) to 8.1(c) show the responses to the 0.004 step in δH_o. The gauge out of the first stand increases immediately, and after the delay of 2 seconds

it takes the error in gauge to reach the last stand the gauge out of the last stand increases significantly. However, the error in gauge is reduced by the inherent attenuation of the mill stands even with the decrease in tensions which tend to increase the gauge error.

Up to 0.99 seconds the torque δG_1 is increased by eight ton-inches (4 volts) and substitution of the values at this time in the δG_1 equation of Appendix D.2.1 shows that the major effects are from the thickness changes, with the tension contributing little due to its small change in this period. Checking the value of δF_1, which is 4.3 volts, for this period in the equation for δF_1 also confirms its value. There is also little change in the velocities as the torque and slip changes have been small. Thus for the time interval it takes the strip gauge error to reach the second stand there is a substantial change in δH_1 only. When the step error in gauge reaches the second stand it affects the variables associated with stand 2. The stand 2 slip, δF_2, is increased which increases the output velocity δV_2, and the increased strip thickness into stand 2 results in $\delta V_1'$ being reduced. The rolling torque, δG_2, required is decreased and this tends to increase the strip velocity from the stand,

although its effects are slightly delayed due to the motor dynamics. The velocity and thickness changes acting in accordance with the continuity and interstand tension equation (equation 4.9) reduce the tension $\delta\sigma_1$. This decrease in back tension and the increase in outgoing gauge of stand 2 offset the effects of the increase in incoming gauge to reduce the stand 2 rolling torque required. The reduction in $\delta\sigma_1$ effects the stand 1 variables - Fig. 7.7 shows the tension being fed back to stand 1. The rolling torque δG_1 required is increased and the roll force required is changed, hence there is a new equilibrium point (Fig. 2.4) due to the stand spring action; which is indicated by the slight increase in δH_1 at a time greater than 0.99 seconds.

During the period the strip gauge error takes to travel from stand 2 to stand 3, (0.99 to 1.58 seconds) there is a small reduction in $\delta\sigma_2$, due to the increase in δV_2, which reduces the rolling torque δG_3 required at stand 3. The reduction in required δG_3 and the change in slips increase δV_3 which causes a reduction in $\delta\sigma_3$ as shown, and so δG_4 is reduced slightly; which as in the case of stand 3 results in an increase in the strip velocity issuing from stand 4.

The step in gauge reaches stand 3; 1.58 seconds after its application to stand 1. This results in another major change in many of the variables. The effects at stand 3 are similar to those which occurred at stand 2 when the step passed it. There is an increase in δF_3, a decrease in $\delta\sigma_2$ and δG_3. Here however, the change in torque is not so great as the effects of the incoming gauge is greater as indicated by the coefficient for this variable in the δG_3 equation of Appendix D.2.1. As before the effects of the step arriving at stand 3 are fed back down the mill to the preceding stands and ahead to the following stands. A decrease of $\delta\sigma_2$ increases the torque required at stand 2, reduces the slip and results in a new force equilibrium which yields a slight increase in the gauge from stand 2. A small increase in $\delta\sigma_1$ has also occurred which reduces slightly the gauge from stand 1 and the torque required at stand 1. At stand 4 the decrease in tension $\delta\sigma_3$ has resulted in a small increase in the gauge issuing from stand 4.

At time 2.0 seconds after application of the step at stand 1 the step reaches the fourth stand. The output gauge δH_4 increases and the back tension $\delta\sigma_3$

decreases as a result of a decrease in $\delta V_3'$ in accordance with the equation 4.9. The reduction in $\delta\sigma_3$ results in an increase in the rolling torque δG_3 and a reduction in δG_4.

From the traces for rolling torque it is evident that each time the step reaches a stand there is a large increase in the torque required at the preceding stand. Except for stand 3 torque (δG_3) there is not such a noticeable effect on the preceding stands. It is also evident that it is the major change in the back tensions which occurs when the step reaches a stand which is responsible for these torque changes, and the remaining variable changes which occur at the preceding stands. In each case the arrival of the step at a stand has much less effect on the front tension of that stand and so the changes in the gauges and torques at the following stands are smaller than those for the preceding stands.

In Fig. 8.1(a) the traces of δH_1^* and δH_4^*, the gauge measurements made by the x-ray gauges, are shown. The δH_1^* and δH_4^* are the strip characteristics. The gauge signal read and produced by the x-ray gauge is also shown. The smoothing effect of the gauge dynamics is evident.

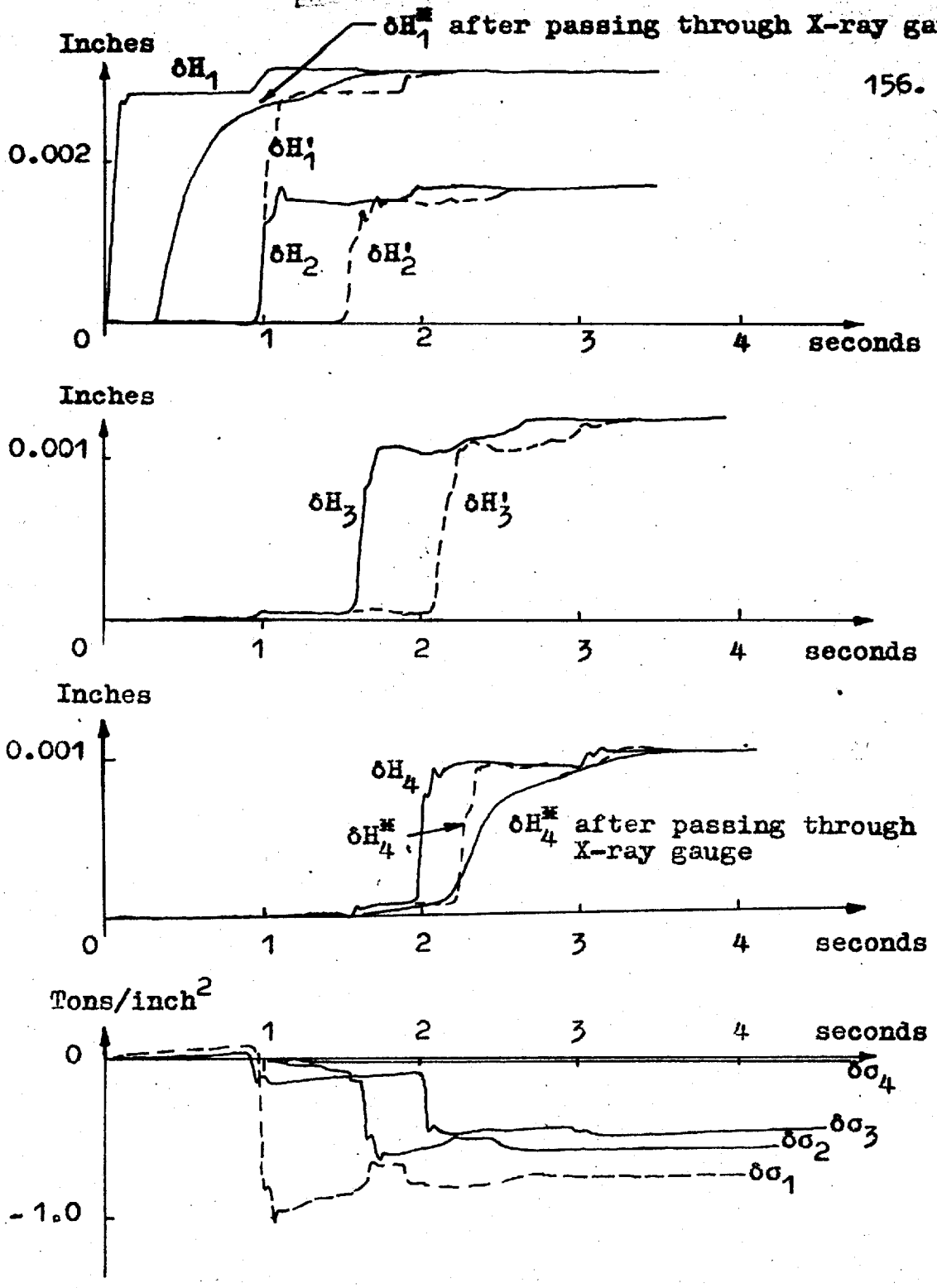

Fig. 8.1(a) Responses to 0.004 inch Step at 1950 feet per minute With Slip.
(Ref. Section 8.2 Experiment (1))

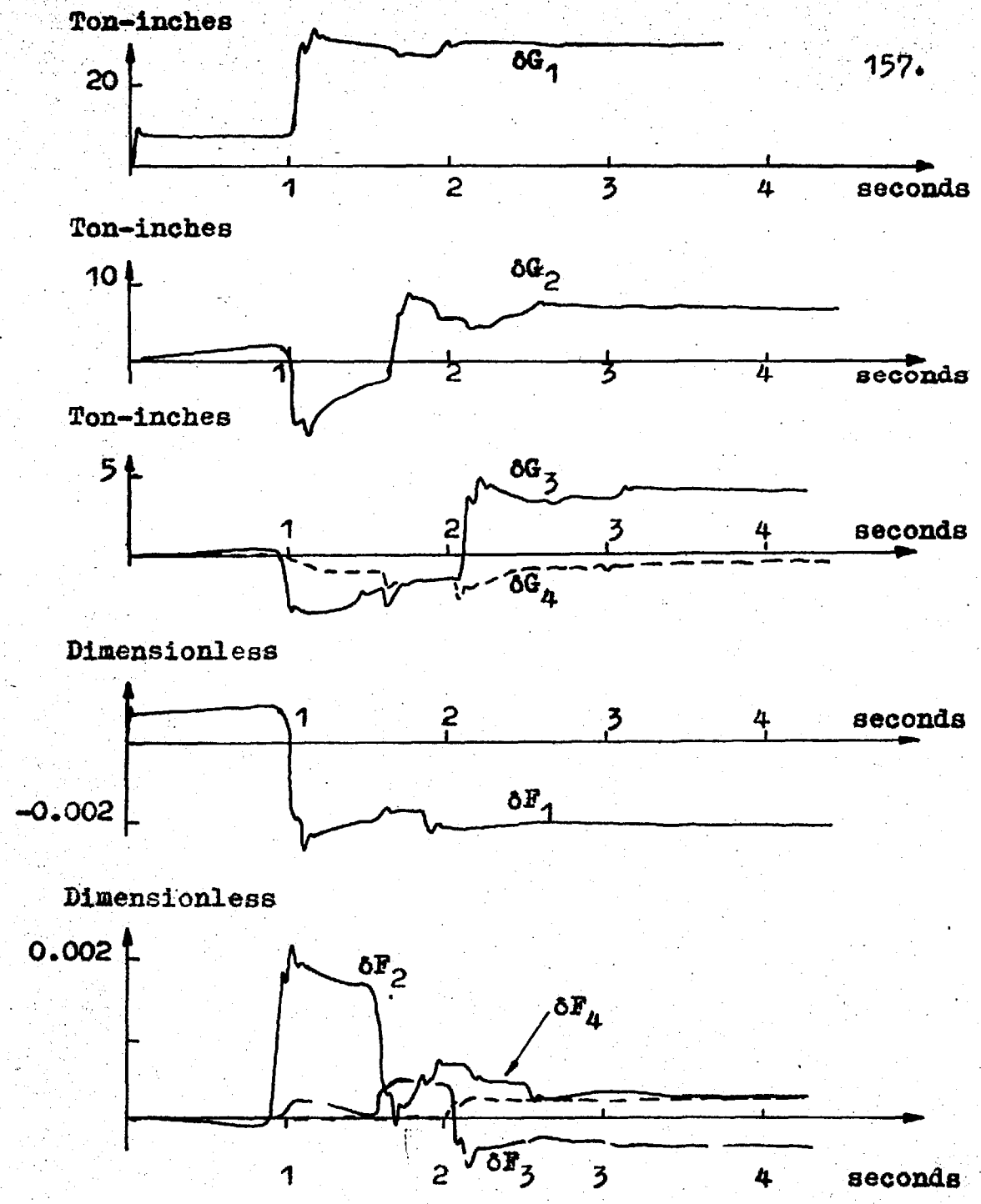

Fig. 8.1(b) Continuation of Fig. 8.1(a)

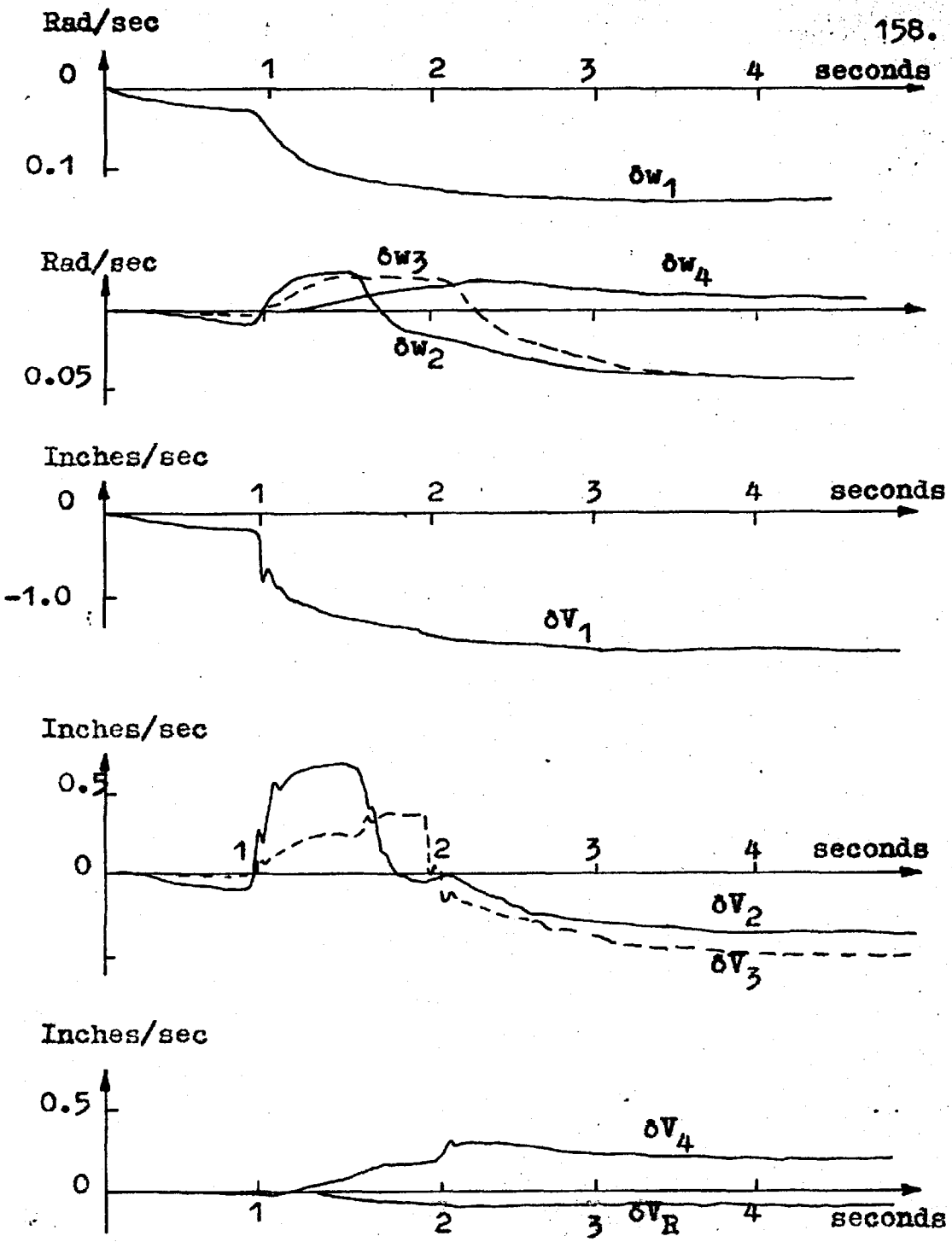

Fig. 8.1(c) Continuation of Fig. 8.1(a)

Experiment (2) - With Slip Not Included

With the simulation set for the 1950 feet per minute case and the slips removed from the simulation experiment (1) was repeated. The effects of slip may be removed from the simulation simply by removing the output lead from the amplifiers which have slip as their outputs (Fig. 7.7).

Figures 8.2(a) and 8.2(b) are traces of the results obtained. Comparing these to Figures 8.1(a) to 8.1(c) obtained from experiment (1) indicates little difference in the steady-state values of the variables. The gauge δH_4 has increased slightly (0.0001 inches) and δG_2 has decreased slightly as have the tensions (0.1 tons/inch^2). However with the slips removed it is evident that the stand rolling torque transients are larger and more varied than for the case with slip included which indicates that the slip tends to have a smoothing effect on the rolling torque requirements.

The Experiments (1) and (2) were repeated with the wind reel circuit omitted from the simulation. This case corresponds to $\delta\sigma_4$ becoming zero and since this is the value to which it was held in the previous experiments by the diode limiter preventing $\delta\sigma_4$ from going negative there should be negligible change in

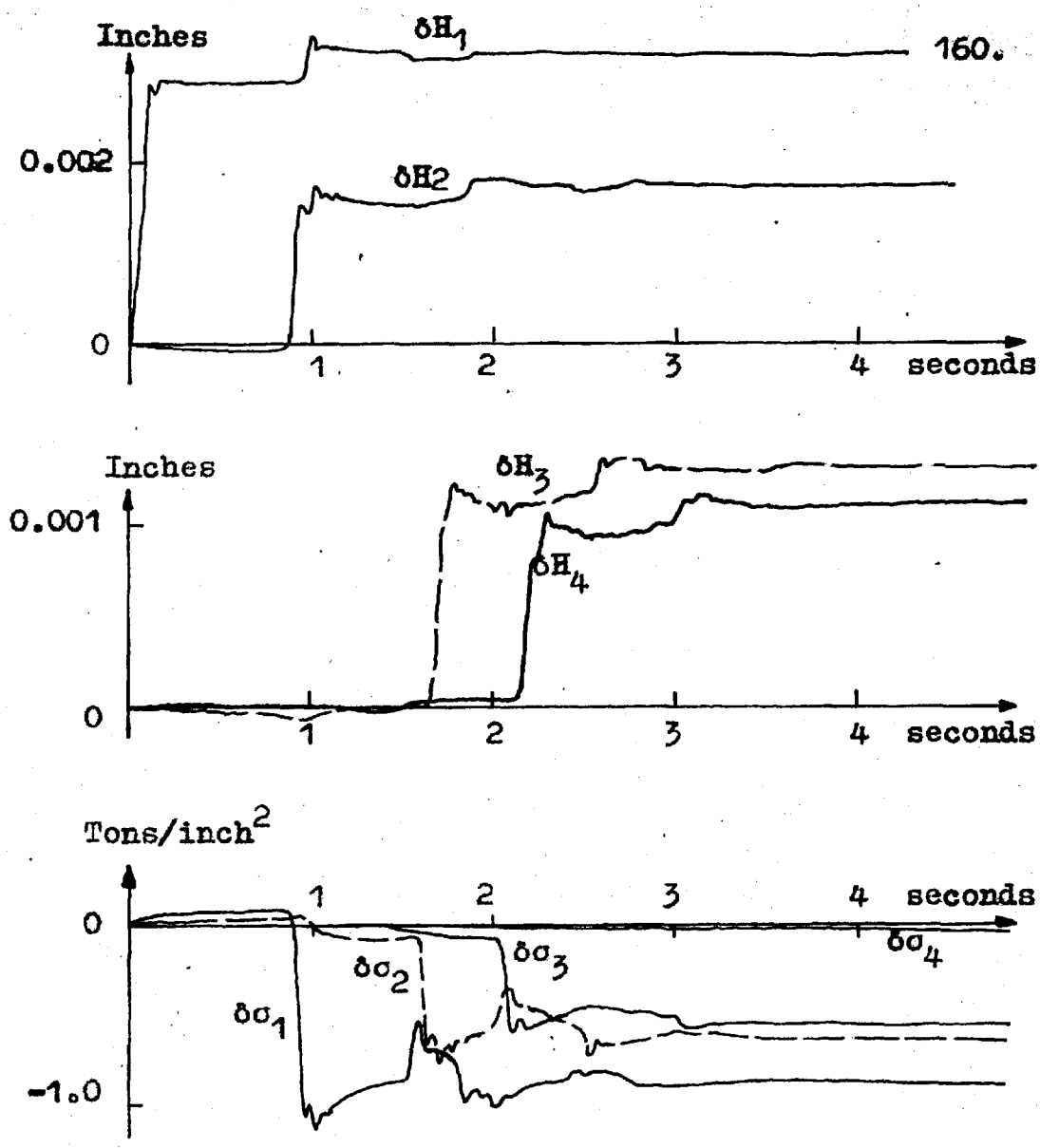

Fig. 8.2(a) Responses to 0.004 inch Step at 1950 feet per minute Without Slip (Ref. Section 8.2 Experiment (2)).

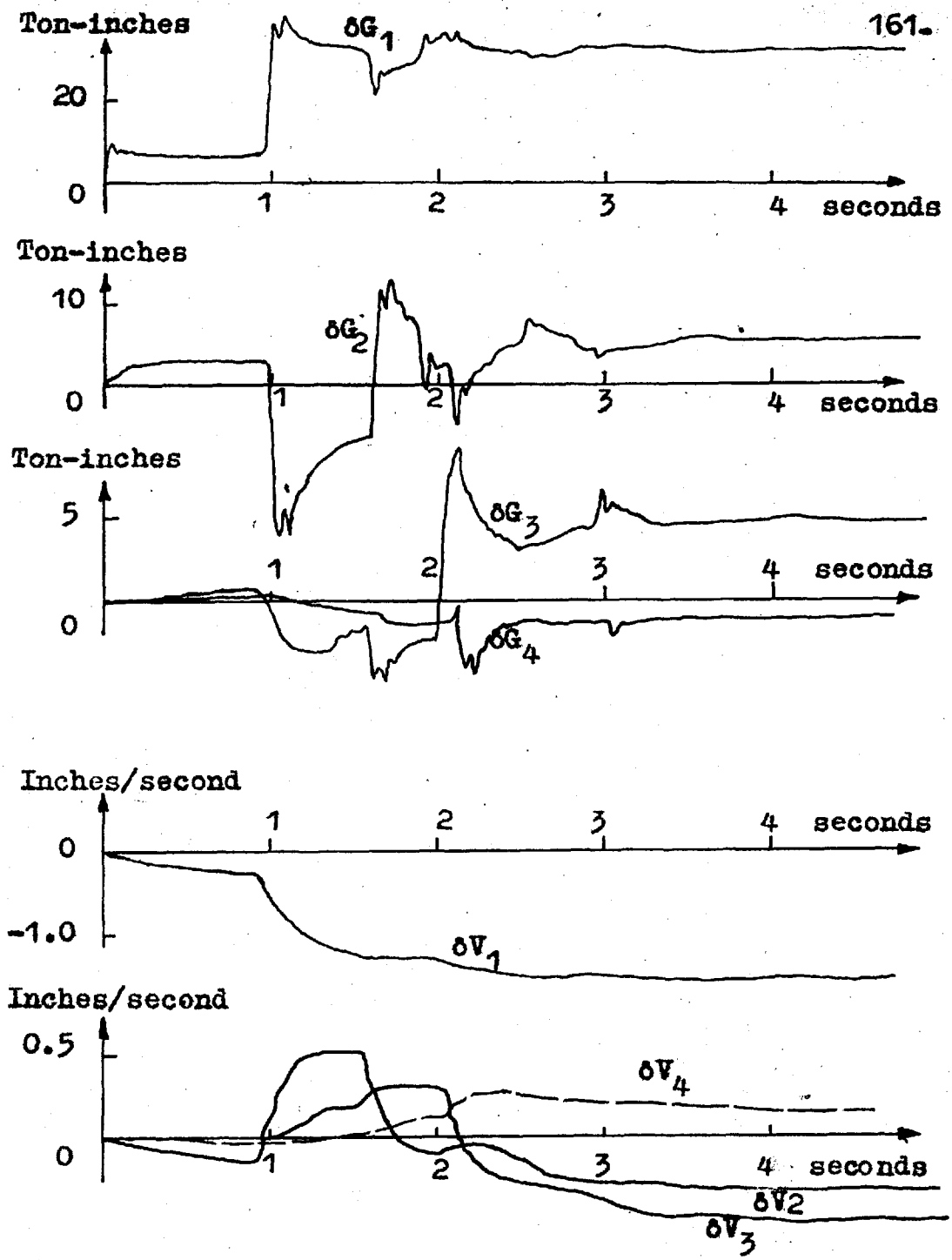

Fig. 8.2(b) Continuation of Fig. 8.2(a)

in the results. There was a small increase of 5% in $\delta\sigma_3$ and of 2% in δH_4 due to the fact that $\delta\sigma_4$ had not been perfectly limited and did have a small negative value in the experiment with the reel included as shown in Fig. 8.1(a)

Experiment (3) With a Second Order Motor Torque - Speed Relationship and With Slip Included

With the coefficient settings still at the 1950 feet per minute case the motor torque-speed dynamics were changed to second order relations for each stand (Fig. 7.8).

The results with slip included are shown in Figures 8.3(a) to 8.3(c). The steady-state values for a 0.004 inch step (20 volts) in δH_o are identical to those for Experiment (1) which is a check on the simulation. The most noticeable effect is the more oscillatory nature of the variable transients. This is expected as the second order relation allows overshoot which the first order lag or exponential relation used previously does not.

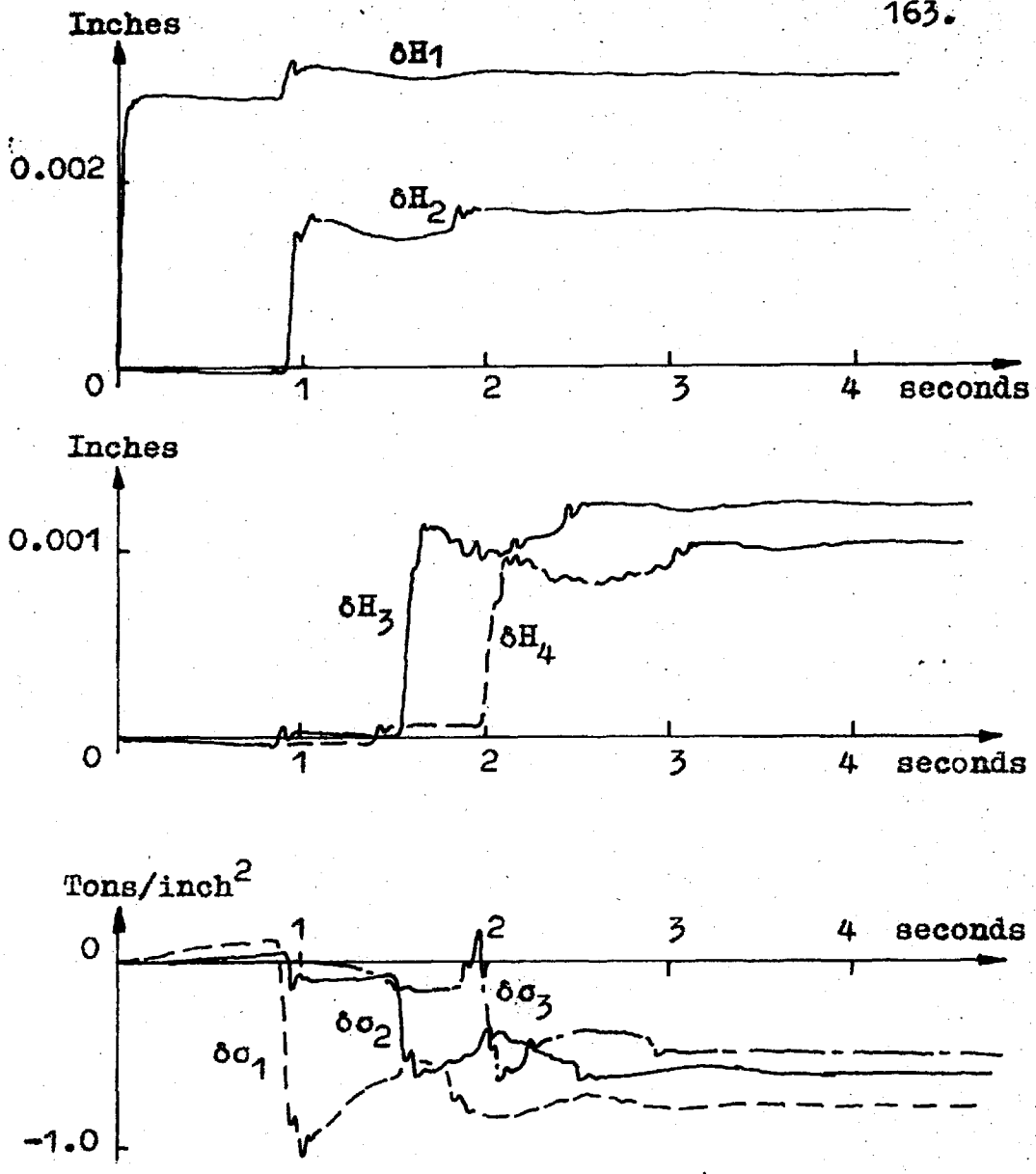

Fig. 8.3(a) Responses to 0.004 inch Step at 1950 feet per minute With Second Order Torque-Speed Relation and Slip (Ref. Section 8.2 Experiment (3)).

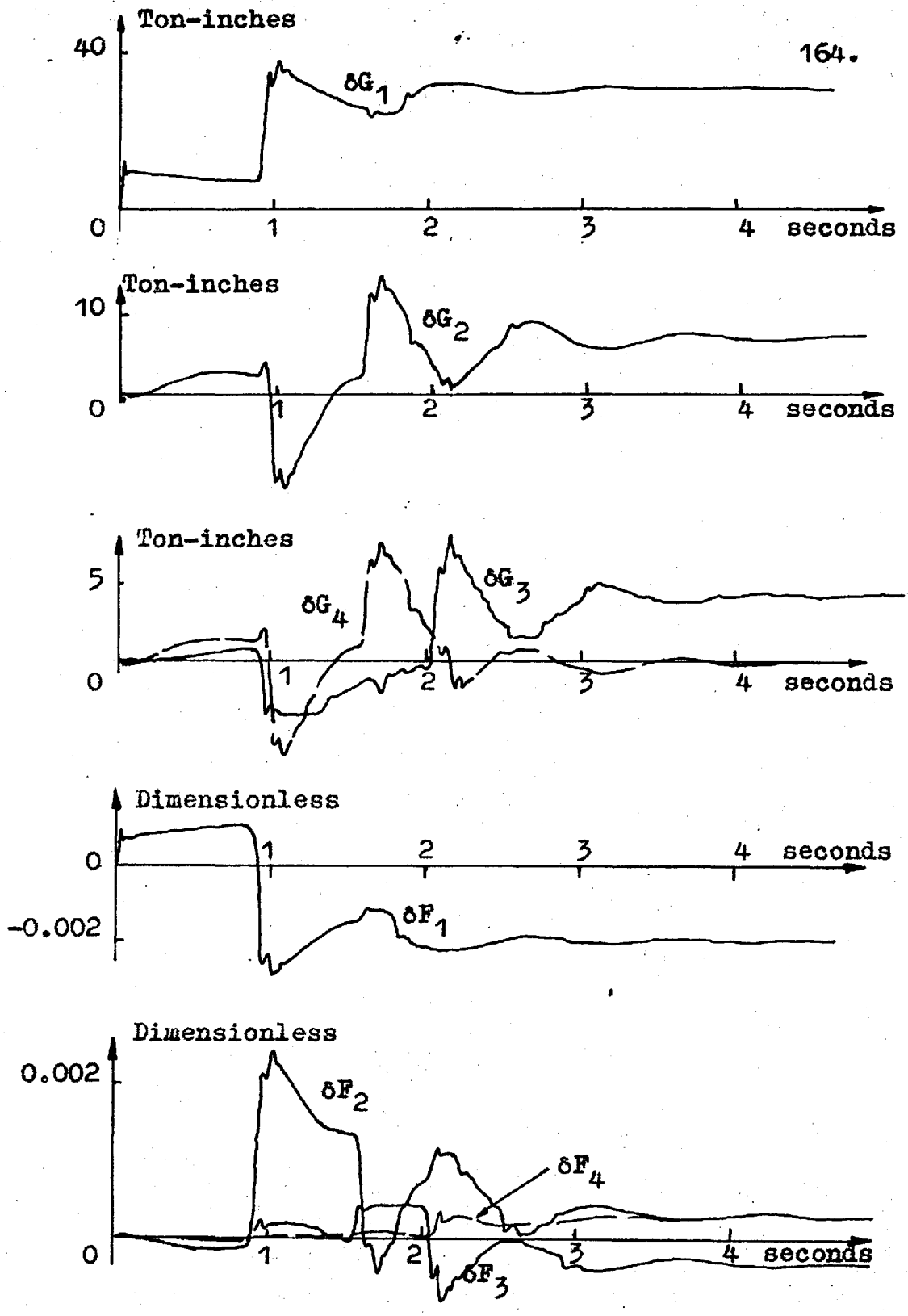

Fig. 8.3(b) Continuation of Fig. 8.3(a)

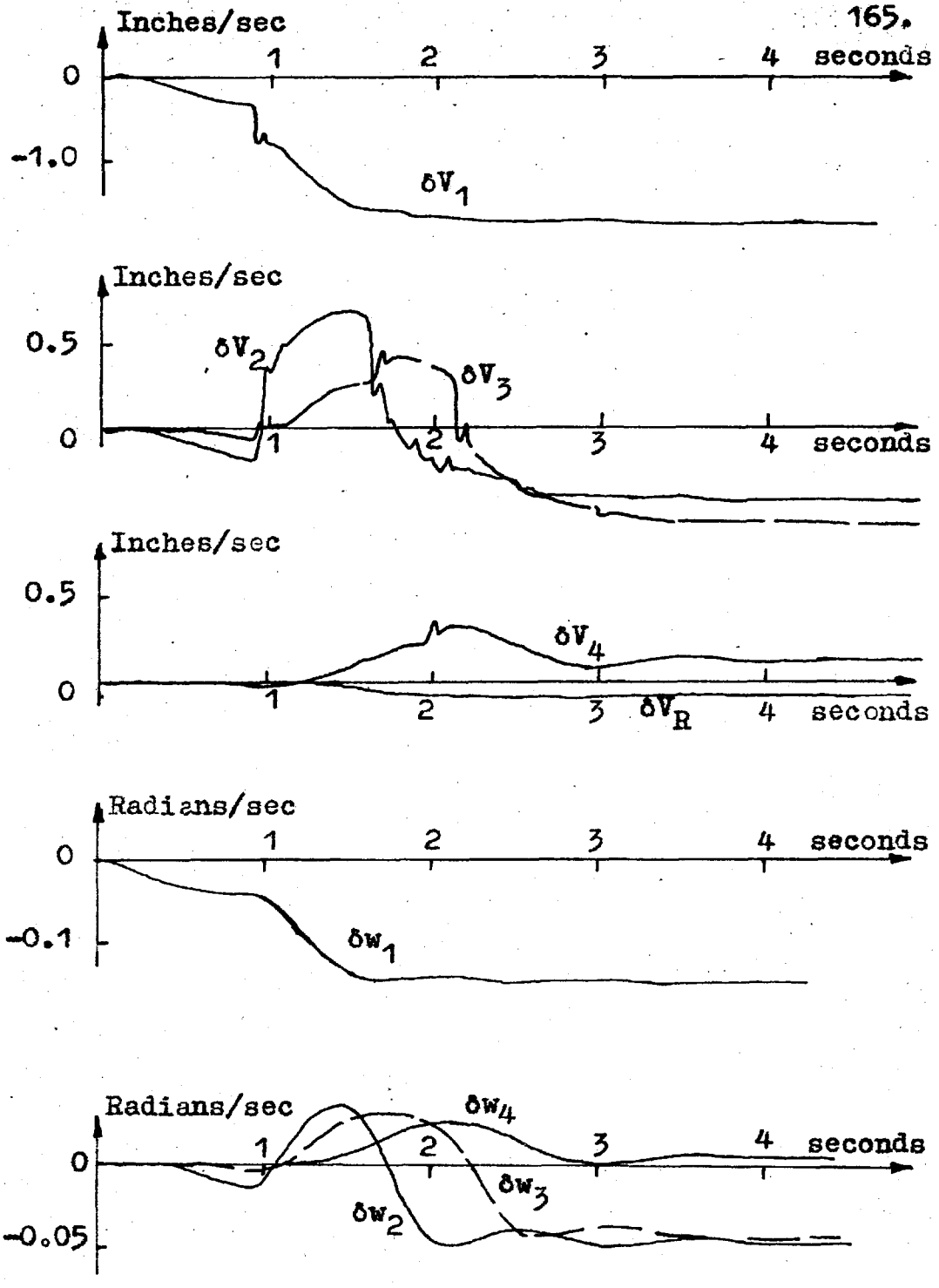

Fig. 8.3(c) Continuation of Fig. 8.3(a)

Experiment (4) - With a Second Order Motor Torque Speed Relationship and With Slip Not Included

Removing the slip as a variable in the simulation of experiment (3) and imposing a 0.004 inch (20 volt) step in δH_o resulted in the traces of Figures 8.4(a) and 8.4(b). Here all the variables are noticeably more oscillatory than for experiment (3) with slip included; and even more so than the tests with the first order lag. Comparing the results with those for experiment (3) it is obvious that slip has a smoothing effect on all variables, thus its elimination from a rolling mill simulation would result in the simulation yielding more oscillatory results than would actually be obtained from the rolling mill in which the slip is an inherent feature.

As can be seen from Fig. 7.7 the slip acts through the strip velocities which determine the nature of the interstand tensions. For the present case without slip the strip velocity traces are much more oscillatory than for the case with slip included. The nature of the slip changes are such that they tend to cancel the roll speed fluctuations, which results in smoother velocity transients and hence less varied transients for the tensions and other variables.

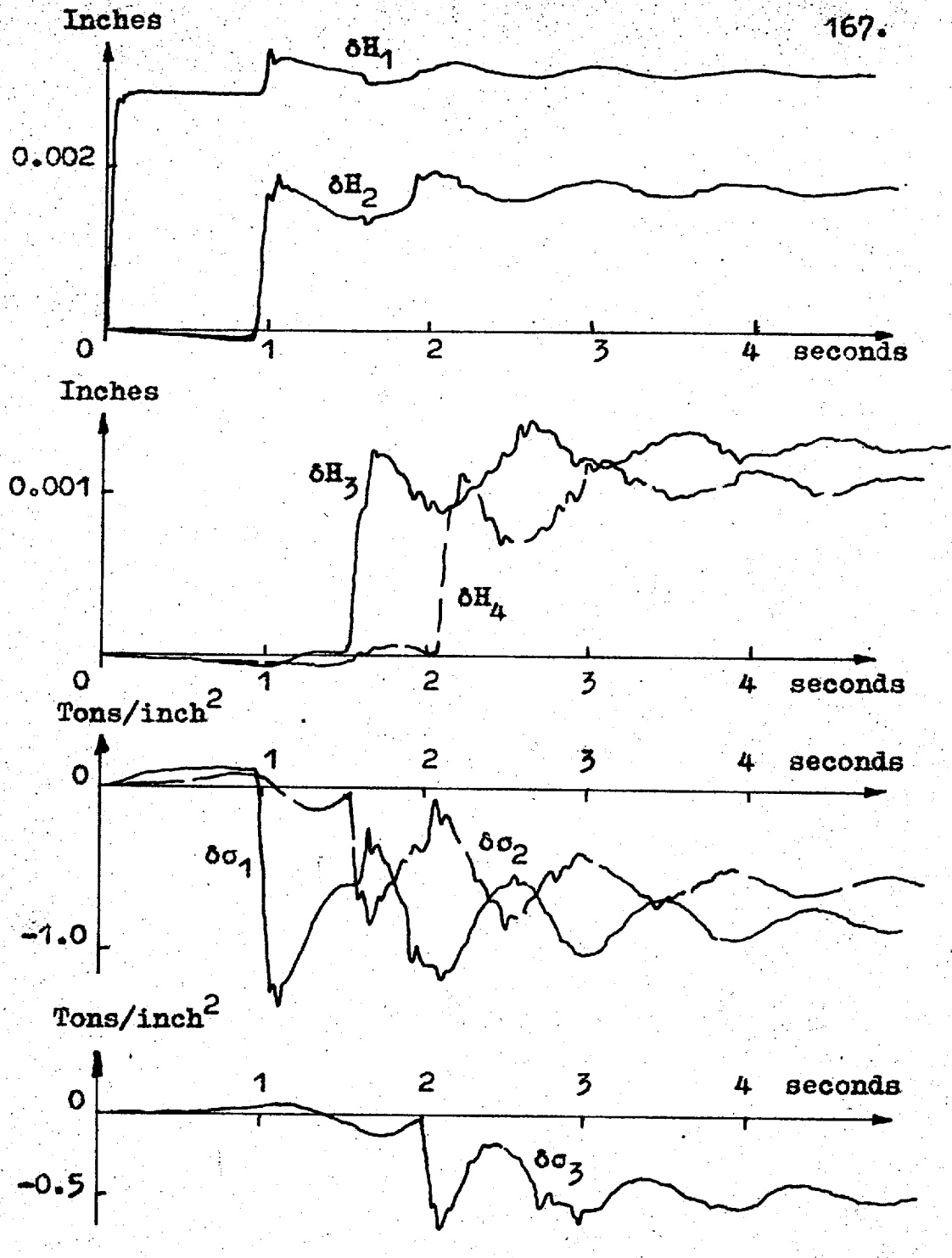

Fig. 8.4(a) Responses to 0.004 inch Step at 1950 feet per minute with Second Order Torque-Speed Relation Without Slip (Ref. Section 8.2 Experiment (4)).

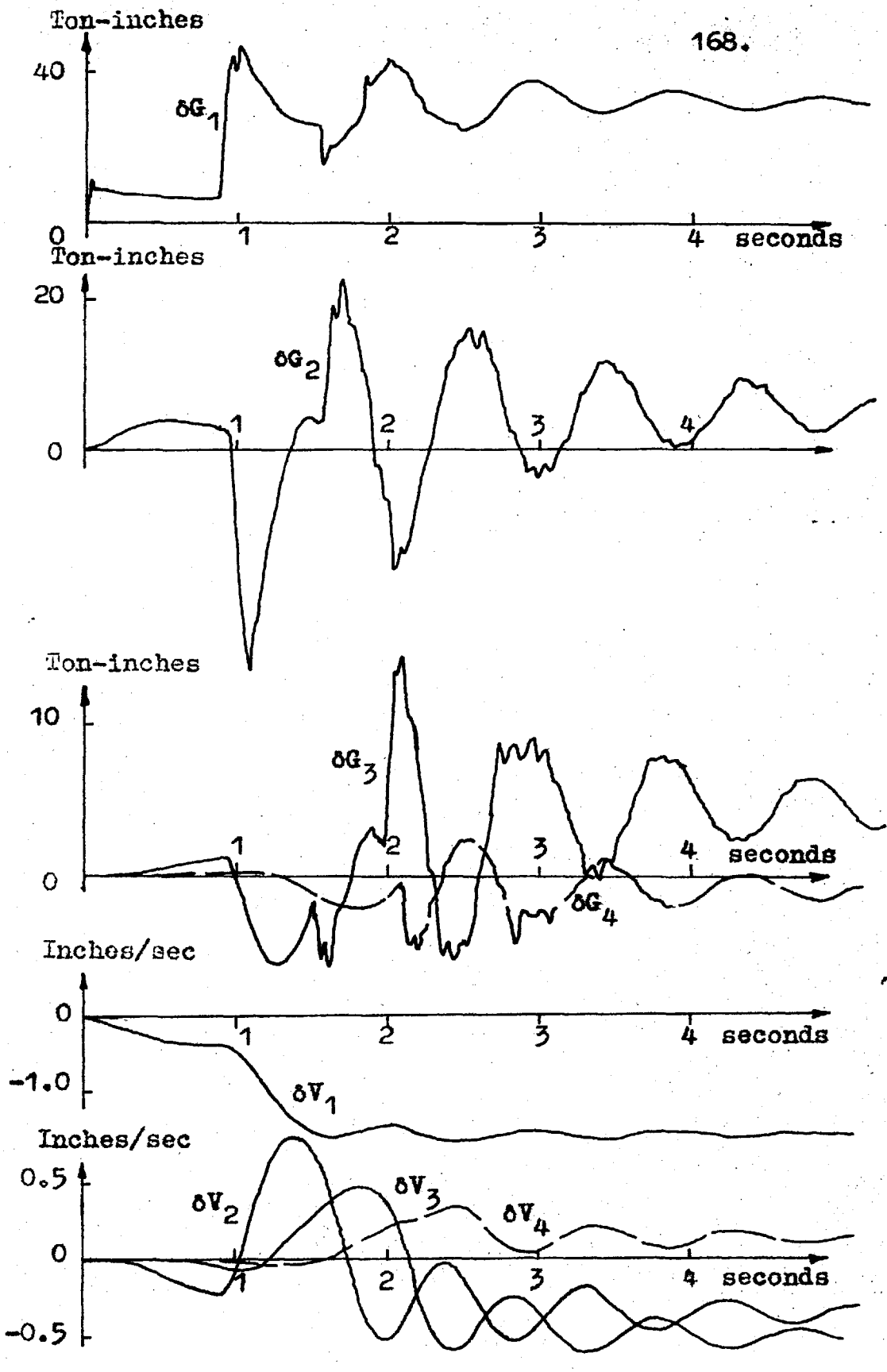

Fig. 8.4(b) Continuation of Fig. 8.4(a)

That many of the tests use first order lags rather than the second order relations for the torque speed relation which gives a more oscillatory transient is, as discussed in section 7.7, a generalisation, as often the response of the motors in practice is a lag. The experiments with the second order relationship indicate the effects as the motor responses become more complex.

Experiment (5) Response to a Sinusoidal Gauge Variation

Fig. 8.5 shows the response of the simulation of Fig. 7.2 to a sinusoidal incoming gauge error of 0.008 inch peak to peak magnitude and a frequency of 0.1 cycles per second. The traces show the mill variables following the sinusoid and the gauge error being attenuated as in the case for the step responses.

8.2.2. With Strip Output Speed 975 Feet per Minute

The experiment numbers are continued from the previous section.

Experiment (6) - With Slip Included

The coefficients in the simulation of Fig. 7.7 were set for the 975 feet per minute output speed case by bringing the servomultiplier potentiometers to the bottom. The results of testing this simulation with a 0.004 inch (20 volt) step in δH_o are shown in Fig. 8.6(a)

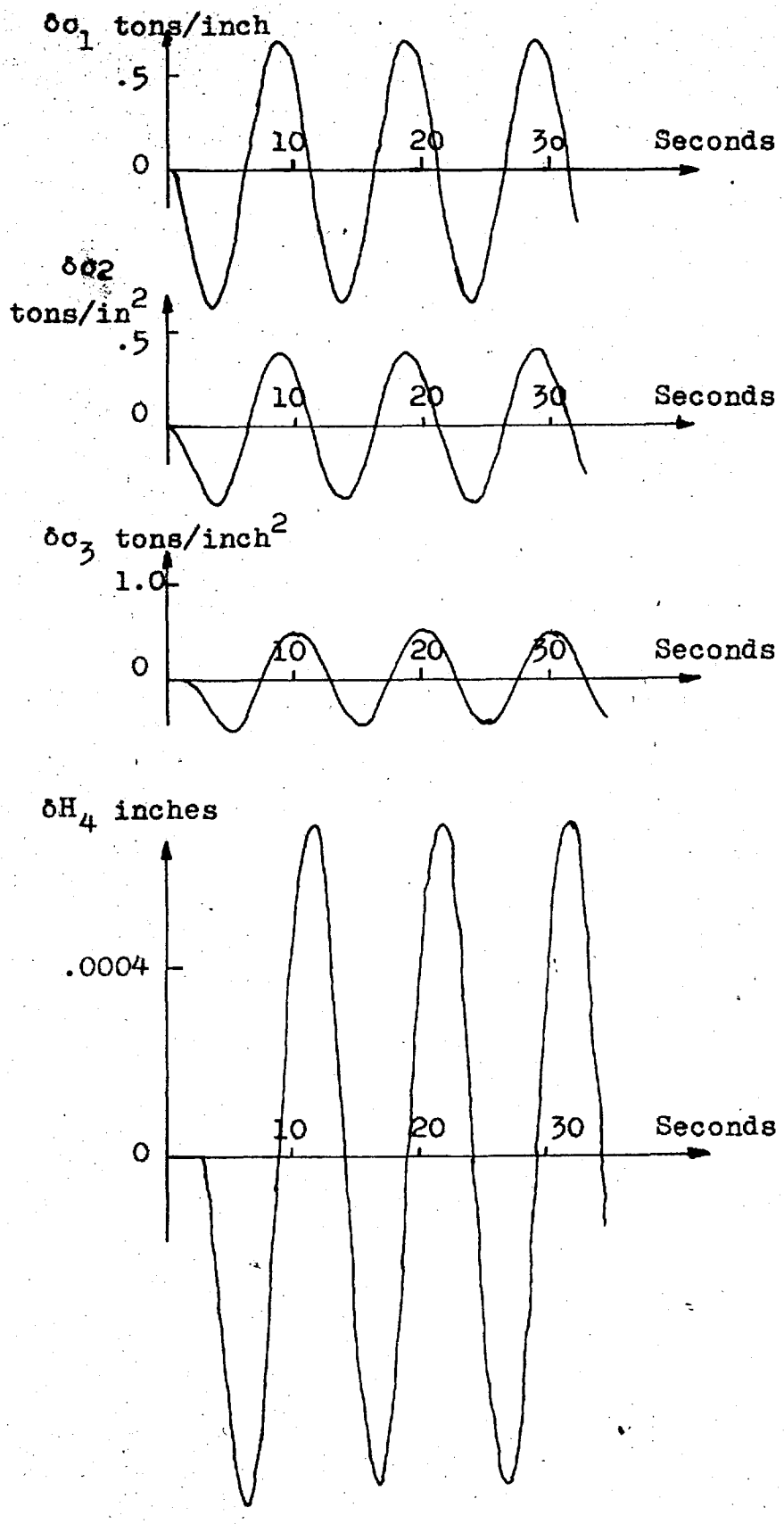

Fig. 8.5 Responses to a 0.008 peak-peak sine of 0.1 cps at 1950 feet per minute (Ref. Section 8.2 Experiment (5)).

to 8.6(d). There is a noticeable change in the transients and in the steady-state values of the variables compared with those of experiment (1), the 1950 feet per minute case. The steady-state values for a 40 volt step can be compared in Table 8.1.

The major reason for the change in the steady-state values is the change in the coefficients of the interstand tension equations and the motor droops as indicated by comparison of the relevant equations in Appendix D.2. Referring to equation 4.9 it can be seen that the coefficients for the gauge deviation terms are direct functions of the nominal strip speed. Since the nominal strip speed has been halved, the tension transients are correspondingly reduced. It is interesting to note that the resulting δH_4 is also halved due to this smaller decrease in the interstand tensions and due to $\delta\sigma_4$ having a positive value in this experiment.

Figure 8.6(a) shows overshoots in the gauges from stands 2, 3 and 4, that is, they assume a negative value before rising to their steady-state positive values. This is due to the interstand tension transients (Fig. 8.6(a)) which are seen to be positive for some time before becoming negative which results in

thinner strip issuing from the stands. This effect results in part from the increase in the motor droops for the lower speed case which give velocity transients of a larger magnitude. This results in a tendency for the tensions to increase while the step is travelling between stands. Since the tension changes due to the step arriving at a stand, which tend to make the tensions negative, are smaller than for the 1950 feet per minute case a positive value for some interstand tensions results during the transient period.

Another factor operating to provide the overshoot in gauge values is that once the gauge has overshot at stand 2 as shown it causes an increase in tensions at the following stands, in the same way that it was previously shown in Experiment (1) that an increase in gauge operates to reduce the tension. The increase in tensions reduces the gauge from the stands concerned.

The smaller reduction of tensions gives a smaller increase in the rolling torque required at stand 1 and an increase in that required at stand 4 over the values for Experiment (1). The rolling torques δG_2 and δG_3 have also increased over the values for Experiment (1).

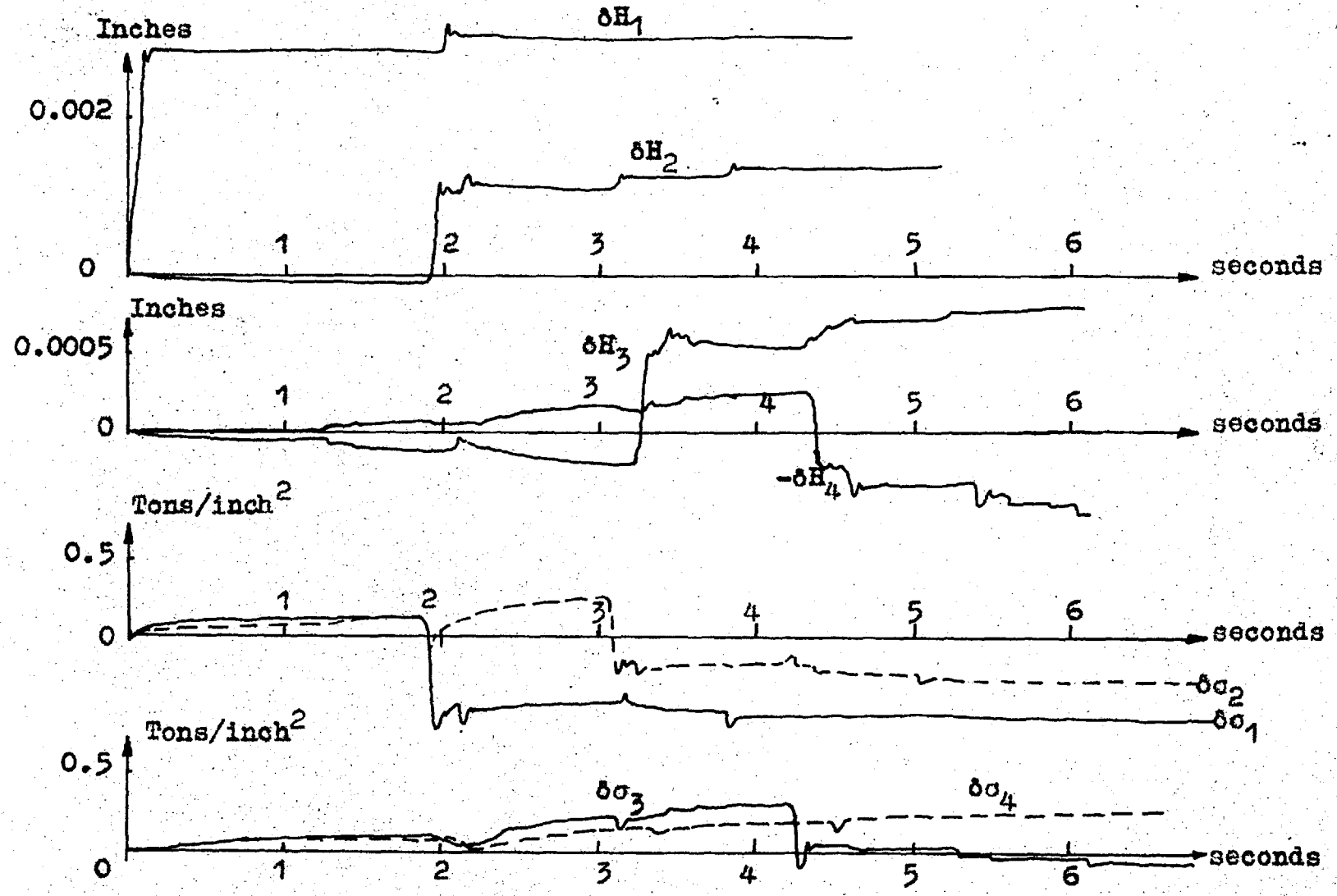

Fig. 8.6(a) Responses to a 0.004 inch Step at 975 feet per minute With Slip (Ref. Section 8.2 Experiment (6)).

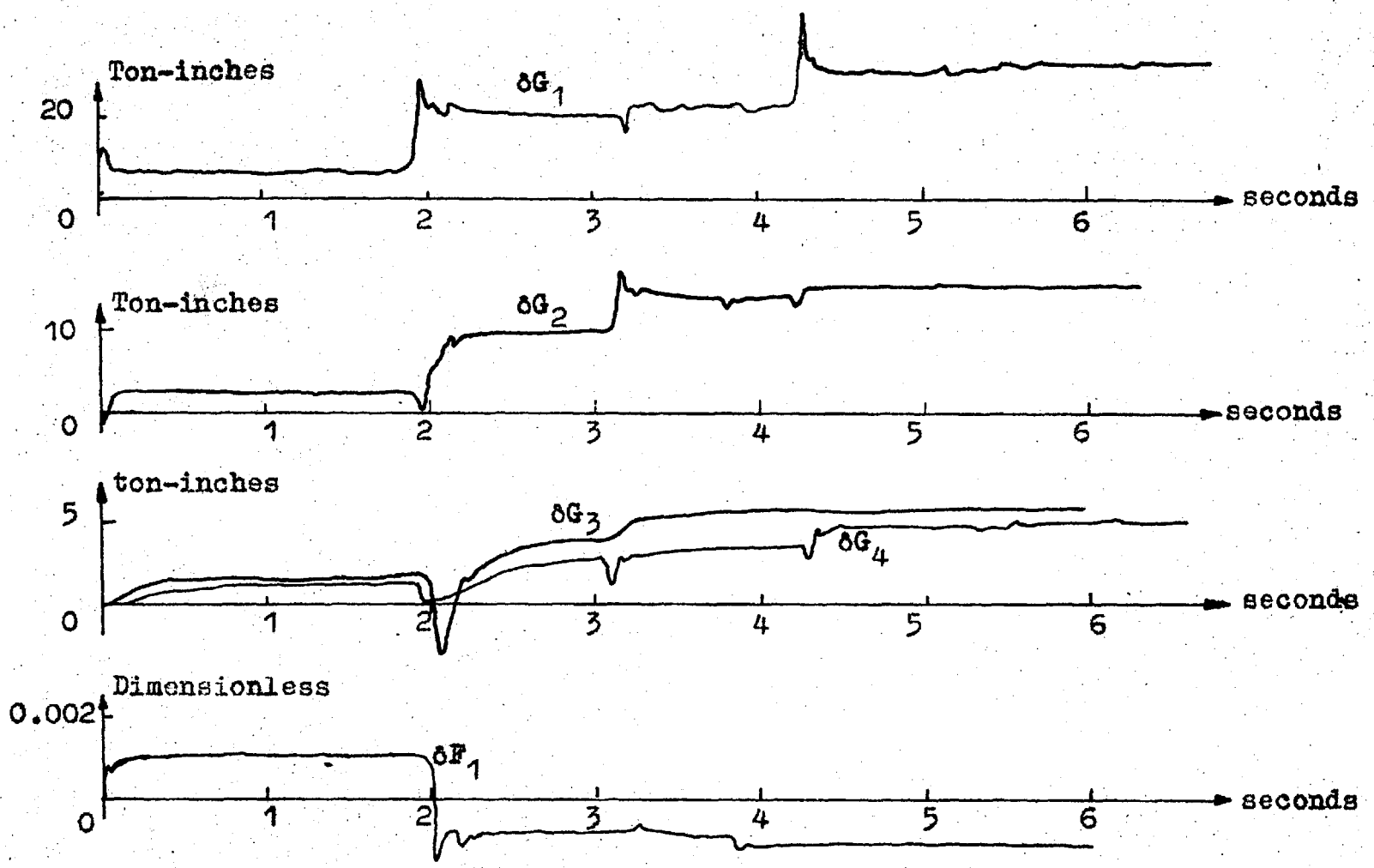

Fig. 8.6(b) Continuation of Fig. 8.6(a)

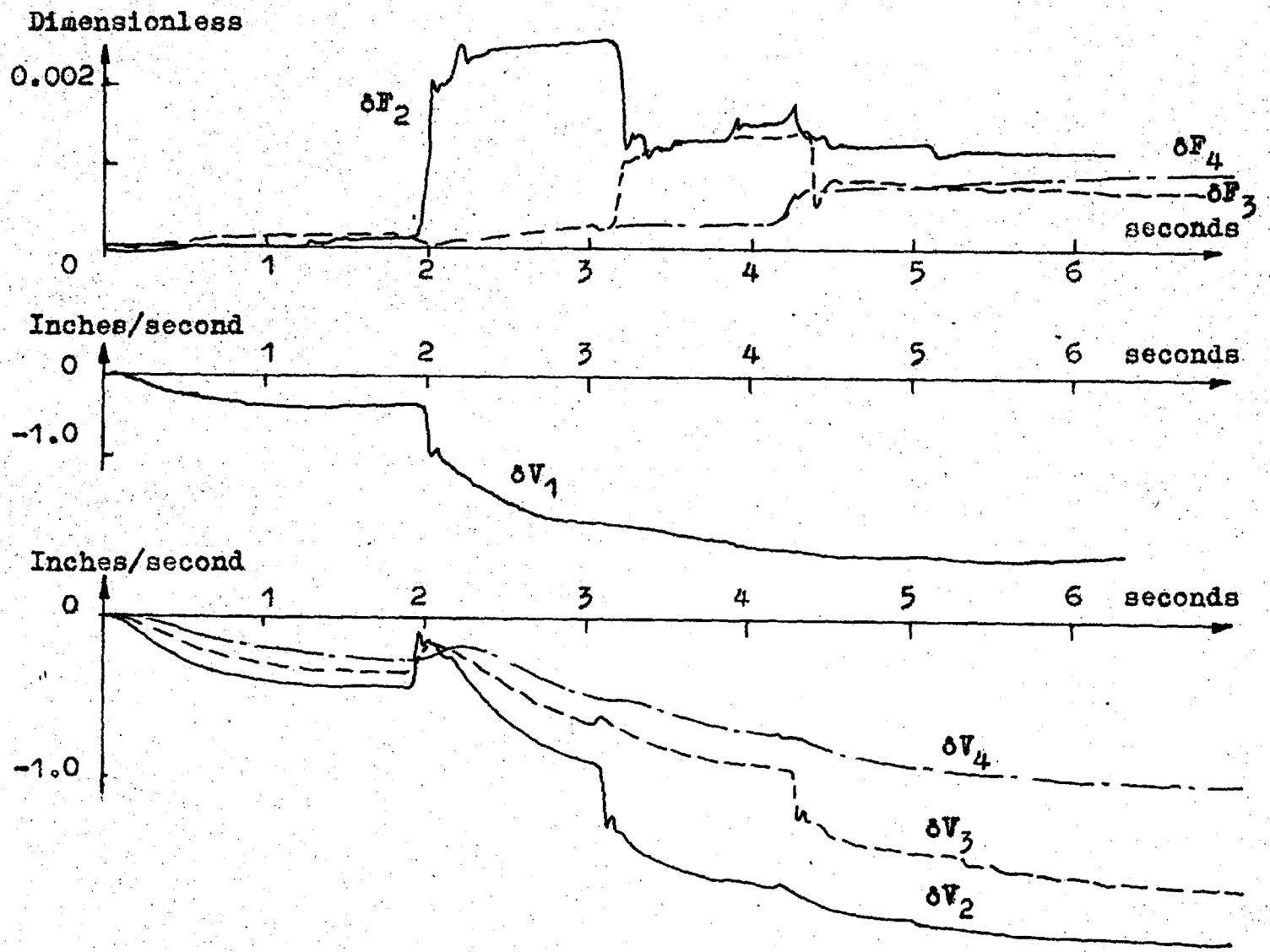

Fig. 8.6(c) Continuation of Fig. 8.6(a)

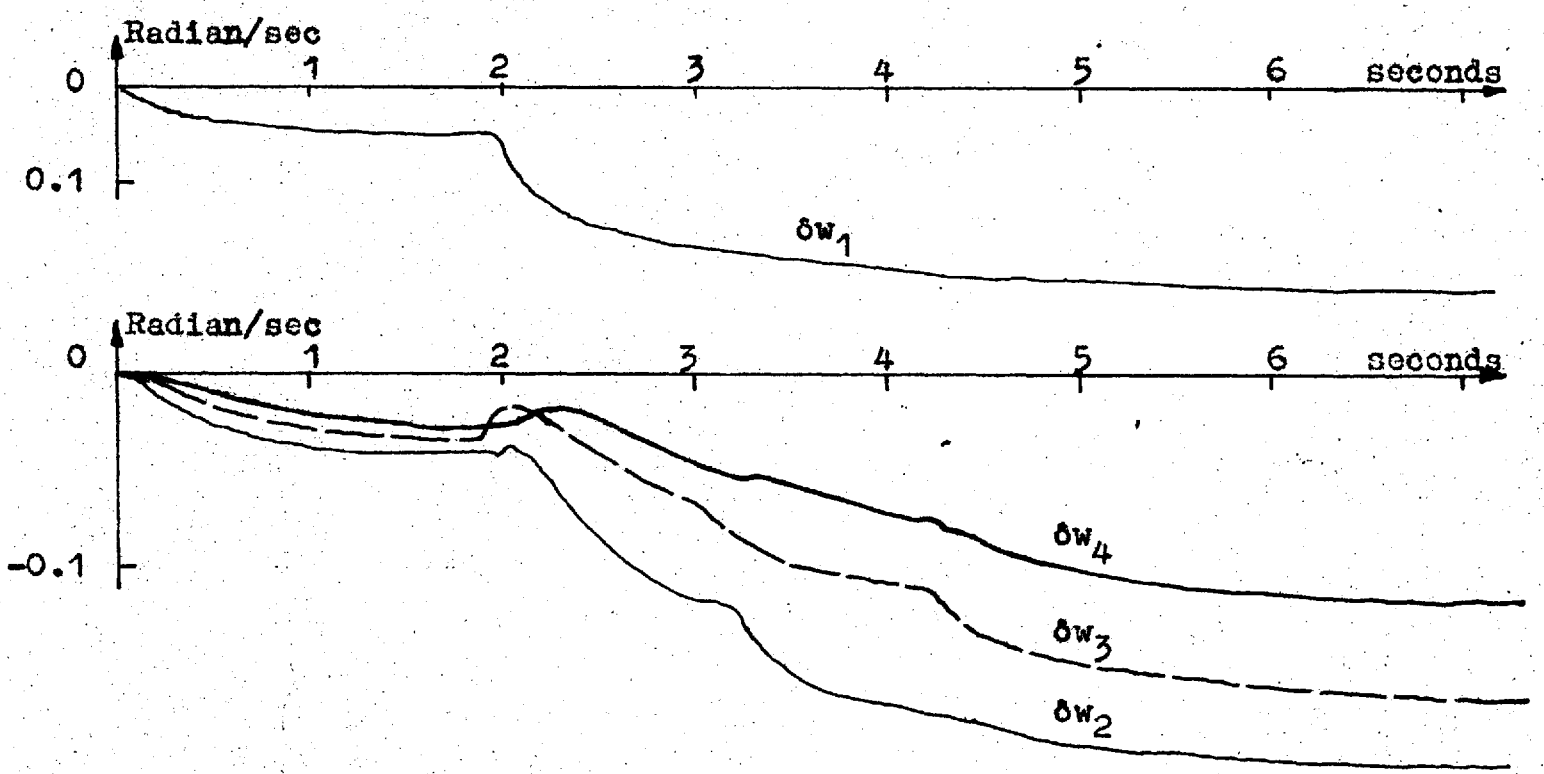

Fig. 8.6(d) Continuation of Fig. 8.6(a)

Comparing the gauges issuing from the stands to those for Experiment (1), the values for stand 1 are close; as the tension $\delta\sigma_1$ has not changed greatly and the tension coefficient is small in the relevant gauge equation (Appendix D.2) compared to the coefficient for the incoming thickness at stand 1. At the other stands the stand output gauge deviations become progressively smaller for the present case.

As in the 1950 feet per minute case little change was noticed for traces made of the primary variables with the reel circuit removed except for a small increase in $\delta\sigma_3$ of 0.08 tons/inch^2 and in δH_4 of 0.0001 inches.

This experiment was repeated with the reel circuit omitted with only slight changes noted in the variables associated with the last stand.

Experiment (7) - With Slip Not Included

As in Experiment (2) the slips were removed from the simulation with all coefficients still set for the 975 feet per minute case. Fig. 8.7 shows some of the results. Here the time scale is 2 seconds per inch. Comparing the results to those for the case with slip, Experiment (6), there is a noticeable change in the tension and rolling torque transients.

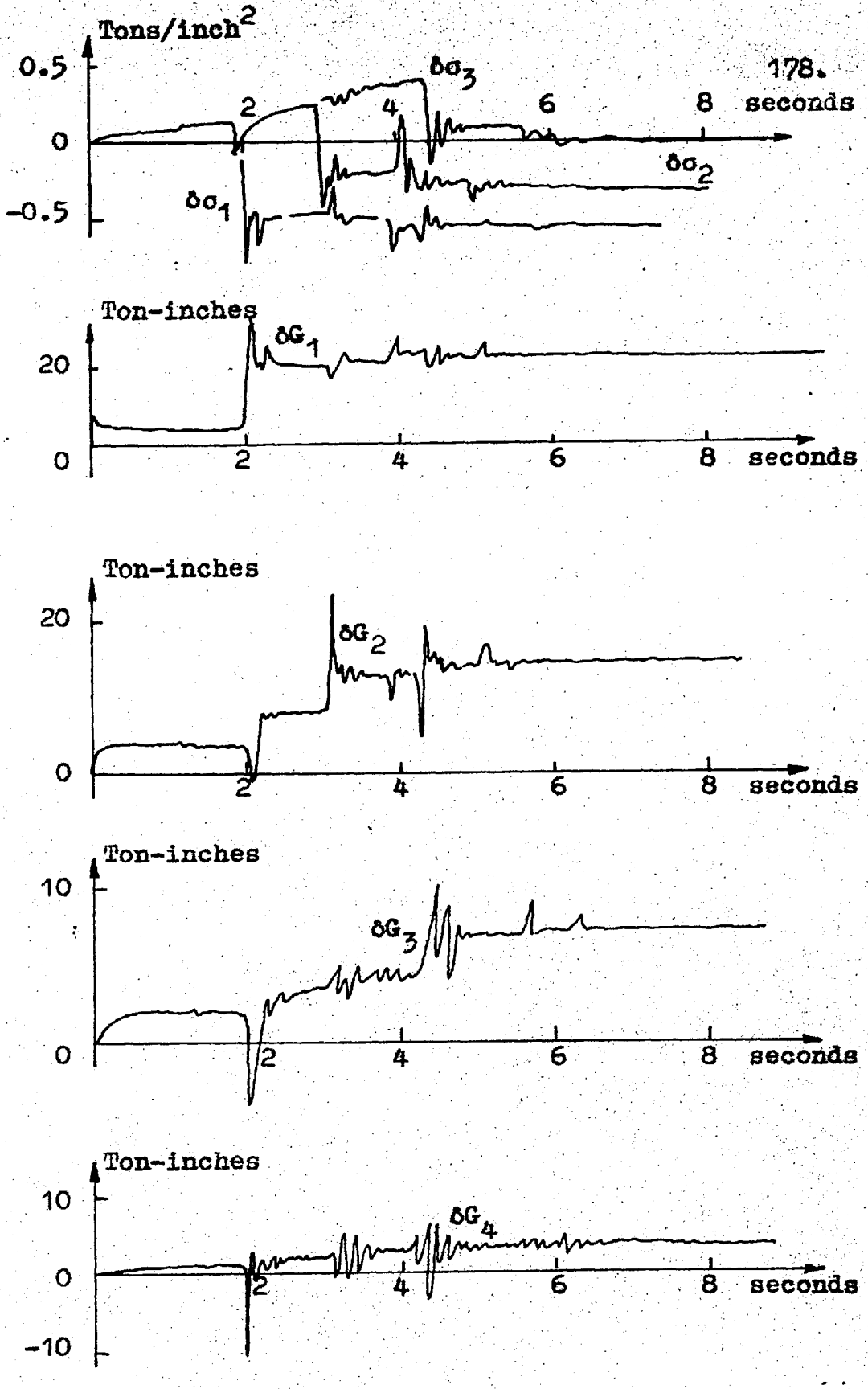

Fig. 8.7 Some Responses to a 0.004 inch Step at 975 feet per minute Without Slip (Ref. Section 8.2 Experiment (7)).

As in the 1950 feet per minute experiment the slip has a noticeable smoothing effect which is even more pronounced for the present 975 feet per minute case.

There is a small change in the steady-state values of the variables with the slip removed, δH_2 is slightly decreased and δH_4 is increased slightly over the values for Experiment (6).

To conduct this experiment, it was necessary to reduce to reel circuit gain from 0.1277 to 0.018 in order to prevent $\delta\sigma_4$ from oscillating. This was not required when the slip was included.

8.3. EXPERIMENTS WITH VARIABLE MILL VELOCITY

For the following experiments the simulation of Fig. 7.7 was used.

8.3.1. Acceleration and Deceleration in the Range 975 to 1950 feet per minute Output Speed

The experiment numbers are continued from the previous section.

Experiment (8) Acceleration and Deceleration With Bearing Roll Neck Oil Film and a Roll Force Schedule Deviation

Table 8.2 lists the values of the bearing roll neck oil film thickness change (ΔS_{or}) and the deviation from the roll force schedule (ΔP_r) used in this experiment. The ΔS_{or} values are of the same order as would be experienced in practice (11, 22, 30, 37) for the speed range considered. The deviations from the roll force schedule (ΔP_r) are arbitrary values corresponding to the case in which the stand roll gaps have not been sufficiently increased during acceleration or decreased during deceleration to maintain the schedule. Dividing the roll force deviations by the stand spring constants yields the equivalent screw movement causing ΔP_r. This may be summed to the oil film effect, allowing both signals to be introduced into the simulation from one servomultiplier potentiometer as shown Fig. 7.7.

Table 8.2 Schedule Deviations for Experiment (8)

Quantity	Units	Stand			
		1	2	3	4
ΔS_{or}	thou	-4	-4	-5	-5
ΔP_r	tons	-67.6	-65.3	-82.7	-155.5
$\Delta P_r/M$	thou	-6.76	-6.53	-8.27	-15.55
$\Delta S_o+\Delta P_r/M$	thou	-10.76	-10.53	-13.27	-20.55

Table 8.2(a) Oil Films for Experiment 8(a)

Quantity	Units	1	2	3	4
ΔS_{or}	thou	-4	-4	-5	-5

Table 8.2(b) Schedule Deviations for Experiment 8(b)

Quantity	Units	1	2	3	4
ΔS_{or}	thou	-4	-4	-5	-5
ΔP_r	tons	-67.6	-65.3	-82.7	-155.5
$\Delta P_r/M$	thou	-6.76	-6.53	-8.27	-15.55
$\Delta S_o+\Delta P_r/M$	thou	-10.76	-10.53	-13.27	-20.55
Δw_r	Rad/sec	9.44	27.28	21.30	25.2

To obtain the change in roll gap from the screw movements, the screw movements must be operated on by a factor (sometimes called the stand transfer function) as indicated by the gauge equations in Appendix D.2.1.

The values in Table 8.2 are the total variations over the speed range considering the 975 feet per minute case as base when the values of these parameters would be zero. The traces shown in Figs. 8.8(a) to 8.8(r) are variations from the values existing at 975 feet per minute. In these figures the traces of the variables for acceleration and deceleration are shown side by side.

The servomultiplier drive signal, or mill velocity profile, is shown in Fig. 8.8(a). Acceleration is constant at approximately 200 feet per minute per second, as is the deceleration. For this test the drive motor dynamics are represented by first order lags.

The effect of the acceleration and deceleration on the gauges issuing from the stands is shown in Figs. 8.8(b) and 8.8(c). As expected during acceleration the gauges decrease and during deceleration they increase over the values existing at high speed.

The traces in Figs. 8.8(b) to 8.8(r) show the changes that occur in the mill variables. To assess the changes,

the steady-state changes at each stand may be considered in turn. In Table D.2, of Appendix D, the steady-state values of the variables for a -0.010 inch movement in screw position, δS_r, at each stand in turn are listed. The screw down motion is shown to be most effective at changing the gauges.when applied at stand 1 and least effective when applied at stand 4. This is in agreement with practical experience. It is also noted that when the stand 2, 3 or 4 are closed the gauge out of the preceding stand increases. This is because of the large decrease in back tension. This does not apply at stand 1 where the back tension is taken as constant. This large decrease in back tensions results in a much larger roll torque required at the preceding stand as shown in Table D.2. The results in Table D.2 (and D.3) were obtained with the mill set at the high and low speed cases in turn as in the experiments of Section 8.2.

The change in the variables as noted in the Figs. 8.8(b) to 8.8(r) during acceleration and deceleration can now be shown to be in agreement with the results of Table D.2. That this is so indicates that the simulation of Fig. 7.7. does represent the acceleration

and deceleration phases of mill operation for the ΔS_{or} and ΔP_r selected as the Figures were recorded during simulated acceleration and deceleration. The gauge out of each stand decreases during acceleration and increases during deceleration (Figs. 8.8(b) and 8.8(c)). During acceleration the large reductions in the stand back tensions noted in the Table leads to a net reduction of all interstand tensions (Figs. 8.8(d) to 8.8(f)). The large decrease in $\delta\sigma_3$ overcomes the effects of the smaller decrease in $\delta\sigma_4$ to reduce the rolling torque required at stand 4 (Fig. 8.8(i)). The rolling torques at the remaining stands have increased (Figs. 8.8(g) to 8.8(h)) primarily due to the decrease in front tensions at these stands being larger than the decrease in back tensions; the difference in strip cross sectional areas being accounted for. Since the torques required have increased at stands 1, 2 and 3, leading to reduction in roll speed; and the slips have decreased, except for the small increase at stand 1 (Figs. 8.8(j) and 8.8(k)), there is a reduction in the strip velocities from the stands. This is a small decrease over the existing nominal strip velocities out the stands. The changes in torques, roll speeds and velocities are again supported by the results in Table D.2.

In reference (22) an actual mill, accelerated to 300 meters per minute showed a net decrease in strip output thickness and an increase in roll force with a simultaneous reduction in interstand tensions. When accelerating the reverse occurred. This is in agreement with the simulation results described. The mill results (22) were more complex; as a more non-linear relationship between roll speed and oil film thickness was noted. Also a lower speed range and different schedule was used.

Fig. 8.8(s) from Reference (30) shows roll force changes lagged directly while varying the mill speed as shown in the lower curve. As noted the roll force increases during acceleration and decreases during deceleration. The equivalent roll neck oil film thickness change causing this is noted (M = 12 tons/thou) and agrees with the values used for the speed range studied in the present simulation.

The progressively longer time it takes the gauge from each following stand to reach the steady state when acceleration or deceleration has terminated (Fig. 8.8(b) and 8.8(c)) is due to the delay times. The time taken to reach the steady state is longer when decelerating; close to 9 seconds although deceleration is complete in 5 seconds. The remaining 4 seconds is the time it takes for perturbations at the 1st stand to reach the last

stand at low speed. The effect of the increasing time delays and droops during deceleration also tends to make the gauges traces less linear than for the acceleration case.

In Figs. 8.8(d) to 8.8(f), the interstand tension traces, there is a tendency for the tensions to overshoot. In this experiment the tension σ_4 was not restrained from going negative. The overshoot in tensions is due to the velocities continuing to vary when acceleration or deceleration is complete, due to the time delays. The mill velocity profile used (Fig. 8.8(a)) brings the mill simulation sharply to a constant speed which seems to contribute to larger overshoots, as later experiments using a mill velocity profile with a less severe corner do not show such large overshoots. That the motor droops are larger for the low speed case contributes to the overshoots being larger when completing deceleration than when completing acceleration.

In the Figs. 8.8(b) to 8.8(c) the dashed line traces are for the case with slip removed from the simulation. As discussed in Section 8.2, slip effects the strip velocities, and hence the tensions. The tension changes noted cause small changes in the δH_1 and $\delta H_2'$ traces.

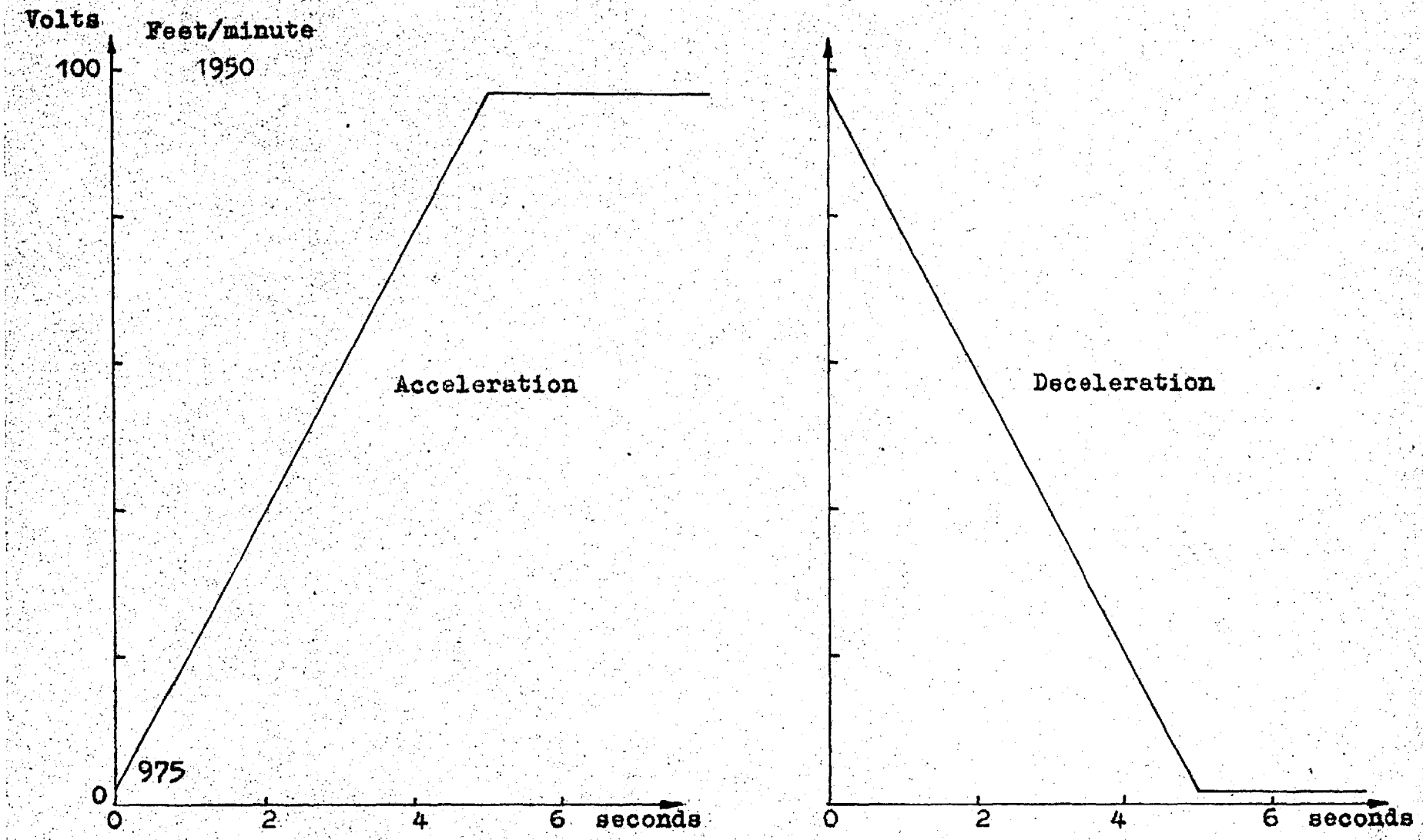

Fig. 8.8(a) Mill Velocity Characteristics Imparted to Servomultipliers in Fig. 7.7 (Ref. Section 8.3 Experiment (8)).

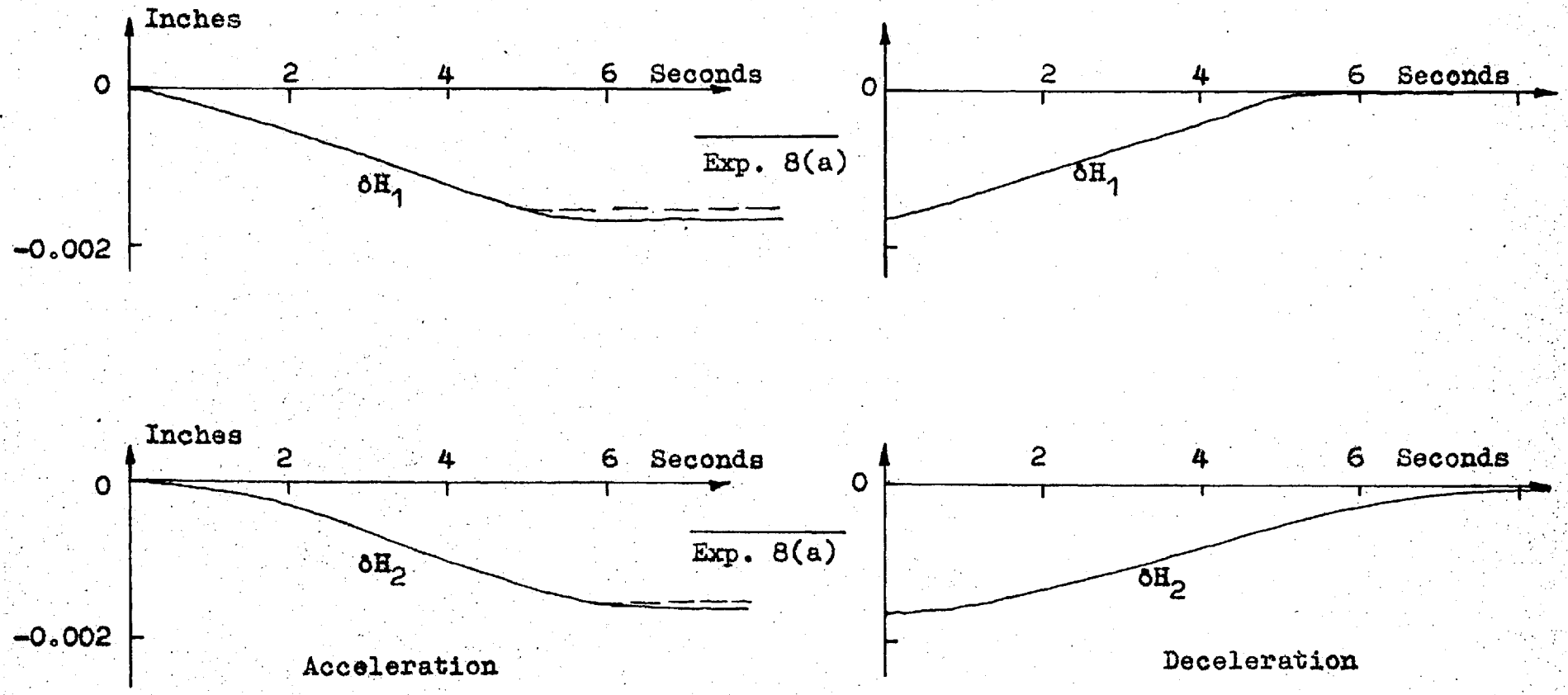

Fig. 8.8(b) Responses to Schedule Deviations of Table 8.2 When Subjected to the Mill Velocity Characteristics of Fig. 8.8(a) (Ref. Section 8.3 Experiment (8)).

— — — — Without Slip

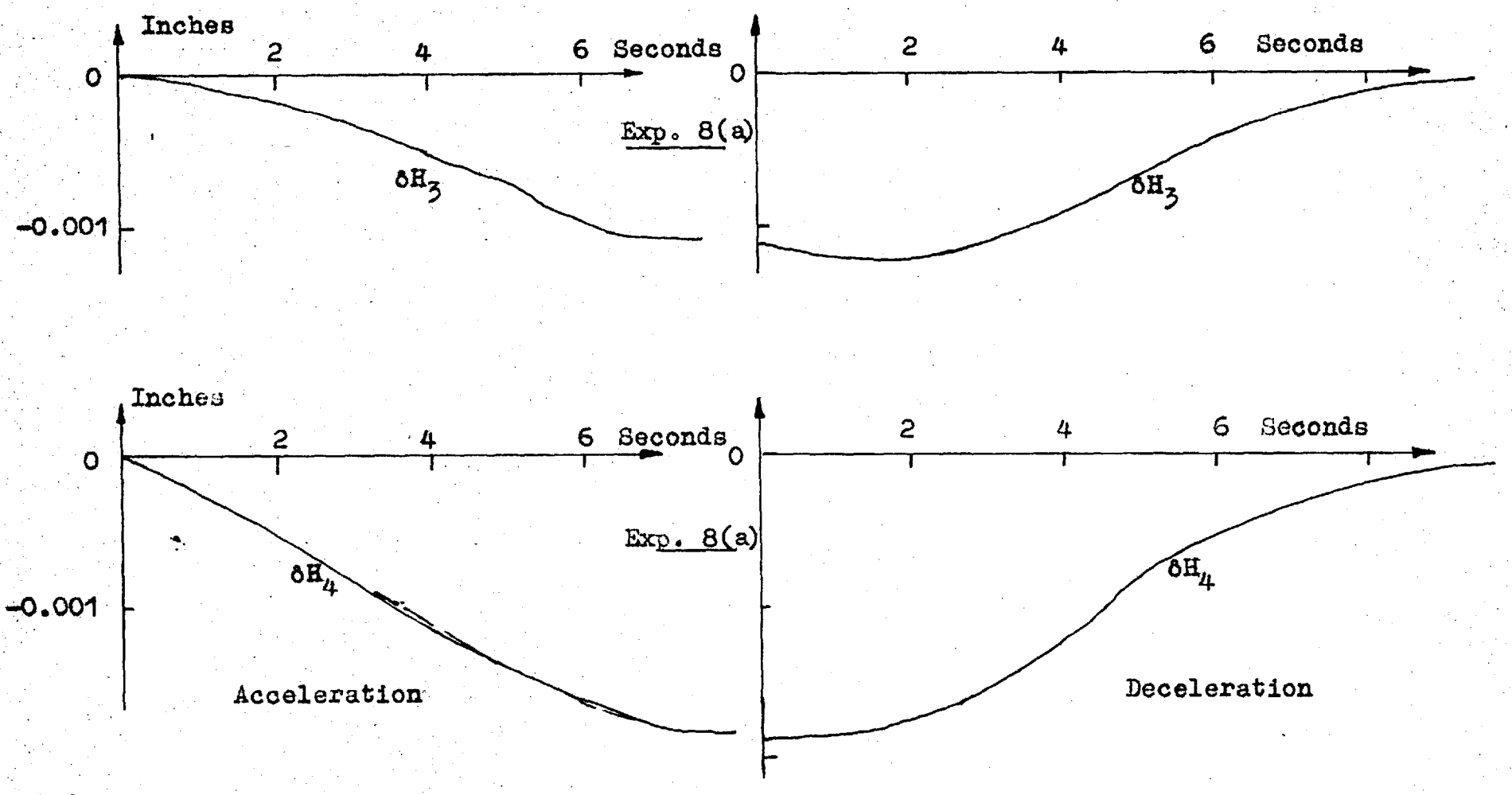

Fig. 8.8(c) Continuation of Fig. 8.8(b)

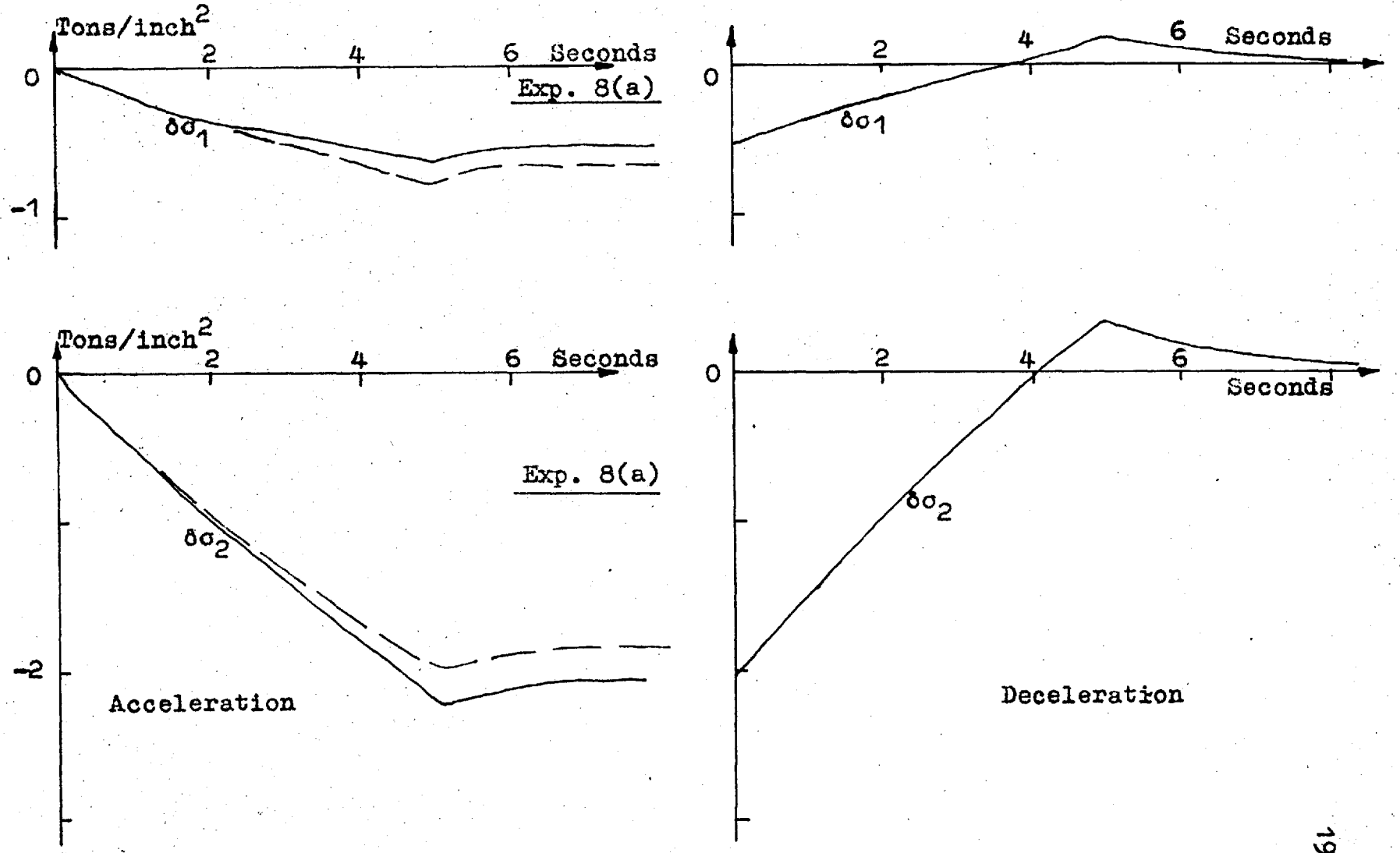

Fig. 8.8(d) Continuation of Fig. 8.8(b)

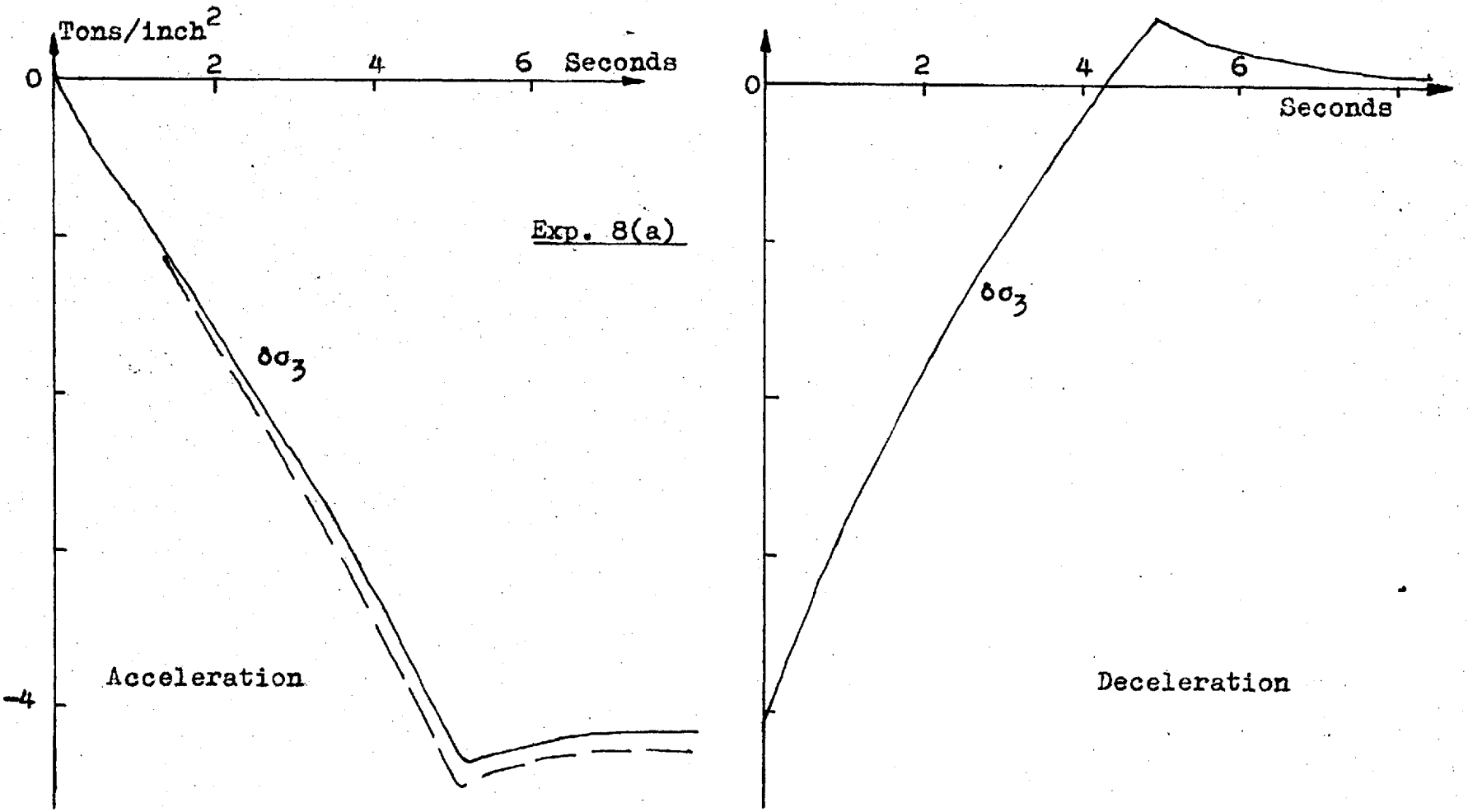

Fig. 8.8(e) Continuation of Fig. 8.8(b)

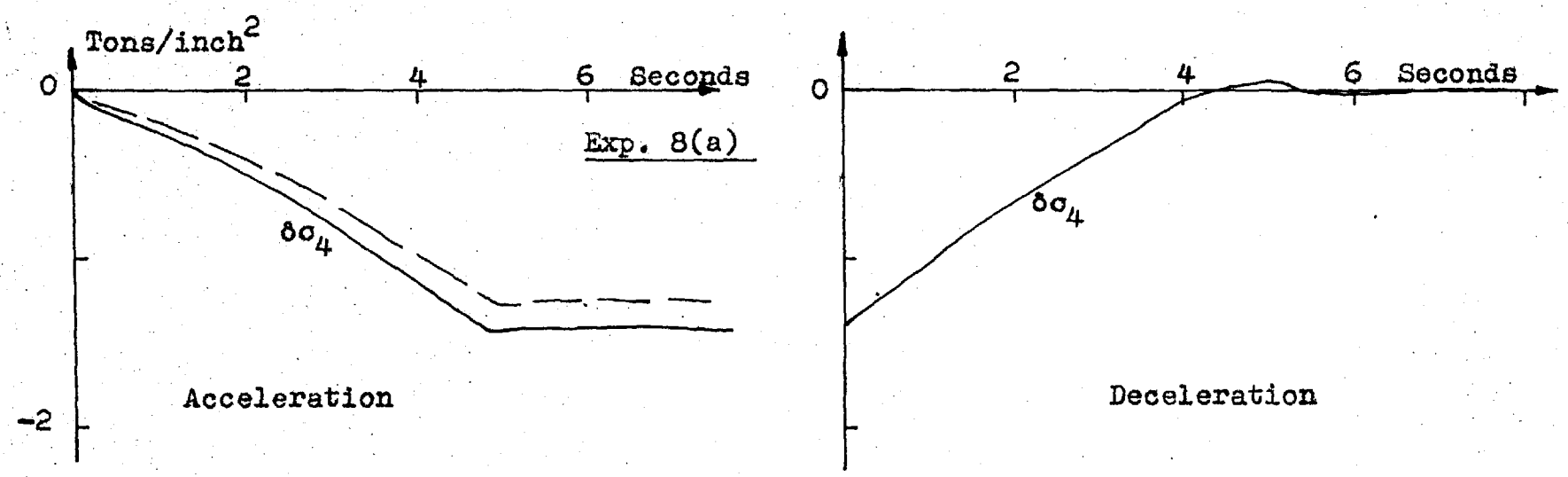

Fig. 8.8(f) Continuation of Fig. 8.8(b)

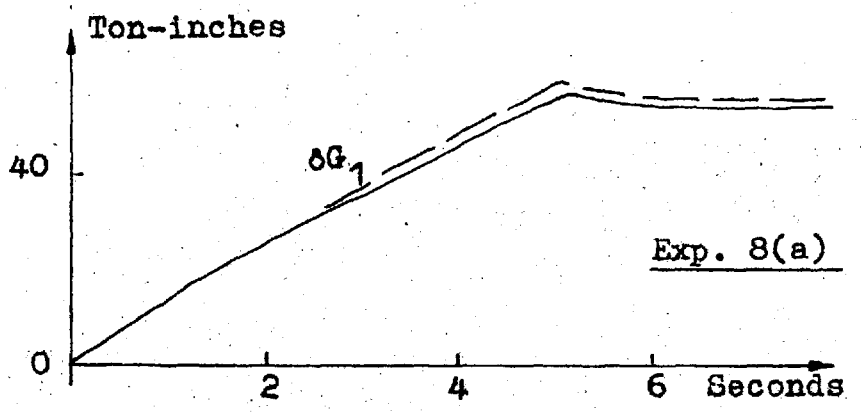

Acceleration

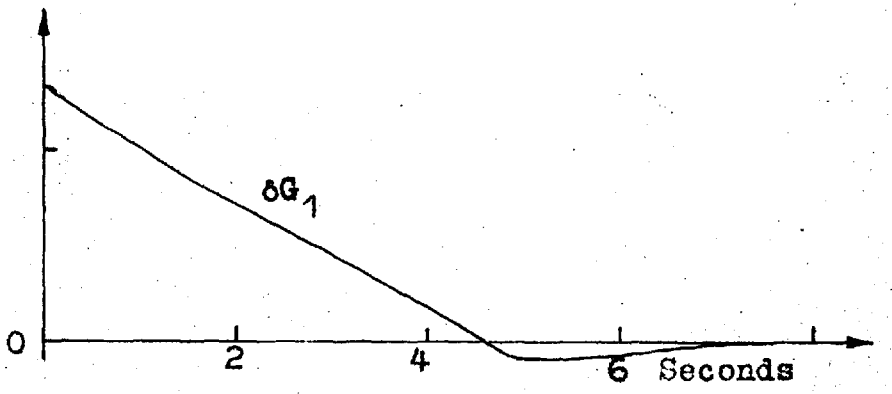

Deceleration

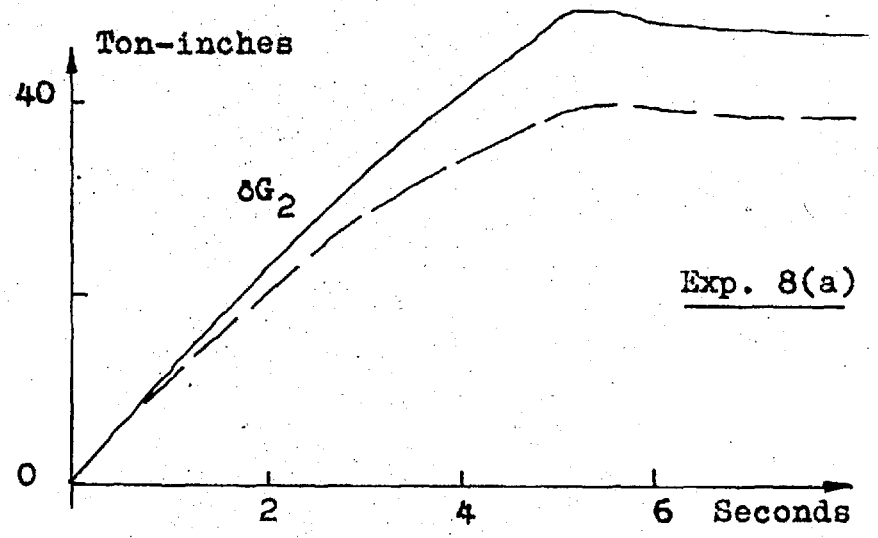

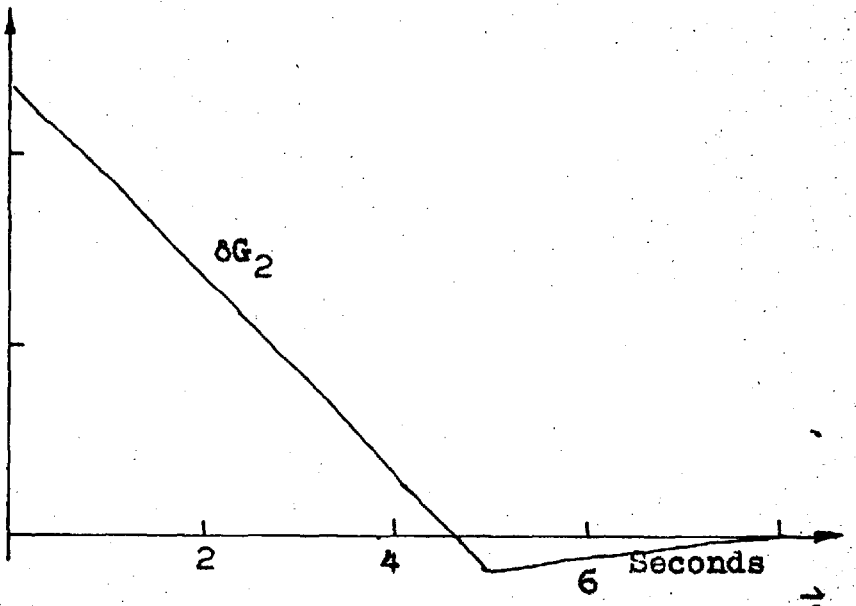

Fig. 8.8(g) Continuation of Fig. 8.8(b)

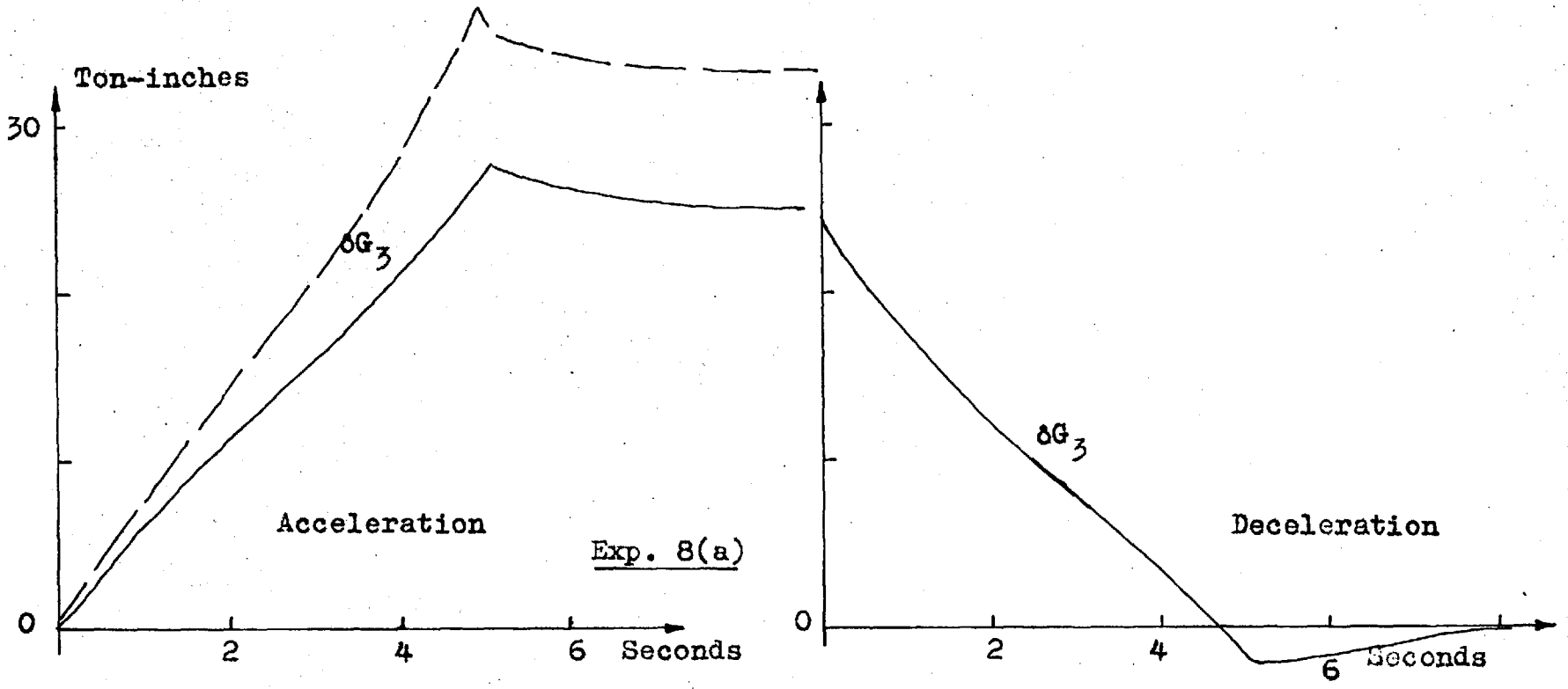

Fig. 8.8(h) Continuation of Fig. 8.8(b)

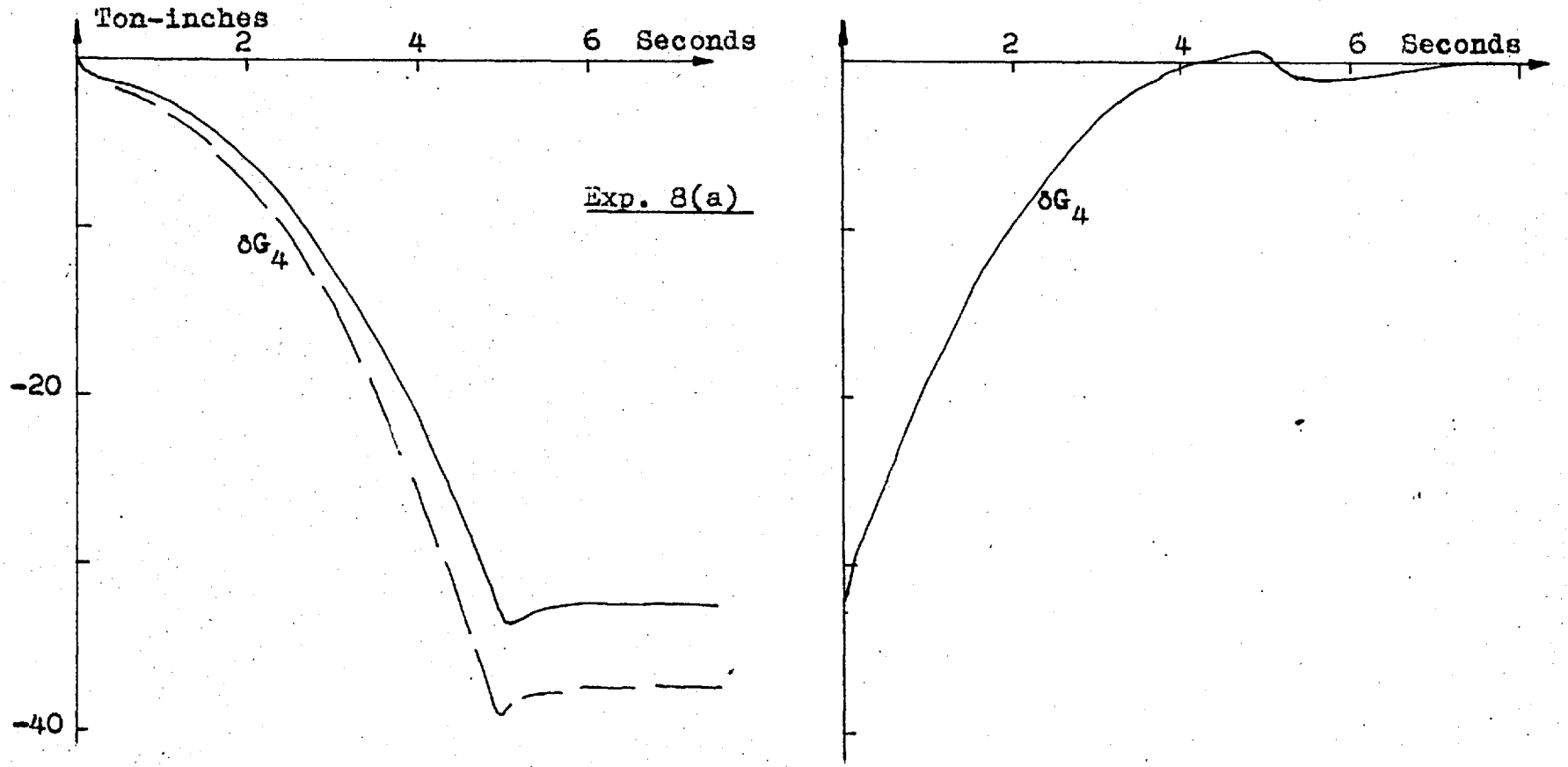

Acceleration

Deceleration

Fig. 8.8(i) Continuation of Fig. 8.8(b)

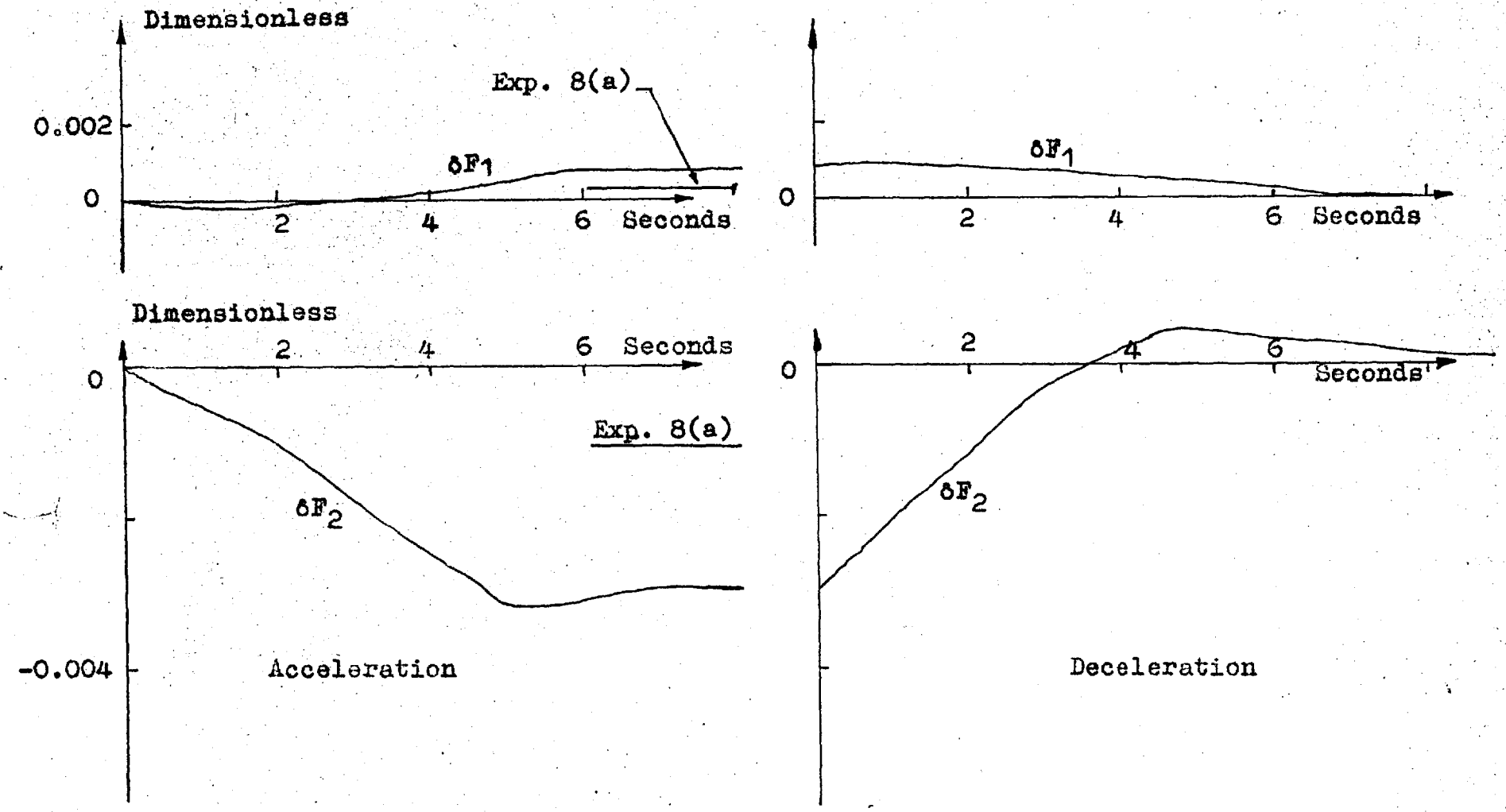

Fig. 8.8(j) Continuation of Fig. 8.8(b)

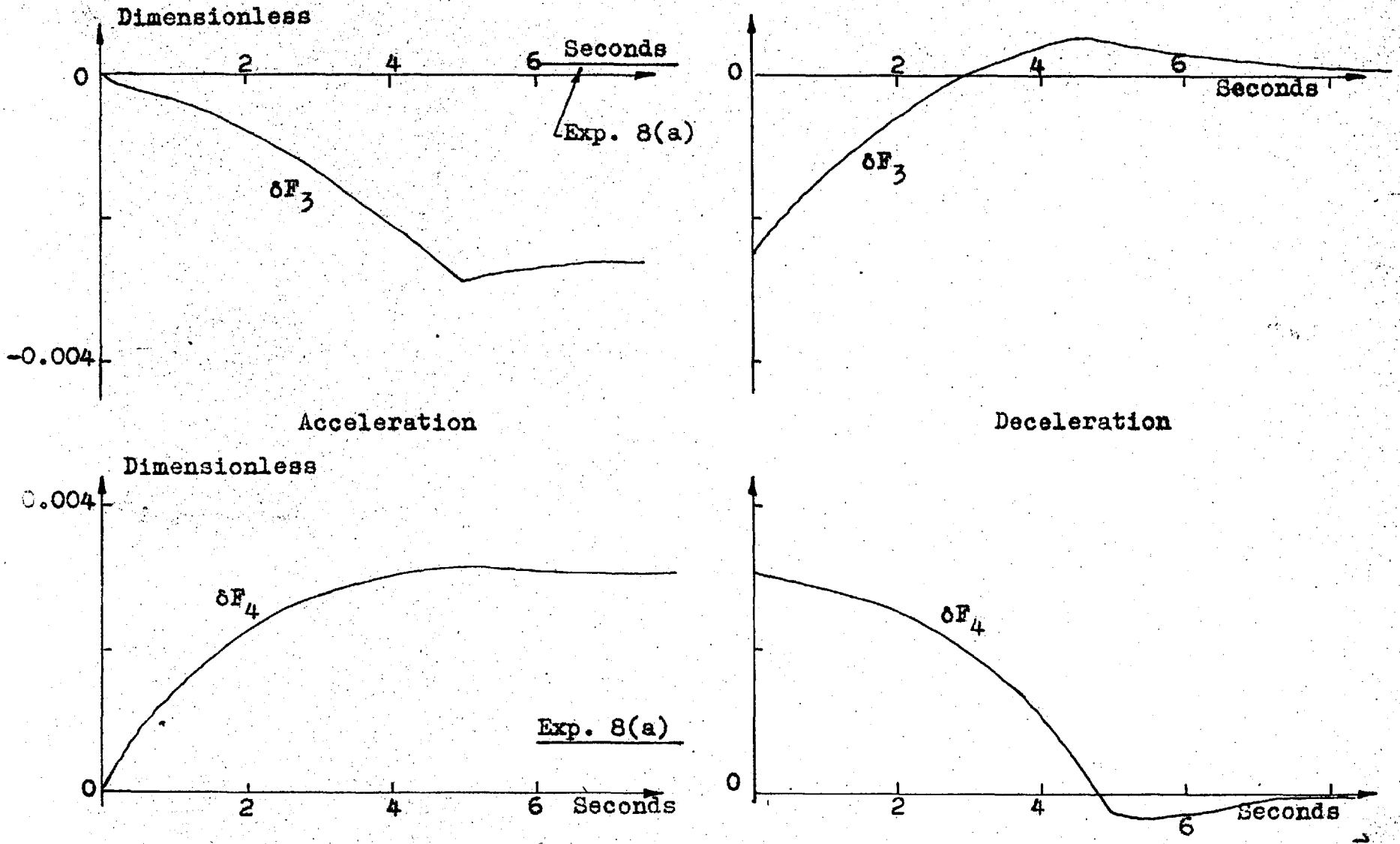

Fig. 8.8(k) Continuation of Fig. 8.8(b)

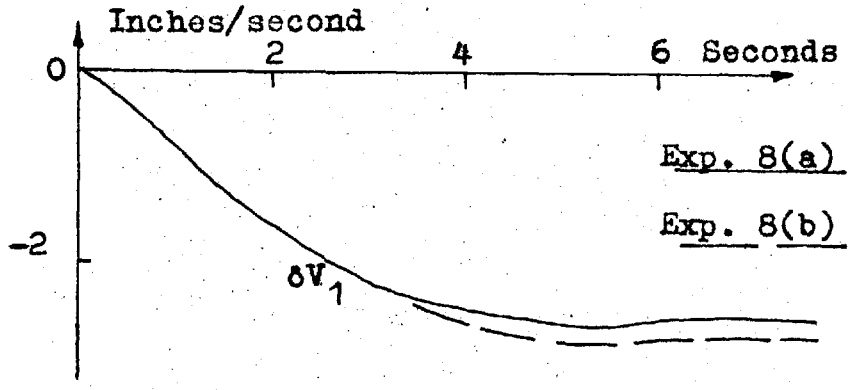

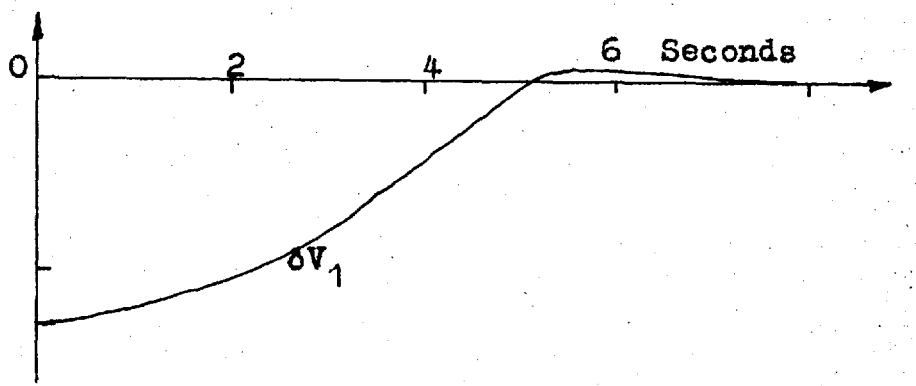

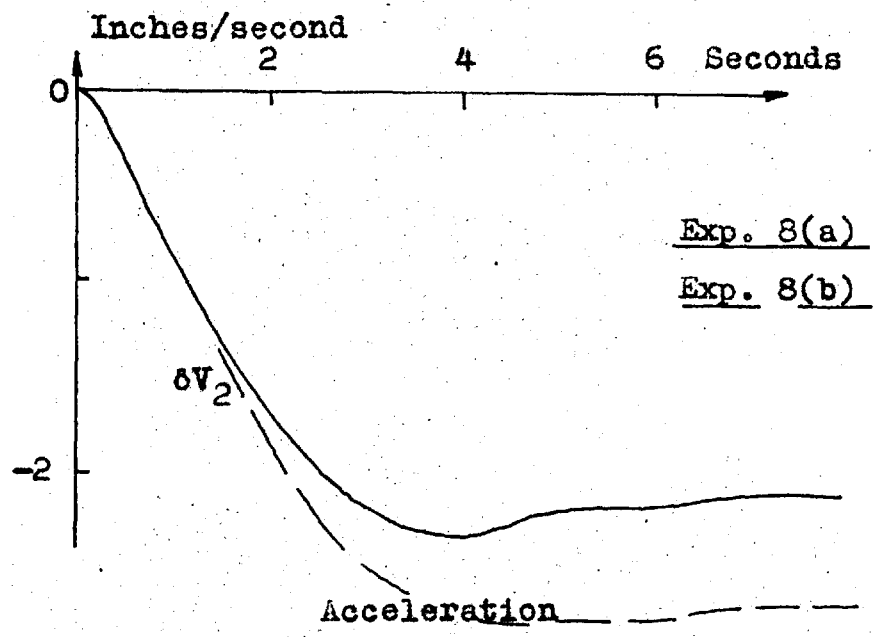

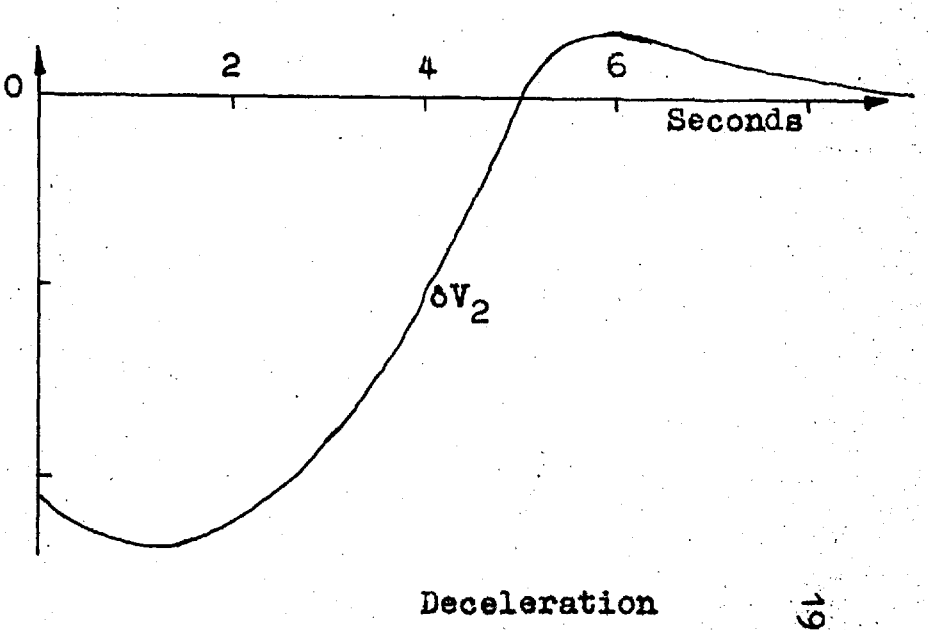

Fig. 8.8(1) Continuation of Fig. 8.8(b)

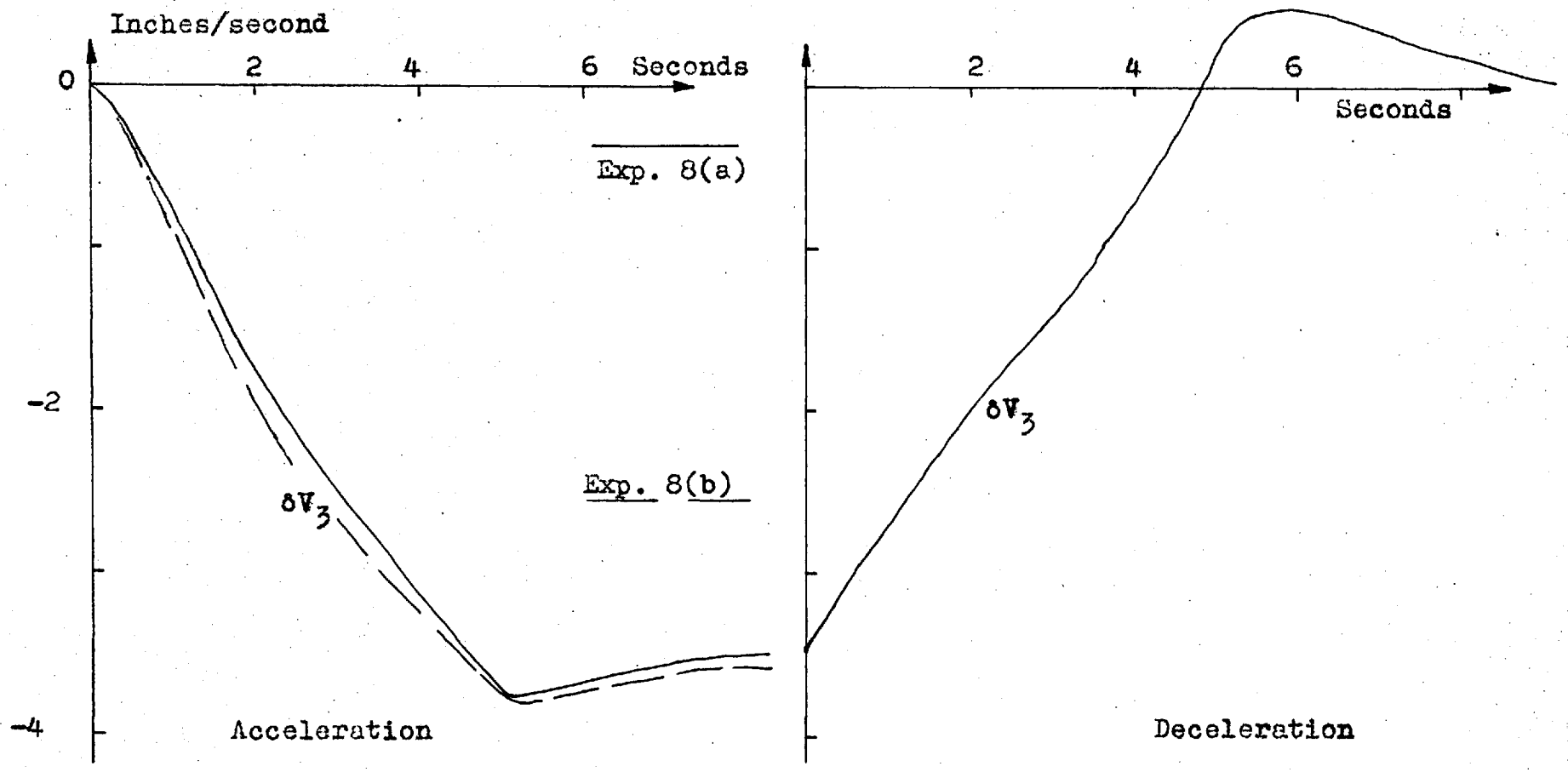

Fig. 8.8(m) Continuation of Fig. 8.8(b)

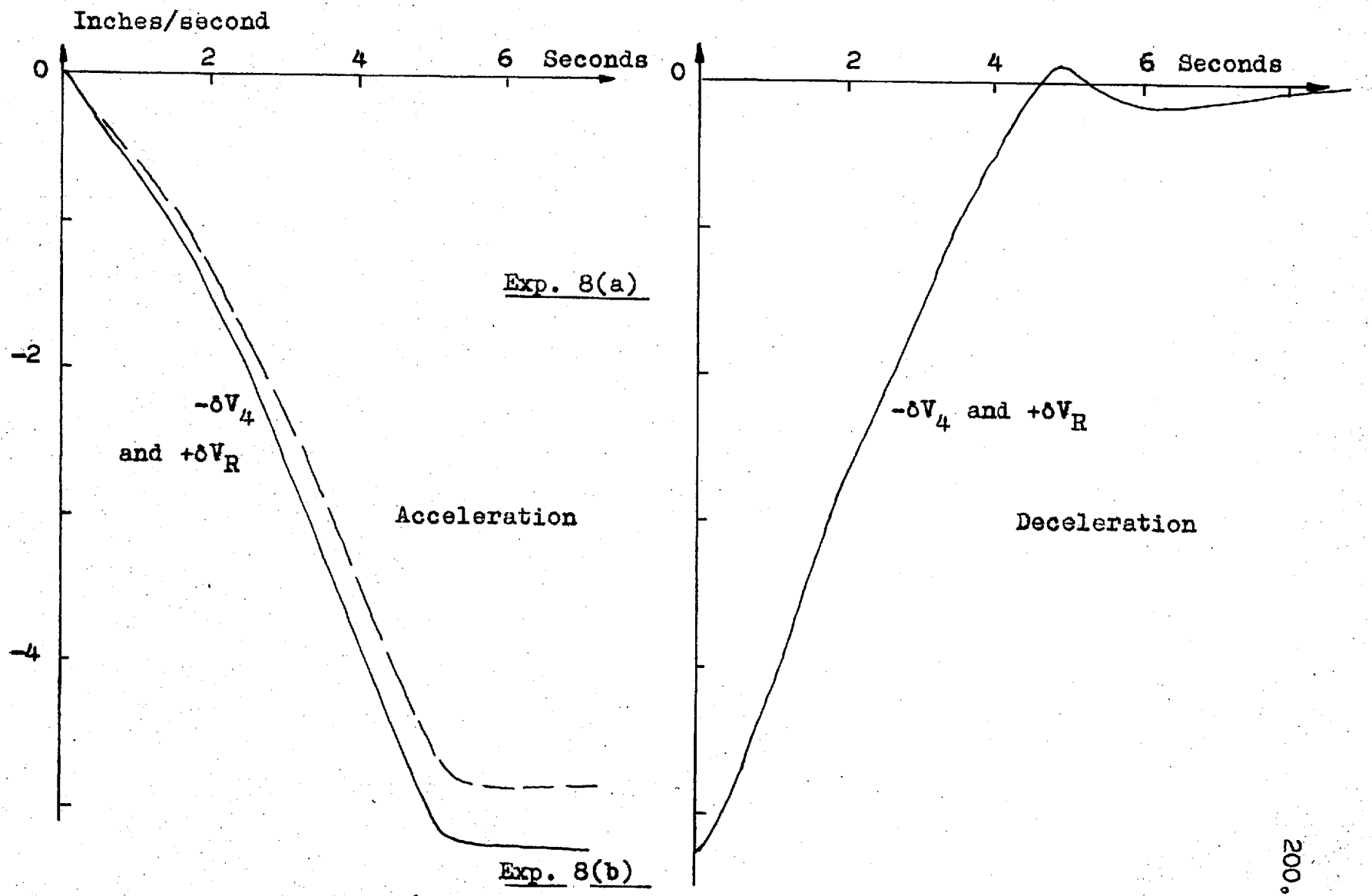

Fig. 8.8(n) Continuation of Fig. 8.8(b)

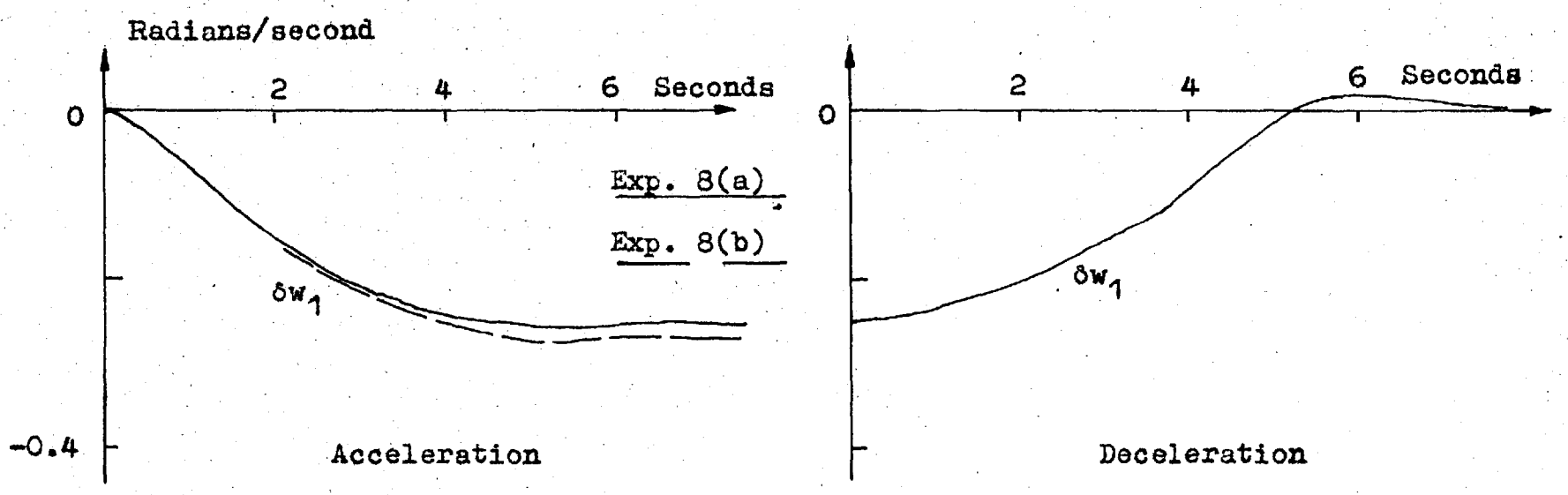

Fig. 8.8(c) Continuation of Fig. 8.8(b)

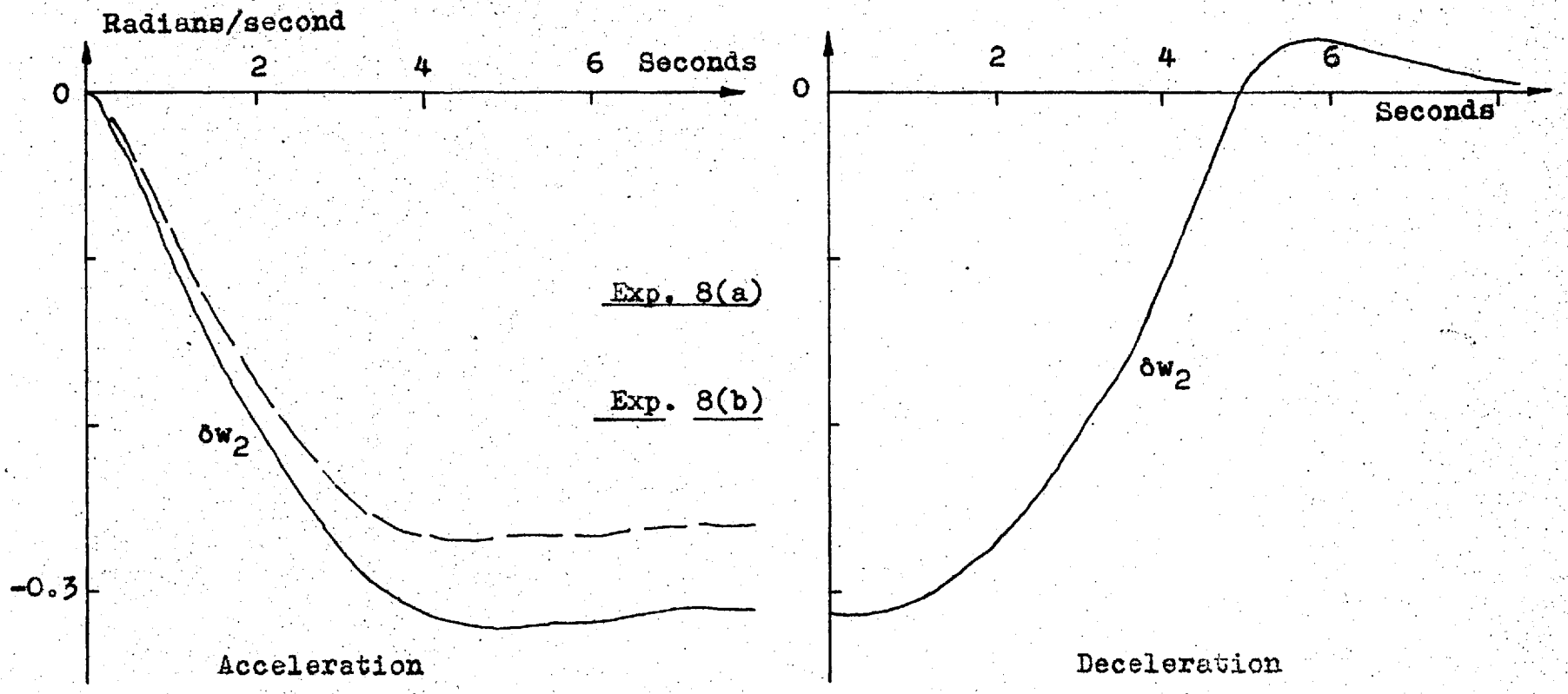

Fig. 8.8(p) Continuation of Fig. 8.8(b)

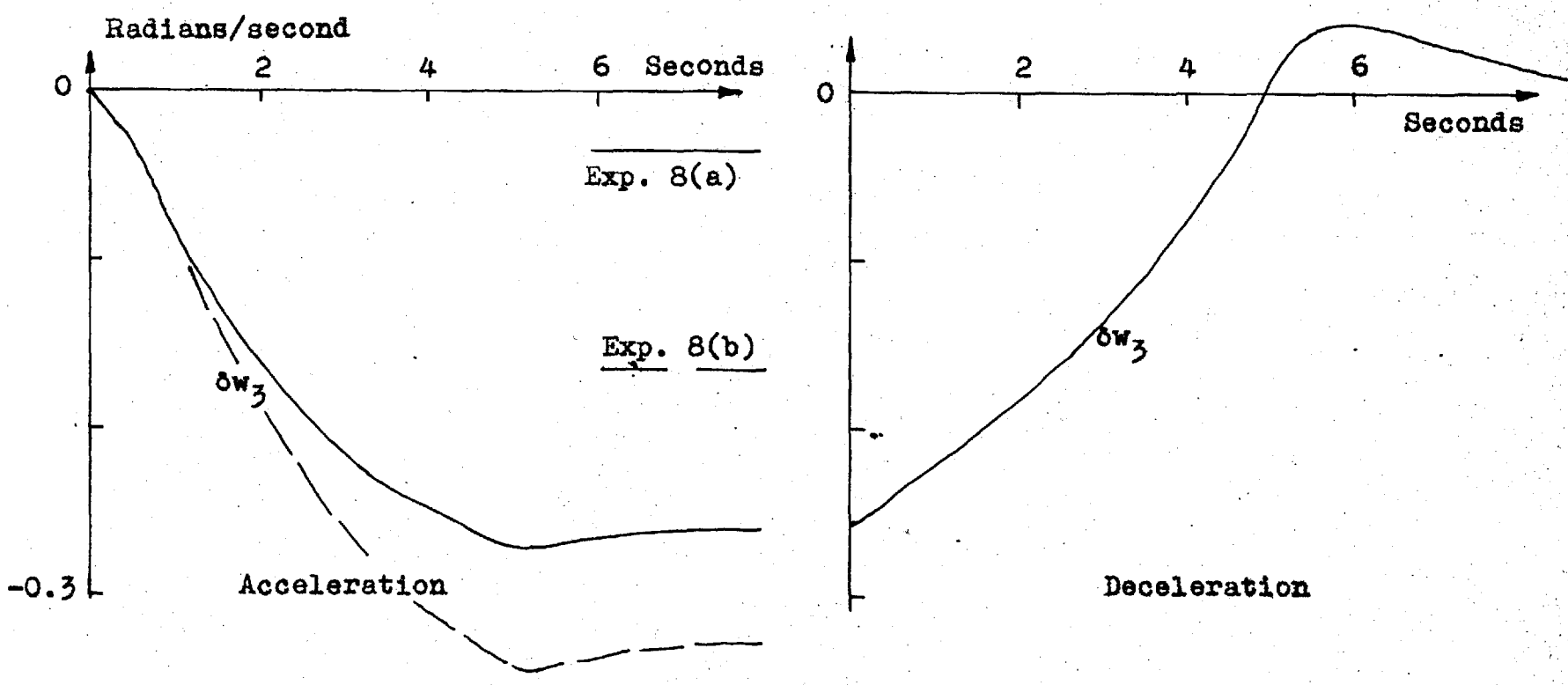

Fig. 8.8(q) Continuation of Fig. 8.8(b)

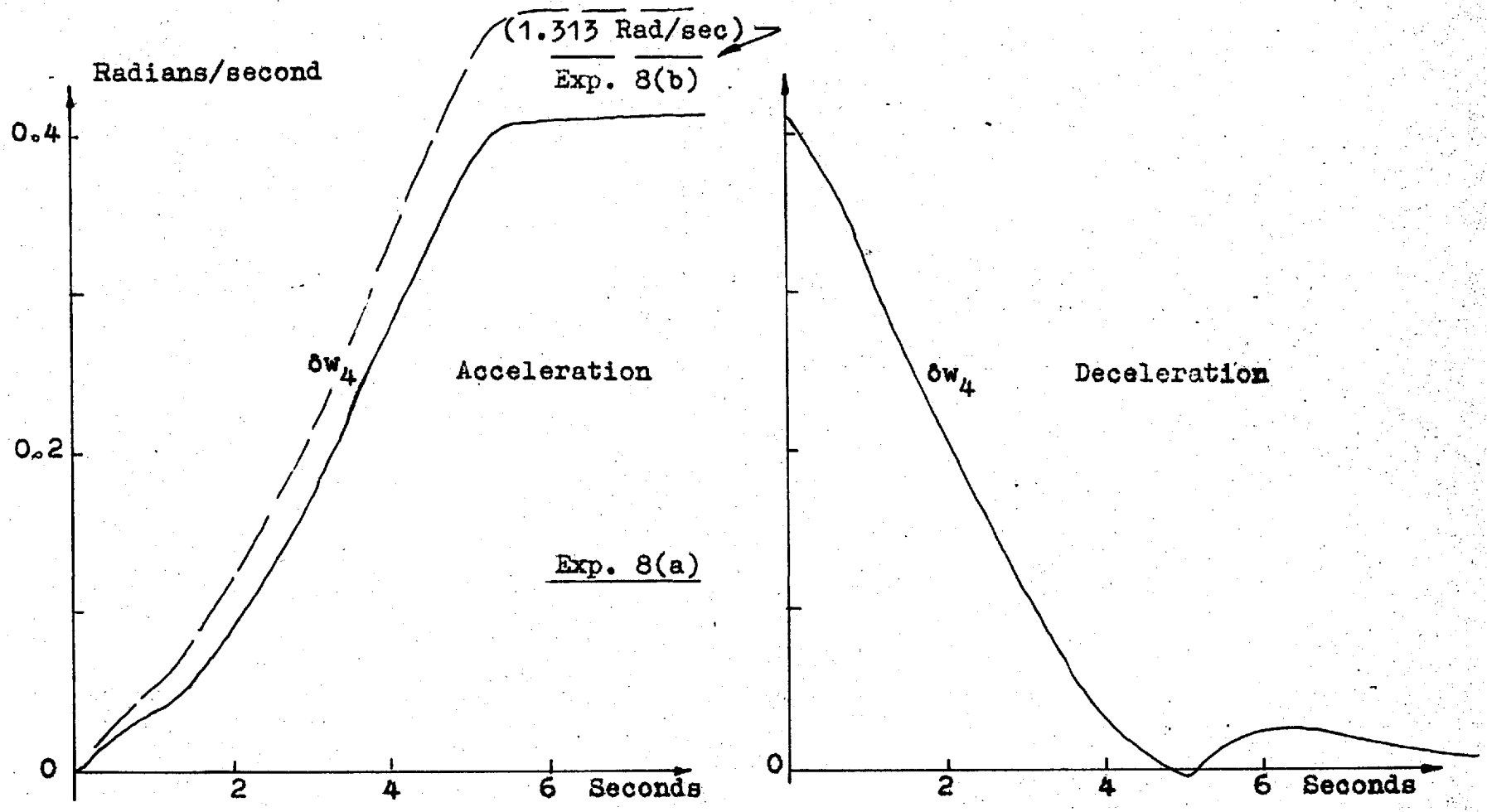

Fig. 8.8(r) Continuation of Fig. 8.8(b)

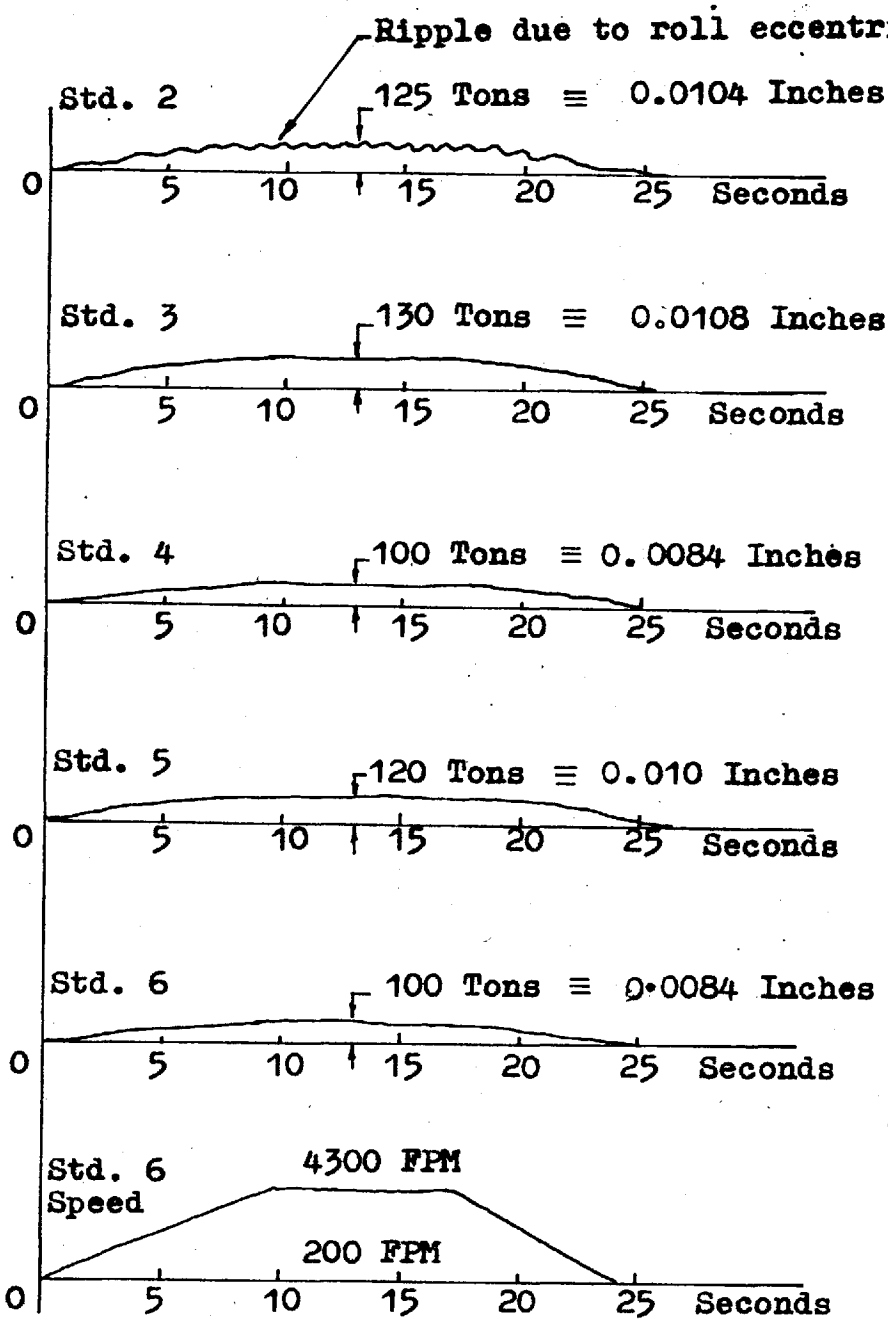

Fig. 8.8s. Total Roll Force and Bearing Roll Neck Oil Film on a Six Stand Mill With No Strip in Mill. From H.N. Cox (Ref. 30)

The tension $\delta\sigma_1$ has become more negative, hence δH_1 tends to become less negative. At stand 2 the increase in $\delta\sigma_2$ is offset by the decrease in $\delta\sigma_1$ to give a slightly less negative value for δH_2. The tension changes and gauge changes lead to changes in the torques and other variables. Again the inclusion of slip in a simulation appears necessary.

This experiment, with slip included, was repeated with the mill being accelerated over the speed range of Fig. 8.8(a) in 10 seconds rather than 5 seconds. The traces were similar to those discussed except for the longer time taken to reach steady-state in view of the longer acceleration time.

Experiment 8(a) Acceleration With Bearing Roll Neck Oil Film

This experiment is identical to Experiment (8) except that only the oil film effects are included as shown in Table 8.2(a). The steady-state values reached are shown on Figs. 8.8(b) to 8.8(r) by the solid lines. The form of the trace was identical to that for Experiment (8). Due to the much smaller screw movements involved, the variable changes are smaller. The stand 3 slip change, δF_3, has taken a slightly positive value compared with its former negative change.

Experiment 8(b) Acceleration and Deceleration With Bearing Roll Neck Oil Film and a Roll Force and Speed Schedule Deviation

The Table 8.2(b) shows the signals introduced into the simulation of Fig. 7.7 at 1950 feet per minute, Figs. 8.8(l) to 8.8(r).show the steady-state values of the mill variables reached. The changes in gauges, tensions, torques and slips have been small and are not noted. This is due to the nature of the speed schedule deviation chosen. From Table D.3 the values may or new steady-state values calculated for speed schedule deviations.

A speed deviation has been used as it is convenient and is related to a torque schedule deviation which would manifest itself as a speed change.

The speed deviation is included to indicate its effects as roll speed is used in chapter (9) to control strip tensions and gauges.

8.3.2. Continuous Acceleration and Deceleration In the Range 975 to 1950 feet per minute Output Speed

The experiment numbers are continued from the previous section.

Experiment (9) Continuous Acceleration and Deceleration With Bearing Roll Neck Oil Film and a Roll Force Schedule Deviation

Fig. 8.9(a) shows the velocity profile used in this experiment. The oil film and roll force deviation of Table 8.2 are used. The traces recorded in Figs. 8.9(b) to 8.9(g) indicate a behaviour similar to those for Experiment (8) except that the traces are now continuous due to the continuous nature of the velocity. The velocity profile is equivalent to accelerating the mill in 10 seconds from low speed to high speed, holding constant speed for 10 seconds then deceleratin in 10 seconds. It is a clipped sine wave.

It is noticeable that the slopes of the traces for $\delta\sigma_3$ and $\delta\sigma_4$ (Fig. 8.9(d)) and for δG_3 and δG_4 (Fig. 8.9(f)) are different for the acceleration and deceleration cases. The nature of the droop and delay time changes would be responsible for this.

Experiment (10) Continuous Acceleration and Deceleration With Bearing Roll Neck Oil Film, Roll Force Schedule Deviation and With a Step in Gauge Introduced.

This is a repeat of Experiment (9) but with a -0.004 inch step in gauge error introduced at the

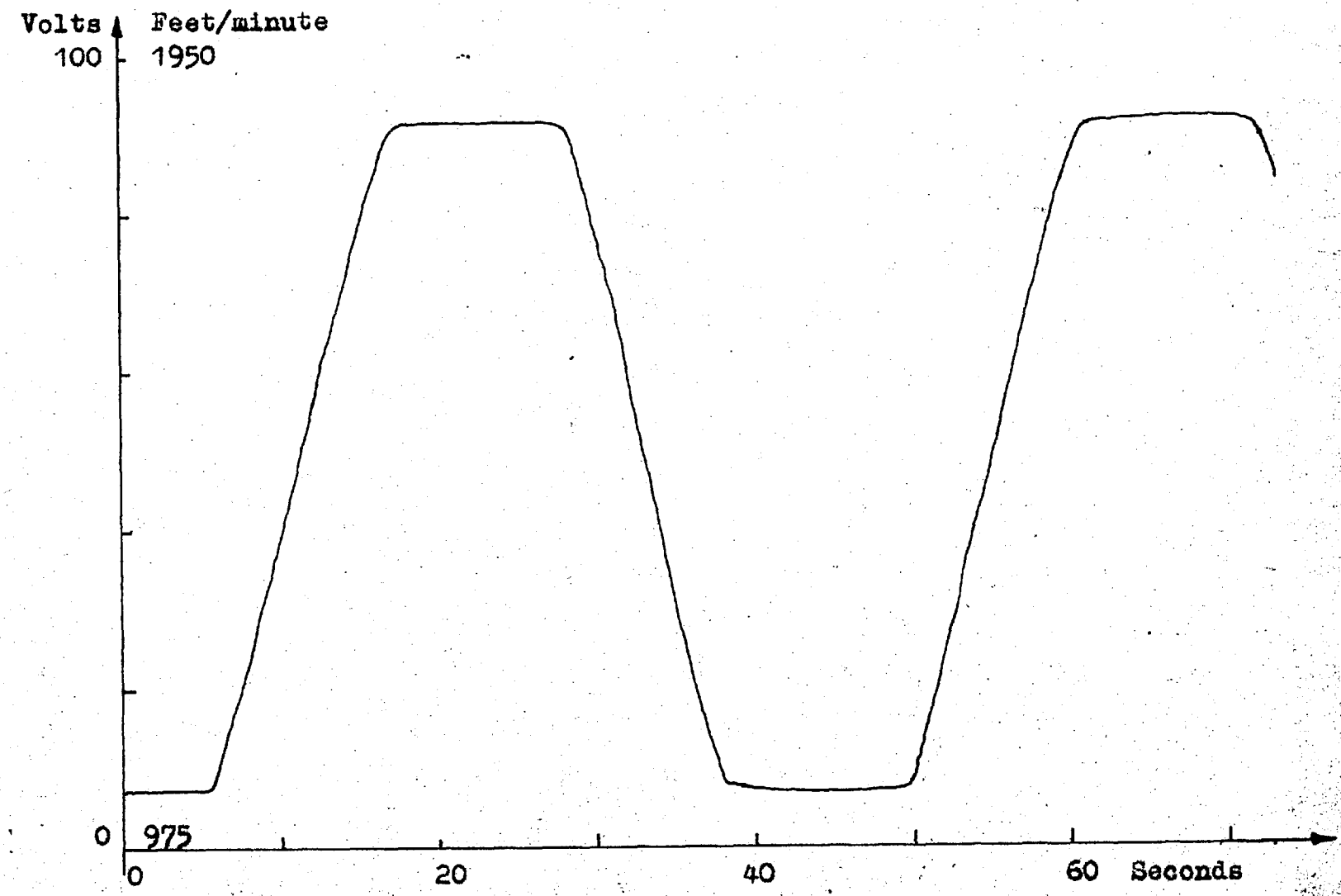

Fig. 8.9(a) Mill Velocity Characteristic Imparted to Servomultipliers In Fig. 7.7 (Ref. Section 8.3 Experiment (9))

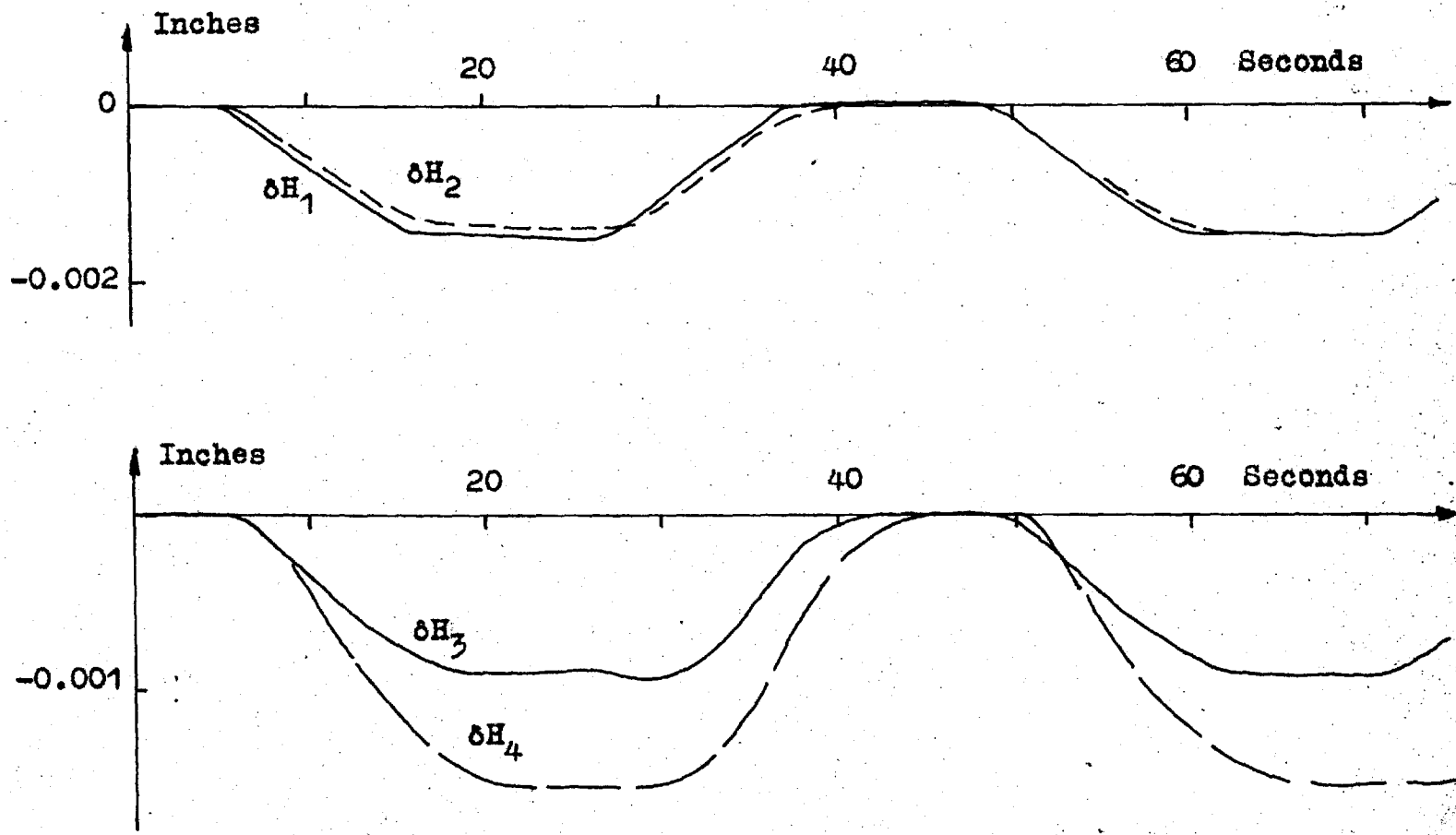

Fig. 8.9(b) Responses to Schedule Deviations of Table 8.2 When Subjected to the Mill Velocity Characteristic of Fig. 8.9(a) (Ref. Section 8.3 Experiment (9))

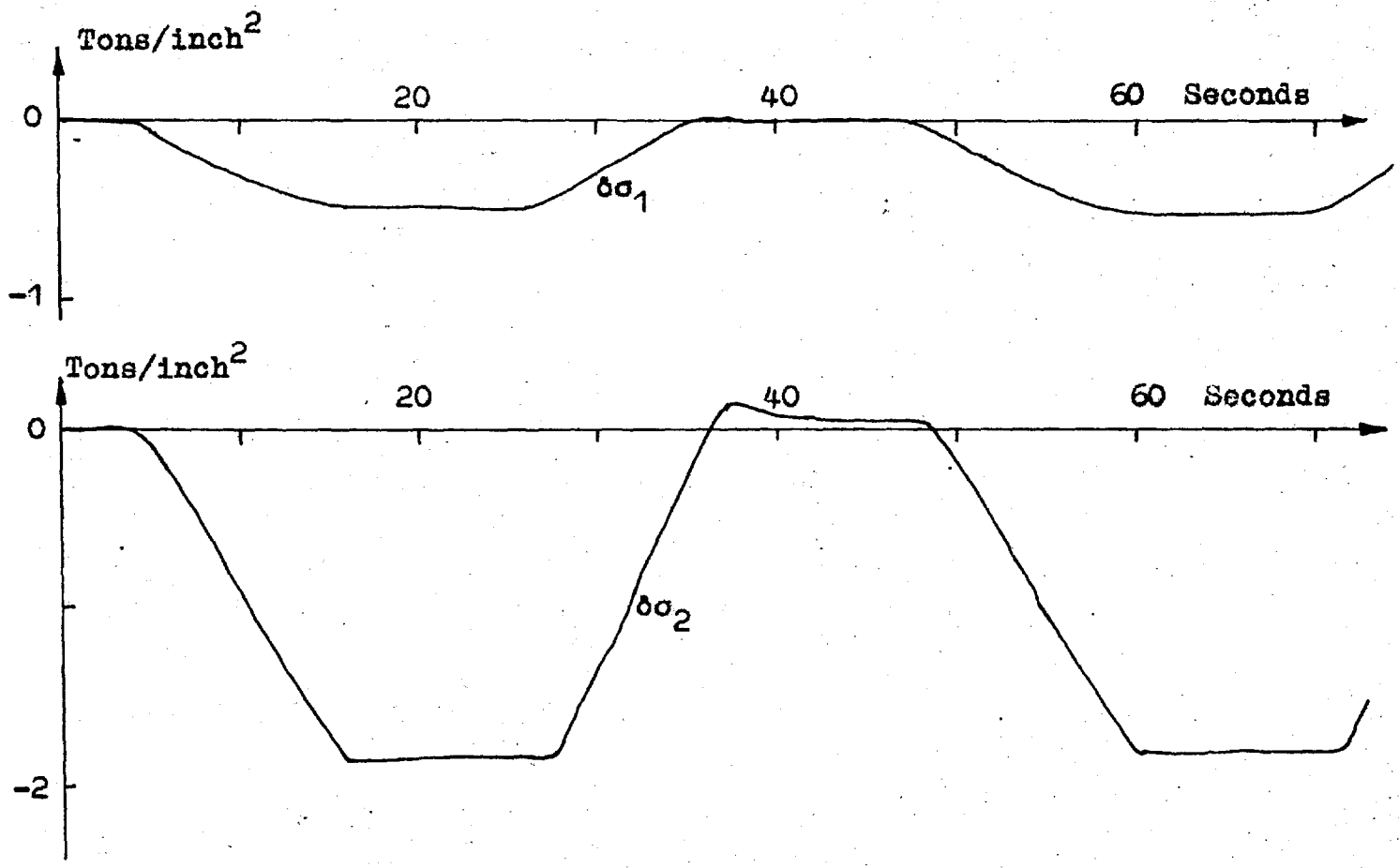

Fig. 8.9(c) Continuation of Fig. 8.9(b)

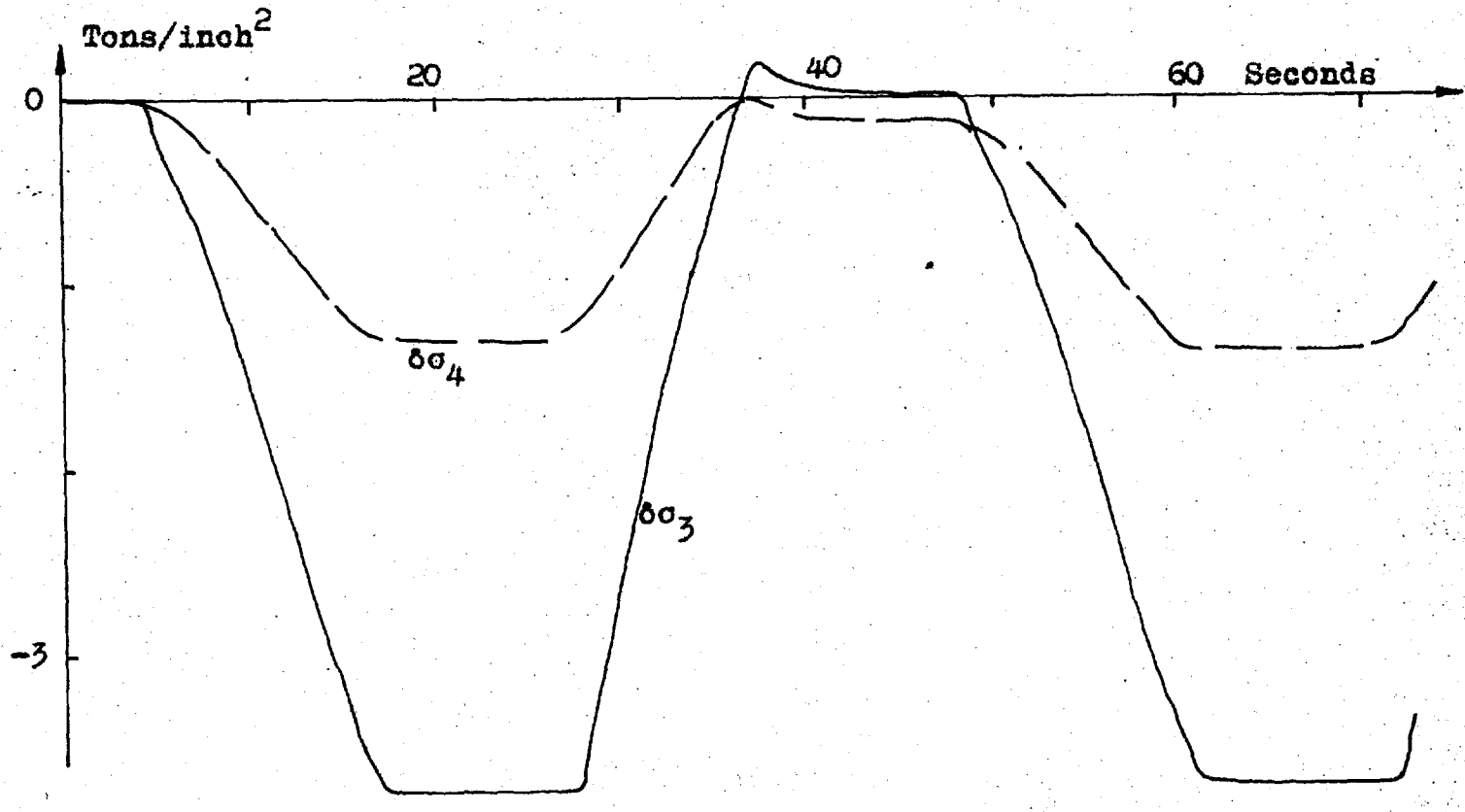

Fig. 8.9(d) Continuation of Fig. 8.9(b)

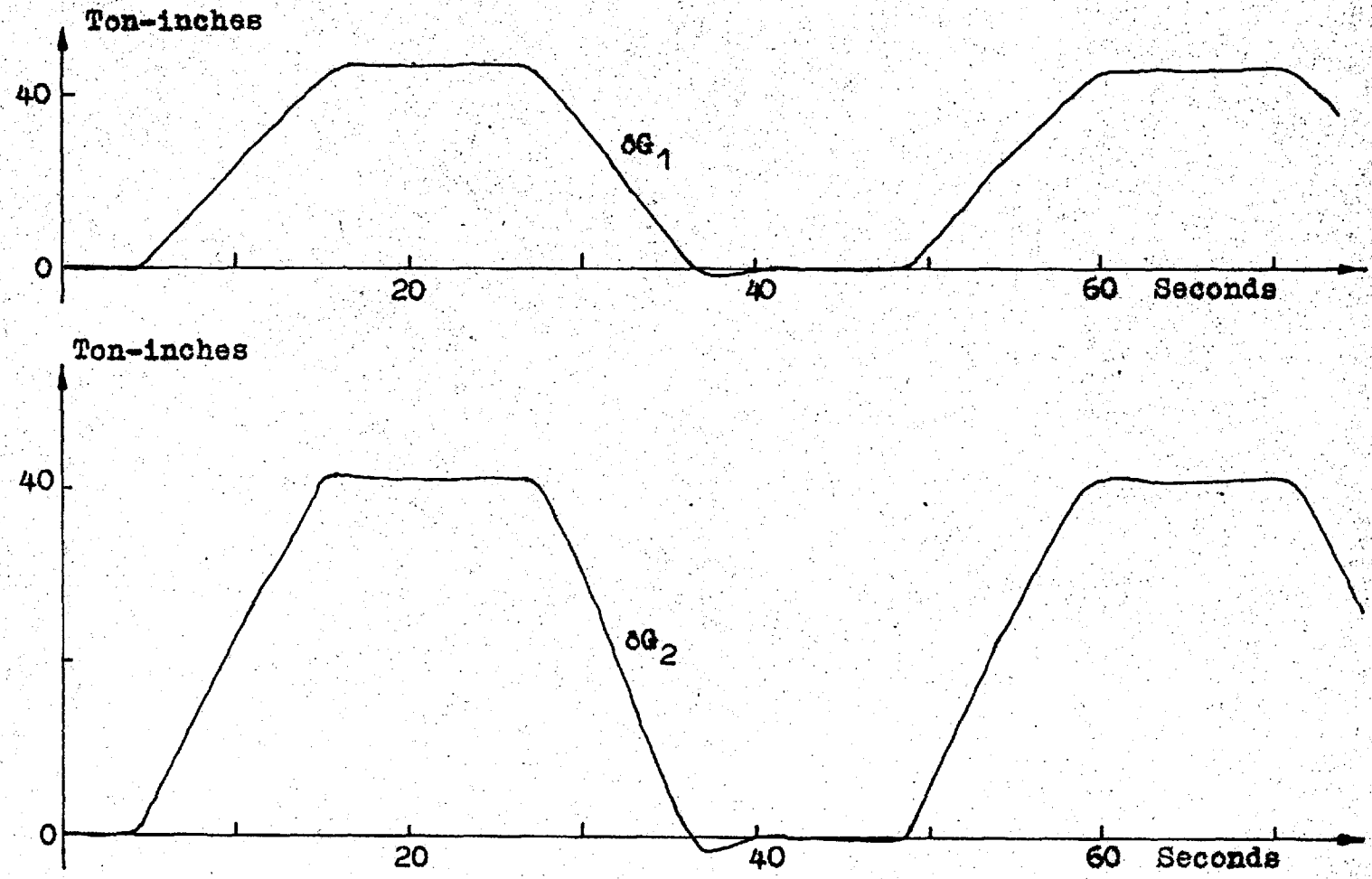

Fig. 8.9(e) Continuation of Fig. 8.9(b)

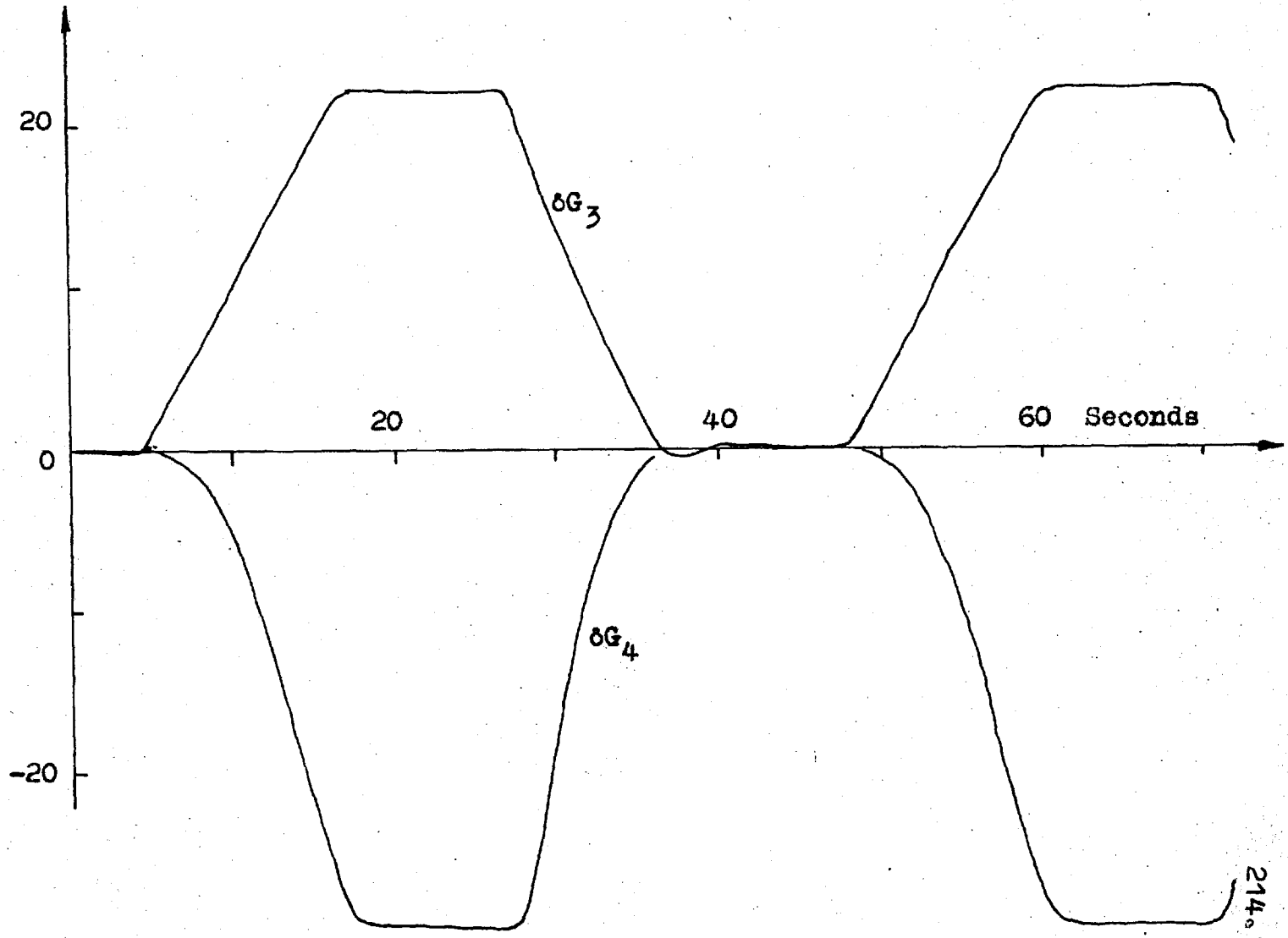

Fig. 8.9(f) Continuation of Fig. 8.9(b)

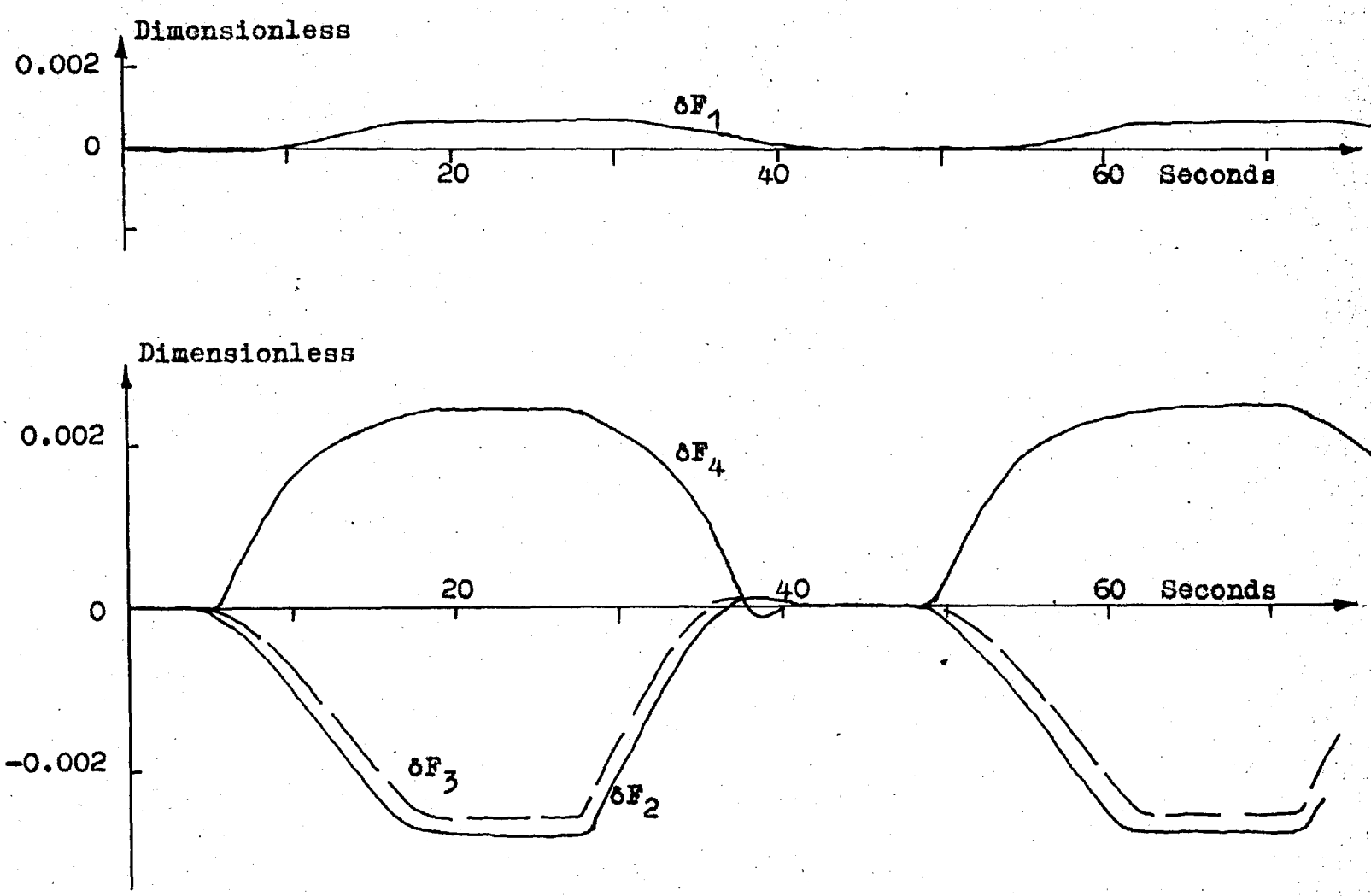

Fig. 8.9(g) Continuation of Fig. 8.9(b)

mid-point of a constant speed plateau. Figures 8.10(a) and 8.10(b) show the traces for the gauges and tensions. The negative step in gauge causes the stand output gauges to be decreased and the interstand tensions to be increased which concurrs with the results achieved in the experiments of Section 8.2.

Due to the greater time scale of the recording, the x-y plotter has probably overshot in attempting to follow such a rapidly changing trace. However the transients due to the step compare with those obtained in the experiments of Section 8.2; and its duration is of the same order of time.

As discussed in Chapter 7 any schedule deviation or gauge error may be introduced into the simulation. The experiments of this Section 8.3 indicate the procedure. Knowing the function of a desired input signal, in terms of time or velocity, allows it to be introduced in the manner and at the time desired.

Experiment 11 Continuous Acceleration and Deceleration With a Constant Gauge Error

This experiment shows the changes that occur in the variables when the mill is accelerated and decelerated with the schedule being maintained, but

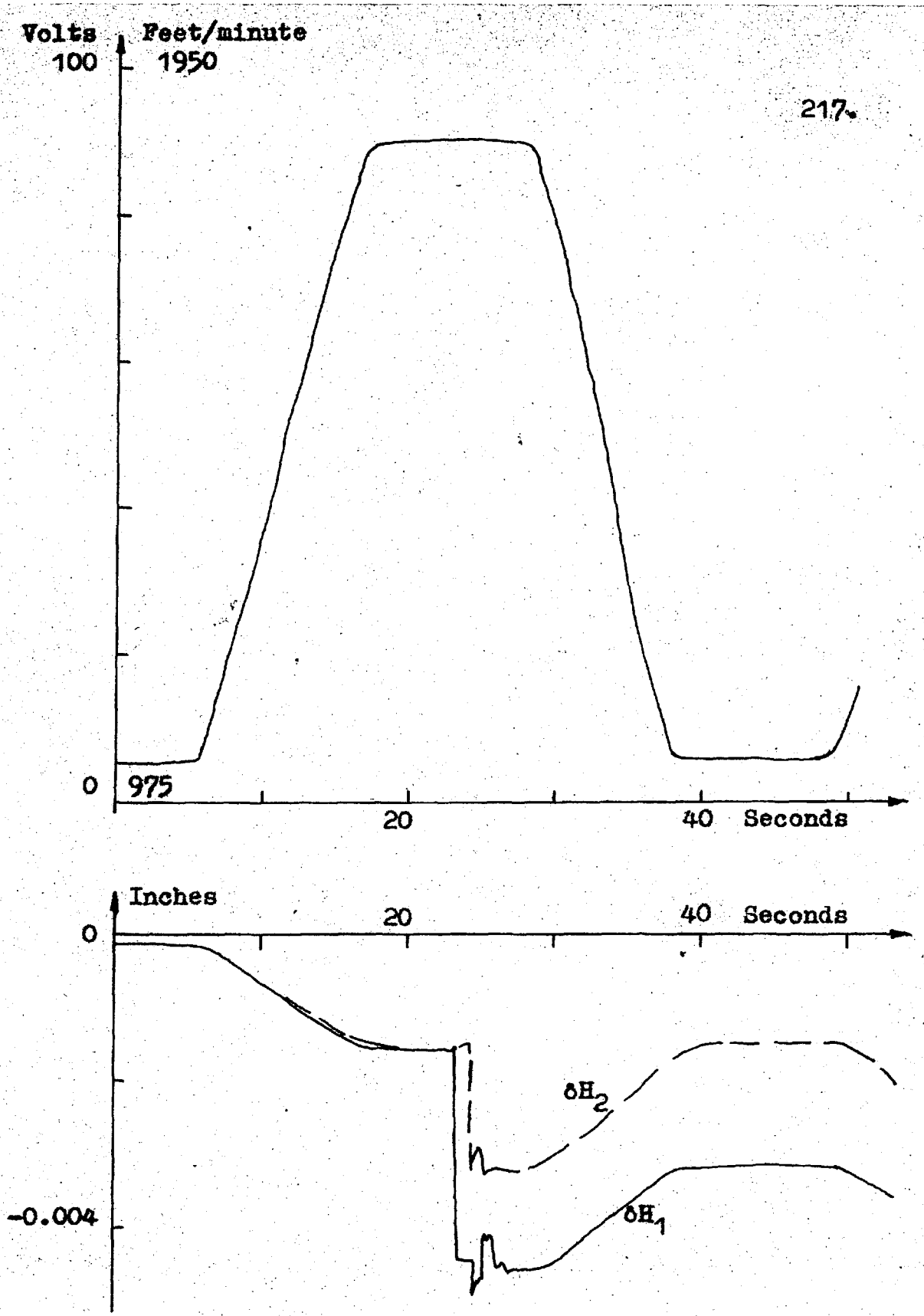

Fig. 8.10(a) Mill Velocity Characteristic Imparted to Servomultipliers In Fig. 7.7 (Ref. Section 8.3 Experiment (10))

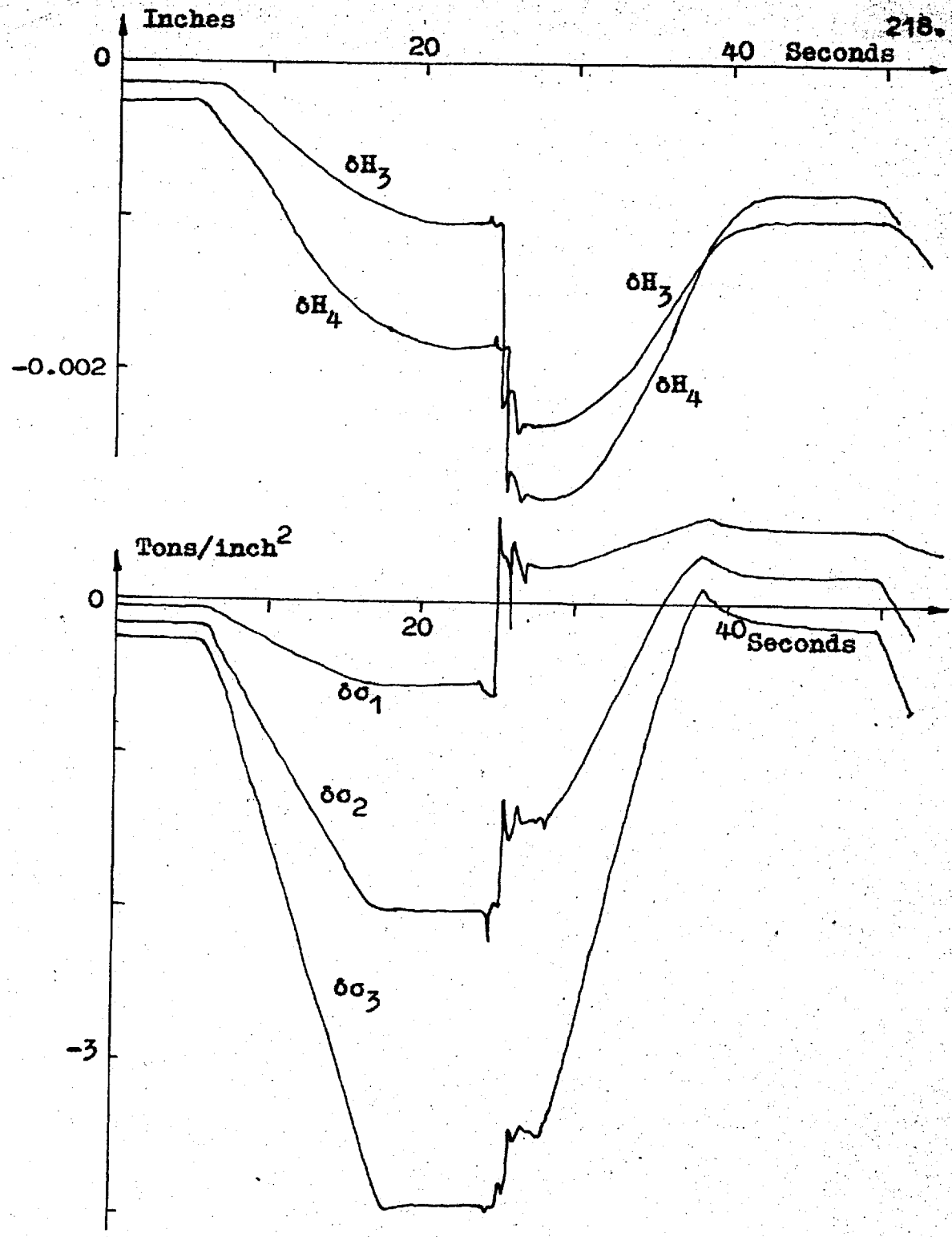

Fig. 8.10(b) Responses to Schedule Deviations of Table 8.2 When Subjected to the Mill Velocity Characteristic of Fig. 8.10(a) and a Step Input of-0.004 Inches at High Speed (Ref. Section 8.3 Experiment (10))

with a steady error of 0.004 inches existing on the incoming strip. The mill velocity profile used is that of Fig. 8.9(a). The changes that occur in the variables with changing speed are now entirely due to the changing coefficients in the simulation (Figs. 8.11(a) and 8.11(b)).

The variations in the traces are quantitatively in agreement with the steady-state values noted for the experiments at constant mill speed of 975 and 1950 feet per minute (Section 8.2).

There are only small changes in the steady-state values due to slightly less than the full speed range being utilised in the present experiment.

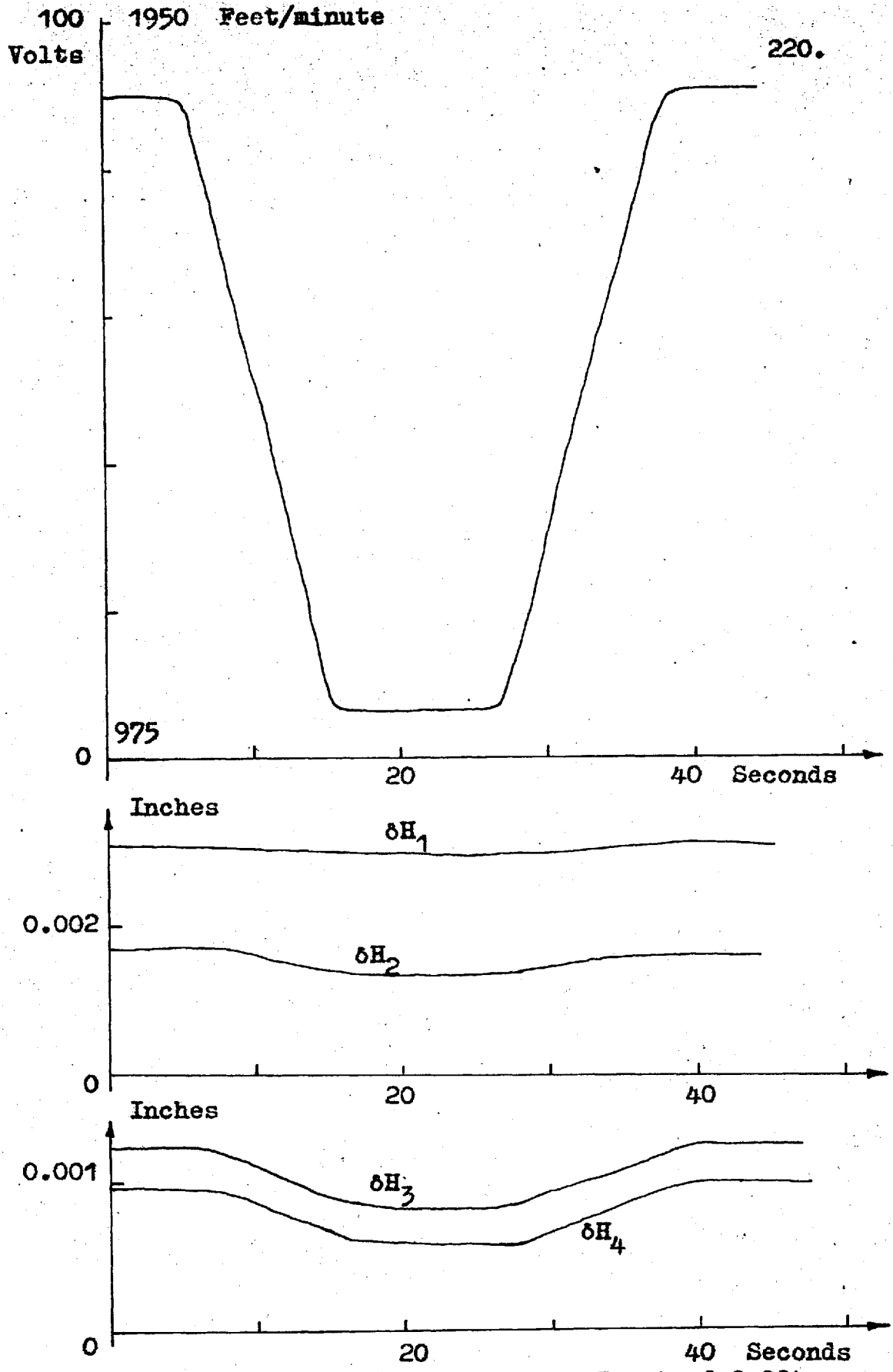

Fig. 8.11(a) Responses to the a Step Input of 0.004 Inches When Subjected to the Velocity Characteristic above (Ref. Section 8.3 Experiment (11))

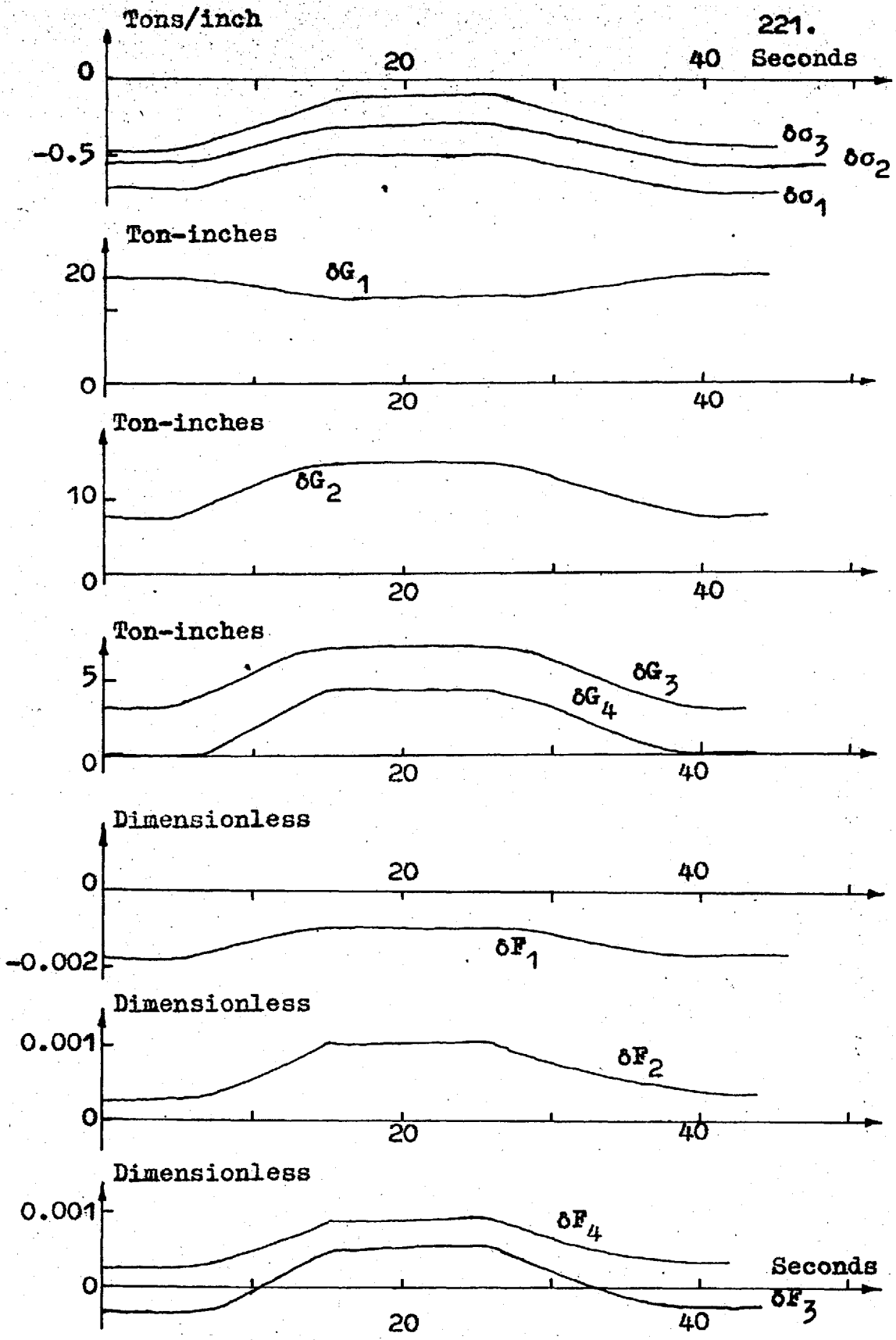

Fig. 8.11(b) Continuation of Fig. 8.11(a)

9 AUTOMATIC GAUGE CONTROL EXPERIMENTS

With a model of the rolling mill developed and simulated on the analogue computer it is possible to simulate and impose automatic gauge control systems on the process (9, 10, 19).

The testing and comparison of the gauge control systems was done mainly with step, and sine wave errors on the incoming strip and with a number of mill velocity profiles. In practice the actual variations in the incoming gauge are of many types (Section 1.2) the welded strip joints, which constitute a step, being the most severe. A profile of incoming gauge is given in reference (9).

Several types of gauge control systems were tested using the simulations of Figs. 7.2 and 7.7. Some of these systems are similar to those used in practice. The more complex ones are similar to those tested in reference (9, 10) with some modifications. Control system number 6 (Fig. 9.21) is a new system. Apart from these basic systems variations of them were tried. Those discussed in the following sections proved the most satisfactory. They are shown in Figs. 9.2, 9.7, 9.11, 9.15, 9.17 and 9.21.

The diagrams show the transfer function in the box representing the particular component of the system. The crossed circles represent comparators, an operation that can be performed with a summing amplifier. In these diagrams the rolling mill itself is represented by the symbolic rolls, strip and reels. The comparators compare the measured mill variables (strip gauges and tensions) with the desired values of these controlled variables. However, since the simulations of the rolling mill (Figs. 7.2 and 7.7) are expressed in terms of small deviations from nominal values, the control systems must conform to this method and must be viewed as attempting to bring the strip gauges and tensions back to their scheduled values in the presence of perturbations in the process. Therefore the desired value of these small deviations in the variables is zero. The error signal then becomes the measured values of the deviations in the variables being controlled, but of opposite sign to give the negative feedback required in control systems.

The effects of the controller gain settings were noted and in most cases adjusted to give the best response; which in this case is assumed to be a dead-beat response (9). A dead beat response is

one in which the transient response, or response to a step input, of the controlled variable is without overshoot. This is not the optimum response but this adjustment is considered consistent with the large masses of the equipment being controlled.

A controller gain in the simulation is the ratio of the voltage applied to a motor to the voltage into the controller. The voltage gains are converted to the physical gains using the scale factors in Tables 7.2 and 7.5.

When an integral controller is used the gain contains the unit seconds^{-1} which cancels with the units of the integral term (seconds).

The evaluation of each control system is based on the criterion noted in Section 3.2; that is, minimum steady state error, minimum overhsoot and fast response with no oscillation.

A complete analogue block diagram of the process and control system number 5 (Fig. 9.15) is shown in Fig. 7.2 for the 1950 feet per minute constant output speed case.

Fig. 9.1 shows three velocity profiles used to drive the servomultipliers in the control system experiments. At the point denoted by 'A' step errors in incoming gauge of 0.004 inches were introduced.

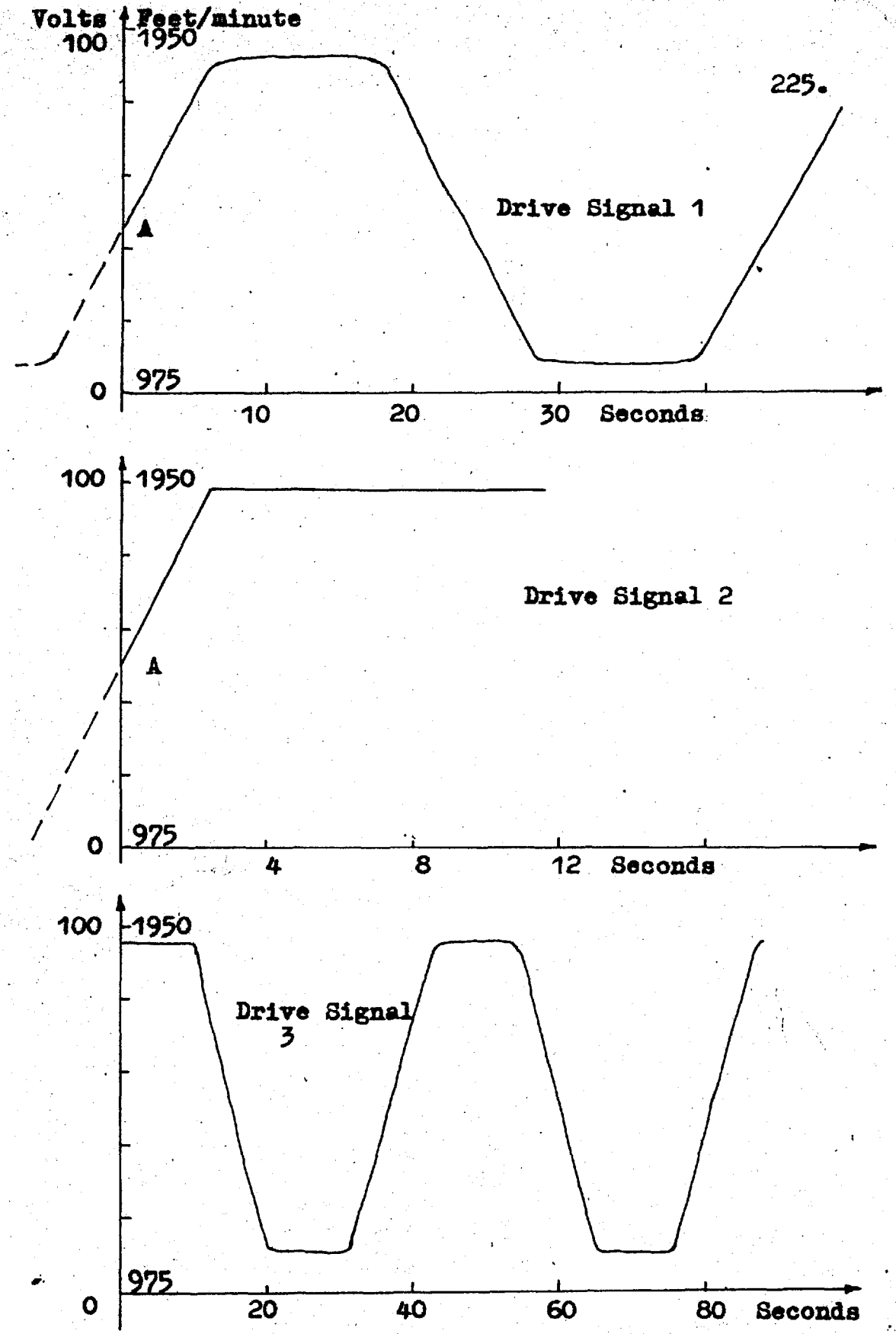

Fig. 9.1 Mill Velocity Characteristics to Drive Servomultipliers in Fig. 7.7.

9.1. CONTROL SYSTEM NUMBER 1

Control system 1 (Fig. 9.2) shows the output strip gauge error, or deviation, being monitored by the x-ray gauge (Section 7.1.1.) then operated on by an integral controller (section 3.4) and fed into the stand 1 drive motor. If the gauge is too thick the error signal will cause the motors to reduce speed and so increase the interstand tension between stands 1 and 2. This action will decrease the strip gauge until the gauge issuing from stand 4 is at the desired value, at which point, δH_4 will be zero.

9.1.1. Responses Using the Simulation of Fig. 7.2

Applying control system number 1, and a step of 0.004 inches, to the simulation of Fig. 7.2 caused a damped oscillation of the process with a controller gain, K_1 equal to 2 r.p.m./thou-second, and a dead-beat response with a gain of 0.5 r.p.m./thou-second as shown in Fig. 9.3. With the latter gain the peak overshoot in δH_4 is +0.00084 inches with the gauge error reduced to 0.0005 inches in 10 seconds and to 0.001 inches in 15 seconds. The steady-state value of the controlling variable, $\delta\sigma_1$, is increased to cause the reduction in strip gauge error. In the initial few seconds the $\delta\sigma_1$ response parallels the response for the system

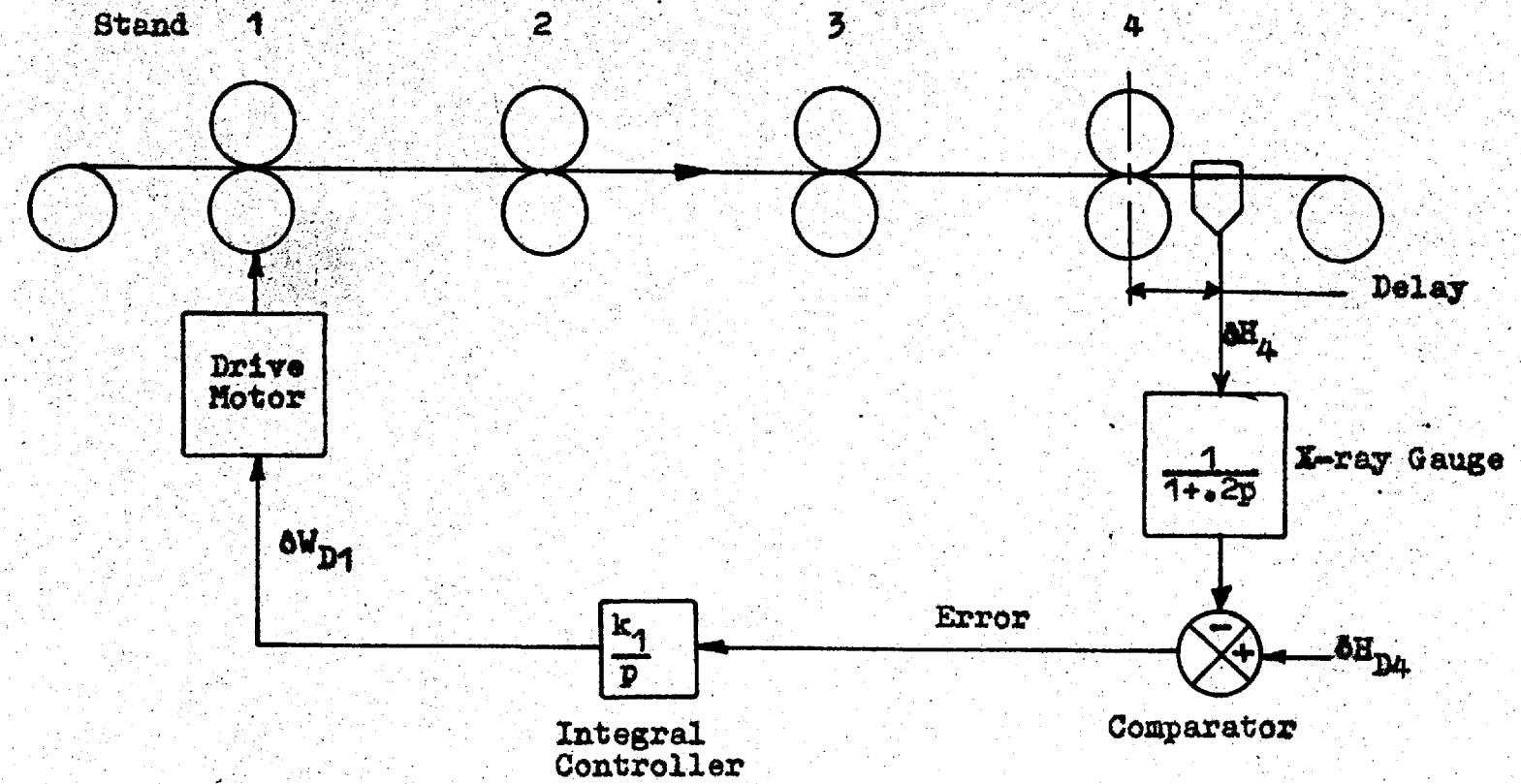

Fig. 9.2. Control System Number 1

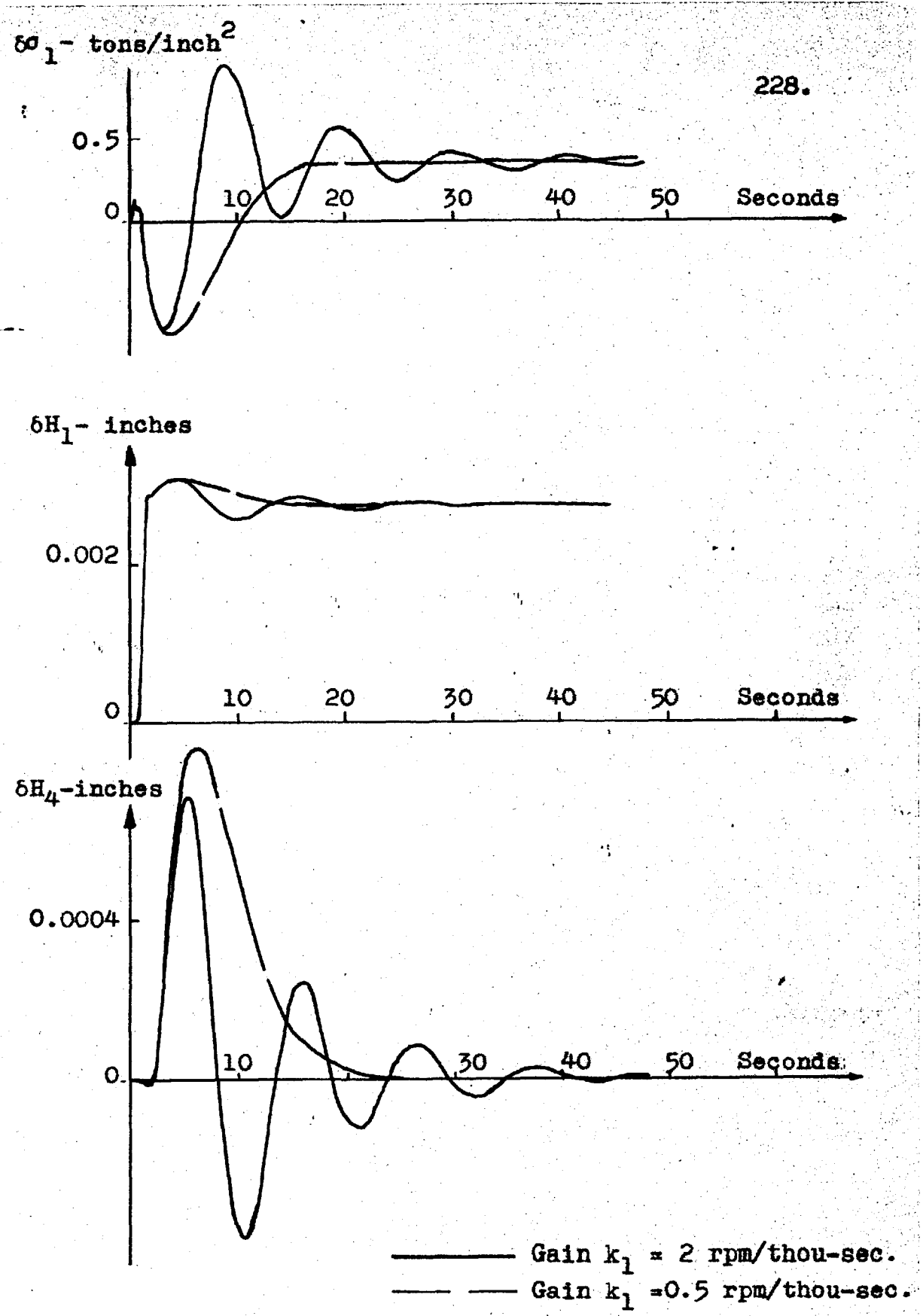

Fig. 9.3 Responses with Control System No. 1. to a .004 inch Step.

without any control. When, 2 seconds after application of the step, a signal is received by the x-ray gauge which operates on the stand 1 drive motor, $\delta\sigma_1$ is brought to a value which gives the required output gauge.

The response of the process, with this type of control to a 0.1 c/s, 0.008 inch peak to peak sine wave imposed on the incoming strip is shown in Fig. 9.4. The experiment was performed with and without slip. Without slip the fluctuations are larger which is in agreement with the open-loop results discussed in chapter 8. With slip the $\delta\sigma_1$ peak is 0.9 tons/inch^2 and the δH_4 peak is 0.00084 inches. The large tension and gauge changes indicate that the system can be improved upon.

9.1.2. Responses Using the Simulation of Fig. 7.7

The control system number 1 was applied to the mill simulation of Fig. 7.7. With no oil film effects or schedule deviations, drive signal number 1 (Fig. 9.1) was applied to the servomultipliers. At point 'A' a step of 0.004 inches in δH_o was introduced and the responses shown in Fig. 9.5 were obtained. They are similar in nature to those of Fig. 9.3 except that the varying coefficients during acceleration and

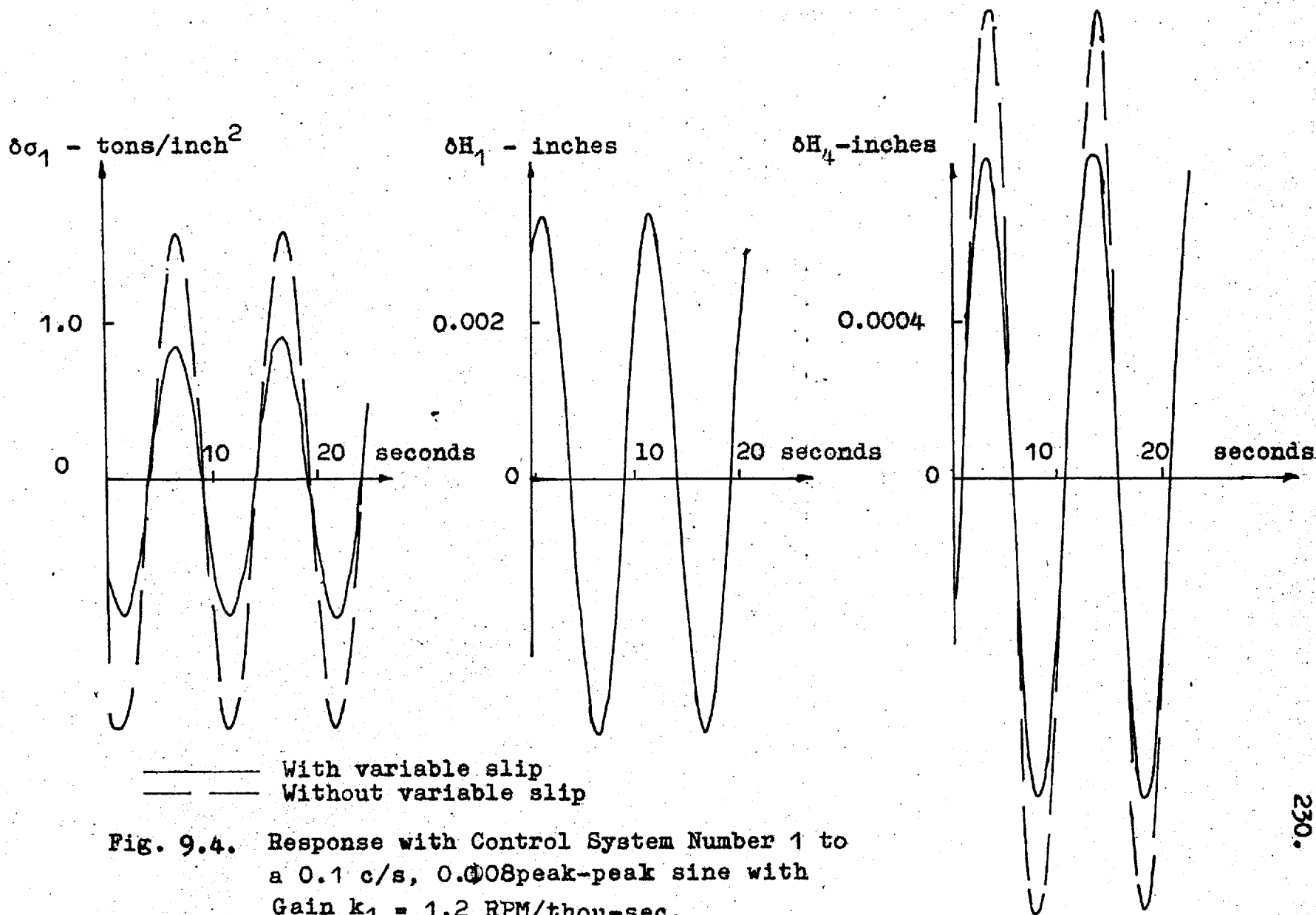

Fig. 9.4. Response with Control System Number 1 to a 0.1 c/s, 0.008peak-peak sine with Gain k_1 = 1.2 RPM/thou-sec.

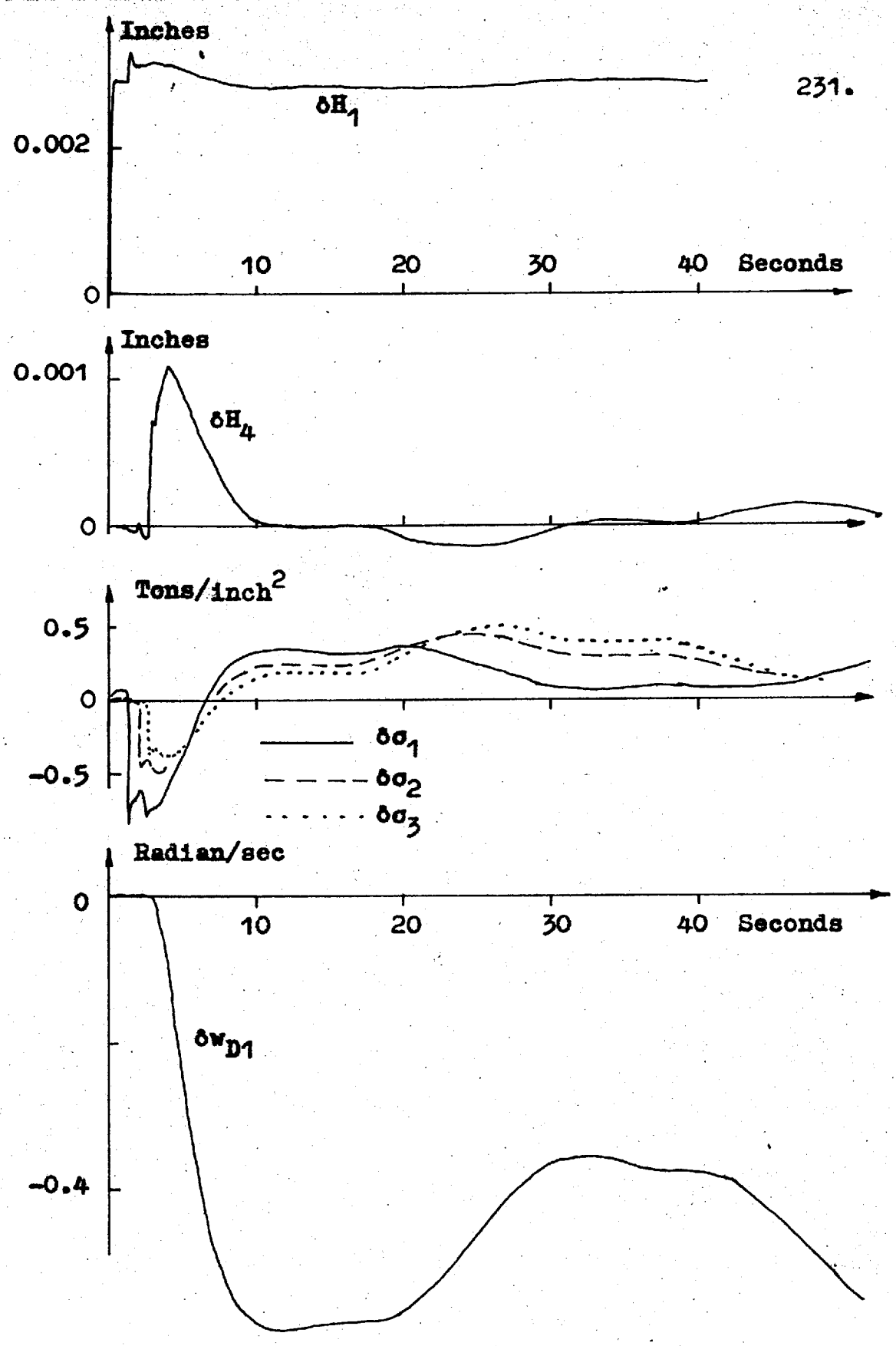

Fig. 9.5 Responses With Control System Number 1
(Ref. Section 9.3.2)

deceleration cause changes in the variables. The demanded stand 1 roll speed, δw_{D1}, as shown by its trace, attempts to correct these variations in δH_4. For this and the next experiment the controller gain was 1.6 r.p.m./thou-second.

With the same set-up the servomultipliers were driven by drive signal number 2 (Fig. 9.1), but with no step in δH_o applied at point A. The oil film and roll force schedule deviations of Table 8.2 were introduced as mill acceleration was simulated.

The traces of Fig. 9.6 show that δH_4 was brought to 0.0005 inches in 8 seconds and to 0.0001 inches in 10 seconds. However, there were large tension changes. With the reel circuit omitted, $\delta\sigma_3$ was -5.3 tons/inch^2. Such a large change would almost bring the interstand tension σ_3 to zero as its scheduled value is 5.77 tons/inch^2 (Table 2.1). Each interstand tension is reduced more than for the same case without control action (Section 8.3 Experiment (8)). This is understandable as this type of control uses the tensions for gauge control. Since the gauge tends to be too thin due to the roll gap having been insufficiently increased during acceleration a decrease in the tensions is required to increase the gauge issuing from the stands. With the

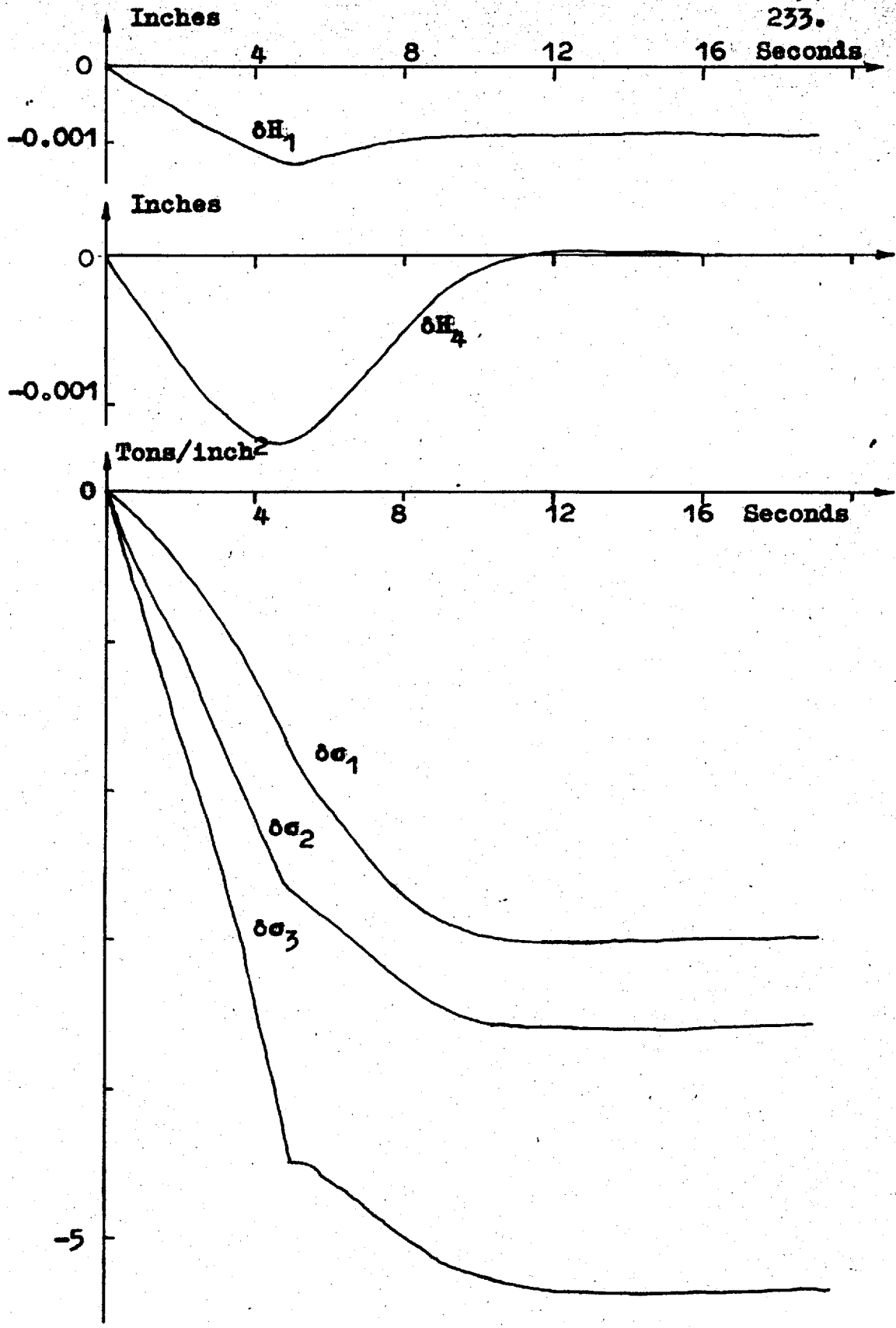

Fig. 9.6 Responses With Control System Number 1
(Ref. Section 9.1.2)

reel circuit included, $\delta\sigma_3$ was only -4.3 tons/inch^2, as, $\delta\sigma_4$ decreased to assist in increasing the output gauge. For the reel-in case, the steady-state value of δw_{D1} was 9.9 r.p.m. and with the reel out δw_{D1} was 11.5 r.p.m.

This experiment was repeated with the mill being accelerated in 10 seconds instead of 5 seconds with no change in the nature of the traces noted.

The scheduled deviations were inserted in this experiment to indicate the capabilities of the mill simulation of Fig. 7.7. Any type of deviation may be inserted in a similar manner. In the remaining control system experiments it is assumed that the schedule is maintained. The evaluation of the control systems is thus based on their ability to control incoming gauge errors with the effects of the varying coefficients included when the simulation of Fig. 7.7 is used. This allows a comparison of the control systems to be made without an arbitrary schedule deviation. Future studies using schedule deviations actually determined from a rolling mill would be useful.

9.2. CONTROL SYSTEM NUMBER 2

As shown in Fig. 9.7 the output gauge error is used to operate the stand 1 screw down motors so as to adjust the roll gap to eliminate the error. A proportional type controller is used here, as the screw down motor transfer function contains an integral term. In the tests the control loop was applied to the screw down motor of each stand in turn.

9.2.1. Responses Using the Simulation of Fig. 7.2

Applying this type of control, and a step input in δH_o of 0.004 inches, to the simulation of Fig. 7.2 with a gain k_1 of 10 thou/thou, caused the process to oscillate as shown in Fig. 9.8. Reducing the gain to 1 thou/thou produced the desired dead beat response which reduced δH_4 to 0.0005 inches in 15 seconds; and to 0.0001 inches in 30 seconds. The response is somewhat slower than that for control system 1.

The strip input error must travel through the mill and be measured by the x-ray gauge which produces the error. This is then acted on by the controller before operating the screw down motor. The corrected gauge is noted by the x-ray gauge after a further 2 seconds. These delays combined with the time required to reduce the strip error results in the peak overshoot in δH_4 occurring at about 7 seconds. The tension, $\delta\sigma_1$, has

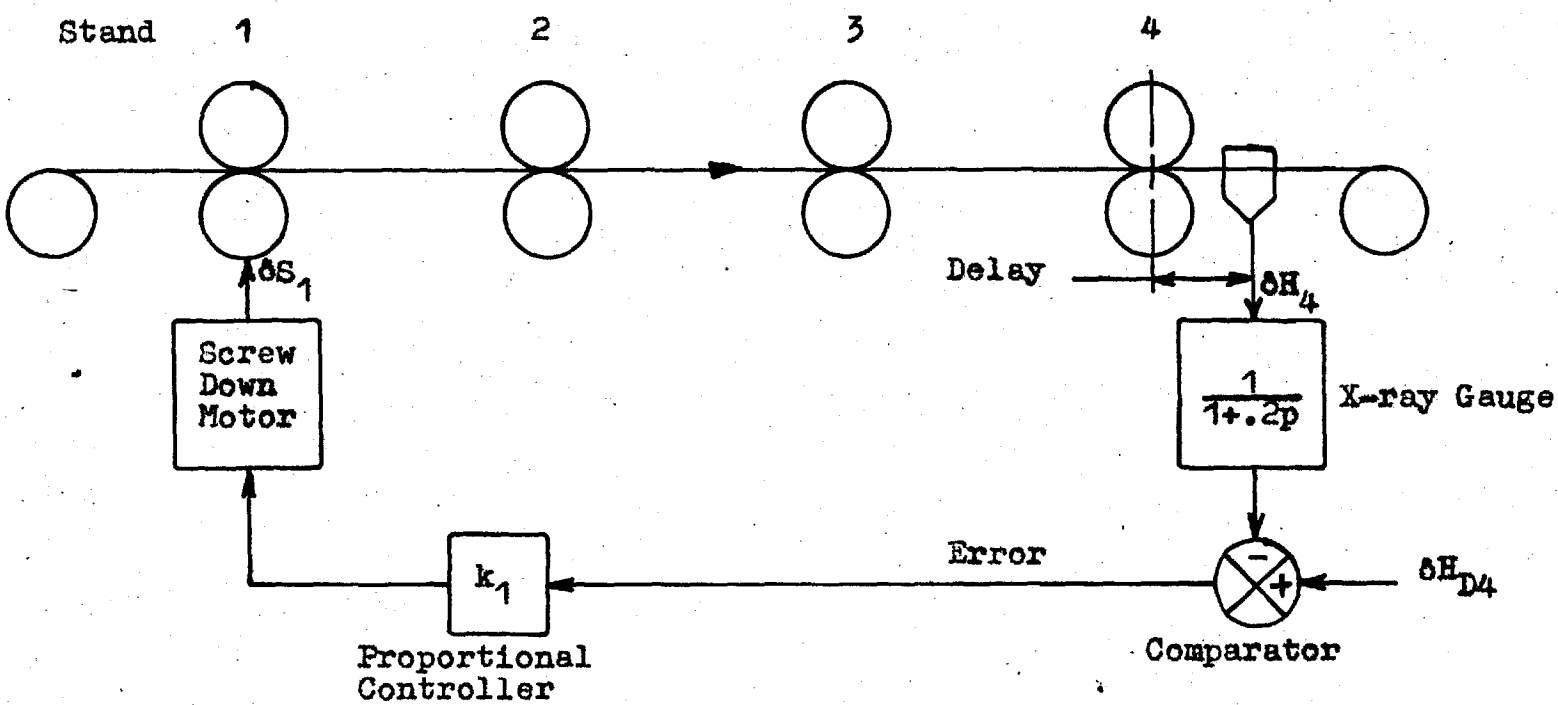

Fig. 9.7. Control System Number 2

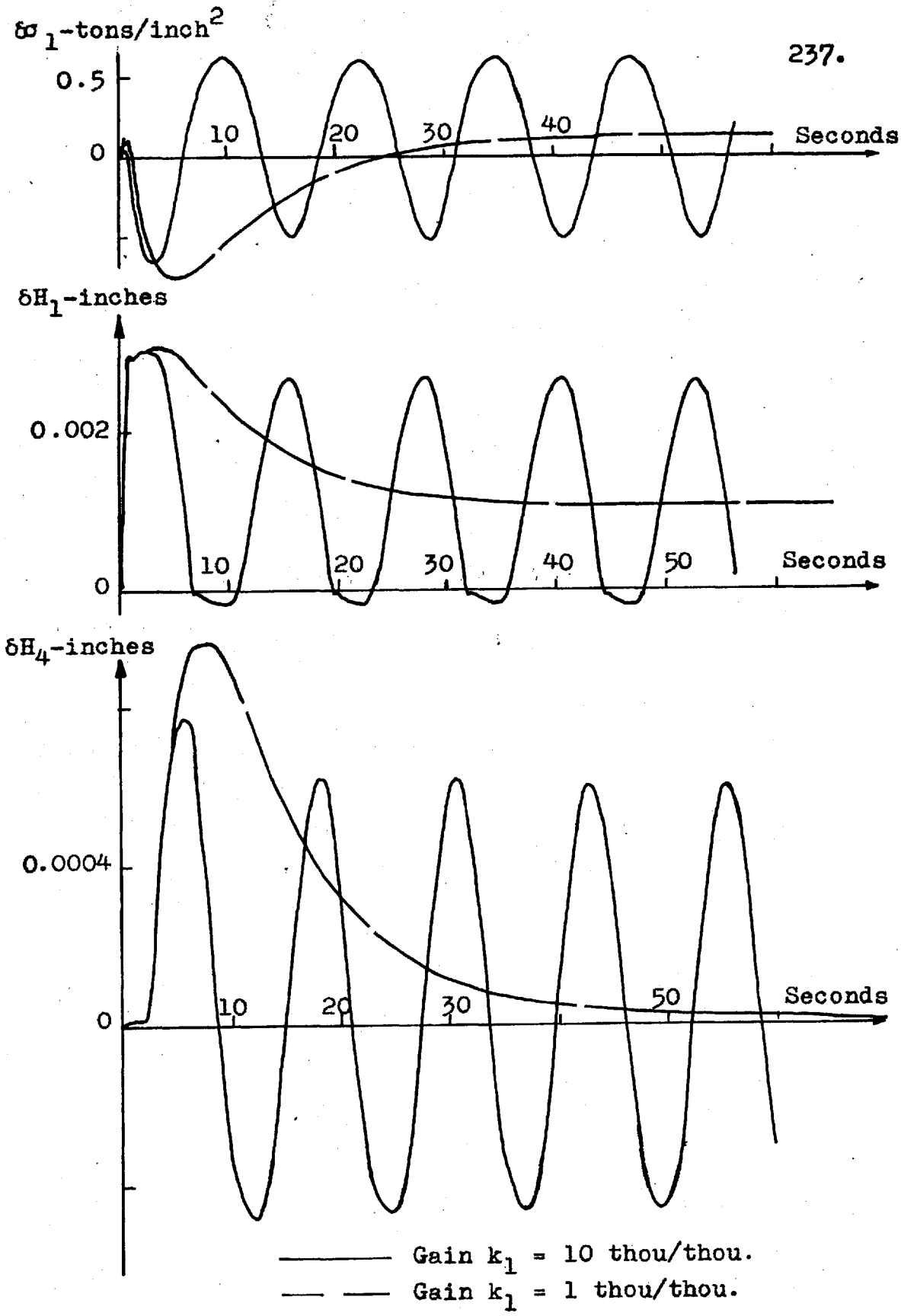

Fig. 9.8. Response with Control System No. 2 to a .004 inch Step.

increased in the steady state due to the screw down action. Such an increase is confirmed by Table D.2 which shows the tensions increasing under screw down action. This action overcomes the effects of the step which tend to make interstand tensions decrease. The net change in $\delta\sigma_1$ is +0.11 tons/inch^2, the negative peak being -0.75 tons/inch^2, which is the same as for control system 1. These peaks are equal as they occur before control action commences.

9.2.2. Responses Using the Simulation of Fig. 7.7

Control system number 2 was applied to the simulation of Fig. 7.7 and the servomultipliers driven with drive signal number 1 (Fig. 9.1). A step in δH_e of 0.004 inches was applied when the drive signal reached a voltage corresponding to mid speed (point A). As with control system number 1 the responses (Fig. 9.9) show that control action is exerted to reduce δH_4 in the presence of the varying coefficients in the simulation. This system does not hold δH_4 as close to zero as does number 1, as the stand 1 screw down control is slower than the tension or drive motor control.

The traces of Fig. 9.10 are the result of applying drive signal number 2 with the screw down control exerted on stands 1, 2, 3 and 4 in succession. A step

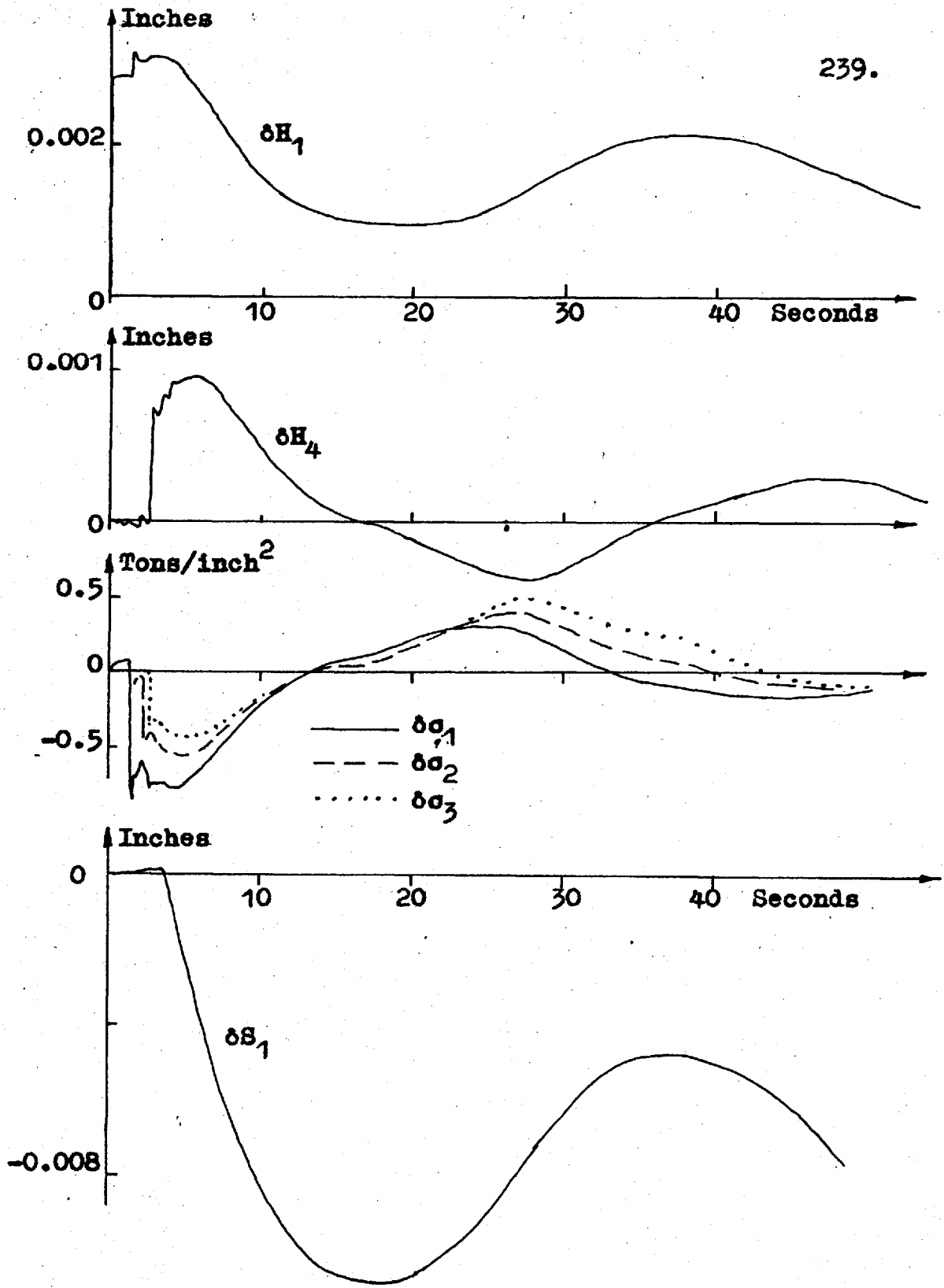

Fig. 9.9 Responses With Control System Number 2
(Ref. Section 9.2.2)

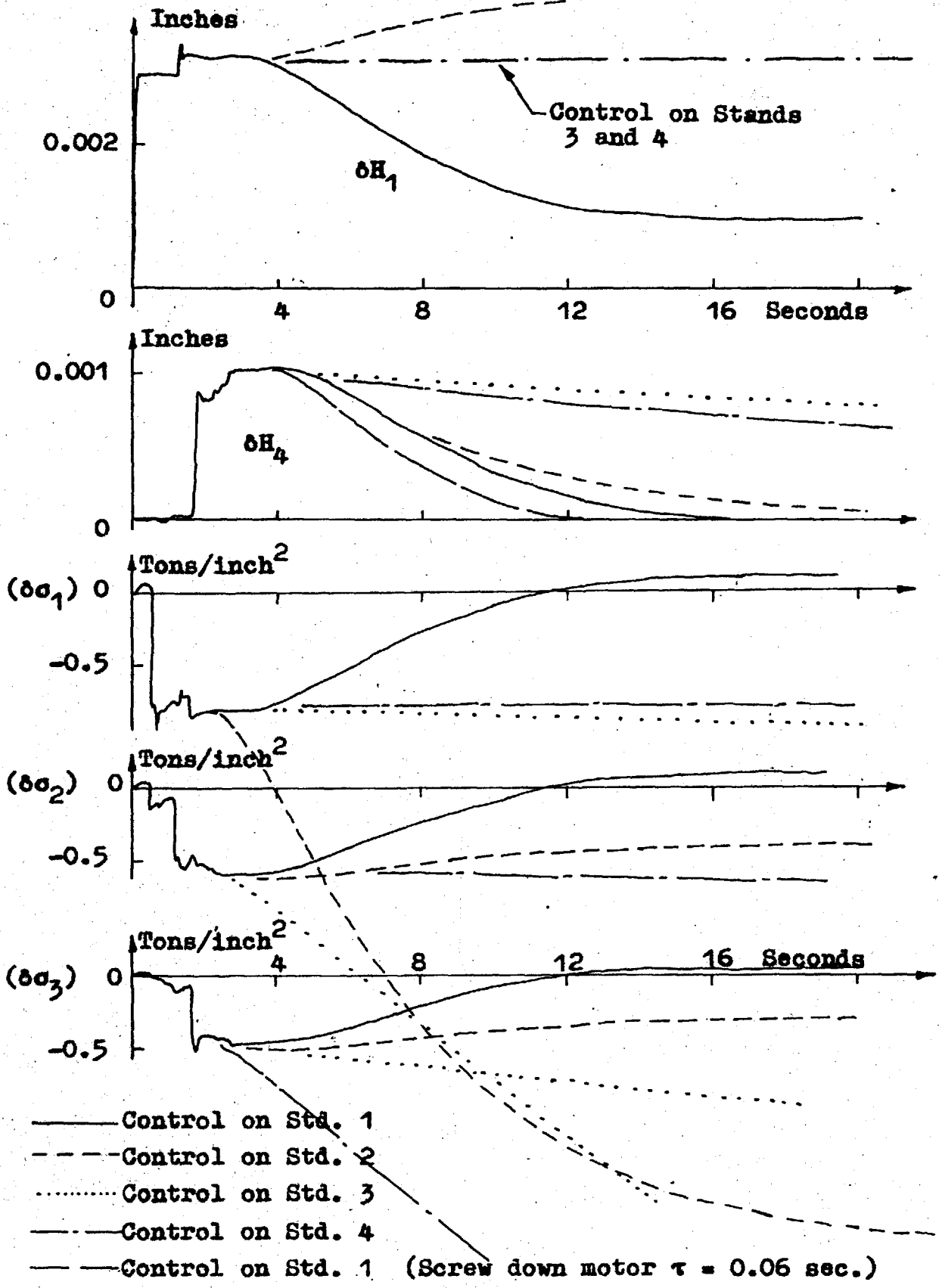

Fig. 9.10 Responses With Control System Number 2
(Ref. Section 9.2.2)

in δH_o of 0.004 inches was introduced in each case when the drive signal reached point A corresponding to mid speed. The traces show that when the control is on other than stand 1, large tension changes are obtained. In each case it is the back tension of the stand being controlled which exhibits a large decrease. This agrees with the results of screw down action discussed in Section 8.3. In some instances the final values of the tensions are not shown as overloading of the computer amplifiers occurred and it was not considered worthwhile rescaling to obtain the value. It could be calculated from Table D.2.

With control on stand 1, the screw down motor time constant was changed to 0.06 seconds from 0.6 seconds. This would correspond to a hydraulic type screw down mechanism, and as the trace for δH_4 indicates, the required output gauge is reached more rapidly with this type of control.

In this and the subsequent experiments the reel circuit has been omitted as it contributes little and its omission facilitates comparison of results from the two simulations.

9.3. CONTROL SYSTEM NUMBER 3

The system of Fig. 9.11 utilises screw down control on the first stand and speed control of the stand 4 drive motors to control the strip output gauge. The drive motor loop contains an integral term that will remove steady-state errors. The control of the stand 4 motors will tend to remove the more rapidly occurring strip errors as the drive motors have a smaller time constant (0.25 sec.) than the screw down motors (0.60 sec.). The drive motor control can be considered a fine control of strip gauge as opposed to the coarse control of the screw down motors.

9.3.1. Responses Using the Simulation of Fig. 7.2.

With this control system applied to the simulation of Fig. 7.2 and a step input of gauge error of 0.004 inches the responses of Fig. 9.12 were obtained. The gain k_1 was 1.0 thou/thou and k_2 was 7.32 r.p.m./thou-second. The value of δH_4 was reduced to 0.0005 inches in 11.5 seconds and to 0.0001 inches in 18 seconds, which is an improvement over the previous two systems.

The tension $\delta\sigma_3$ increased by 1 ton/inch^2 to provide a reduction in gauge. A 1 ton/inch^2 change in $\delta\sigma_3$ is not as severe for the strip as a similar change in tension between the preceding stands as the strip has

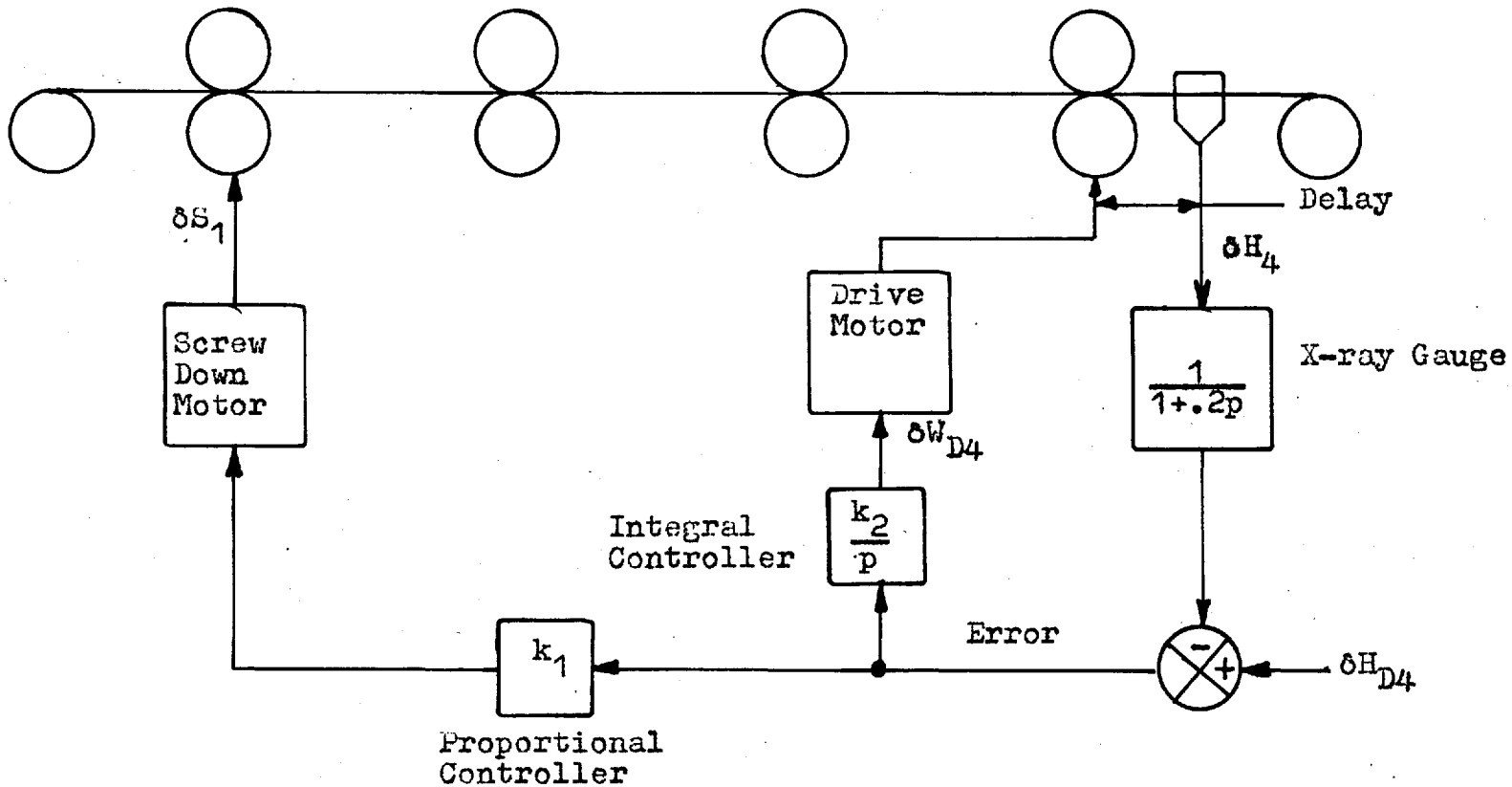

Fig. 9.11. Control System Number 3

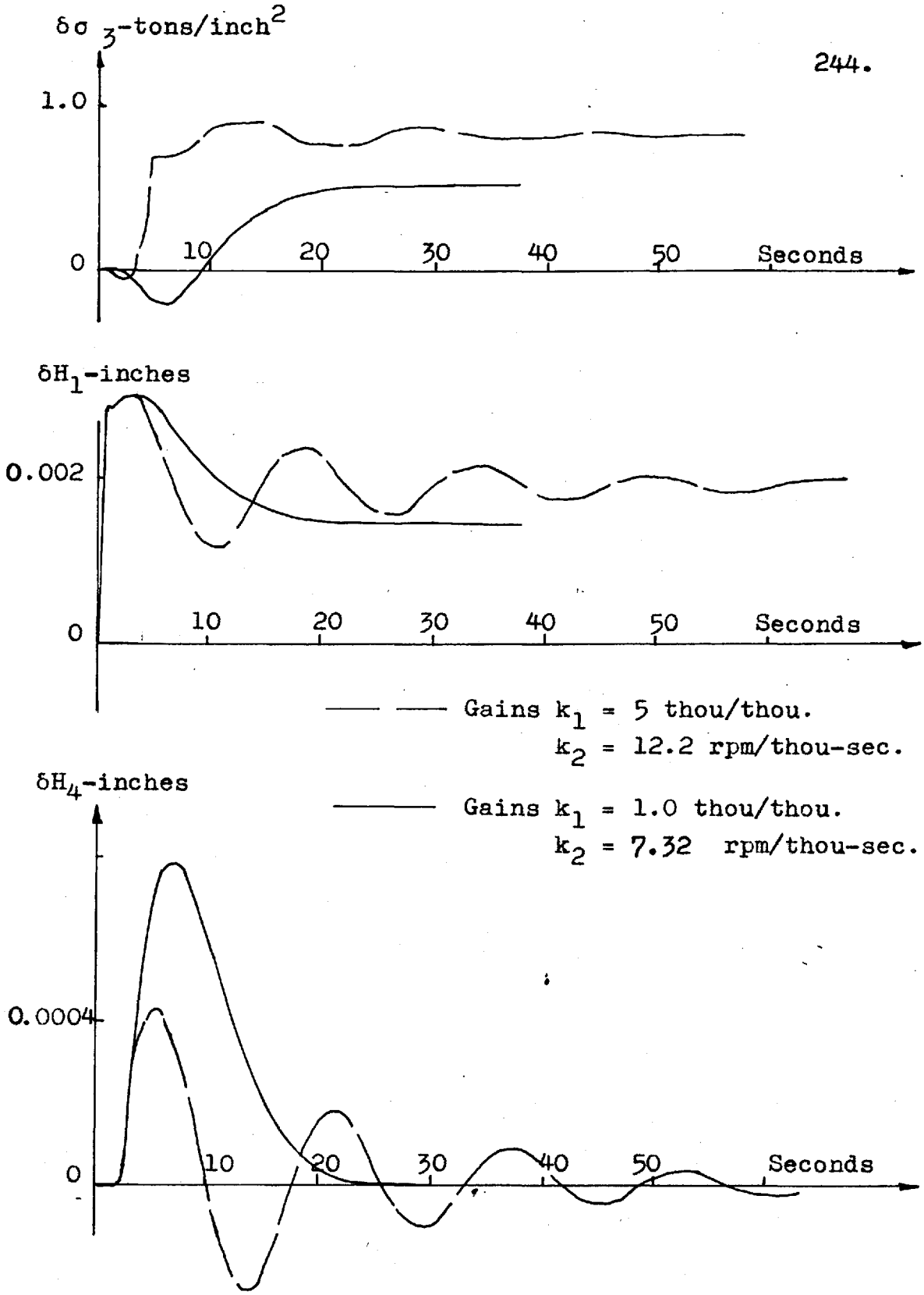

Fig. 9.12 Response with control System Number 3 to a Step of .004 inches.

been work hardened. At the output of stand 1 the yield stress is 33.8 tons/inch^2 while at the output of stand 3 the yield stress is 47.3 tons/inch^2. Because of this control of gauge by tension, the correction made by the stand 1 screws is less than that for the previous control system. This can be seen by comparing the values of δH_1 in Figs. 9.8 and 9.12. The value of the peak overshoot in δH_4 is the same as for system number 2 as it occurs before control action commences.

Fig. 9.13 shows responses to a 0.5$^{c/s}$, 0.008 inch peak to peak sine wave for δH_o. The amplitude of δH_4 is of the same order as for the similar case of control system number 1, indicating that the control action is still not sufficient to remove this type of error on the incoming strip. The traces of Fig. 9.13 have been corrected for attenuation in the pen recorder.

9.3.2. Responses Using the Simulation of Fig. 7.7

With the simulation of Fig. 7.7, drive signal number 2 (Fig. 9.1) and a step in δH_o of 0.004 inches introduced at point A of the drive signal the traces of Fig. 9.14 were obtained. The controller gains were k_1 equal 1.4 thou/thou and k_2 equal 10 r.p.m./thou-second. The transients are slightly more varied than

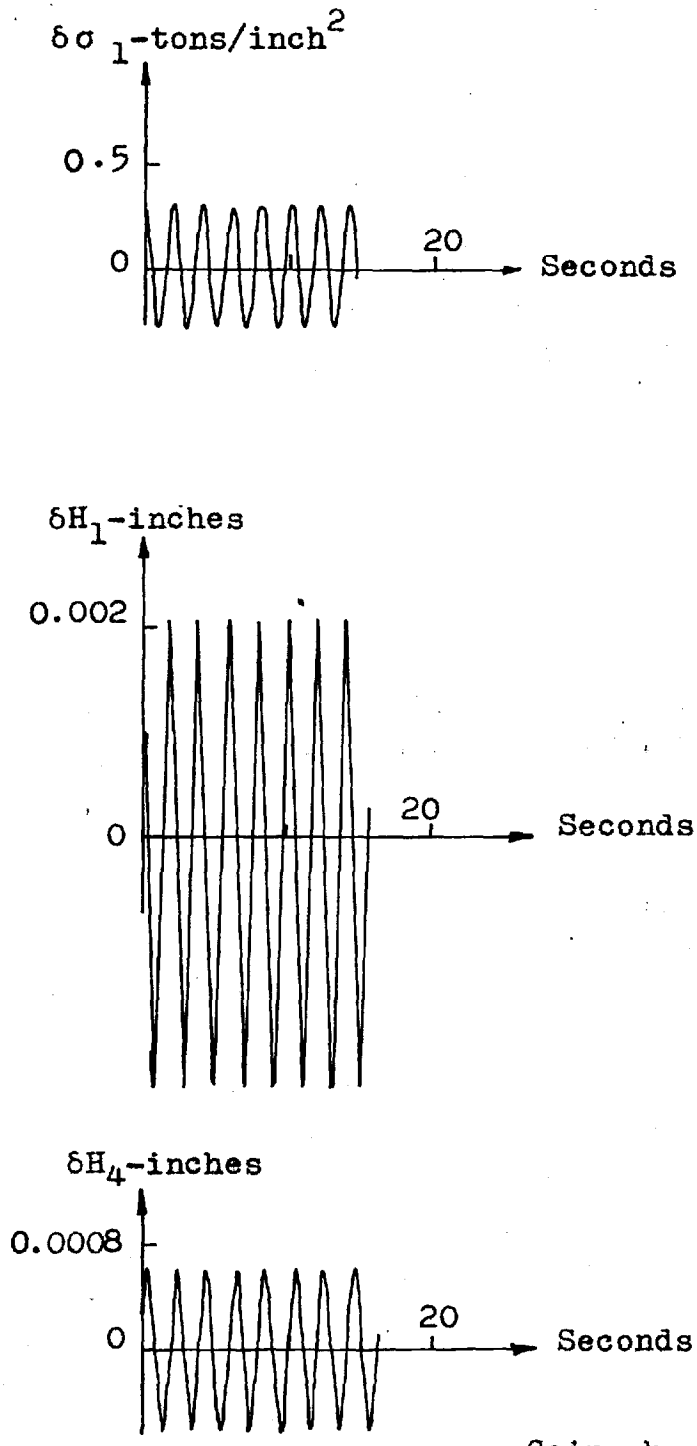

Gains k_1 = 1.0 thou/thou.
k_2 = 0.732 rpm/thou-sec.

Fig. 9.13 Response with Control System Number 3 to a 0.5 c/s, 0.008 inch peak-peak sine.

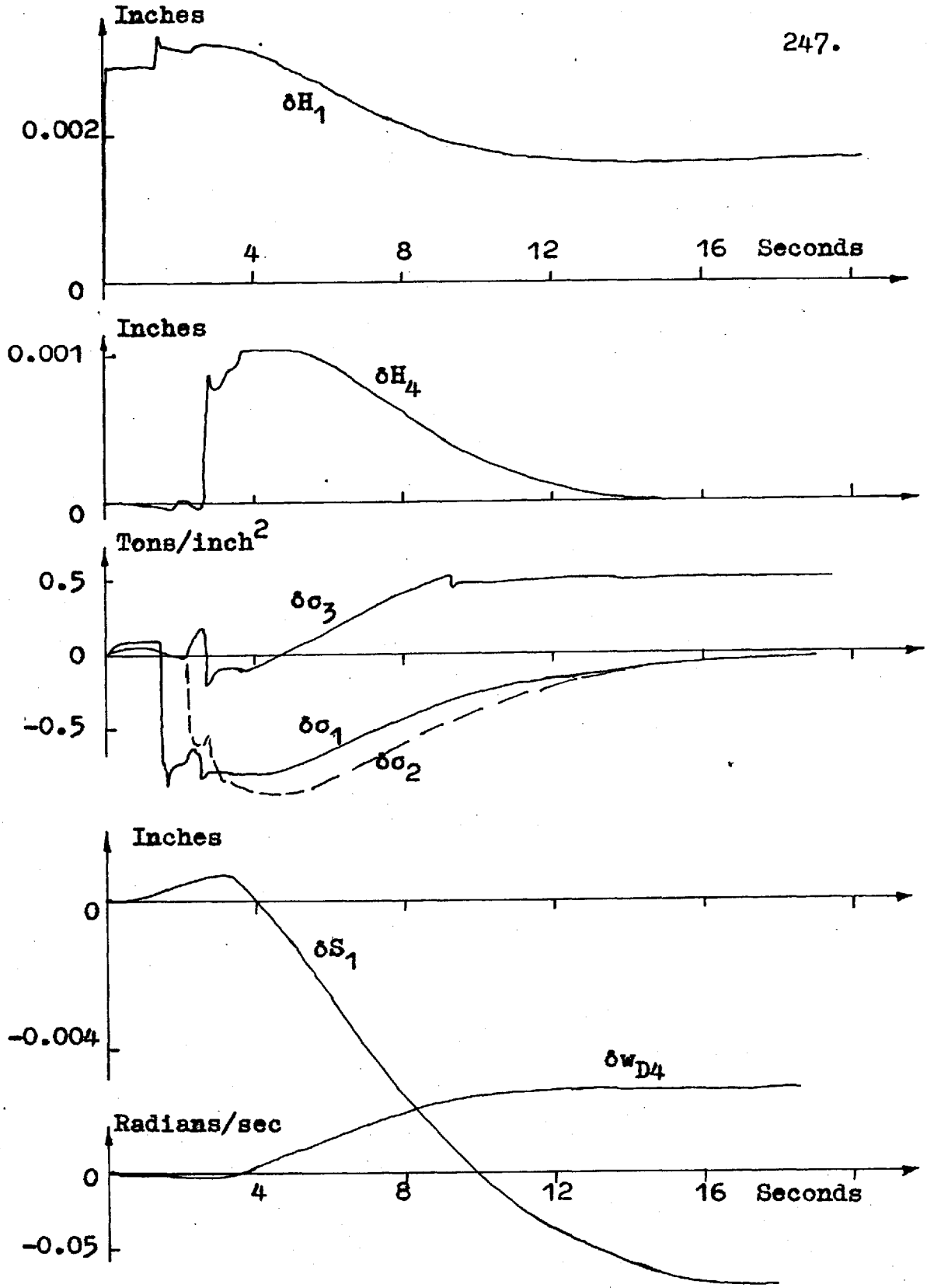

Fig. 9.14 Response With Control System Number 3
(Ref. Section 9.3.2)

those for Fig. 9.12 due to the acceleration, but with the larger gains δH_4 is brought to zero more rapidly. The control action traces show δS_1 decreasing to reduce the gauge and δw_{D4} increasing to increase the tension $\delta \sigma_3$ causing further gauge reduction as discussed.

9.4. CONTROL SYSTEM NUMBER 4

Control system number 4 (Fig. 9.15) consists of controls centered about the first two stands. The output gauge of the first stand is monitored by an x-ray gauge and the error signal used to operate the stand 1 screw down motors. The tension between stands 1 and 2 is monitored by a tensiometer (Section 7.1.2) and its signal applied to the stand 2 drive motor to keep the tension, σ_1, to the scheduled value.

9.4.1. Responses Using the Simulation of Fig. 7.2.

This system was tested in conjunction with the simulation of Fig. 7.2 to indicate the unsatisfactory response of control centered solely about the first two stands. Fig. 9.16 shows the results of applying a 0.004 inch step in δH_o. The δH_4 trace shows that the output gauge has been overcompensated by 0.00064 inches, although δH_1 and $\delta \sigma_1$ are brought to their scheduled values. With this system δH_1 is brought to zero in

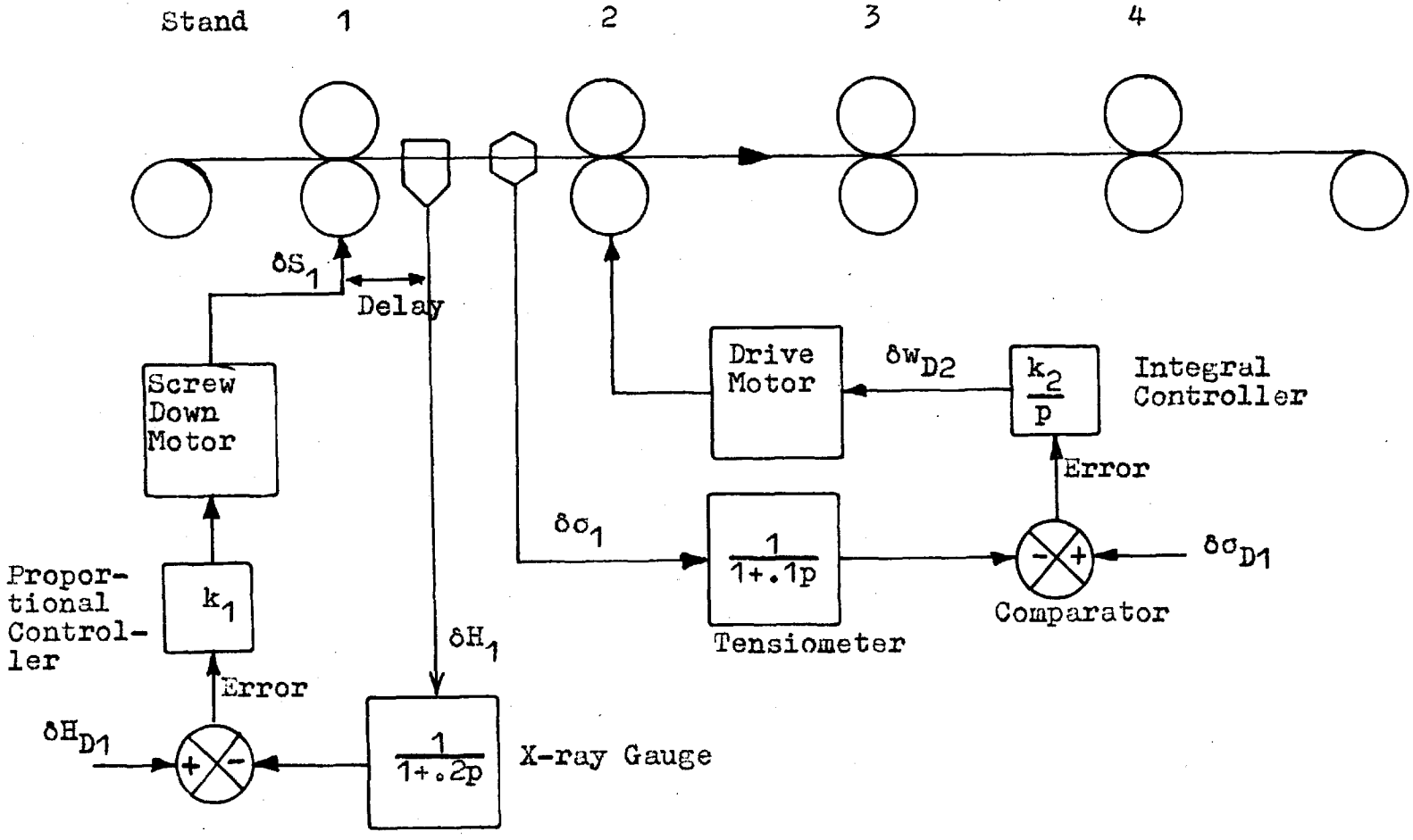

Fig. 9.15. Control System Number 4

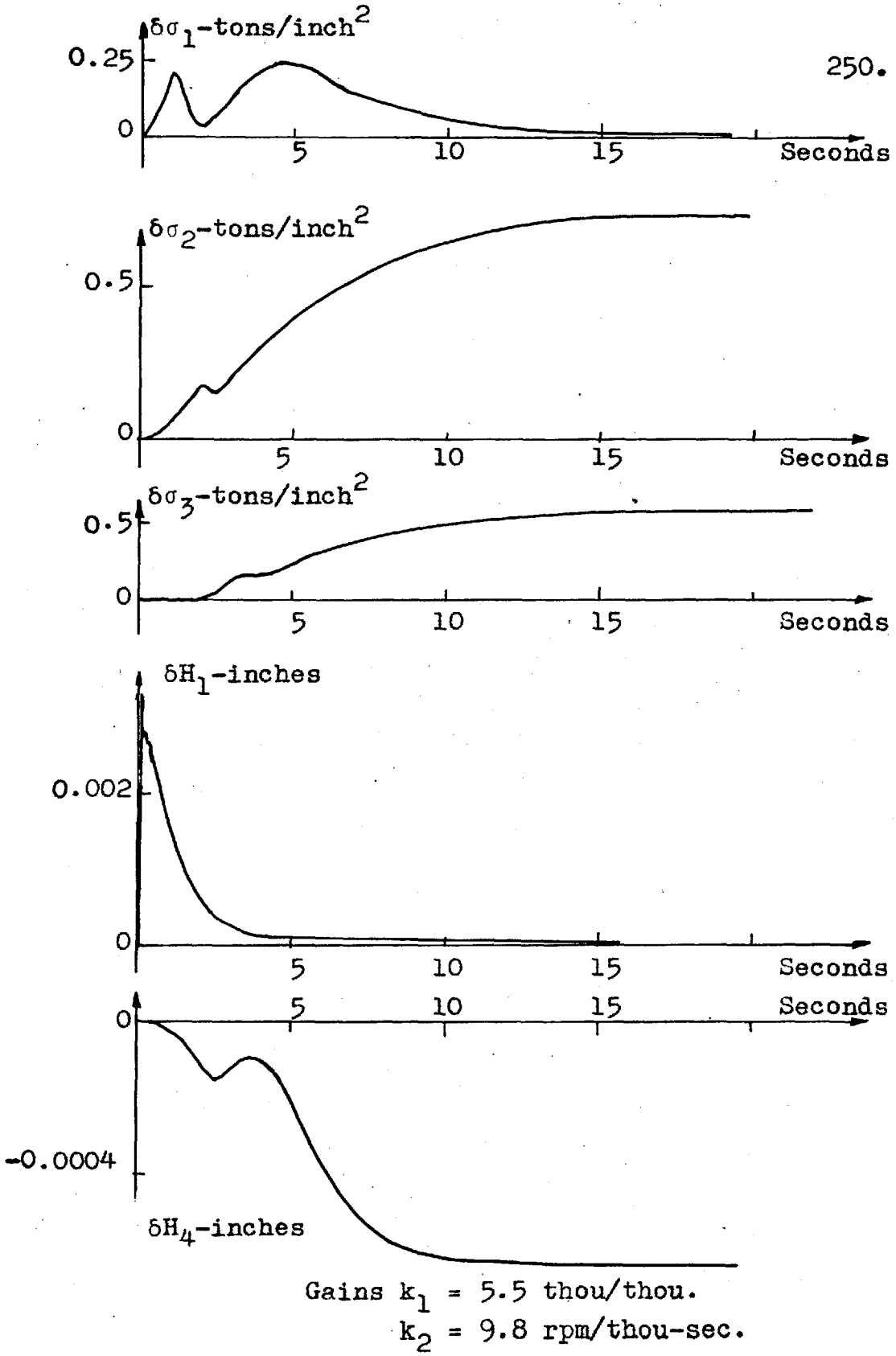

Fig. 9.16. Response with Control System Number 4 to a 0.004 inch step.

about 5 seconds due to the x-ray gauge being after the first stand.

Overcompensation results from the increase in $\delta\sigma_2$ and $\delta\sigma_3$ which reduce the gauge from the latter stands. The step into stand 1 reduces its output velocity initially, thereby increasing $\delta\sigma_1$. When the tension control loop acts to bring $\delta\sigma_1$ to zero by decreasing stand 2 roll speed, the tension $\delta\sigma_2$ is increased. An increase in $\delta\sigma_2$ results in an increase in rolling torque required at stand 3; as it is not supplied, the stand roll speed decreases resulting in an increase of $\delta\sigma_3$.

9.5. CONTROL SYSTEM NUMBER 5

Fig. 9.17 illustrates the fifth type of control system tested to keep the strip on gauge. The three interstand tensions are controlled and the output gauges of stands 1 and 4 are measured and controlled.

The control of the stand 1 front tension and gauge is intended to remove long term and large errors. The stand 1 and 4 gauge control loops contain dead zones (Appendix B) to prevent the screw down motors from operating continuously, thus eliminating overheating of the motors and excessive wear of the screws. The dead zones were set at $\pm$ 0.001 inches for the stand 1 loop and at $\pm$ 0.0005 inches for the stand 4 loop.

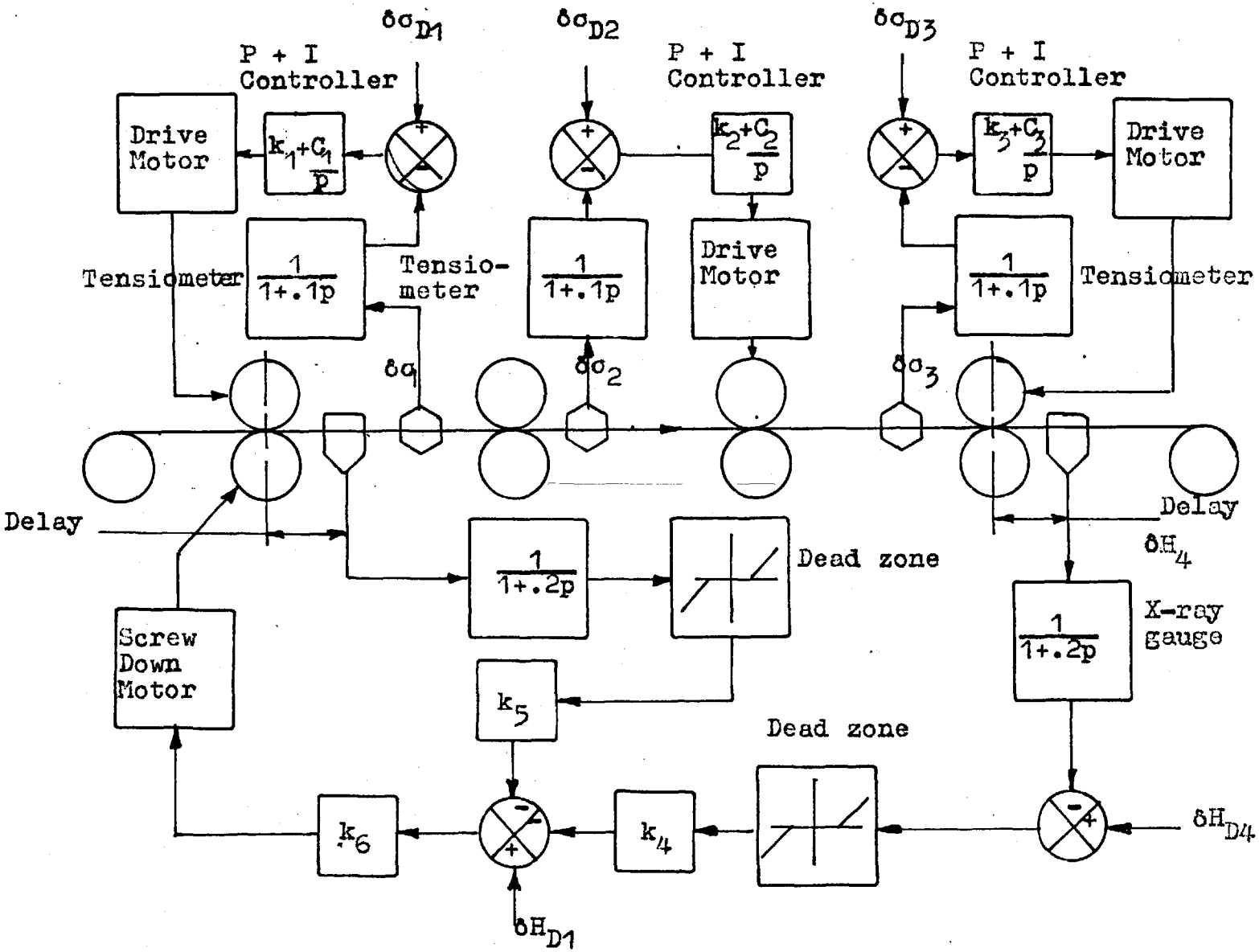

Fig. 9.17. Control System Number 5

The tension control loops contain proportional plus integral type controllers. The integral action being used to remove steady state errors. Controlling the tensions also helps to prevent strip breakage and cobbles.

9.5.1. Responses Using the Simulation of Fig. 7.2.

With the control system applied to the simulation of Fig. 7.2 each sub-loop gain was set in turn to the required value.by testing with a step input of 0.004 inches. Figs. 9.18(a) and 9.18(b) were recorded with the following gain settings.

k_1 = 0.2 rpm/ton/inch^2 c_1 = 8 rpm/ton/inch^2/sec
k_2 = 0.1 rpm/ton/inch^2 c_2 = 5 rpm/ton/inch^2/sec
k_3 = 0.05 rpm/ton/inch^2 c_3 = 1 rpm/ton/inch^2/sec
k_4 = 0.75 thou/thou
k_5 = 0.1 thou/thou
k_6 = 10 thou/thou

Without the dead-zones in the gauge control loops the peak value of δH_4 for the 0.004 inch step input is under 0.0001 inches, which is an order of magnitude better than for the previous gauge control systems discussed. The maximum tension change associated with the step input is; $\delta\sigma_1$ equal to 0.15 tons/inch^2.

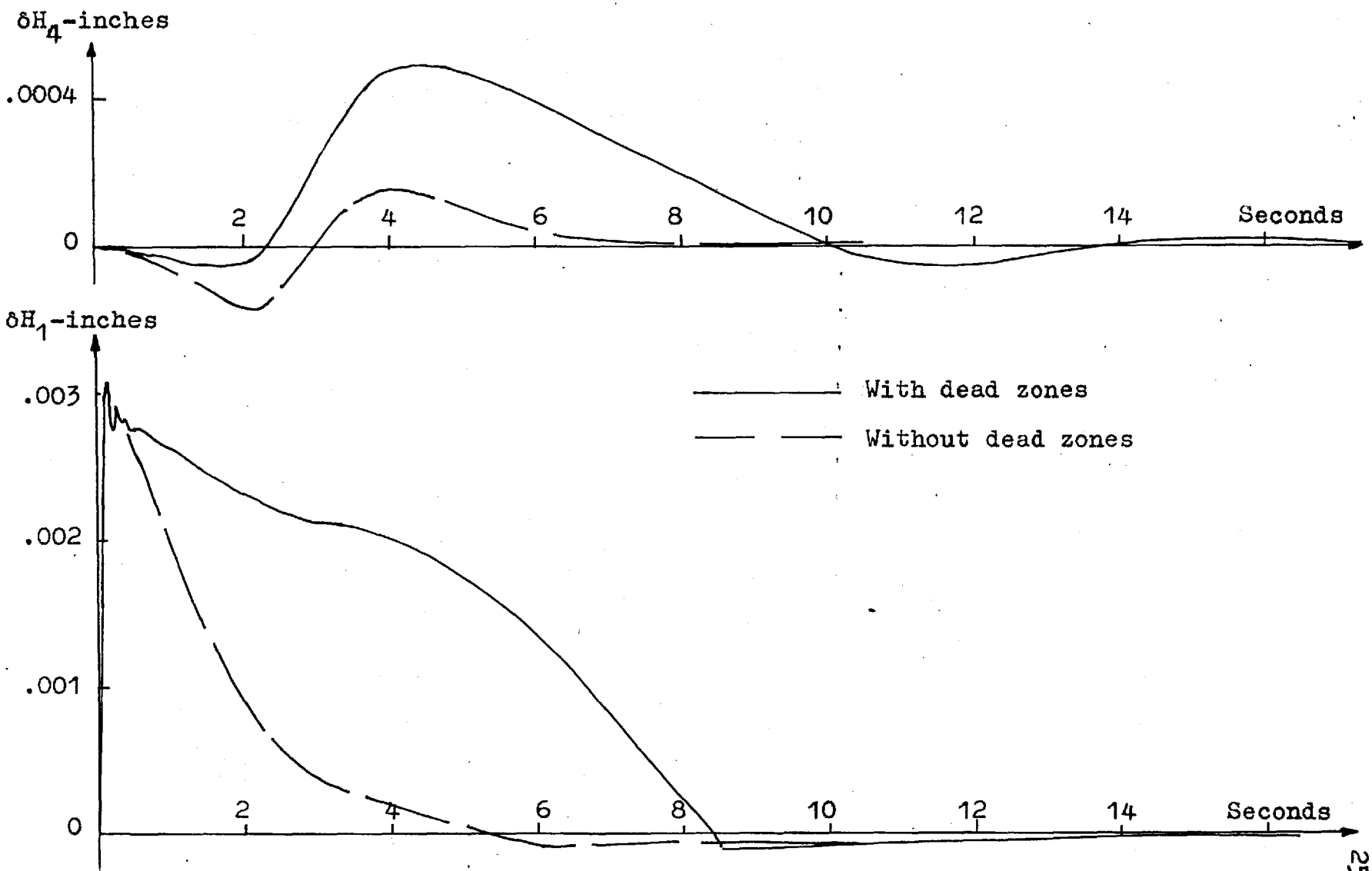

Fig. 9.18(a) Response with Control System Number 5 to a 0.004 inch step.

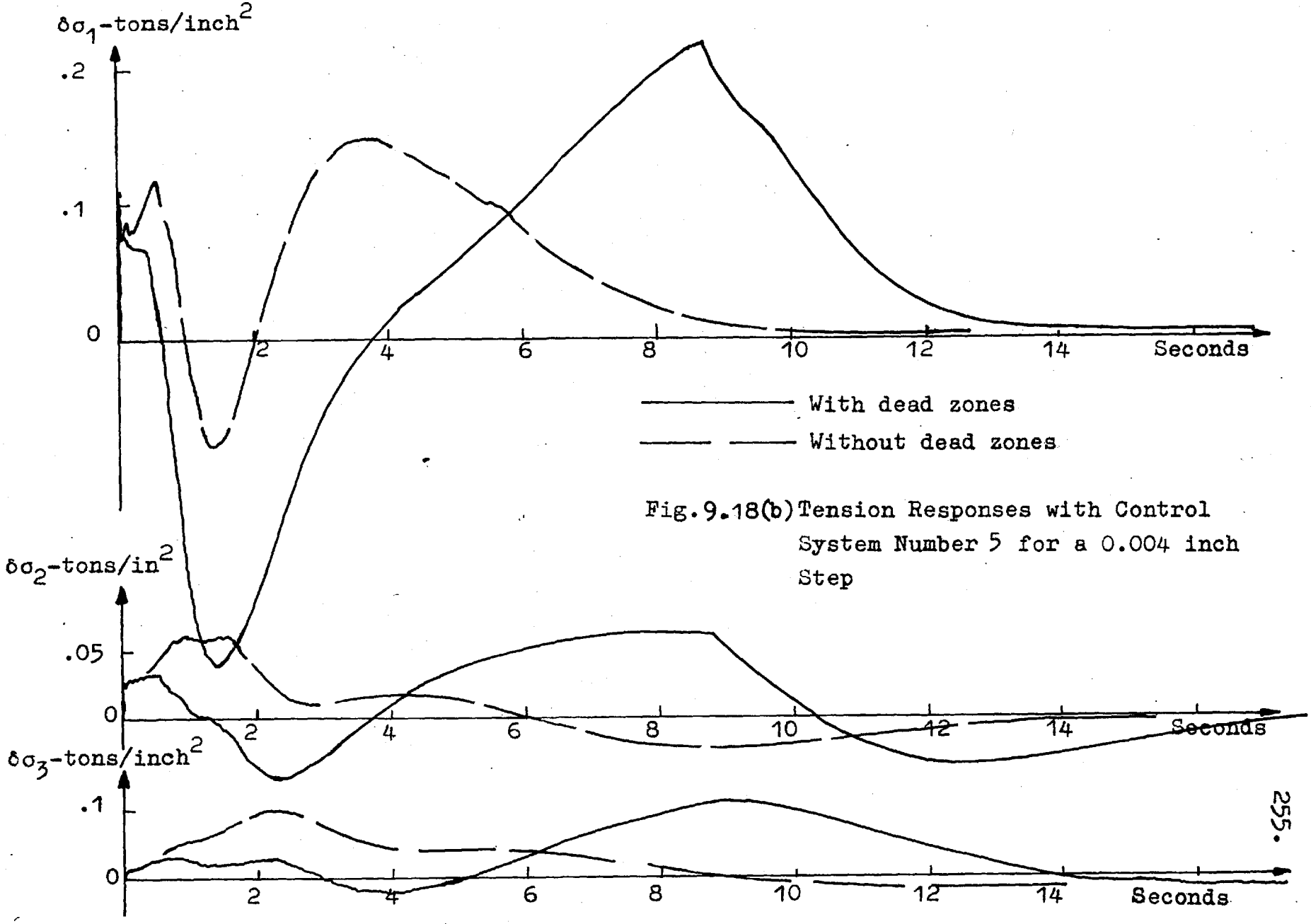

Fig. 9.18(b) Tension Responses with Control System Number 5 for a 0.004 inch Step

With the dead zones included the performance of the control system is reduced, as would be expected since there is no gauge control signal for errors that do not exceed the limits of the dead zones. The peak value of the tension changes is $\delta\sigma_1$ equal to -0.24 tons/inch^2 and +0.22 tons/inch^2. The output gauge deviation, δH_4, is reduced to 0.0001 inches in 8 seconds.

Both with and without the dead zones, δH_1 reaches a peak of 0.0031 inches, but is then reduced to the scheduled value with little overshoot. The tensions, after several overshoots, commence decreasing to their scheduled values when δH_1 has been reduced to near zero (8.5 seconds), as would be expected since there is little gauge error to travel down the mill to cause further fluctuations. This control system acts to keep the tensions and gauges at scheduled values.

The application of a 0.5c/s, 0.008 inch peak to peak sine wave for δH_o produced the response shown in Fig. 9.19 with the dead zones included in the control loops. The amplitude of δH_4 is held to $\pm$ 0.0013 inches.

This system although more complex than the previous system results in more strip being rolled to gauge and a reduction in the amplitude of the gauge errors.

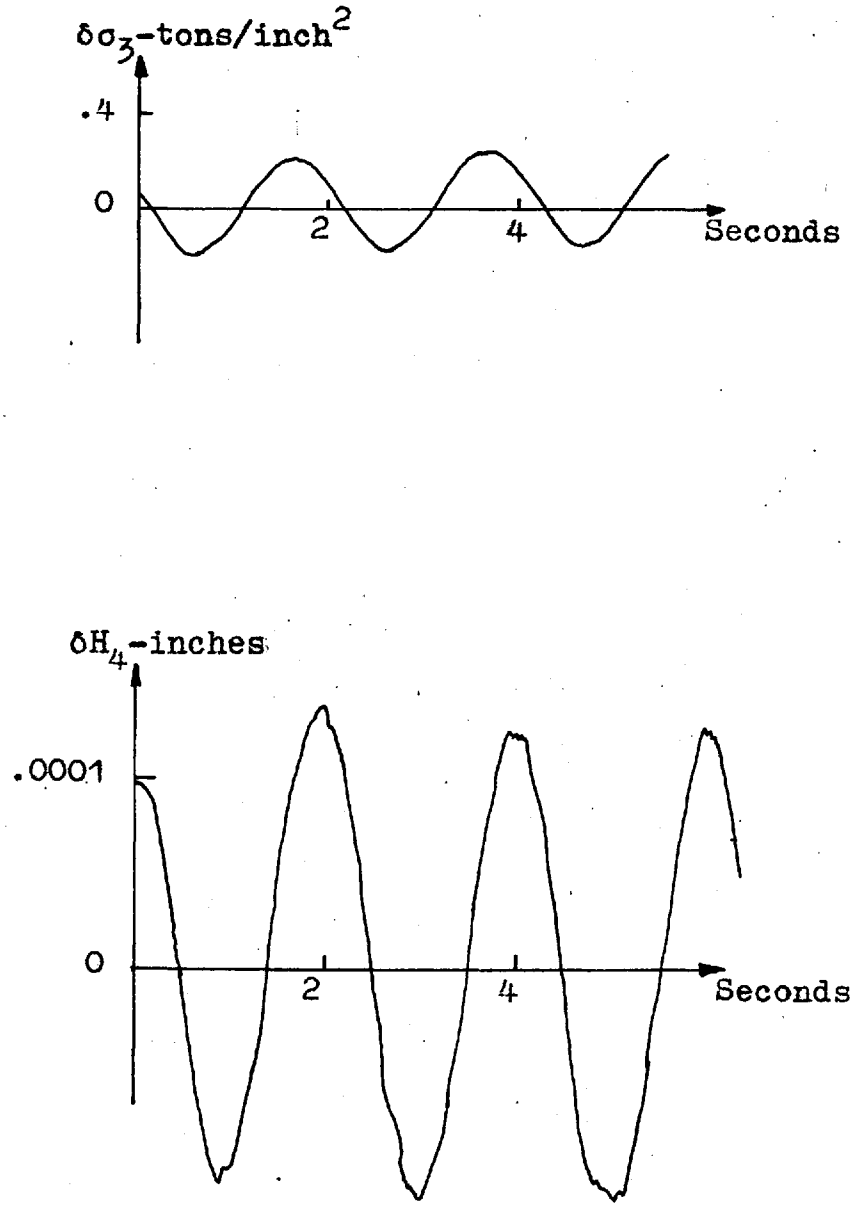

Fig. 9.19. Response with Control System Number 5 to a 0.5 c/s sine, 0.008 inches peak to peak with Dead Zones Included.

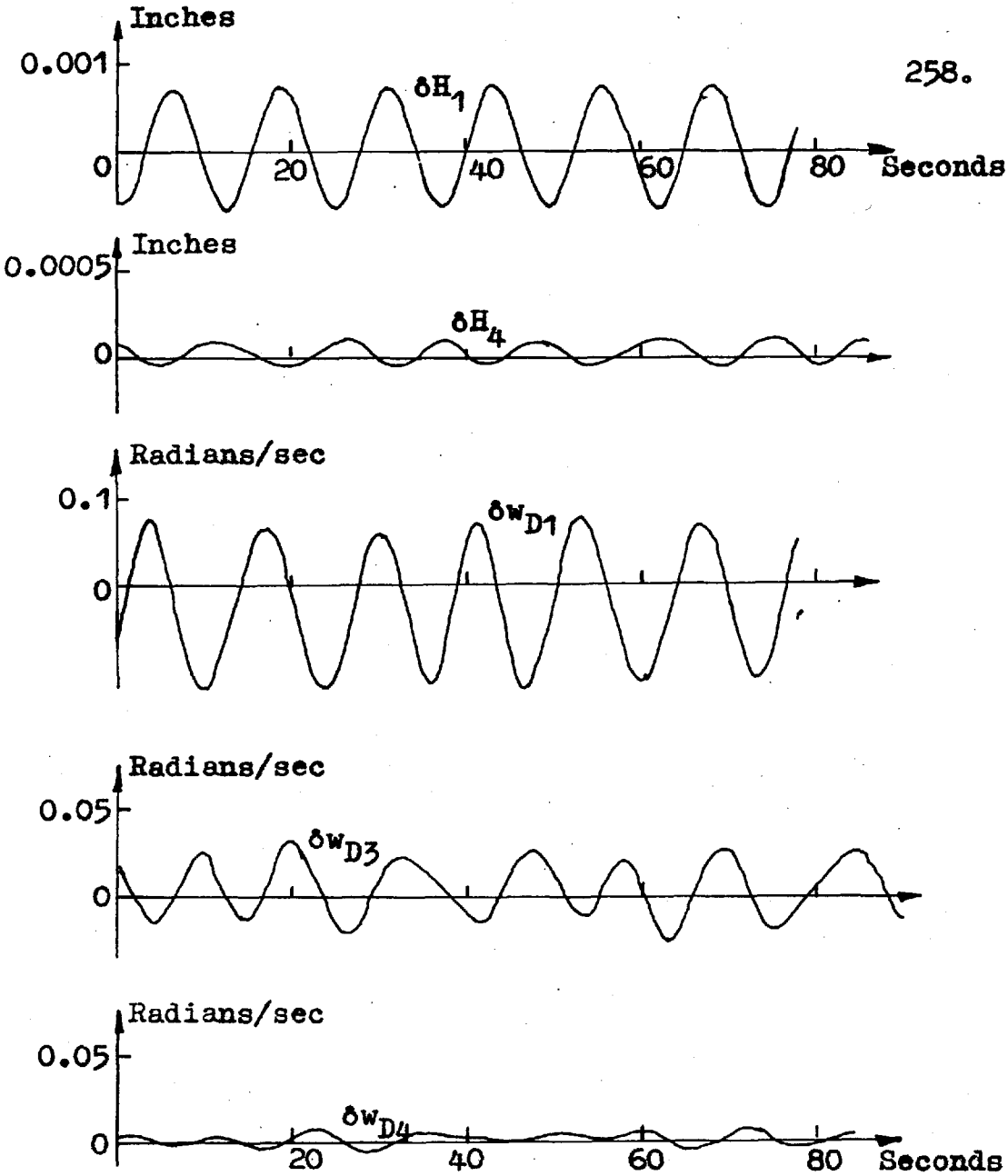

Fig. 9.20 Responses With Control System Number 5
(Ref. Section 9.5.2)

9.5.2. Responses Using the Simulation of Fig. 7.7

Using the simulation of Fig. 7.7 and drive signal number 3, a sine wave of 0.5 radians/second and 0.002 inches peak to peak for δH_0 was applied. The values of k_1, k_2 and k_3 were reduced to zero to indicate the effects of such a decrease. Recordings (Fig. 9.20) showed δH_1 held to limits of ± 0.0014 inches and δH_4 to ± 0.00017 inches. During acceleration and deceleration there is a change in the period of δH_4 due to the changing delay times. The change in gains has caused the system performance to be reduced.

9.6. CONTROL SYSTEM NUMBER 6

Control system number 6 (Fig. 9.21) includes tension control on stands 1, 2 and 3 to maintain constant σ_1, σ_2 and σ_3. As in number 5, the gauges out of stands 1 and 4 are monitored by x-ray gauges and the signals used to operate the stand 1 screw down motors after passing through dead zones. Here the measurement of the output gauge deviation, δH_4, is also used to operate the stand 4 drive motors to provide rapid control of the gauge from stand 4 by tension between stands 3 and 4. The dead zones were set at ± 0.001 inches for the stand 1 loop and at ± 0.00025 inches for the stand 4 loop.

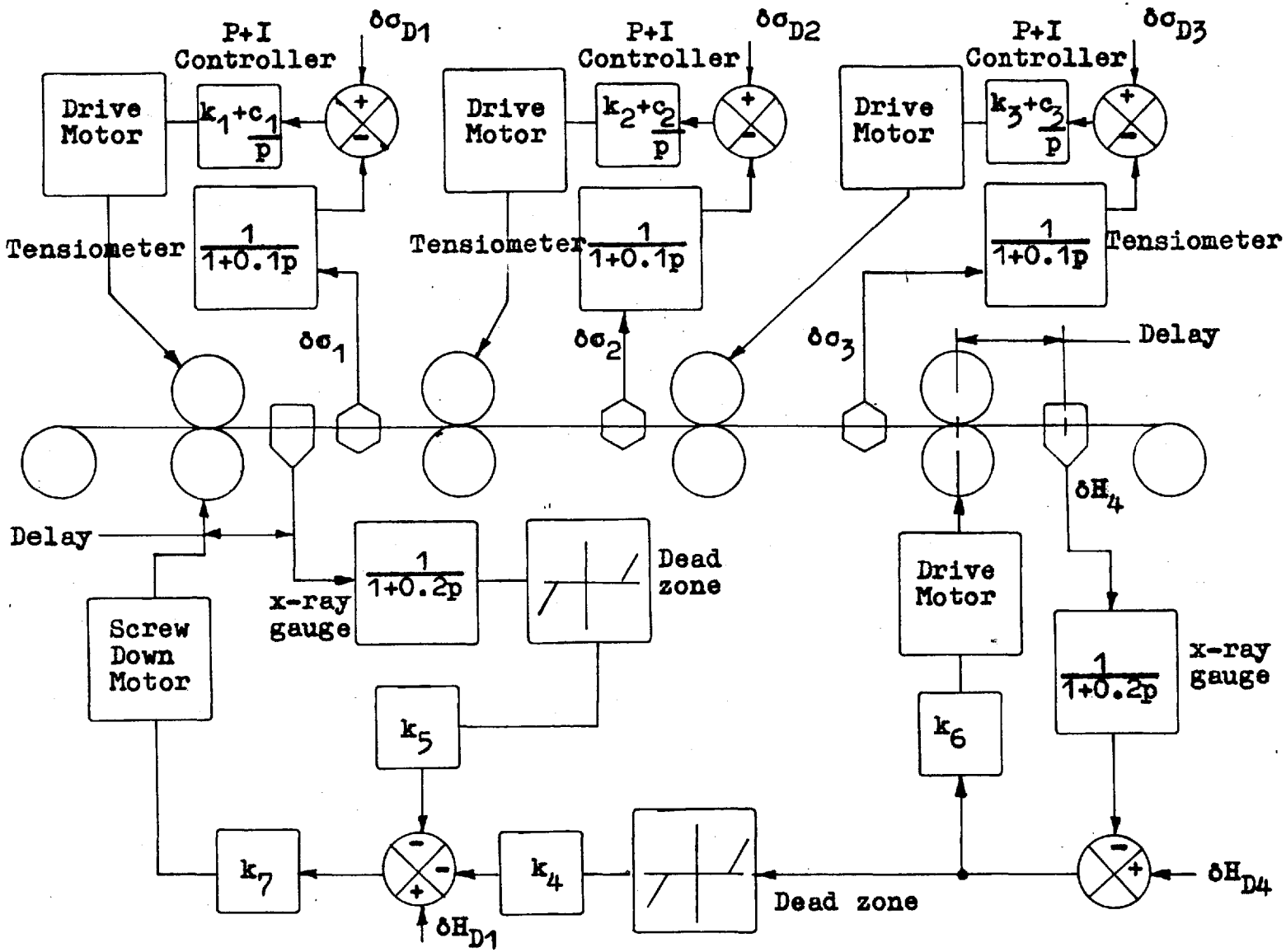

Fig. 9.21 Control System Number 6

9.6.1. Responses Using the Simulation of Fig. 7.7

Control system number 6 was applied to the simulation of Fig. 7.7 and the loop gains adjusted to the following values with the reel circuit eliminated

$k_1 = 0$ $\quad c_1 = 5$ rpm/ton/inch^2-sec.

$k_2 = 0$ $\quad c_2 = 5$ rpm/ton/inch^2-sec.

$k_3 = 0$ $\quad c_3 = 0$

$k_4 = 0.18$ thou/thou

$k_5 = 0.5$ thou/thou

$k_6 = 3$ rpm/thou-second

$k_7 = 10$ thou/thou

The values of k_3 and c_3 were set equal to zero, in effect removing the loop tending to hold σ_3 constant as it proved unsatisfactory. This was expected as the stand 4 drive motor is being used to vary σ_3 to control the strip gauge.

The traces of Fig. 9.22 show the results of applying drive signal number 2 with a step of 0.004 inches in δH_o at point A. Although δH_4 exhibits some overshooting it is held to a range of $\pm$0.00055 inches and brought to 0.0001 inches in 8.5 seconds. The responses are similar to those for a step input with control system number 5 although a direct comparison cannot be made due to mill acceleration being simulated

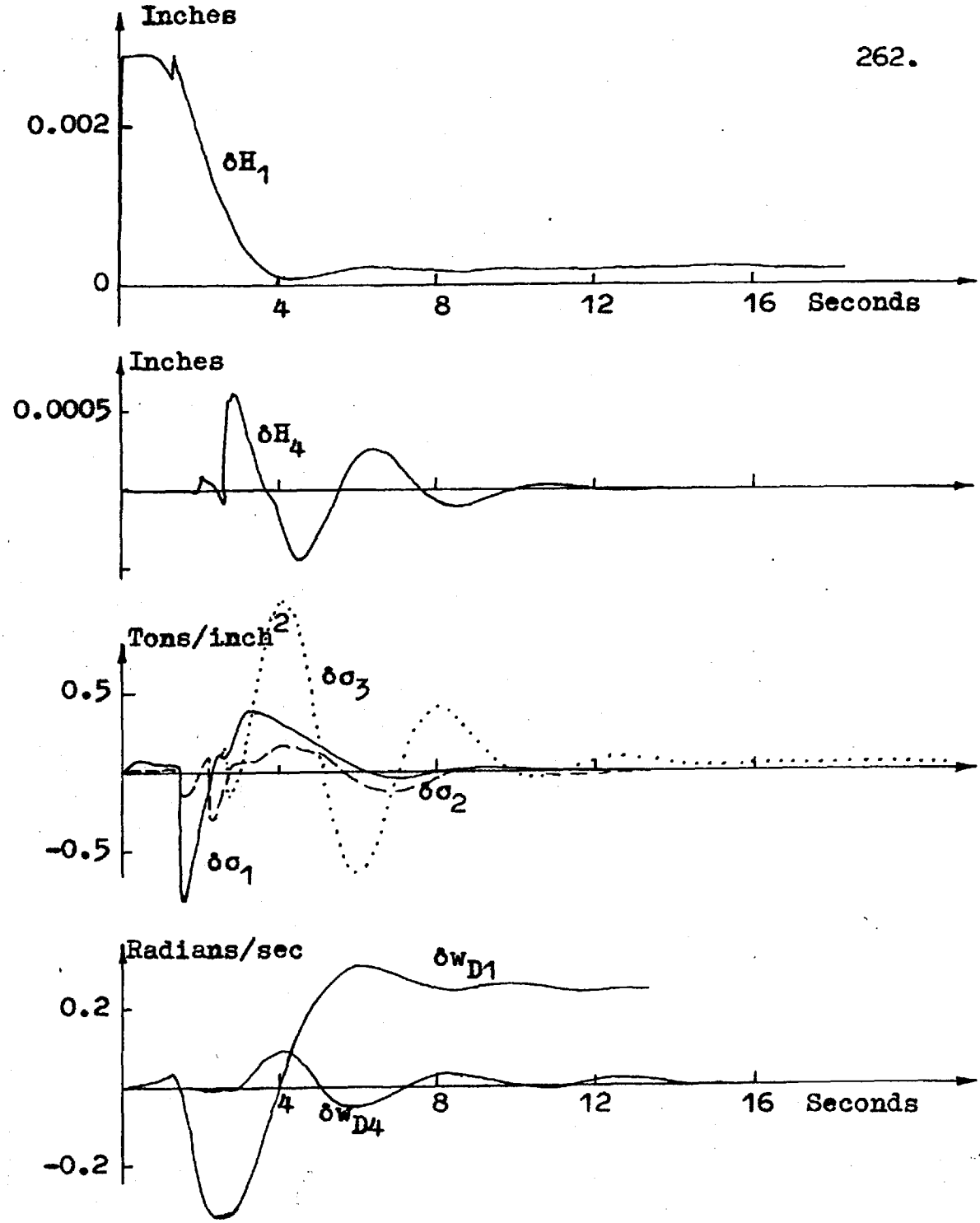

Fig. 9.22 Responses With Control System Number 6
(Ref. Section 9.6.1)

here. By more refined adjustment of the gain settings the response could probably be improved. The trace for $\delta\sigma_3$ shows it increasing when δH_4 increases and decreasing when δH_4 goes negative which it should do to assist in maintaining the desired gauge. There is, however, some phase difference between the two signals due to the delay taken for the strip to reach the x-ray gauge. The traces of the control signals to the stands 1 and 4 drive motors show that the demanded stand 1 roll speed has increased while that for stand 4 merely varies about its nominal value to yield tension changes that control the strip gauge at the last stand.

The results of applying a 0.5 radians per second, 0.002 inch peak to peak sine wave for δH_0 are shown in Fig. 9.23. Here δH_4 is shown held between limits better than ± 0.00005 inches. This is better than for the similar test with control system number 5 and shows the advantage of using the fast acting tension control at the latter stands. To provide this fine control, $\delta\sigma_3$ varied between limits of +0.6 tons/inch^2 and -0.1 tons/inch^2. This unbalance is due to δH_1 not being symmetrical, as shown by the trace. This would appear to be due to their being a bias on the sine wave input.

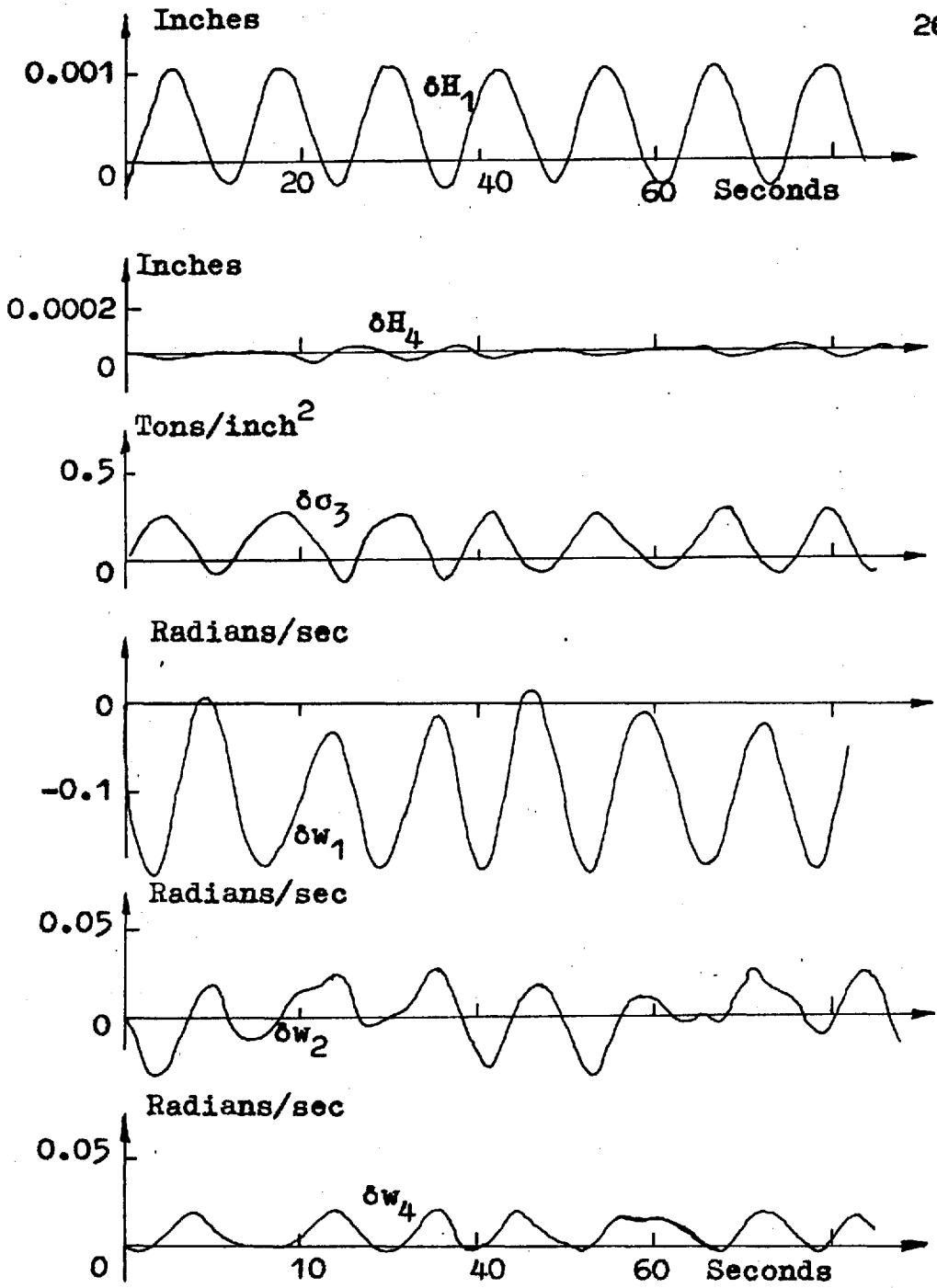

Fig. 9.23 Responses with Control System Number 6 (Ref. Section 9.6.1)

The trace of δw_1 would support this as it has a negative bias which means the stand 1 rolls have been slowed thereby increasing the average value of σ_1. The variation of δw_1 about this average value would tend to remove the input error.

A 0.0004 inch per second ramp was applied for δH_o with drive signal number 3 (Fig. 9.1) applied to the servomultipliers. The control system held δH_4 to within 0.00005 inches. A similar test with control system number 5 showed δH_4 rising steadily at 0.00004 inches per second. It was found that $\delta\sigma_3$ rose in number 6 to eliminate this error whereas control system 5 held $\delta\sigma_3$ constant. Again tension control of gauge on the last stand appears beneficial. Repeating the test with control system 3 showed the tension $\delta\sigma_3$ able to control δH_4 but within much wider limits than control system number 6.

10. CONCLUSIONS

1) For any given schedule and range of mill speed, the cold rolling mill control equation coefficients - including a forward slip equation - can be calculated using the digital computer and equations for the rolling mechanics which include the effects of the elastic zones.

2) Utilising variable time delays, modified servo-multipliers and a general purpose analogue computer an analogue simulation of a multistand rolling mill enabling the acceleration and deceleration phases of operation to be represented is possible.

3) With the aid of this simulation the effects of schedule deviations during acceleration and deceleration may be evaluated, as well as the effects of variations in the character of the incoming strip.

4) The mill simulation shows forward slip to have a smoothing effect on the transient response of the mill variables which becomes more apparent as the drive motor dynamics become more complex. The forward slip operates through the strip velocities which determine the nature of the strip tension variations.

5) The analogue simulation of the mill further shows that the bearing roll neck oil films cause the gauges and interstand tensions to be reduced during acceleration

and increased during deceleration for the schedule used.

6) The simulation may be used to evaluate forms of automatic gauge control during acceleration and deceleration as well as at a constant mill speed setting.

11. SUGGESTIONS FOR FURTHER STUDY

1) The effects of the elastic recovery zone on the strip thickness in the stand spring equation. It now assumes that the stand output gauge is equal to the strip thickness at the Ø equal zero plane.

2) A mill simulation based on a schedule in which the interstand tensions are reduced with mill speed with attention to the tendency for the neutral angle to approach zero for low roll gap coefficients of friction. A limitation may be the range of scheduled tension change over which the control equation coefficients remain accurate.

3) The effects of various representative drive motor transfer functions and various motor droops.

4) Extension of the speed range of the mill simulation; particularly the low speed end. Capacitor-ring type time delays (Ref. 48) would allow this or those used (Section 6.10) with a sacrifice in frequency response.

5) Extension of servomultiplier equipment to handle all varying coefficients.

6) Utilise a strip input error signal recorded from actual strip (Ref. 9, 10).

7) Compare analogue simulation tests to results of identical tests on an actual mill.

8) Attempt to determine a simpler analogue circuit which approximates that used (Fig. 7.7).

9) Determine and evaluate other types of mill controls for rescheduling and gauge control such as screw down control on every stand (Ref. 11).

10) An extensive but useful study would be to link the analogue simulation of the mill to digital computer equipment. The best means of rescheduling the mill during acceleration and deceleration and digital control to compensate for incoming strip variations could be studied.

REFERENCES

1. Peck, P.E., and Morgan, H.D. "Development of Electric Drives and Control for High-Speed Tandem Cold Reduction Mill"
Jour. Iron and Steel Instit., vol. 199, Dec. 1961, pp. 361-374.

2. British Iron and Steel Research Association, "Research on the Rolling of Strip"
A symposium of selected papers 1948-1958, Waterloo and Sons Ltd., London.

3. Bland, D.R., and Ford, H. "The Calculation of the Roll Force and Torque in Cold Strip Rolling with Tensions"
Proc. I.Mech.E., vol. 159, p. 144, 1948.

4. Ford, H., Ellis, F., and Bland, D.R. "Cold Rolling with Strip Tension Part I - A New Approximate Method Calculation and a Comparison with Other Methods"
J. Iron and Steel Instit., May 1951, 168, pp. 57-72.

5. Ford, H., and Ellis F. "Cold Rolling with Strip Tensions Part II - Comparison of Calculated and Experimental Results"
J. Iron and Steel Instit., July 1952, 171, pp. 239-245.

6. Bland, D.R., and Ford, H. "Cold Rolling with Strip Tensions Part III - An Approximate Treatment of the Elastic Compression of the Strip in Cold Rolling.
J. Iron and Steel Instit., July 1952, 171, pp. 245-249.

7. Sekulic, M.R., and Alexander, J.M. "Investigation of the Behaviour of a Four-Stand Tandem Mill, Using an Electronic Analogue"
J. Mech. Eng. Sc., vol. 4, no. 4, 1962.

8. Shohet, K.N. "A Method of Evaluating the Coefficients in the Perturbation Equations of a Cold Rolling Mill"
D.I.C. Dissertation - 1963, Imperial College, Mechanical Engineering Department.

9. Bryant, G.F. "Assessing Automatic Gauge Control Systems for a Cold Reduction Tandem Rolling Mill"
B.I.S.R.A., P/17/62, (ITW/A/43/62), London.

10. Bryant, G.F., and Butterfield, M.H. "Simulator Assessment of Tandem Cold-Rolling-Mill Automatic Gauge-Control Systems.
Inst. Elect. Engrs., Dec. 1963.

11. Butterfield, M.M., and Killick, R.D. "The Control of a Cold Steel Tandem Rolling Mill" B.I.S.R.A., PE/B/71/63.

12. Hessenberg, W.C.F., and Sims, R.B. "Principles of Continuous Gauge Control in Sheet and Strip-Rolling" Proc. Inst. Mech. Engrs., 1952, 166, pp. 75-81.

13. Sims, R.B., and Arthur, D.F. "Speed Dependent Variables in Cold Strip Rolling" J. Iron and Steel Instit., vol. 172, Pt. 3, Nov. 1952, pp. 285-295.

14. Sims, R.B., Place, J.A., and Briggs, P.R.A. "Control of Strip Thickness in Cold Rolling by Varying the Applied Tensions" J. Iron and Steel Instit., vol. 173, Pt. 4, Apr. 1953, pp. 343-354.

15. Sims, R.B., and Briggs, P.R.A. "Control of Strip Thickness in Hot and Cold Rolling" Iron and Coal Trades Review, Vol. 168, no. 1482, 5 Mar 1954, pp. 559-566.

16. Hessenberg, W.C.F., and Jenkins, W.N. "Effects of Screw and Speed-Setting Changes on Gauge Speed and Tension in Tandem Mills" Proc. Inst. Mech. Engrs., 1955, 169, pp. 1051-1058.

17. Courcoulas, J.H., and Ham, J.M. "Incremental Control Equations for Tandem Rolling Mills" Trans. A.M. Inst. E. Eng., 1956, pp. 56-656, Preprint.

18. Lianis, G., and Ford, H. "Control Equations of Multistand Cold Rolling Mills" Proc. Inst. Mech. Engrs., 1957, 171, pp. 757-772.

19. Phillips, R.A. "Analysis of Tandem Cold Reduction Mill with Automatic Gauge Control" Applications and Industry, A.I.E.E., Jan. 1957.

20. Reider, J.F., and Spergel, P. "Modern Computer Analysis for the Design of Steel Mill Control Systems" A.I.E.E. General Meeting, N.Y., Jan. 1957.

21. Phillips, R.A., and Maxwell, H.S. "Automatic Gauge Control for Cold Reduction Mills" Iron and Steel Engineer, June 1957, pp. 149-158.

22. Muller, H.G., and Lueg, W. "Conclusions from Rolling Trials on a Four Stand Cold Mill for Wide Strip" Stahl und Eisen, 1959, Mar. 19, pp. 325-331.

23. Doganovskii, S.A., and Fel'dbaum, A.A. "Analysis of the Compensation for Strip Thickness Variations by Means of an Electronic Analogue Computer" Automation and Remote Control, vol. 20, no. 2, Feb. 1959, pp. 185-197.

24. Varner, D. "Automatic Gauge Control as a Function of Transport Distance"
Iron and Steel Engineer, vol. 38, no. 9, Sep. 1961, pp. 188-195.

25. Visochanskii, V.S. "Automatic Tension Regulator for Cold Rolling Mills"
Engineers Digest, vol. 22, no. 12, Dec. 1961, pp. 76-78.

26. Orellana, I.G. "Recent Developments in Strip Thickness Control"
Iron and Steel Engineer, Nov. 1962.

27. Billigmann, J., and Lenze, J. "Experiences and Findings in a High-Speed Tandem Cold Reduction Mill"
Stahl und Eisen, 1962, 82,(6), March 15, pp. 313-337.

28. Shou-Te, Ch. U. "Automatic thickness Control of Cold Roll Strip"
Automation and Remote Control, Vol. 22, no. 8, 1962, p. 943.

29. Sekulic, M.R., and Alexander, J.M. "A Theoretical Discussion of the Automatic Control of Multi-Stand Tandem Cold Strip Mills"
J. Mech. Sc., 1963, vol. 5, pp. 149-163.

30. Cox. H.N. "New Features in Tandem Cold Strip Mills"
Iron and Steel Engineer, Jan. 1965.

31. Kaflanoglu, B.
University of London, Ph.D. Thesis (1965).

32. Ovens, G., and Dodd, C.A. "Modern Developments of the Ward-Leonard Principle and Applications in Steel Works"
J. Iron and Steel Instit., vol. 188, Mar. 1958, pp. 266-276.

33. Fitzgerald, A.E., and Kingsley, C. "Electric Machinery"
McGraw Hill Book Co. Inc., (1961).

34. Thorpe, J.M. "Mechanisms of Lubrication in Cold Rolling"
Proc. I. Mech. E., vol. 175, no. 11, 1961.

35. Whitton, P.W., and Ford, H. "Surface Friction and Lubrication in Cold Strip Rolling"
Proc. I. Mech. Eng., 1955, 169, pp. 123-133.

36. Wallquist, G., and Berg, B. "Investigation of Effect of Strip Tensions and Rolling Speed on Roll Pressure, Energy Consumption and Forward Slip in Cold Rolling Steel Strip"
Jernkontorets Annaler, vol. 145, no. 9, 1961, pp. 563-614.

37. Duke, R.L., and Hulls, L.R. "An Automatic Gauge Controller for a 56" Reversing Mill" Canadian Westinghouse Co., unpublished.

38. Meerov, M.V. "Automatic Regulating of Electrical Machines" Butterworths, London (1961).

39. Raven, F.H. "Automatic Control Engineering" McGraw-Hill Book Co. Inc., (1961).

40. Thaler, G.J., and Brown, R.G. "Analysis and Design of Feedback Control Systems" McGraw-Hill Book Co. Inc., (1960).

41. Stockdale, L.A. "Servomechanisms" Pitman and Sons Ltd., 1962.

42. Douce, J.L. "An Introduction to the Mathematics of Servomechanisms" English Universities Press (1963).

43. Nixon, F.E. "Principles of Automatic Controls" MacMillan and Co. Ltd., 1958.

44. Mishkin, E., and Braun, L. "Adaptive Control Systems" McGraw-Hill Book Co. Inc., 1961.

45. West, J.C. "Servomechanisms" English Universities Press Ltd. (1957).

46. Korn, G.A. and Korn, T.M. "Electronic Analogue Computers"
McGraw-Hill Book Co. Inc., (1956).

47. Fifer, S. "Analogue Computation" - 4 Vols
McGraw-Hill Book Co. Inc., (1961).

48. Huskey, H.D. and Korn, G.A. "Computer Handbook"
McGraw-Hill Book Co. Inc., (1962).

49. Pfeifer, G. "Four Methods of Scaling Analog Computers"
Control Engineering (New York), Aug. 1963, pp. 73-77.

50. Margolis, S.G. and O'Donnell, J.J. "Rigorous Treatment of Variable Time Delays"
I.E.E.E. Trans on Elect. Computers, Jan. 1963.

51. Single, C.H. "An Analog for Process Lags"
Control Engineering, vol. 3, pp. 113-115, Oct. 1956.

APPENDIX A

A.1 EQUATIONS FOR THE PLASTIC ZONE

Geometrical relations:

$$H = H_o + 2R'(1 - \cos \phi) \simeq H_o + R'\phi^2 \qquad A.1$$

$$\delta = H - H_o = R'\phi^2 = x^2/R' \qquad A.2$$

$$r = \frac{H}{H_f} \qquad A.3$$

$$x = R'\phi = \sqrt{R'\delta} \qquad A.4$$

Horizontal equilibrium of forces in Fig. A.1 yields:

$$(p + \delta p)(H + \delta H) - pH = 2sR'\delta\phi \sin\phi \pm 2usR'\delta\phi\cos\phi$$

Which is:

$$\frac{d(pH)}{d\phi} = 2sR'(\phi \pm u) \qquad A.5$$

Condition of plasticity:

$$q = k + p \qquad A.6$$

Substituting A.6 in A.5 with s = q and rearranging:

$$\frac{d}{d\phi}\left(kH\left(\frac{s}{k} - 1\right)\right) = 2R's(\phi \pm u) \qquad A.6$$

Since k = f(ϕ), we get:

$$\left(\frac{s}{k} - 1\right)\frac{d}{d\phi}(Hk) + Hk\frac{d}{d\phi}\left(\frac{s}{k}\right) = 2sR'(\phi \pm u) \qquad A.7$$

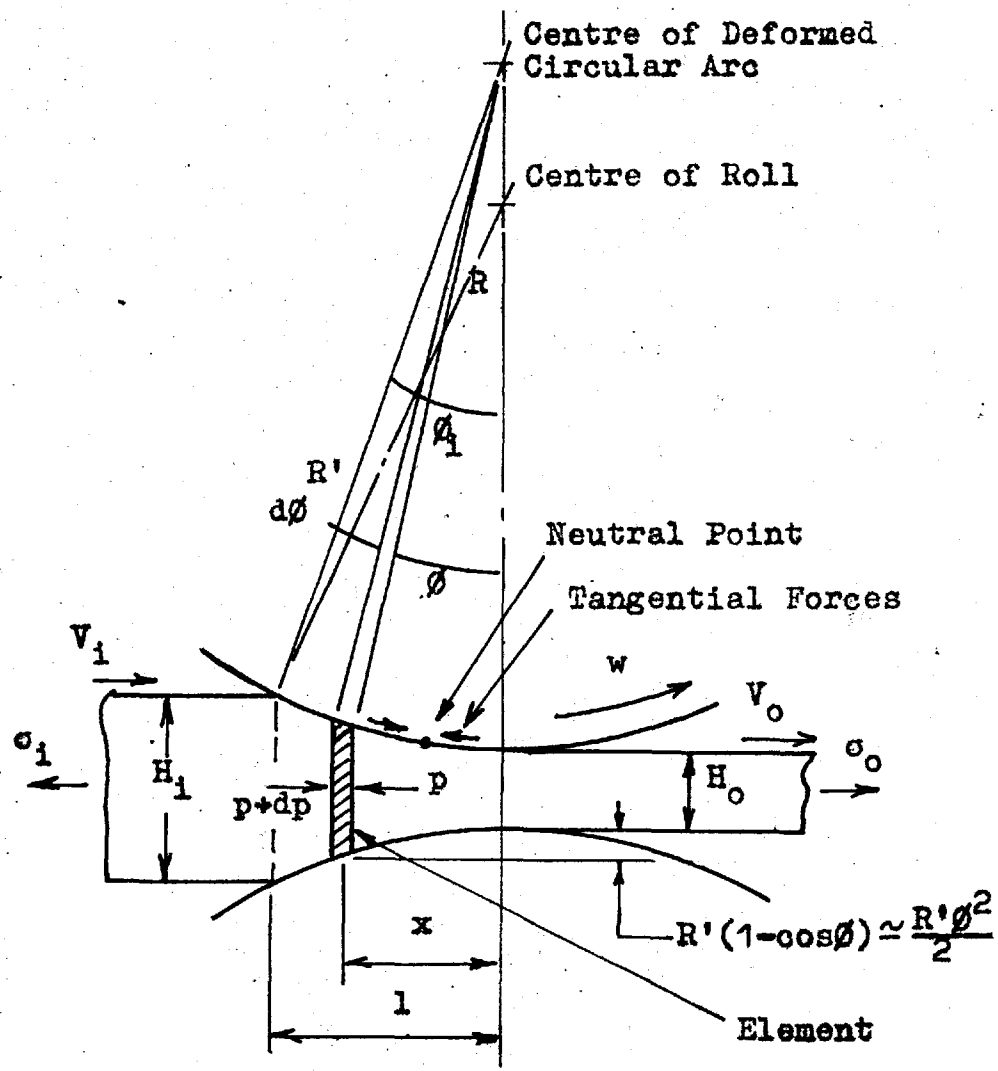

Fig. A.1 Roll Gap Geometry

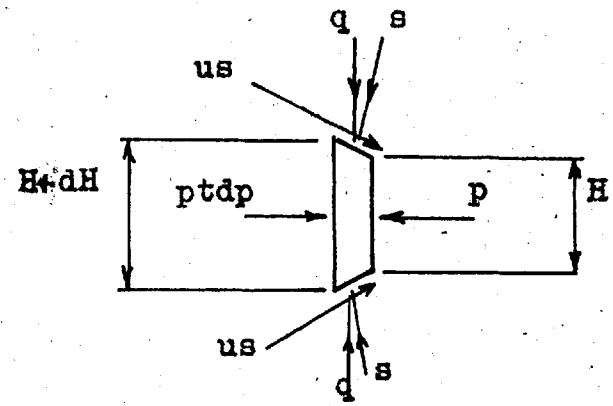

Forces on Element

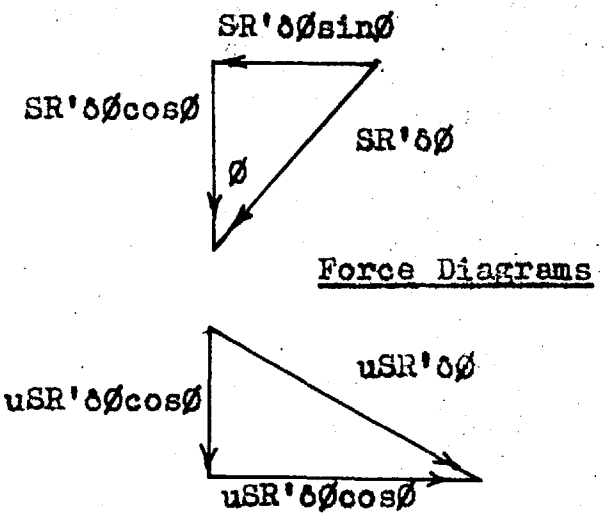

Force Diagrams

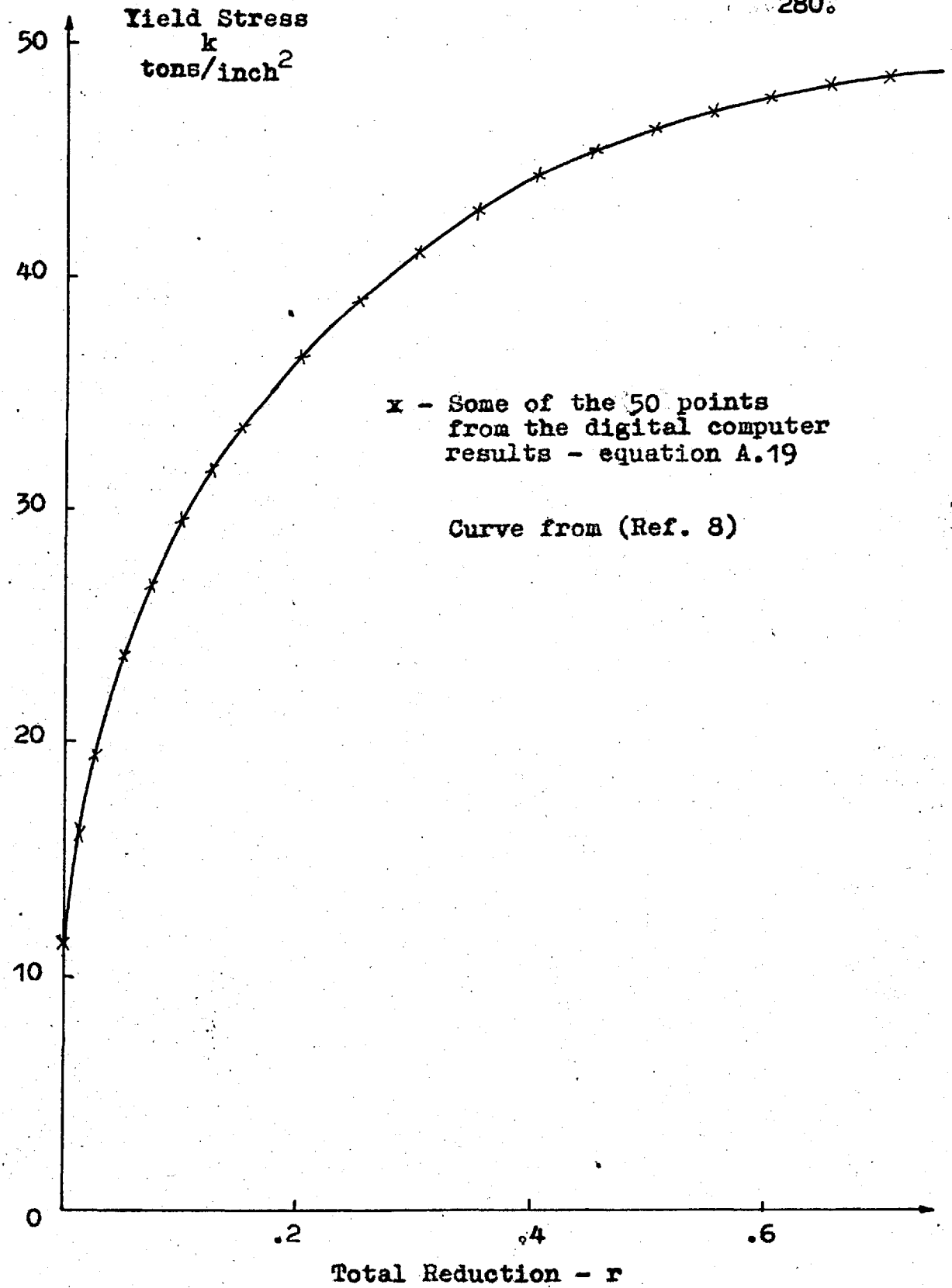

Fig. A.2 Yield Stress Curve of Mild Steel Strip

The first term on the L.H.S. is negligible as $\left(\frac{s}{k} - 1\right)$ is small and Hk is approximately constant.

The equation becomes:

$$\frac{d\left(\frac{s}{k}\right)}{\frac{s}{k}} = \frac{2R'}{H}(\phi \pm u)$$

Using A.1 and integrating gives:

$$s = c\frac{kH}{R'}e^{\pm Ju} \qquad \text{A.8}$$

\+ on entry side of neutral point.

\- on exit side of neutral point.

c is a constant of integration.

$$J = 2\sqrt{\frac{R'}{H_o}}\ \text{Arctan}\left(\phi\sqrt{\frac{R'}{H_o}}\right) \qquad \text{A.9}$$

At exit $\phi = 0$, therefore $J = 0$ and $s_o = k_o - \sigma_o$

At entry $\phi = \phi_i$, therefore:

$$J_i = 2\sqrt{\frac{R'}{H_i}}\ \text{Arctan}\left(\phi_i\sqrt{\frac{R'}{H_i}}\right) \qquad \text{A.10}$$

$$S_i = K_i - \sigma_i$$

Therefore from $\phi = 0$ to $\phi = \phi_n$:

$$s^+ = \frac{kH}{H_o}\left(1 - \frac{\sigma_o}{k_o}\right)e^{+uJ} \qquad \text{A.11}$$

And from $\phi = \phi_n$ to $\phi = \phi_i$

$$s^- = \frac{kH}{H_i}\left(1 - \frac{\sigma_i}{k_i}\right) e^{u(J_i - J)} \qquad \text{A.12}$$

At the neutral point:

$$s^+ = s^-; \quad J = J_n; \quad \phi = \phi_n$$

$$J_n = \frac{J_i}{2} - \frac{1}{2u}\ln\left[\frac{H_i}{H_o}\frac{\left(1 - \frac{\sigma_o}{k_o}\right)}{\left(1 - \frac{\sigma_i}{k_i}\right)}\right] \qquad \text{A.13}$$

$$\phi_n = \sqrt{\frac{H_o}{R'}}\tan\left(\sqrt{\frac{H_o'}{R'}}\frac{J_n}{2}\right) \qquad \text{A.14}$$

Hitchcocks formula was used (3) to give the radius of the arc of contact under load. It is based on an elliptical distribution of load and is widely used.

$$R' = R\left(1 + \frac{2cP}{\delta}\right) \qquad \text{A.15}$$

$c = 1.67 \times 10^{-4}$ in^2/ton for steel rolls

The roll force may now be evaluated from the expression:

$$P = \int_o^{\phi_n} s^+ R' d\phi + \int_{\phi_n}^{\phi_i} s^- R' d\phi \qquad \text{A.16}$$

The roll torque equation may be expressed by an equation similar to A.15, however this would involve the

subtraction of two numbers of comparable size. An alternate form was developed (3) and is noted below.

$$G = RR'\left(\int_{o}^{\phi_i} s\phi d\phi + \frac{\sigma_i H_i - \sigma_o H_o}{2R'}\right) \qquad A.17$$

For the first approximation in the solution for P, the roll force, the following formula was used.

$$P = \text{arclength} \times 1.2\bar{k} = \sqrt{R'\delta}\ 1.2\bar{k} \qquad A.18$$

$\bar{k}$ = the mean yield stress in plastic zone

$= 0.4k_i + 0.6k_o$

The formula for yield stress, as a function of reduction, discussed in section 2.1.1, is:

$$k = A(B + r)^{\theta} \qquad A.19$$

Where A, B, θ are constants to be evaluated with the digital computer. From section 2.1.2.

A = 55.2982

B = 0.00202317

θ = 0.271503

Slip is used to relate roll speed to strip velocity. It is defined as shown by equation 4.10 as:

$$F = \frac{V_o - wR}{wR}$$

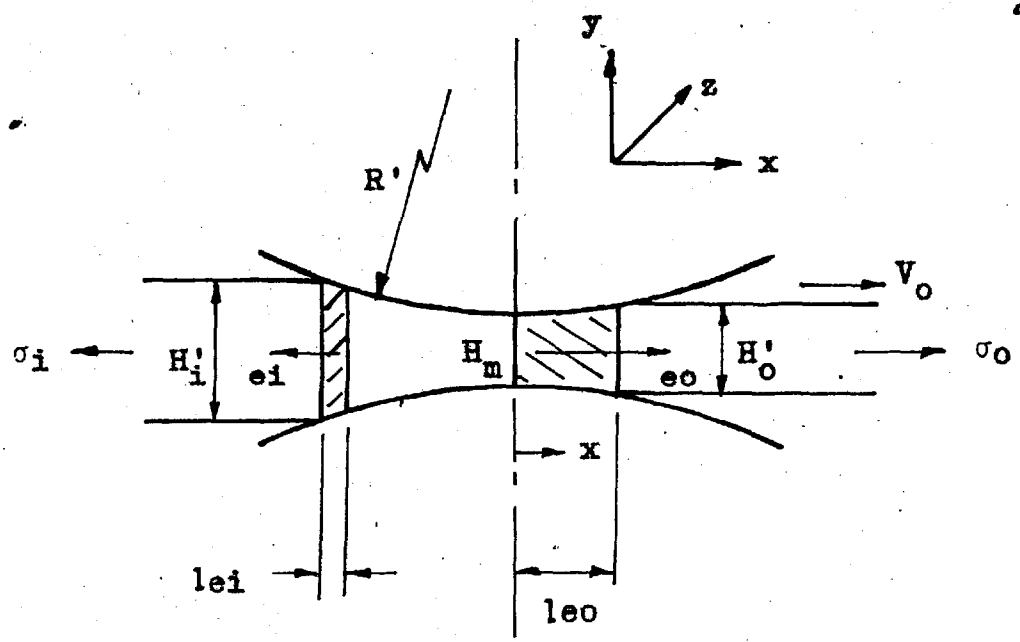

l_{ei} - Length of entry elastic zone.

l_{eo} - Length of exit or recovery elastic zone.

H_i' - Input thickness with tension σ_i applied.

H_o' - Output thickness with tension σ_o applied.

Fig. A.3 The Elastic Zones.

Using equations A.1 and 4.6 it is easily shown that

$$F = \frac{R'}{H_o} \phi_n^2 \qquad \text{A.20}$$

A.2 ELASTIC ZONE EQUATIONS

With the axes in the direction of the principal stresses, that is, x in the direction of strip flow; y in the vertical direction; and z in the transverse horizontal, Hookes Law may be written:

$$\left.\begin{aligned} e_x &= 1/E\,(\sigma_x - \nu(\sigma_y + \sigma_z)) \\ e_y &= 1/E\,(\sigma_y - \nu(\sigma_x + \sigma_z)) \\ e_z &= 1/E\,(\sigma_z - \nu(\sigma_x + \sigma_y)) \end{aligned}\right\} \qquad \text{A.21}$$

For the plane-strain condition $\sigma_z = 0$, and the equations become:

$$\left.\begin{aligned} e_x &= 1/E\,(\sigma_x - \nu^2(\sigma_x + \sigma_y) - \nu\sigma_y) \\ e_y &= 1/E\,(\sigma_y - \nu^2(\sigma_x + \sigma_y) - \nu\sigma_x) \end{aligned}\right\} \qquad \text{A.22}$$

A.2.1. Exit Zone Equations

At the exit of the elastic zone $\sigma_y = 0$, therefore from A.22:

$$e_y = \frac{\nu(1 + \nu)\sigma_o}{E}$$

At any point x in the elastic zone the total strain will be:

$$e_y = \frac{\gamma(1+\gamma)\sigma_o}{E} - \frac{l_{eo}^2 - x^2}{R'H_o'} \qquad \text{A.23}$$

Neglecting shear gives:

$$\sigma_x \simeq \sigma_o \qquad \text{A.24}$$

From A.22 and A.24:

$$\sigma_y = \frac{E_{ey}}{1-\gamma^2} + \frac{\gamma\sigma_o}{1-\gamma} \qquad \text{A.25}$$

Substituting A.23 in A.25:

$$\sigma_y = -\frac{E}{1-\gamma^2}\frac{(l_{eo}^2 - x^2)}{R'H_o'} \qquad \text{A.26}$$

From the yield criterion:

$$\sigma_x - \sigma_y = k \qquad \text{A.27}$$

At the plastic-elastic junction a compressive stress approximately equal to $\frac{2uP_{eo}}{H_o}$ is applied to the plastic zone. Therefore at x = 0:

$$\sigma_x = \sigma_{eo} = \sigma_o - \frac{2uP_{eo}}{H_o} \qquad \text{A.28}$$

The force exerted on the rolls due to this elastic zone is P_{eo}. Using A.26:

$$P_{eo} = \int_0^{l_{eo}} s\,dx = \frac{2}{3}\frac{E l_{eo}^2}{(1-\gamma^2)R'H_o'} \qquad A.29$$

Substituting A.26, A.27 and A.28 in A.29 and assuming $H_o \simeq H_o'$ we arrive at:

$$P_{eo} = \frac{2}{3}(k_o - \sigma_{eo})\sqrt{\frac{R'H_o(1-\gamma^2)(k_o - \sigma_{eo})}{E}} \qquad A.30$$

The torque due to the recovery elastic zone aids the motor torque and is therefore considered negative.

$$G_{eo} = -uRP_{eo} \quad \text{Per roll} \qquad A.31$$

A.2.2. Entry Zone Equations

By a similar analysis to that used in the exit zone derivations, the following equations may be developed for the entry zone.

$$P_{ei} = \frac{1-\gamma^2}{4E} H_1 \sqrt{\frac{R'}{H_i - H_o}} (K_i - \sigma_{ei})^2 \qquad A.32$$

$$G_{ei} = +uRP_{ei} \qquad A.33$$

$$\sigma_{ei} = \sigma_i - 2u\frac{P_{ei}}{H_i} \qquad A.34$$

A.2.3. Roll Force and Torque for the Three Zones

The total roll force becomes:

$$P = P_p + P_{eo} + P_{ei} \qquad \text{A.35}$$

The total roll torque becomes:

$$G = G_p + G_{eo} + G_{ei} \qquad \text{A.36}$$

A.3 MODIFIED ARC RADIUS

By considering the effect of the strip deflections in the elastic zones it is shown that (6) δ in equation A.16 must be replaced by the expression:

$$\left(\sqrt{\delta + \delta_{eo} + \delta t} + \sqrt{\delta_{eo}}\right)^2$$

Where:

$$\left.\begin{aligned} \delta &= H_i - H_o \\ \delta_{eo} &= \frac{1 - \gamma^2}{E} H_o (K_o - \sigma_o) \\ \delta_t &= \frac{\gamma(1 + \gamma)}{E} (\sigma_o H_o - \sigma_i H_i) \end{aligned}\right] \qquad \text{A.37}$$

The expression for the modified R' becomes:

$$R' = R\left[1 + \left(\sqrt{\frac{2cP}{\delta + \delta_{eo} + \delta_t}} + \sqrt{\delta_{eo}}\right)^2\right] \qquad \text{A.38}$$

A.4. MILL DRIVE MOTOR DROOP EQUATION

$$W_{\text{full load}} = W_{\max}\left(1 - \frac{\%\ \text{Droop}}{100}\right)$$

Full load torque in ton-inches is:

$$G_{or} = \frac{\text{h.p. x 33000 x 12}}{2\pi\ w \times 2240}$$

$$D_r = \frac{W_{\max} - W_{\text{full load}}}{G_{or}} \qquad \text{A.39}$$

A.5. WIND REEL EQUATION

For 1% droop; $D_r = -0.0173$ rad/sec-Ton-in.

Change in strip speed at reel (δV_R) can be approximated by:

$$\delta V_R = R_o^2 A_4 D_R \delta\sigma_4$$

R_o = coil radius (10.5 ins. to 36 ins.)

= 20 ins. average value say.

Therefore; $\delta V_R \simeq -11.5\ \delta\sigma_4$

Assumed dynamic equation

$$\delta V_R = \frac{\delta V_{DR}}{(1 + 0.20p)} - \frac{11.5\ \delta\sigma_4}{(1 + 0.30p)}$$

A.5.1. Strip Tension between Stand 4 and Reel

$$\delta\sigma_4 = \frac{E}{L} \int (\delta V_R - \delta V_4)dt$$

$\frac{E}{L}$ = 111.67 tons/inch^2

Coefficients $\frac{\partial P_4}{\partial \sigma_4}$, $\frac{\partial G_4}{\partial \sigma_4}$ and $\frac{\partial F_4}{\partial \sigma_4}$ are estimated as in Tables 7.3 and 7.4.

APPENDIX B

B.1. THE LAPLACE TRANSFORMATION

The direct Laplace transform of a function of time is defined by the equation (39, 40, 41, 42):

$$\mathcal{L}(f(t)) = \int_0^\infty f(t)e^{-pt}dt = F(p)$$

The symbol $\mathcal{L}(f(t))$ is a shortand notation for the Laplace integral. Evaluation of the integral results in a function F(p) which has p as the variable. The variable p is a complex quantity of the form $\sigma + jw$. The lower limit of the integral is zero as we are not concerned with the value of f(t) for negative time.

B.1.1. Transforms of Basic Functions Used

1) A step function is fixed change occurring instantly although it cannot always be put into a system as it takes a definite length of time to make the change in input. Providing the system is satisfactory the output must eventually reach a constant value. The Laplace transform of a step r(t) is:

$$\mathcal{L}(r(t)) = \int_0^\infty r(t)e^{-pt}dt = -\frac{re^{-pt}}{p}\Bigg|_0^\infty = \frac{r}{p}$$

2) Sinusoid; $f(t) = \sin wt$:

$$\mathcal{L}(\sin wt) = \frac{w}{p^2 + w^2}$$

3) Integration with initial conditions = 0:

$$\mathcal{L}\left(\int f(t)\right) = \frac{F(p)}{p}$$

4) Differentiation:

$$\mathcal{L}\left(\frac{df(t)}{dt}\right) = pF(p)$$

5) A constant $f(t) = A$:

$$\mathcal{L}(A) = A$$

6) Exponential; $f(t) = e^{-at}$

$$\mathcal{L}(e^{-at}) = \frac{1}{a + p} = F(p)$$

B.2. TRANSFER FUNCTION OF A SIMPLE LAG

The first order or simple lag is represented by the first order differential equation.

$$a\frac{dc}{dt} + bc = r$$

Where r is the input and c is the output and b is a constant. In Laplace notation the transfer function

becomes:

$$\frac{c(p)}{r(p)} = \frac{1}{b + ap} = \frac{1}{b(1 + \frac{a}{b}p)} = \frac{k}{H\tau p} = G(p)$$

Where in control system analysis k is termed the gain, τ the time constant and G(p) the transfer function in general form.

To solve the differential equation for a specified input when the equation is in the transformed state, the input function is Laplace transformed then the resulting expression for the output is transformed back to the time domain. Thus for a step input r(t) we get:

$$c(p) = \frac{r(p)}{p} \frac{k}{(1 + \tau p)}$$

Using partial fraction techniques the equation becomes:

$$c(p) = k \frac{r(p)}{p} - \frac{r\tau}{(p\tau + 1)}$$

Using transforms (1) and (6) in section B.1.1 to revert to the time domain results in:

$$c(t) = kr(t) \left(1 - e^{-t/r}\right)$$

This is the expression for a first order lag; an exponentially rising function with time.

B.2.1. Analogue Simulation of a Lag

The first order lag may be represented by the analogue circuit of Fig. B.1. By applying an analysis similar to that in section 6.2 it can be shown that the transfer function is approximately:

$$\frac{e_o}{e_1} = -\frac{k_1 R}{k_o R_1} \frac{1}{1 + \frac{R}{k_o} Cp} \qquad \text{B.1}$$

$\frac{k_1 R}{k_o R_1}$ is the d.c. gain

$\frac{R}{k_o} C$ is the time constant.

Both factors are variable with the potentiometer settings which facilitates set-up of the desired transfer function.

B.3. ANCILLARY CIRCUITS USED IN ANALOGUE SIMULATION

B.3.1. Analogue Simulation of a Dead Zone

Fig. B.2 shows an analogue circuit which simulates a dead zone (Ref.47). Its characteristic is given in Fig. B.3. Diode 1 conducts when $e_i > E_1$ and then holds e_i at voltage E_1 giving $e_o = -k(E_1 - e_i)$. Diode 2 conducts when $e_i < -E_2$ and then holds e_i at voltage $-E_2$

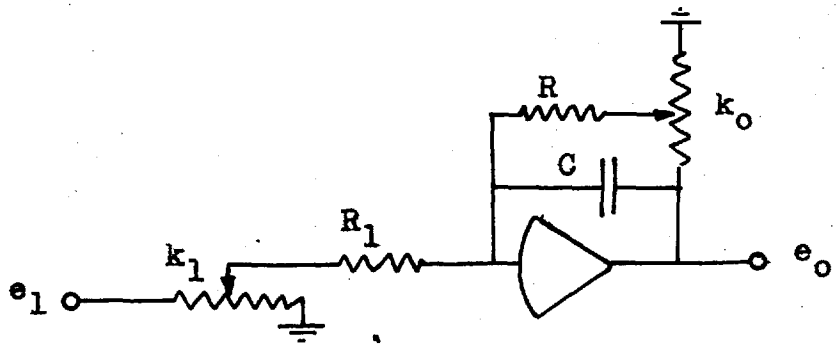

Fig. B.1 Analogue of a First Order Lag.

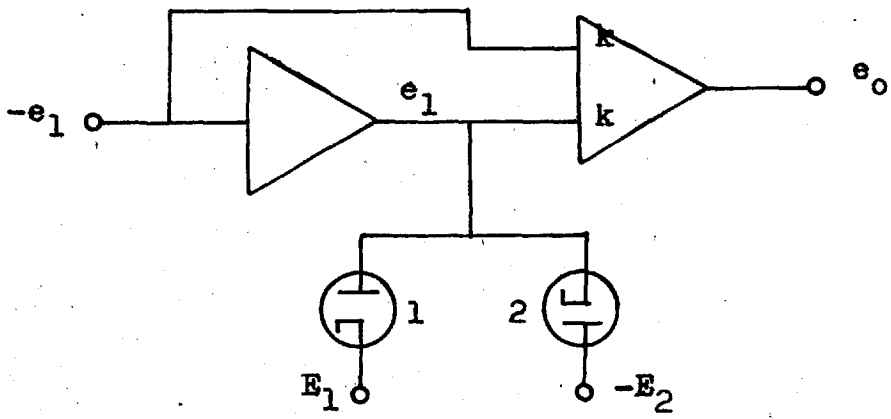

Fig. B.2 Analogue of a Dead Zone.

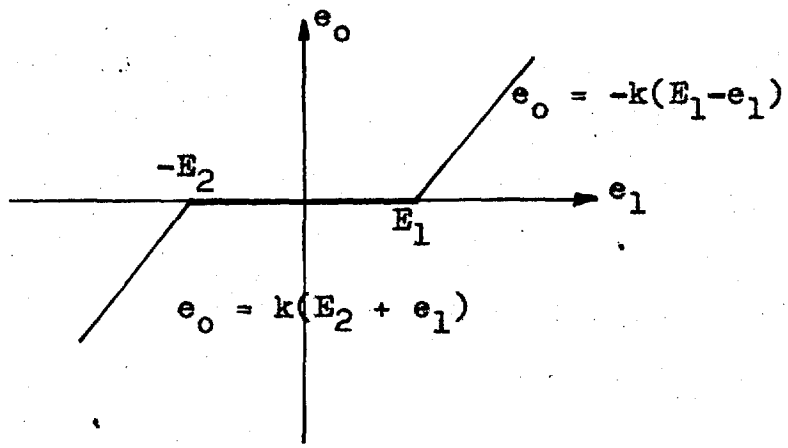

Fig. B.3 Dead Zone Characteristic.

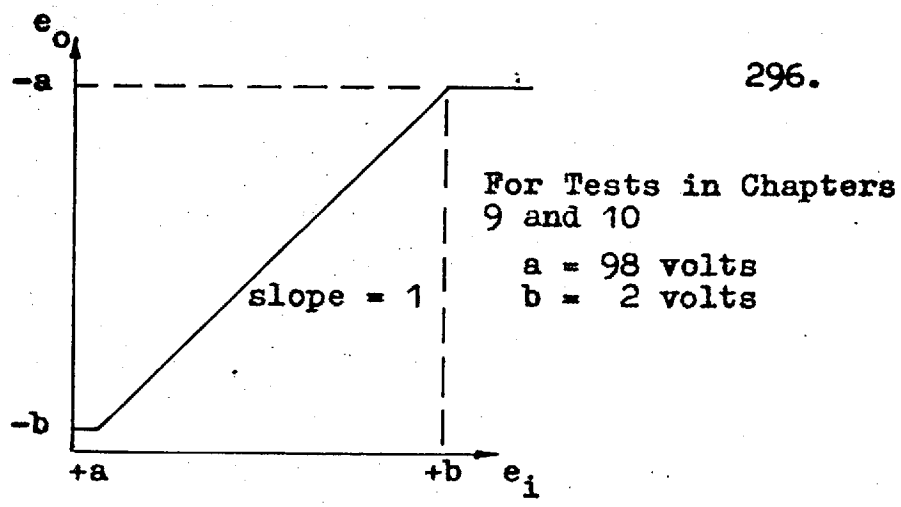

Fig. B.4 Characteristic of Limiter Circuit of Fig. B.5

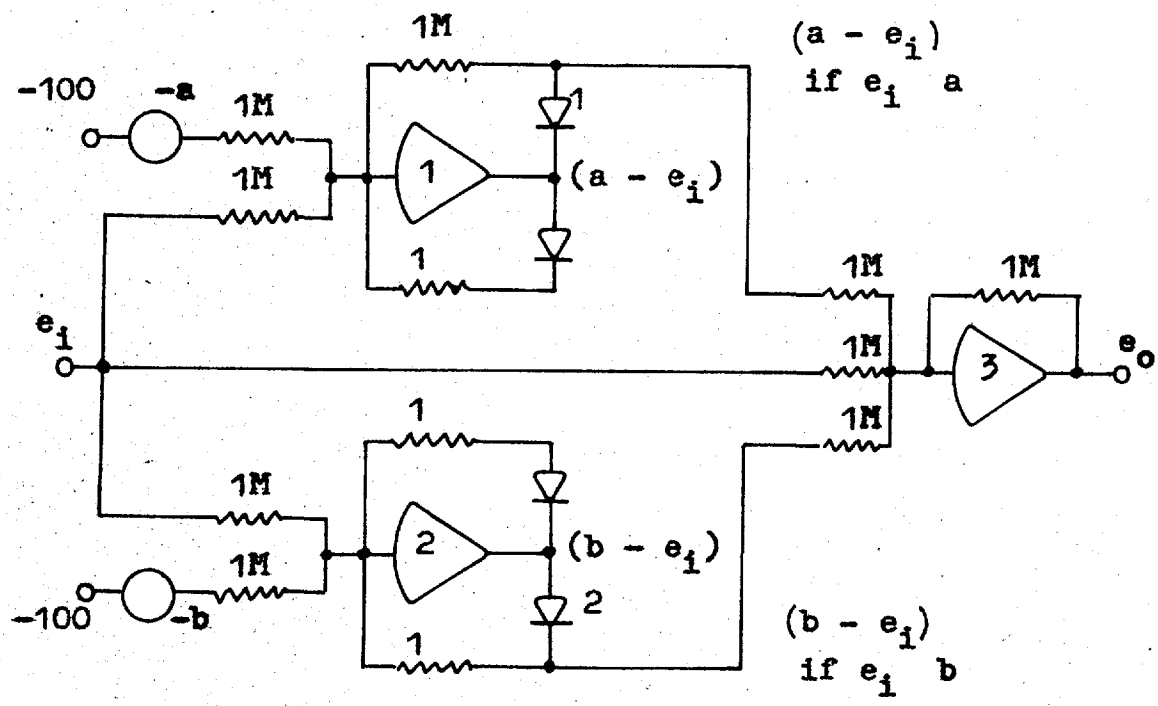

Fig. B.5 Limiter Circuit

giving $e_o = -k(-E_2 - e_i)$. Neither diode conducts in the range $-E_2 \leq e_i \leq E_1$; which gives $e_o = 0$.

B.3.2. Limiter Circuit

The characteristic of the limiter is shown in Fig. B.4. A voltage signal e_i is limited to the range -2 volts to -98 volts. It is used to prevent the servo drive signal from causing the potentiometer wipers from the overshooting which would occur if the full range of 0 to -100 volts was used. A negative drive voltage is used as the servomultiplier feedback is positive.

Fig. B.5 gives the circuit used to obtain the above action. The output of amplifier 1 is $(a - e_i)$, and of amplifier 2 it is $(b - e_i)$. When $e_i > a$ diode 1 conducts, when $e_i < b$ diode 2 conducts. The remaining diodes give feedback when these relations are not satisfied and do not conduct when the relations are satisfied. Thus for amplifier 3:

When $e_i < a$ and $e_i > b$ we have; $e_o = -e_i$

When $e_i > a$; $e_o = -(e_i + a - e_i) = -a$

When $e_i < b$; $e_o = -(e_i + b - e_i) = -b$

This yields the characteristic of Fig. B.4.

B.3.3. Servomultiplier and Plotter Drive

When a computation on the analogue computer is started it is necessary to commence the recording of results simultaneously with the start of the experiment. The circuit in Fig. B.6 does this by supplying the time signal to drive the X-Y plotter as it supplies the servomultiplier drive signal for the acceleration or deceleration tests.

When switch 1 is opened the relay is thrown a signal of 1 volt is supplied to the integrator which supplies a ramp of 1 volt per second to drive the plotter arm. Switch 2 is previously set for an acceleration or deceleration run as is potentiometer 4. The settings of potentiometers 5 and 6 determine the slope of the servo drive signal and hence the acceleration or deceleration rate, and potentiometer 4 sets the required initial condition. As shown there would be a -2 volt initial condition and the negative voltage from potentiometer 5 would be integrated to add to this. The limiter circuit is placed in series to limit the servo drive signal to the range of -2 volts to -98 volts.

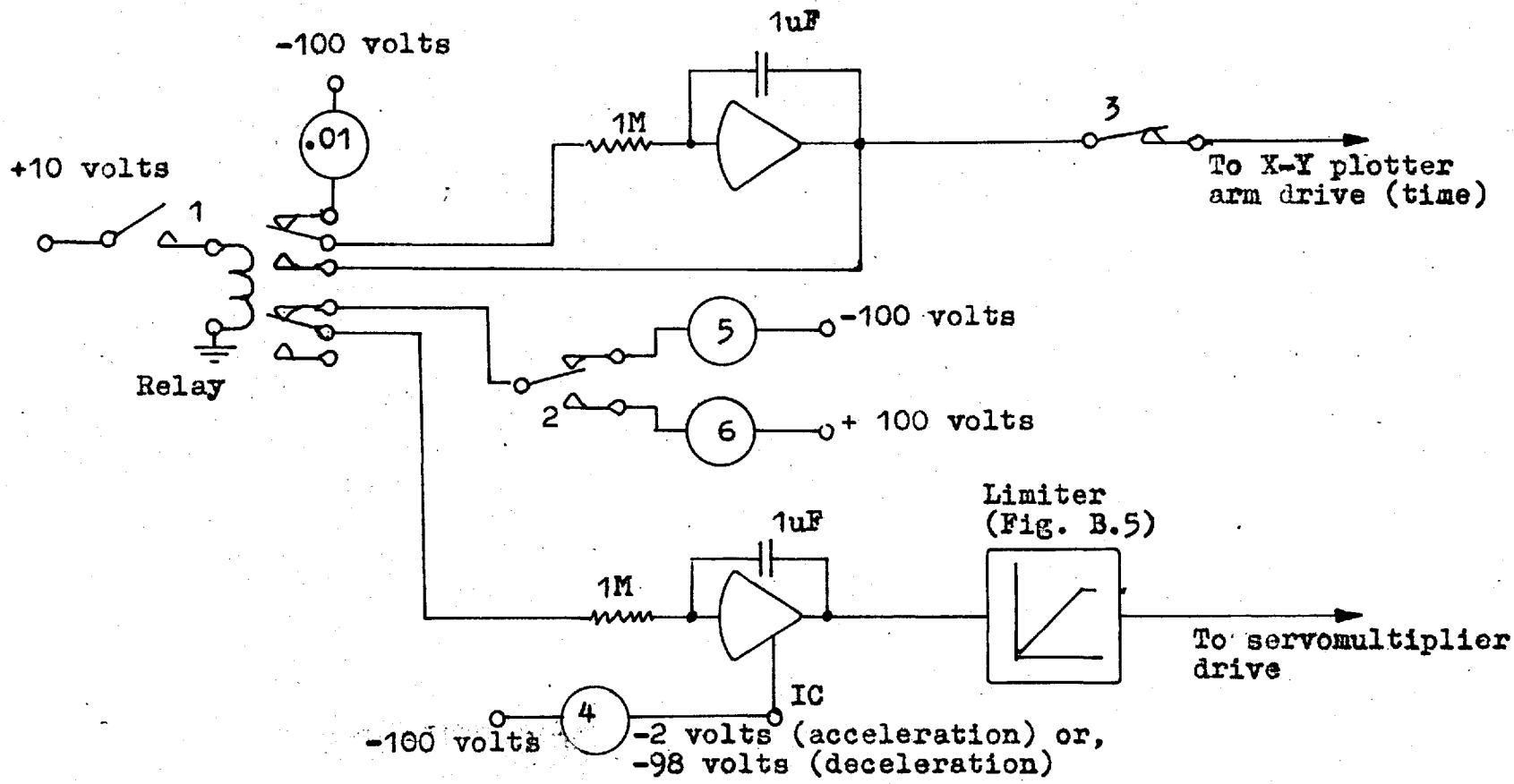

Fig. B.6 Servomultiplier and X-Y Plotter Drive

APPENDIX C

C.1 CONTROL EQUATION COEFFICIENTS

The roll force, torque and slip for a range of u values are given in Tables C.1 and C.2.

The coefficients for the control equations of chapter 4 are listed in Tables C.3 to C.6 for a range of u.

The contents of these tables is discussed in chapter 5.

C.2 BISRA CONTROL EQUATIONS

The control equations used by BISRA are listed below.

$$\delta H_{1r} = a_{1r}\delta T_r + a_{2r}\delta T_{r-1} + a_{3r}\delta S_r + a_{4r}\delta H'_{r-1} \qquad C.1$$

$$\delta w_r = b_{1r}\delta T_r + b_{2r}\delta T_{r-1} + b_{3r}\delta S_r + b_{4r}\delta H'_{r-1} \qquad C.2$$

The 'a' and 'b' partial differential coefficients may be expressed in terms of the 'p' and 'g' coefficients used in this report (8). The coefficients are given in terms of the full strip width and including the effects of both rolls in the case of equation C.2.

$$a_{1r} = -\frac{1}{A_r}\,\frac{p_{4r}}{p_{2r} - M_r} \quad \text{inches/ton}$$

$$a_{2r} = -\frac{1}{A_r - 1}\,\frac{p_{3r}}{p_{2r} - M_r} \qquad \text{inches/ton}$$

$$a_{3r} = -\frac{M_r}{p_{2r} - M_r} \qquad \text{inches/inch}$$

$$a_{4r} = -\frac{p_{1r}}{p_{2r} - M_r} \qquad \text{inches/inch}$$

$$b_{1r} = D_r\,\frac{g_{4r}}{A_r} + g_{2r}\,a_{1r} \qquad \text{RPM/ton}$$

$$b_{2r} = D_r\,\frac{g_{3r}}{A_r - 1} + g_{2r}\,a_{2r} \qquad \text{RPM/ton}$$

$$b_{3r} = D_r g_{2r} a_{3r} \qquad \text{RPM/inch}$$

$$b_{4r} = D_r\,g_{1r} + g_{2r}\,a_{4r} \qquad \text{RPM/inch}$$

The values of these coefficients are given in Tables C.7 and C.8 for a range of u. In the tables thousandths are used rather than full inches.

C.3. DIGITAL COMPUTER PROGRAMME

```
JOB
LSC44EL1, DARLINGTON RUN 1 MAY 8 64
COMPUTING 50000 INSTRUCTIONS
OUTPUT
0 LINE PRINTER 1100 LINES
STORE 15 BLOCKS
COMPILER EMA

IGNORE QUERIES


TITLE
COLD ROLL TANDEM MILL     COEFF WITH ELASTIC ZONES
TITLE
R.F.DARLINGTON MECH ENG IC        U1173/Q

CHAPTER 1

A→30
B→40
C→30
D→30
E→30
F→30
G→30
H→30
U→100

3)JUMP4, J'≥1

B10=A6+2A6A10B8/B6?
4)B11=ΨSQRT(B6/B10)?
B12=ΨSQRT(B10/A3)

B13=ΨARCTAN(1,B11B12)
B13=2B12B13

B14=1-A4/B3
B15=1-A5/B4
B16=A2/A3

B17=ΨLOG(B16B15/B14)
```

```
B17=.5B13-.5B17/A7 ?

B19=ψSQRT(A3/B10)
B20=ψTAN(.5B19B17)
B20=B19B20  ?

B21=.16667B20
B22=B11-B20
B22=.083332B22

K=0(1)6
CK=KB21
DK=B12CK
DK=ψARCTAN(1,DK)

DK=2B12DK
DK=ψEXP(A7DK)
EK=A3+B10CKCK

FK=ψLOG(A19+1-EK/A1)
FK=ψEXP(A20FK)
FK=A18FK

EK=EKFKB15DK/A3
GK=EKCK
REPEAT

K=7(1)18
L=K-6
CK=B20+LB22
DK=B12CK

DK=ψARCTAN(1,DK)

DK=2B12DK
DK=ψEXP(A7B13-A7DK)
EK=A3+B10CKCK

FK=ψLOG(A19+1-EK/A1)
FK=ψEXP(A20FK)
FK=A18FK

EK=FKEKB14DK/A2
GK=EKCK
```

```
REPEAT

B25=.33332B21
B26=.33332B22
B27=E0+4E1+2E2+4E3+2E4+4E5+E6
B27=B25B27

B28=E6+4E7+2E8+4E9+2E10+4E11+2E12+4E13+2E14
B28=B28+4E15+2E16+4E17+E18

B28=B26B28
B30=B10B27+B10B28   ?

B8=B30

ACROSS7/0

PSA

ψARCTAN
ψTAN
ψSQRT
ψEXP

CLOSE
```

```
CHAPTER2

VARIABLES1

1)H6=-2A7A6H5
H10=2A7A6H10

B32=E0C0+4E1C1+2E2C2+4E3C3+2E4C4+4E5C5+E6C6
B32=B25B32

B33=E6C6+4E7C7+2E8C8+4E9C9+2E10C10+4E11C11+2E12C12
B33=B33+4E13C13+2E14C14+4E15C15+2E16C16+4E17C17+E18C18

B33=B26B33

B32=A6B10B32+A6B10B33
B33=A4A2-A5A3
B33=.5B33A6
B33=B32+B33
B33=2B33

H17=B33+H6+H10

H18=A6B20B20/A3

JUMP10,Q>0
NEWLINE
CAPTION
IV    PT    PP    PE0    PE1    GT    F    R'    Ψ1    ΨN
```

```
NEWLINE

P=o(I)8
SPACE
REPEAT
JUMPII

IO)PRINT(AN')I,5
II)PRINT(H8)I,5
PRINT(B3O)I,5
PRINT(H5)I,5
PRINT(H9)I,5
PRINT(HI7)I,5
PRINT(HI8)I,5
PRINT(BIO)I,5
PRINT(BII)I,5
PRINT(B2O)I,5
NEWLINE

JUMP3O,Q=O

JUMP2O,Q=I
JUMP2I,Q=2
JUMP2O,Q=3
JUMP2I,Q=4
JUMP2O,Q=5
JUMP2I,Q=6
JUMP2O,Q=7
JUMP2I,Q=8

2O)E=H8
F=HI7
G=HI8
AI=X
JUMP3O

2I)E'=H8
F'=HI7
G'=HI8
AN'=B
AI=X

U=ψDIVIDE(E'-E,A-C)
U=46.25U
```

```
V=ψDIVIDE(F'-F,A-C)
V=46.25V
W=ψDIVIDE(G'-G,A-C)

S=S+1
US=U
S=S+1
US=V
S=S+1
US=W

JUMP6,Q=8
30)ACROSS8/0

6)P=0(1)3
NEWLINE
REPEAT

U20=U4-A23
U20=1/U20

U21=-U10U20/A22
U22=-U7U20/A21
U23=-A23U20
U24=-U1U20

U25=-A24U11/A22
U26=-A24U8/A21
U27=-A24U5
U28=-A24U2

U29=U25+U27U21
U30=U26+U27U22
U31=U27U23
U32=U28+U27U24

NEWLINE
CAPTION
   NIV      DPT/DIV     DGT/DIV     DF/DIV      A       B
NEWLINE

PRINT(A2)1,5
PRINT(.001U1)1,5
PRINT(.001U2)1,5
```

```
PRINT(.001U3)1,5
PRINT(1000U21)1,5
PRINT(U29)1,5

NEWLINE
PRINT(A3)1,5
PRINT(.001U4)1,5
PRINT(.001U5)1,5
PRINT(.001U6)1,5
PRINT(1000U22)1,5
PRINT(U30)1,5

NEWLINE
PRINT(A4)1,5
PRINT(U7)1,5
PRINT(U8)1,5
PRINT(U9)1,5
PRINT(U23)1,5
PRINT(.001U31)1,5

NEWLINE
PRINT(A5)1,5
PRINT(U10)1,5
PRINT(U11)1,5
PRINT(U12)1,5
PRINT(U24)1,5
PRINT(.001U32)1,5

ACROSS8/0

PSA
CLOSE
```

```
CHAPTER 0

VARIABLES1

READ(Q')
R'=1(1)Q'

P=0(1)5
NEWLINE
REPEAT

R=0(1)3
N'=1
S=0

1)Q=0(1)8
JUMP1 5,Q≥1
K'=0

P=0(1)7
NEWLINE
REPEAT

I=1(1)24
READ(AI)
PRINT(AI)0,5
```

```
K'=K'+1
JUMP6,K'≠8
NEWLINE
K'=0
6)REPEAT
NEWLINE
NEWLINE

JUMP16,Q=0
15)READ(A)
JUMP12,Q=1
JUMP13,Q=2
JUMP12,Q=3
JUMP13,Q=4
JUMP12,Q=5
JUMP13,Q=6
JUMP12,Q=7
JUMP13,Q=8

12)N'=N'+1
B=AN'
C=A
AN'=A
JUMP29

13)D=A
AN'=A

29)JUMP16,R>0
JUMP16,N'>2
X=A1
A1=AN'

16)B0=1-A2/A1
JUMP30,B0≥0
B0=0
30)B1=1-A3/A1
B2=.4B0+.6B1

I=3(1)5
I'=I-3
BI=ψLOG(A19+BI')
BI=ψEXP(A20BI)
BI=A18BI
```

```
JUMP4,Q>o
PRINT(BI)2,4
4)REPEAT

B6=A2-A3
B7=ΨSQRT(A6B6)
B8=I.2B5B7+I.44B5B5AIoA6 ?

J'=o(I)3
ACROSS3/I

7)JUMPIo,J'≥I
H7=A4
H2=A5
JUMP2o,J'=o
Io)A4=HI9
A5=H2o

2o)N=o(I)6
H3=B4-H2
H4=I-AI4AI4
H5=ΨSQRT(A3BIoH4H3/AI5)
H5=.6667H3H5?
H2=A5-2A7H5/A3?
REPEAT

22)N=o(I)6
H8=B3-H7
H4=I-AI4AI4
H9=ΨSQRT(BIo/B6)
H9=.25H4A2H9H8H8/AI5 ?
H7=A4-2A7H9/A2?
REPEAT

23)H8=B3o+H5+H9
HII=B4-A5
HII=A3H4HII/AI5
HI2=AI4+AI4AI4
HI3=A3A5-A2A4
HI2=HI2HI3/AI5

HI4=ΨSQRT(B6+HII+HI2)
HI5=ΨSQRT(HII)
```

```
HI4=HI4+HI5
HI4=HI4HI4
HI6=2AIOH8A6/HI4
HI6=A6+HI6

HI9=A4
H2O=A5

A4=H7
A5=H2

BIO=HI6
REPEAT

A4=HI9
A5=H2O

ACROSS 1/2
8)REPEAT
REPEAT
REPEAT

END

PSA

ψARCTAN
ψTAN
ψSQRT
ψEX 1

CLOSE
```

	Coefficient of Friction										
	.03	.04	.05	.06	.07	.08	.09	.10	.11	.12	.15
P_{p1}	12.45	12.85	13.28	13.73	14.20	14.70	15.23	15.78	16.38	17.02	19.18
P_{p2}	18.90	20.19	21.50	22.87	24.34	25.95	27.73	29.69	31.90	17.02	44.42
P_{p3}	18.58	20.10	21.69	23.43	25.39	27.62	30.21	33.27	36.95	34.39	64.37
P_{p4}	15.44	16.65	17.95	19.40	21.05	22.97	25.25	28.00	31.38	35.64	58.63
G_{p1}	.110	.227	.350	.479	.613	.754	.902	1.058	1.222	1.395	1.975
G_{p2}	7.58	8.00	8.42	8.87	9.35	9.86	10.43	11.04	11.72	12.47	15.35
G_{p3}	7.11	7.45	7.82	8.21	8.64	9.13	9.68	10.31	11.40	11.91	15.98
G_{p4}	4.67	4.79	4.93	5.08	5.24	5.43	5.64	5.89	6.19	6.55	8.35
F_{p1}	.03920	.04037	.04108	.04156	.04190	.04216	.04237	.04253	.04266	.04277	.04302
F_{p2}	.01150	.02374	.03329	.04063	.04636	.05095	.05470	.05783	.06048	.06276	.06807
F_{p3}	.01263	.02329	.03132	.03740	.04212	.04589	.04898	.05157	.05377	.05569	.06032
F_{p4}	.00770	.01254	.01603	.01861	.02059	.02215	.02343	.02449	.02539	.02617	.02804

Table C.1. Roll Force, Roll Torque and Slip for the Plastic Zone.
P_p - tons/inch; G_p - ton-inches/inch; F_p - dimensionless

	Coefficient of Friction										
	.03	.04	.05	.06	.07	.08	.09	.10	.11	.12	.15
P_1	13.26	13.72	14.20	14.71	15.26	15.84	16.45	17.11	17.80	18.55	21.13
P_2	19.83	21.22	22.65	24.16	25.79	27.59	29.58	31.82	34.34	37.22	49.04
P_3	19.53	21.17	22.91	24.84	27.03	29.55	32.50	36.03	40.33	45.70	74.40
P_4	16.30	17.62	19.07	20.70	22.60	24.86	27.60	31.01	35.37	41.18	82.24
G_1	-0.392	-0.450	-0.508	-0.566	-0.624	-0.681	-0.738	-0.795	-0.851	-0.907	-1.070
G_2	6.96	7.15	7.35	7.57	7.81	8.08	8.38	8.71	9.11	9.56	11.47
G_3	6.40	6.48	6.57	6.67	6.80	6.94	7.13	7.36	7.65	8.06	10.59
G_4	3.683	3.426	3.138	2.813	2.442	2.013	1.505	0.885	0.098	-0.967	-12.67
F_1	.03328	.03432	.03494	.03533	.03560	.03579	.03593	.03603	.03609	.03614	.03620
F_2	.00782	.01831	.02678	.03334	.03849	.04260	.04595	.04878	.05107	.05309	.05786
F_3	.00834	.01735	.02436	.02971	.03387	.03719	.03989	.04218	.04416	.04598	.05191
F_4	.00393	.00771	.01055	.01268	.01431	.01559	.01663	.01751	.01830	.01907	.02263

Table C.2. Roll Forces, Roll Torques and Slips Including Elastic Zones.
P - tons/inch; G - ton-inches/inch; F - dimensionless

	Coefficient of Friction										
	.03	.04	.05	.06	.07	.08	.09	.10	.11	.12	.15
p_{11}	28.28	29.87	31.54	33.32	35.24	37.31	39.54	41.97	44.61	47.49	57.95
p_{21}	-30.64	-32.60	-34.69	-36.93	-39.34	-41.96	-44.81	-47.92	-51.33	-55.08	-68.88
p_{31}	-	-	-	-	-	-	-	-	-	-	-
p_{41}	-12.33	-13.04	-13.73	-14.44	-15.18	-15.96	-16.81	-17.73	-18.72	-19.81	-23.79
g_{11}	14.30	14.72	15.16	15.62	16.11	16.64	17.20	17.81	18.46	19.15	21.62
g_{21}	-17.22	-17.74	-18.28	-18.85	-19.46	-20.10	-20.79	-21.53	-22.33	-23.18	-26.19
g_{31}	-	-	-	-	-	-	-	-	-	-	-
g_{41}	-36.15	-35.80	-35.42	-35.01	-34.59	-34.14	-33.67	-33.18	-32.66	-32.12	-30.30
f_{11}	-.00107	-.00023	.00028	.00063	.00088	.00107	.00122	.00134	.00143	.00152	.00169
f_{21}	.00125	.00026	-.00035	-.00076	-.00106	-.00128	-.00146	-.00160	-.00171	-.00181	-.00202
f_{31}	-	-	-	-	-	-	-	-	-	-	-
f_{41}	.00889	.00675	.00544	.00456	.00392	.00344	.00307	.00276	.00252	.00231	.00185

Table C.3. Stand 1 Coefficients With Elastic Zone Effects Included.
p_{1r} and p_{2r} - tons/thou; p_{3r} and p_{4r} - tons/ton/inch^2
g_{1r} and g_{2r} - ton-inch/thou; g_{3r} and g_{4r} - ton-inch/ton/inch^2
f_{1r} and f_{2r} - -/thou; f_{3r} and f_{4r} - -/ton/inch^2

	Cofficient of Friction										
	.03	.04	.05	.06	.07	.08	.09	.10	.11	.12	.15
p_{12}	6.78	8.82	10.67	12.53	14.48	16.61	18.99	21.68	24.79	28.44	44.51
p_{22}	-19.38	-23.39	-27.46	-31.88	-36.83	-42.51	-49.15	-57.00	-66.45	-77.98	-133.88
p_{32}	-29.05	-28.62	- 29.11	-30.19	-31.75	-33.76	-36.25	-39.30	-43.00	-47.54	-69.09
p_{42}	-6.24	-9.05	-11.30	-13.35	-15.39	-17.54	-19.90	-22.57	-25.68	-29.36	-46.41
g_{12}	13.13	14.13	15.18	16.30	17.50	18.82	20.28	21.91	23.74	25.83	34.40
g_{22}	-18.88	-20.36	-21.95	- 23.68	-25.58	-27.70	-30.09	-32.83	-35.99	-39.70	-56.31
g_{32}	24.03	23.73	23.38	22.94	22.41	21.79	21.07	20.22	19.23	18.05	12.73
g_{42}	-24.46	-24.36	-24.22	-24.05	-23.83	-23.60	-23.34	-23.07	-22.81	-22.55	-22.09
f_{12}	-.00079	-.00057	-.00021	.00013	.00042	.00066	.00087	.00105	.00120	.00134	.00167
f_{22}	.00046	.00003	-.00045	-.00088	-.00123	-.00153	-.00178	-.00200	-.00218	-.00235	-.00279
f_{32}	-.00351	-.00405	-.00393	-.00365	-.00336	-.00309	-.00284	-.00262	-.00243	-.00226	-.00187
f_{42}	.00276	.00318	.00309	.00288	.00266	.00245	.00226	.00209	.00194	.00181	.00147

Table C.4. Stand 2 Coefficients with Elastic zone Effects Included.
(Ref. Table C.3 for units)

	Coefficient of Friction										
	.03	.04	.05	.06	.07	.08	.09	.10	.11	.12	.15
p_{13}	17.81	21.31	24.85	28.69	33.07	38.21	44.41	52.07	61.84	74.72	156.22
p_{23}	-26.61	-32.75	-39.47	-47.29	-56.70	-68.36	-83.18	-102.85	-128.66	-165.13	-432.10
p_{33}	-23.40	-23.65	-24.71	-26.41	-28.74	-31.79	-35.76	-40.95	-47.85	-57.29	-120.48
p_{43}	- 6.34	- 9.02	-11.35	-13.69	-16.25	-19.22	-22.82	-27.38	-33.35	-41.47	-97.44
g_{13}	19.43	20.92	22.54	24.33	26.35	28.67	31.37	34.58	38.50	43.44	72.16
g_{23}	-20.99	-22.99	-25.18	-27.64	-30.45	-33.75	-37.68	-42.51	-48.65	-56.76	-112.32
g_{33}	18.53	18.32	18.05	17.71	17.28	16.76	16.11	15.29	14.22	12.77	2.80
g_{43}	-17.95	-17.72	-17.44	-17.11	-16.74	-16.33	-15.88	-15.38	-14.87	-14.34	-13.66
f_{13}	-.00038	.00013	.00064	.00107	.00143	.00172	.00197	.00218	.00237	.00255	.00315
f_{23}	-.00003	-.00076	-.00142	-.00195	-.00239	-.00275	-.00306	-.00334	-.00360	-.00386	-.00513
f_{33}	-.00240	-.00259	-.00245	-.00224	-.00204	-.00185	-.00170	-.00156	-.00144	-.00135	-.00127
f_{43}	-.00204	.00220	.00209	.00192	.00175	.00159	.00146	.00133	.00122	.00112	.00078

Table C.5. Stand 3 Coefficients With Elastic Zone Effects Included.
(Ref. Table C.3 for units)

	Coefficient of Friction										
	.03	.04	.05	.06	.07	.08	.09	.10	.11	.12	.15
p_{14}	47.21	53.66	60.61	68.52	77.83	89.07	103.01	120.73	143.90	175.05	310.99
p_{24}	-55.21	-64.15	-74.29	-86.36	-101.20	-119.99	-144.54	-177.70	-224.37	-293.44	-980.61
p_{34}	-18.12	-18.42	-19.43	-21.01	-23.20	-26.14	-30.09	-35.46	-43.02	-54.11	-165.23
p_{44}	-	-	-	-	-	-	-	-	-	-	-
g_{14}	24.73	26.86	29.26	32.03	35.31	39.27	44.22	50.64	59.43	72.45	355.79
g_{24}	-23.05	-25.37	-27.93	-30.83	-34.17	-38.10	-42.82	-48.65	-56.08	-65.88	-71.69
g_{34}	16.63	16.65	16.66	16.67	16.69	16.73	16.81	16.98	17.33	18.09	56.44
g_{44}	-	-	-	-	-	-	-	-	-	-	-
f_{14}	.00059	.00137	.00199	.00246	.00284	.00315	.00341	.00365	.00387	.00411	.00521
f_{24}	-.00093	-.00183	-.00252	-.00304	-.00346	-.00379	-.00409	-.00436	-.00463	-.00495	-.00724
f_{34}	-.00119	-.00123	-.00114	-.00103	-.00092	-.00083	-.00076	-.00060	-.00064	-.00061	-.00069
f_{44}	-	-	-	-	-	-	-	-	-	-	-

Table C.6. Stand 4 Coefficients With Elastic Zone Effects Included.
(Ref. Table C.3 for units)

	Coefficient of Friction										
	.03	.04	.05	.06	.07	.08	.09	.10	.11	.12	.15
a_{11}	-.0841	-.0848	-.0851	-.0852	-.0852	-.0851	-.0850	-.0848	-.0846	-.0843	-.0836
a_{21}	-.1963	-.1924	-.1897	-.1876	-.1859	-.1844	-.1830	-.1817	-.1805	-.1792	-.1745
a_{31}	.2461	.2347	.2238	.2131	.2027	.1924	.1824	.1726	.1630	.1537	.1268
a_{41}	.6960	.7011	.7058	.7102	.7142	.7180	.7214	.7245	.7273	.7297	.7347
a_{12}	-.0835	-.1066	-.1186	-.1254	-.1293	-.1314	-.1323	-.1325	-.1321	-.1312	-.1268
a_{22}	-.2740	-.2375	-.2153	-.1997	-.1878	-.1781	-.1698	-.1625	-.1558	-.1497	-.1330
a_{32}	.3404	.2995	.2670	.2388	.2135	.1904	.1691	.1492	.1308	.1137	.0695
a_{42}	.2307	.2642	.2849	.2991	.3092	.3163	.3210	.3236	.3243	.3232	.3094
a_{13}	-.0913	-.1111	-.1209	-.1259	-.1284	-.1292	-.1291	-.1282	-.1267	-.1248	-.1161
a_{23}	-.2513	-.2175	-.1964	-.1813	-.1695	-.1596	-.1509	-.1431	-.1357	-.1287	-.1072
a_{33}	.2730	.2339	.2021	.1746	.1499	.1276	.1073	.0889	.0721	.0571	.0226
a_{43}	.4863	.4985	.5022	.5009	.4958	.4877	.4766	.4627	.4660	.4266	.3534
a_{14}	-.0558	-.0669	-.0733	-.0775	-.0806	-.0830	-.0852	-.0873	-.0896	-.0924	-.1174
a_{24}	-.1464	-.1309	-.1214	-.1149	-.1099	-.1060	-.1026	-.0996	-.0967	-.0940	-.0879
a_{34}	.1534	.1349	.1186	.1038	.0899	.0769	.0647	.0553	.0427	.0330	.0101
a_{44}	.7239	.7237	.7191	.7111	.6999	.6852	.6666	.6432	.6140	.5769	.3139

Table C.7. BISRA 'a' Coefficients (Units as per Appendix C.2)

	Coeffidient of Friction										
	.03	.04	.05	.06	.07	.08	.09	.10	.11	.12	.15
b_{11}	.3855	.3786	.3715	.3642	.3565	.3486	.3402	.3314	.3222	.3124	.2792
b_{21}	-.4514	-.4503	-.4495	-.4489	-.4484	-.4479	-.4475	-.4472	-.4469	-.4467	-.4467
b_{31}	.1907	.1874	.1841	.1808	.1774	.1741	.1707	.1673	.1638	.1603	.1494
b_{41}	-.1040	-;1026	-.1014	-.1005	-.0998	-.0993	-.0992	-.0994	-.0999	-.1009	-.1070
b_{12}	.5228	.4815	.4499	.4217	.3943	.3666	.3377	.3071	.2740	.2377	.1004
b_{22}	-.7689	-.7417	-.7282	-.7205	-.7158	-.7131	-.7115	-.7108	-.7108	-.7114	-.7161
b_{32}	.4178	.3965	.3809	.3675	.3550	.3429	.3307	.3185	.3060	.2933	.2544
b_{42}	-.5707	-.5688	-.5801	-.5989	-.6237	-.6541	-.6905	-.7336	-.7846	-.8449	-1.1037
b_{13}	.7653	.6882	.6238	.5621	.4987	.4308	.3554	.2697	.1694	.0483	-.5934
b_{23}	-1.2753	-1.2287	-1.2224	-1.2154	-1.2137	-1.2157	-1.2205	-1.2278	-1.2378	-1.2510	-1.3333
b_{33}	.5821	.5458	.5165	.4897	.4635	.4372	.4105	.3834	.3561	.3290	.2579
b_{43}	-.9358	-.9606	-1.0047	-1.0650	-1.1422	-1.2394	-1.3610	-1.5134	-1.7059	-1.9517	-3.2963
b_{14}	.9455	.8565	.7677	.6709	.5600	.4276	.2634	.0503	-.2433	-.6827	-8.2233
b_{24}	-1.4565	-1.4509	-1.4601	-1.4788	-1.5058	-1.5420	-1.5900	-1.6548	-1.7464	-1.8865	-4.3245
b_{34}	.4243	.4106	.3977	.3840	.3688	.3517	.3325	.3111	.2872	.2605	.0868
b_{44}	-.9652	-1.0204	-1.1012	-1.2129	-1.3665	-1.5793	-1.8805	-2.3210	-2.9991	-4.1339	-39.994

Table C.8. BISRA 'b' Coefficients (Units as per Appendix C.2)

APPENDIX D

D.1 MACHINE EQUATIONS FOR CONSTANT NOMINAL MILL OUTPUT SPEED OF 1950 FEET PER MINUTE

$$\delta H_1 = 1.454\delta H_0' + .1628\delta S_1 - 0 - .1525\delta\sigma_1$$
$$\delta H_2 = 1.425\delta H_1' + .267\delta S_2 - 1.945\delta\sigma_1 - .755\delta\sigma_2$$
$$\delta H_3 = .498\delta H_2' + .234\delta S_3 - 1.383\delta\sigma_2 - 1.055\delta\sigma_3$$
$$\delta H_4 = .724\delta H_3' + .1535\delta S_4 - 1.390\delta\sigma_3 - 0$$

$$\delta G_1 = 1.846\delta H_0' - 1.117\delta H_1 + 0 - .817\delta\sigma_1$$
$$\delta G_2 = 1.518\delta H_1' - .439\delta H_2 + 1.169\delta\sigma_1 - 1.211\delta\sigma_2$$
$$\delta G_3 = .418\delta H_2' - .460\delta H_3 + .916\delta\sigma_2 - 1.772\delta\sigma_3$$
$$\delta G_4 = .989\delta H_3' - .922\delta H_4 + 3.326\delta\sigma_3 - 0$$

$$\delta F_1 = 1.440\delta H_0' - .855\delta H_1 - 0 + .630\delta\sigma_1$$
$$\delta F_2 = - .0213\delta H_1' - .0916\delta H_2 - 1.964\delta\sigma_1 + 1.55\delta\sigma_2$$
$$\delta F_3 = .024\delta H_2' - .1534\delta H_3 - 1.299\delta\sigma_2 + 2.219\delta\sigma_3$$
$$\delta F_4 = .1186\delta H_3' - .186\delta H_4 - 1.205\delta\sigma_3 + 0$$

$$\delta V_1 = 1.036\delta W_1 + .3190\delta F_1$$
$$\delta V_2 = 1.284\delta W_2 + .655\delta F_2$$
$$\delta V_3 = 1.272\delta W_3 + .835\delta F_3$$
$$\delta V_4 = 1.255\delta W_4 + .9780\delta F_4$$

$$p\delta\sigma_1 = 48.56\delta V_2 + 98.8\delta H_2 - 349\delta H_1' - 172\delta V_1$$
$$p\delta\sigma_2 = 51.36\delta V_3 + 220\delta H_3 - 164\delta H_2' - 68.8\delta V_2$$
$$p\delta\sigma_3 = 29.8\delta V_4 + 159.6\delta H_4 - 140\delta H_3' - 34.4\delta V_3$$

$$\delta w_1 = \frac{\delta W_{D1}}{(1 + .25p)} - \frac{0.9448 G_1}{(1 + .40p)}$$

$$\delta w_2 = \frac{\delta W_{D2}}{(1 + .25p)} - \frac{1.3648 G_2}{(1 + .40p)}$$

$$\delta w_3 = \frac{\delta W_{D3}}{(1 + .25p)} - \frac{2.138 G_3}{(1 + .40p)}$$

$$\delta w_4 = \frac{\delta W_{D4}}{(1 + .25p)} - \frac{1.268 G_4}{(1 + .40p)}$$

$$\delta s_1 = \frac{\delta S_{D1}}{p(1 + .60p)}$$

$$\delta s_2 = \frac{\delta S_{D2}}{p(1 + .60p)}$$

$$\delta s_3 = \frac{\delta S_{D3}}{p(1 + .60p)}$$

$$\delta s_4 = \frac{\delta S_{D4}}{p(1 + .60p)}$$

$$\delta H_1'(t) = \delta H_1(t - .99)$$
$$\delta H_2'(t) = \delta H_2(t - .595)$$
$$\delta H_3'(t) = \delta H_3(t - .468)$$

$$\delta H_1^{*}(t) = \delta H_1(t - .228)$$
$$\delta H_4^{*}(t) = \delta H_4(t - .123)$$

D.2 MACHINE EQUATIONS FOR VARYING NOMINAL MILL SPEED

D.2.1 At an Output Speed of 1950 Feet per Minute

$$\delta H_1 = 1.4466\delta H_0' + .1765(\delta S_1 + \Delta S_{o1}) - 0 - .1532\delta\sigma_1$$
$$\delta H_2 = .2848\delta H_1' + .2181(\delta S_2 + \Delta S_{o2}) - .3887\delta\sigma_1 - .1596\delta\sigma_2$$
$$\delta H_3 = .9861\delta H_2' + .1808(\delta S_3 + \Delta S_{o3}) - .5532\delta\sigma_2 - .2110\delta\sigma_3$$
$$\delta H_4 = .7120\delta H_3' + .1217(\delta S_4 + \Delta S_{o4}) - .2779\delta\sigma_3 - .155\delta\sigma_4$$

$$\Delta S_{o1} = .19; \quad \Delta S_{o2} = .23; \quad \Delta S_{o3} = .48; \quad \Delta S_{o4} = .50$$

$$\delta G_1 = 1.755\delta H_0' - 1.061\delta H_1 + 0 - .835\delta\sigma_1$$
$$\delta G_2 = 1.518\delta H_1' - 2.195\delta H_2 + 1.1115\delta\sigma_1 - 1.189\delta\sigma_2$$
$$\delta G_3 = 4.184\delta H_2' - 2.299\delta H_3 + 1.754\delta\sigma_2 - 1.703\delta\sigma_3$$
$$\delta G_4 = 2.473\delta H_3' - 2.306\delta H_4 + 1.666\delta\sigma_3 - 1.45\delta\sigma_4$$

$$\delta F_1 = 1.250\delta H_0' - .750\delta H_1 - 0 + .745\delta\sigma_1$$
$$\delta F_2 = 0\delta H_1' - .450\delta H_2 - 1.695\delta\sigma_1 + 1.34\delta\sigma_2$$
$$\delta F_3 = .130\delta H_2' - .380\delta H_3 - 1.110\delta\sigma_2 + .950\delta\sigma_3$$
$$\delta F_4 = .295\delta H_3' - .465\delta H_4 - .53\delta\sigma_3 + .875\delta\sigma_4$$

$$\delta V_1 = 1.037\delta w_1 + .2287\delta F_1$$
$$\delta V_2 = 1.037\delta w_2 + .5102\delta F_2$$
$$\delta V_3 = 1.027\delta w_3 + .6566\delta F_3$$
$$\delta V_4 = 1.009\delta w_4 + .7770\delta F_4$$

$$p\delta\sigma_1 = 51.806\delta V_2 + 493.53\delta H_2 - 348.08\delta H_1' - 171.8\delta V_1$$
$$p\delta\sigma_2 = 67.38\delta V_3 + 548.92\delta H_3 - 818.39\delta H_2' - 85.98\delta V_2$$
$$p\delta\sigma_3 = 73.57\delta V_4 + 796.96\delta H_4 - 699.77\delta H_3' - 85.9\delta V_3$$
$$p\delta\sigma_4 = 111.67\delta V_R - 111.67\delta V_4$$

$$\delta w_1 = \frac{\delta W_{D1}}{(1 + .25p)} - \frac{0.944\delta G_1}{(1 + .40p)}$$

$$\delta w_2 = \frac{\delta W_{D2}}{(1 + .25p)} - \frac{1.364\delta G_2}{(1 + .40p)}$$

$$\delta w_3 = \frac{\delta W_{D3}}{(1 + .25p)} - \frac{1.065\delta G_3}{(1 + .40p)}$$

$$\delta w_4 = \frac{\delta W_{D4}}{(1 + .25p)} - \frac{1.26\delta G_4}{(1 + .40p)}$$

$$\delta V_R = \frac{\delta V_{DR}}{(1 + .20p)} - \frac{11.5\delta\sigma_4}{(1 + .30p)}$$

$$\delta S_1 = \frac{\delta S_{D1}}{p(1 + .60p)}$$

$$\delta S_2 = \frac{\delta S_{D2}}{p(1 + .60p)}$$

$$\delta S_3 = \frac{\delta S_{D3}}{p(1 + .60p)}$$

$$\delta S_4 = \frac{\delta S_{D4}}{p(1 + .60p)}$$

$$\delta H_1'(t) = \delta H_1(t - .99)$$
$$\delta H_2'(t) = \delta H_2(t - .595)$$
$$\delta H_3'(t) = \delta H_3(t - .468)$$

$$\delta H_1^*(t) = \delta H_1(t - .228)$$
$$\delta H_4^*(t) = \delta H_4(t - .123)$$

D.2.2 At An Output Speed of 975 Feet per Minute

$$\delta H_1 = 1.4466\delta H_o' + .1765(\delta S_1 + \Delta S_{o1}) - 0 - .1531\delta\sigma_1$$
$$\delta H_2 = .3212\delta H_1' + .2181(\delta S_2 + \Delta S_{o2}) - .3066\delta\sigma_1 - .1596\delta\sigma_2$$
$$\delta H_3 = .9861\delta H_2' + .1808(\delta S_3 + \Delta S_{o3}) - .4507\delta\sigma_2 - .2433\delta\sigma_3$$
$$\delta H_4 = .7120\delta H_3' + .1217(\delta S_4 + \Delta S_{o4}) - .2086\delta\sigma_3 - .155\delta\sigma_4$$

$$\Delta S_{o1} = 0; \quad \Delta S_{o2} = 0; \quad \Delta S_{o3} = 0; \quad \Delta S_{o4} = 0$$

$$\delta G_1 = 1.755\delta H_o' - 1.061\delta H_1 + 0 - .835\delta\sigma_1$$
$$\delta G_2 = 2.028\delta H_1' - 3.009\delta H_2 + 1.111\delta\sigma_1 - 1.189\delta\sigma_2$$
$$\delta G_3 = 5.734\delta H_2' - 3.375\delta H_3 + 1.754\delta\sigma_2 - 1.703\delta\sigma_3$$
$$\delta G_4 = 3.531\delta H_3' - 3.417\delta H_4 + 1.666\delta\sigma_3 - 1.45\delta\sigma_4$$

$$\delta F_1 = 1.25\delta H_o' - .75\delta H_1 - 0 + .745\delta\sigma_1$$
$$\delta F_2 = .87\delta H_1' - 1.78\delta H_2 - 1.695\delta\sigma_1 + 1.34\delta\sigma_2$$
$$\delta F_3 = 1.72\delta H_2' - 1.375\delta H_3 - 1.110\delta\sigma_2 + .950\delta\sigma_3$$
$$\delta F_4 = 1.42\delta H_3' - 1.73\delta H_4 - .53\delta\sigma_3 + .875\delta\sigma_4$$

$$\delta V_1 = 1.037\delta w_1 + .2287\delta F_1$$
$$\delta V_2 = 1.037\delta w_2 + .2505\delta F_2$$
$$\delta V_3 = 1.027\delta w_3 + .322\delta F_3$$
$$\delta V_4 = 1.009\delta w_4 + .3845\delta F_4$$

$$p\delta\sigma_1 = 51.806\delta V_2 + 246.77\delta H_2 - 174.08\delta H_1' - 171.8\delta V_1$$
$$p\delta\sigma_2 = 67.38\delta V_3 + 274.46\delta H_3 - 409.19\delta H_2' - 85.9\delta V_2$$
$$p\delta\sigma_3 = 73.57\delta V_4 + 398.48\delta H_4 - 349.89\delta H_3' - 85.9\delta V_3$$
$$p\delta\sigma_4 = 111.67\delta V_R - 111.67\delta V_4$$

$$\delta w_1 = \frac{\delta W_{D1}}{(1 + .25p)} - \frac{1.8888\delta G_1}{(1 + .40p)}$$

$$\delta w_2 = \frac{\delta W_{D2}}{(1 + .25p)} - \frac{2.7288\delta G_2}{(1 + .40p)}$$

$$\delta w_3 = \frac{\delta W_{D3}}{(1 + .25p)} - \frac{2.138\delta G_3}{(1 + .40p)}$$

$$\delta w_4 = \frac{\delta W_{D4}}{(1 + .25p)} - \frac{2.528\delta G_4}{(1 + .40p)}$$

$$\delta V_R = \frac{\delta V_{DR}}{(1 + .20p)} \quad \frac{\delta \sigma_4}{(1 + .30p)}$$

$$\delta S_1 = \frac{\delta S_{D1}}{p(1 + .60p)}$$

$$\delta S_2 = \frac{\delta S_{D2}}{p(1 + .60p)}$$

$$\delta S_3 = \frac{\delta S_{D3}}{p(1 + .60p)}$$

$$\delta S_4 = \frac{\delta S_{D4}}{p(1 + .60p)}$$

$$\delta H_1'(t) = \delta H_1(t - 1.98)$$
$$\delta H_2'(t) = \delta H_2(t - 1.19)$$
$$\delta H_3'(t) = \delta H_3(t - .936)$$

$$\delta H_1^*(t) = \delta H_1(t - .456)$$
$$\delta H_2^*(t) = \delta H_4(t - .246)$$

	1950 Feet/minute			975 Feet/minute			1950 Feet/min. Measured Physical Values	
	Measured	Calculated	Δ	Measured	Calculated	Δ		
	1	2	3	4	5	6	7	8
δH_o	40	40		40	40		4	4
δH_1	62.56	62.72	.16	60.85	61.12	.73	3.179	3.128
δH_2	33.89	34.10	.21	27.63	27.64	.01	1.732	1.695
δH_3	50.67	50.80	.13	32.49	32.50	.01	1.236	1.267
δH_4	41.44	41.48	.04	21.90	21.92	.02	0.9964	1.036
$\delta\sigma_1$	-31.9	≤ 0.06	-	-20.62	≤ .020	-	-0.848	-0.798
$\delta\sigma_2$	-24.1	≤ 0.09	-	-11.44	≤ .009	-	-0.537	-0.603
$\delta\sigma_3$	-19.18	≤ 0.09	-	-2.5	≤ .026	-	-0.376	-0.479
δG_1	+29.96	30.45	.49	+22.5	22.56	.06	30.74	29.96
δG_2	+13.26	13.7	.44	+30.84	30.94	.10	3.49	6.63
δG_3	+15.6	-15.8	.20	+32.96	32.97	.01	4.52	3.9
δG_4	-2.07	-1.4	.67	+19.72	19.54	.18	1.335	-0.52
δF_1	-20.69	-20.66	.03	-11.01	-11.00	.01	0.00048	-0.00207
δF_2	+5.38	6.0	.62	+22.68	23.28	.60	0.00161	+0.00027
δF_3	-6.57	-7.0	.43	+13.02	13.17	.15	-0.00036	-0.00018
δF_4	+5.3	5.48	.18	+19.2	19.43	.23	0.000454	+0.00053
δV_1	-34.58	-34.54	.04	-46.8	-46.77	.03	-1.508	-1.729
δV_2	-16.14	-16.18	.04	-80.88	-80.940	.06	-0.033	-0.404
δV_3	-21.8	-21.81	.01	-67.52	-67.67	.15	-0.53	-0.545
δV_4	+6.73	6.73	.00	-42.58	-42.72	.14	0.082	0.168
δw_1	-28.75	-28.3	.45	-42.67	-42.48	.19	-0.1456	-0.1437
δw_2	-18.26	-18.08	.18	-83.53	-84.13	.60	-0.0238	-0.0913
δw_3	-17.03	-16.6	.43	-69.97	-70.20	.23	-0.0478	-0.0851
δw_4	+2.6	2.61	.01	-49.65	-49.69	.04	-0.0169	+0.013

Physical units: δH - thousandths
$\delta\sigma$ - tons/inch^2
δG - ton-inches
δV - inches/sec
δw - radians/sec

Table D.1. Steady-State Values of Variables for Inputs of δH_o shown.

	Units / Stand	1950 Feet Per Minute				975 Feet per Minute			
		1	2	3	4	1	2	3	4
δH_1	Inches	-0.00202	+0.00052	+0.00003	+0.00001	-0.00205	+0.000354	-0.000072	-0.00002
δH_2	"	-0.00141	-0.00081	+0.00026	+0.00002	-0.00150	-0.000169	-0.00068	-0.000136
δH_3	"	-0.00111	-0.00053	-0.00027	+0.00051	-0.00125	-0.000144	+0.000503	-0.000736
δH_4	"	-0.00092	-0.00042	-0.00002	-0.00016	-0.00104	-0.000120	+0.000342	+0.000194
$\delta \sigma_1$	Tons/inch^2	+0.843	-1.695	+0.2	-0.005	+0.962	-1.160	-0.219	-0.039
$\delta \sigma_2$	"	+0.584	+0.195	-2.15	-0.083	+0.835	+0.994	-2.203	-0.323
$\delta \sigma_3$	"	+0.468	+0.157	-0.429	-2.18	+0.690	+0.832	+0.068	-2.179
$\delta \sigma_4$	"	+0.025	-0.0125	-0.286	-0.54	0.046	0.048	-0.143	-0.242
δG_1	Ton-inches	+15.04	+44.66	-5.4	+0	+11.9	+30.58	+5.56	+0.84
δG_2	"	+5.56	-16.42	+43.78	+1.74	+5.52	+8.49	+23.58	+3.44
δG_3	"	-1.275	-3.6	-12.84	+23.79	+1.84	+3.28	+1.83	+10.73
δG_4	"	+1.405	-0.612	-8.92	-1.05	+2.4	+3.68	-2.51	-0.02
δF_1	-	+0.00554	-0.00582	+0	-0	+0.00595	-0.0040	-0.00076	-0.00012
δF_2	-	-0.00059	+0.0131	-0.00067	-0.00023	+0.00008	+0.0098	-0.00662	-0.00096
δF_3	-	+0.00026	+0.00016	+0.0067	-0.0043	-0.00031	+0.00044	+0.00786	-0.0052
δF_4	-	-0.00024	+0.00011	-0.0042	+0.0018	+0.00064	-0.00076	-0.00053	+0.00465
δV_1	Inches/sec	-0.131	-2.91	+0.00018	-0.022	-0.497	-3.463	-0.650	-0.114
δV_2	"	-0.27	-0.74	-0.407	-0.10	-0.693	-1.089	-3.013	-0.452
δV_3	"	+0.225	+0.458	+2.82	-4.05	-0.35	-0.640	+0.884	-3.179
δV_4	"	-0.275	+0.038	+1.08	+2.05	-0.734	-1.080	+0.533	+0.91

Table D.2. Steady-State Responses to -0.01 inch Screw Motor at Each Stand

	Units / Stand	1950 Feet per Minute				975 Feet per minute			
		1	2	3	4	1	2	3	4
δw_r	Rad./sec	0.4	0.4	0.4	0.4	0.4	0.4	0.4	0.4
δH_1	Inches	+0.000258	-0.000135	0	-0	+0.000208	-0.000101	-0.000020	0
δH_2	"	+0.000893	-0.000305	-0.000120	-0.000020	+0.000709	-0.000153	-0.000178	-0.000036
δH_3	"	+0.00161	+0.000010	-0.000268	-0.000140	+0.000739	+0.000090	-0.000253	-0.000184
δH_4	"	+0.00137	+0.000055	-0.000125	-0.000244	+0.000700	+0.000123	+0.000165	-0.000237
$\delta \sigma_1$	Tons/inch^2	-0.831	+0.443	-0.073	+0.0065	-0.698	+0.325	+0.049	+0.012
$\delta \sigma_2$	"	-0.513	-0.229	+0.462	+0.025	-0.243	-0.243	+0.450	+0.079
$\delta \sigma_3$	"	-0.405	-0.174	-0.24	+0.525	-0.649	-0.278	-0.081	+0.523
$\delta \sigma_4$	"	-0.012	-0.01	-0.024	-0.025	-0.013	-0.014	-0.025	-0.024
δG_1	Ton-inches	+22.82	-11.64	+1.08	-0	+18.5	-8.52	-1.14	-0.2
δG_2	"	-22.95	+19.89	-9.37	-0.5	-16.1	+15.4	-4.81	-0.86
δG_3	"	-2.06	-7.79	+15.64	-5.875	-7.55	-6.98	+12.52	-2.6
δG_4	"	-2.56	-3.83	-7.54	+11.23	-6.57	-5.55	-4.56	+10.61
δF_1	-	-0.00295	+0.0015	-0.00012	+0.000024	-0.00239	+0.00111	+0.00017	+0.000044
δF_2	-	+0.00108	-0.00194	+0.00142	+0.000056	-0.00062	-0.00156	+0.00134	+0.00023
δF_3	-	-0.00014	+0.00012	-0.00129	+0.00105	-0.000642	-0.00051	-0.00077	+0.00125
δF_4	-	+0.00024	+0.000116	+0.00016	-0.00045	+0.00048	+0.000095	-0.000123	-0.00030
δV_1	Inches/sec	+2.671	+0.762	-0.055	+0.017	+2.060	+0.967	+0.135	+0.027
δV_2	"	+1.081	+2.24	+0.443	+0.033	+2.059	+1.791	+0.615	+0.1105
δV_3	"	+0.189	+0.908	+1.448	+0.997	+1.533	+1.438	+1.267	+0.764
δV_4	"	+0.420	+0.538	+1.034	+2.423	+1.755	+1.425	+1.130	+1.298

Table D.3. Steady-State Responses to 0.4 rad/sec. change in Roll Speed at Each Stand